ISSN 0711-6659

canadian acoustics
acoustique canadienne

Journal of the Canadian Acoustical Association - Journal de l'Association Canadienne d'Acoustique

SEPTEMBER 2001 | SEPTEMBRE 2001

Volume 29 -- Number 3 | Volume 29 -- Numéro 3

PROCEEDINGS

ACOUSTICS WEEK IN CANADA

SEMAINE CANADIENNE D'ACOUSTIQUE

2001

CAHIERS DES ACTES

canadian acoustics

acoustique canadienne

THE CANADIAN ACOUSTICAL ASSOCIATION
P.O. BOX 1351, STATION "F"
TORONTO, ONTARIO M4Y 2V9

L'ASSOCIATION CANADIENNE D'ACOUSTIQUE
C.P. 1351, SUCCURSALE "F"
TORONTO, ONTARIO M4Y 2V9

CANADIAN ACOUSTICS publishes refereed articles and news items on all aspects of acoustics and vibration. Articles reporting new research or applications, as well as review or tutorial papers and shorter technical notes are welcomed, in English or in French. Submissions should be sent directly to the Editor-in-Chief. Complete instructions to authors concerning the required camera-ready copy are presented at the end of this issue.

ACOUSTIQUE CANADIENNE publie des articles arbitrés et des informations sur tous les domaines de l'acoustique et des vibrations. On invite les auteurs à soumettre des manuscrits, rédigés en français ou en anglais, concernant des travaux inédits, des états de question ou des notes techniques. Les soumissions doivent être envoyées au rédacteur en chef. Les instructions pour la présentation des textes sont exposées à la fin de cette publication.

CANADIAN ACOUSTICS is published four times a year - in March, June, September and December. The deadline for submission of material is the first day of the month preceeding the issue month. Copyright on articles is held by the author(s), who should be contacted regarding reproduction. Annual subscription: $10 (student); $50 (individual, institution); $150 (sustaining - see back cover). Back issues (when available) may be obtained from the CAA Secretary - price $10 including postage. Advertisement prices: $400 (centre spread); $200 (full page); $120 (half page); $80 (quarter page). Contact the Associate Editor (advertising) to place advertisements. Canadian Publication Mail Product Sales Agreement No. 0557188.

ACOUSTIQUE CANADIENNE est publiée quatre fois par année - en mars, juin, septembre et décembre. La date de tombée pour la soumission de matériel est fixée au premier jour du mois précédant la publication d'un numéro donné. Les droits d'auteur d'un article appartiennent à (aux) auteur(s). Toute demande de reproduction doit leur être acheminée. Abonnement annuel: $10 (étudiant); $50 (individuel, société); $150 (soutien - voir la couverture arrière). D'anciens numéros (non-épuisés) peuvent être obtenus du Secrétaire de l'ACA - prix: $10 (affranchissement inclus). Prix d'annonces publicitaires: $400 (page double); $200 (page pleine); $120 (demi page); $80 (quart de page). Contacter le rédacteur associé (publicité) afin de placer des annonces. Société canadienne des postes - Envois de publications canadiennes - Numéro de convention 0557188.

EDITORIAL / ÉDITORIAL

Dalila Guisti, Conference Chair, Acoustics Week in Canada 2001, Alliston, Ontario

Welcome to the 2001 Proceedings Issue of Canadian Acoustics. The CAA Acoustics Conference in Canada 2001 is upon us and we hope that it will be a great learning and social experience for all participants.

Organizing a Conference is a challenge and requires the time, dedication and ideas of many people. It especially requires the participation and attendance of the members. In the case of the Canadian Acoustical Association this challenge is heightened by the small size of the organization, the diversity of the areas of acoustics and the wide spread geographical placement of the members.

One of my goals at the onset of the planning for this year's Conference was to have all the areas of acoustics represented. While most areas will have sessions, there are some areas that will not be represented, despite great efforts by the organizing committee. I am disappointed by this, however we have not let this detail deter us from our goal of making this Conference the best one yet!!

The Conference is being held at the beautiful Nottawasaga Inn in Alliston, Ontario. This year's Conference promises to be interesting and diverse with over 80 papers and discussion sessions. The plenary speakers are world class as is our banquet entertainer. We have been fortunate to have many sponsors for the coffee breaks, wine for the banquet and tote bags. In addition we have over 15 exhibitors. All this has been accomplished through the hard work of the organizing committee. All that is left is for the members to attend and participate in the sessions to make the 2001 Acoustics Conference a resounding success.

I have enjoyed meeting the challenges presented to us in the course of my duties as the Conference Chair. Thank you to all the people who were involved in putting this Conference together and good luck to future Conference Chairs!

WHAT'S NEW ??

Promotions
Deaths
New jobs
Moves
Retirements
Degrees awarded
Distinctions
Other news

Do you have any news that you would like to share with Canadian Acoustics readers? If so, send it to:

QUOI DE NEUF ?

Promotions
Décès
Offre d'emploi
Déménagements
Retraites
Obtention de diplômes
Distinctions
Autres nouvelles

Avez-vous des nouvelles que vous aimeriez partager avec les lecteurs de l'Acoustique Canadienne? Si oui, écrivez-les et envoyer à:

Francine Desharnais, DREA Ocean Acoustics, P.O. Box 1012, Dartmouth NS, Email: desharnais@drea.dnd.ca

SYSTEM 824 SLM/RTA

Five sophisticated acoustical instruments in One!

1 **Integrating Sound Level Meter** meeting Type 1 Standards with simultaneous measurement of sound pressure levels using fast, slow, and impulse detector, and simultaneous A, C, and flat weighting. It measures 48 sound pressure parameters at once! All this with a 105 dB linearity range!

Simple Sound Analyzer with simultaneous sound pressure level measurement and real-time 1/3 octave frequency analysis.

Logging Sound Level Meter permits data gathering of broadband sound pressure levels and frequency spectra over user-defined time intervals.

Real Time Frequency Analyzer with 1/1 and 1/3 octave analysis over a 20kHz frequency range and optimized for characterizing steady-state or high speed transient events.

Fast Fourier Transform Analyzer with 100, 200, and
5 400 lines resolution and 20kHz range for specific frequency investigations.

For use in a wide variety of applications

Research and Development

- Building Acoustics
- Sound Power Determination
- Vibration measurements
- Statistics
- Simple Point Shoot
- Transient Capture

Environmental

- Aircraft Noise
- Industrial Noise
- General Surveys
- Transportation Noise
- Community Noise

Worker Safety

- Noise Exposure Measurements
- Work Place Surveys
- Machinery Noise
- Audiometric Calibration
- Simultaneous C minus A Measurements

Listen with Larson•Davis

Dalimar Instruments Inc.

At your service since 1986

193, Joseph Carrier, Vaudreuil-Dorion, Quebec, Canada J7V 5V5 Tel.: (450) 424-0033 Fax: (450) 424-0030
1234 Reid Street, Suite 8, Richmond Hill, Ontario, Canada L4B 1C1 Tel.: (905) 707-9000 Fax: (905) 707-5333
E-mail: info@dalimar.ca Website: www.dalimar.ca

MAIL

4 July 2001

I am writing to extend a formal apology to Dr. Christian Giguère and Dr. Sharon Abel for an important oversight that has recently been brought to my attention. As author of "An evaluation of three-dimensional audio displays for use in military environments." *Canadian Acoustics,* 28(4), 5-14, 2000, I unintentionally neglected to formally acknowledge that portions of the reported work were drawn from a contract report submitted to the Defence and Civil Institute of Environmental Medicine by Drs. Giguère and Abel entitled "A review of the effect of hearing protective devices on auditory perception: The integration of active noise reduction and binaural technologies" (Contract No. W7711-6-7316/001, 1997), and also Giguère, C., Abel, S.M., and Arrabito, G.R. (2000). "Binaural technology for application to active noise reduction communication headsets: Design considerations." *Canadian Acoustics,* 28(2), 21-31, 2000. Their report and paper should have been quoted and referenced at several places in my own article, particularly in Section 4 (Transition potential of the technology) and Section 6 (Conclusions and recommendations).

This oversight was not intentional and I am genuinely sorry for the discomfort that I have no doubt caused Drs. Giguère and Abel. I understand that Canadian Acoustics strives to promote academic excellence, and I will try to adhere to this high standard in my future work. I am indebted to both Chris and Sharon for all the help they have given me in my research and I sincerely apologize to them, the readership of this journal and my colleagues at DCIEM.

G. Robert Arrabito
Defence Scientist
DCIEM, National Defense
Toronto, ON

Editor's Note: Drs. C. Giguère and S. Abel have read the above letter and have accepted Arrabito's apology.

Proceedings of Acoustics Week In Canada 2001
Actes de la Semaine Canadienne D'Acoustique 2001

Table of Contents / Tables des matières

Human Response to Vibration

Computer Applications

Hearing Loss and Hearing

Industrial Noise

Hearing Protection

Architectural Acoustics

Exhibitors and Sponsors of the 2001 Canadian Acoustical Association Conference
Nottawasaga Inn, Alliston, Ontario, October 1-3, 2001

For our 2001 annual Conference, the CAA has experienced a great deal of interest from both Sponsors and Exhibitors, more than we had originally anticipated! With a great location, an impressive list of technical papers, and the expectation of unprecedented attendance levels, the 2001 CAA Conference is going to be a great event for everyone interested in acoustics, noise and vibration.

Support has come from companies across Canada, and the CAA wishes to recognize the contributions of this year's Sponsors and Exhibitors.

Confirmed Sponsors:

The CAA is grateful to have the following companies support their annual Conference by way of sponsorship, enabling the CAA to hold the Conference at the Nottawasaga Inn and helping to keep registration fees to a minimum for all Conference attendees.

Silex

SPL Control Inc.

ECKEL
NOISE CONTROL TECHNOLOGIES

Durisol

KINETICS Noise Control
VIBRON PRODUCTS GROUP

SOUND SOLUTIONS

Brüel & Kjær

The Canadian Acoustical Association
l'Association Canadienne d'Acoustique

Confirmed Exhibitors:

Silex

Vibro-Acoustics

SOUND SOLUTIONS®

Dalimar Instruments Inc. since 1986

ACOUSTIC SOLUTIONS INC
"Protecting People"

arxx™
BUILDING PRODUCTS

ECKEL
NOISE CONTROL TECHNOLOGIES

MAXXON CANADA

Blachford

environmental analytical systems

instrumentation SOLUTIONS

Owens Corning

The OZAGroup.com

Brüel & Kjær

DODGE-REGUPOL
INCORPORATED
Leaders in recycled products technology

Durisol

WALLWORKS

KINETICS Noise Control

VIBRON PRODUCTS GROUP

SCANTEK, INC.
Sound and Vibration
Instrumentation & Engineering

The Canadian Acoustical Association

l'Association Canadienne d'Acoustique

Exhibitors and Sponsors of the 2001 Canadian Acoustical Association Conference
Nottawasaga Inn, Alliston, Ontario, October 1-3, 2001

For our 2001 annual Conference, the CAA has experienced a great deal of interest from both Sponsors and Exhibitors, more than we had originally anticipated! With a great location, an impressive list of technical papers, and the expectation of unprecedented attendance levels, the 2001 CAA Conference is going to be a great event for everyone interested in acoustics, noise and vibration.

Support has come from companies across Canada, and the CAA wishes to recognize the contributions of this year's Sponsors and Exhibitors.

Confirmed Sponsors:

The CAA is grateful to have the following companies support their annual Conference by way of sponsorship enabling the CAA to hold the Conference at the Nottawasaga Inn and helping to keep registration fees to a minimum for all Conference attendees.

Sponsor Information:

The CAA appreciates the support of all our sponsors; however, special recognition goes out to SPL Control Inc. and Silex Inc. SPL Control has shown their support of the Conference by sponsoring the wine that will accompany our meal during the Tuesday evening banquet dinner and Silex Inc. has donated the attractive CAA tote bags that will be handed out to our Conference attendees.

Silex Inc., Mississauga, ON *Silex designs, engineers and manufactures Silencers, Emission Control Equipment, Enclosures and a wide range of related products for industrial applications and a quieter life. Silex services a broad range of industry sectors throughout the world, and have invested heavily in new technology to assist in the development of the next phase of silencers and acoustical enclosures.*	***Conference Tote Bag Sponsor*** Contact: Marina Polumbo Phone: 905 612 4000 Email: marinap@silex.com Web: www.silex.com
SPL Control Inc., Cambridge, ON *Specializes in the engineering and design of Sound Control Protection Systems.*	***Evening Banquet - Wine Sponsor*** Contact: Rick Hedges Phone: 519 623 6100 Fax; 519 623 7500 Email: rhedges@splcontrol.com
Eckel Industries of Canada, Morrisburg, ON *From product testing to research laboratory, Eckel has played an integral role in technological advances in science, industry and commerce. Today, engineers and scientists utilize Eckel anechoic chambers and noise control products to improve the technology that affects our lives and the environment for our future.*	***Conference Break Sponsor*** Contact: Blake Noon Phone: 613 543 2967 Email: eckel@eckel.ca Web: www.eckel.ca
Brüel & Kjær, Norcross, GA *Brüel & Kjær has been a leading player in the sound and vibration market with over 1,200 employees, offices in 55 countries and 7 accredited calibration centres worldwide. B&K has a wide product range in excess of 450 products, including transducers, a full range of hand-held sound level meters, analyzers, systems, service products and customised solutions.*	***Upscale Conference Break Sponsor*** Contact: Bill Bailey (West & Central Ontario) Phone: 905 945 1900 Email: bkinfo@bksv.com Web: www.bksv.com
Sound Solutions (1997) Inc., Toronto, ON *Manufacturer and distributor of interior architectural finishes for walls and ceilings. Represent the widest range of custom and pre-engineered, interior architectural and acoustical products, including ceiling systems, wall panels and related decorative accessories.*	***Upscale Conference Break Sponsor*** Contact: Tom Richardson Phone: 416 740 0303 Fax: 416 740 0696 Web: www.soundsolutions.ca
Vibron / Kinetics Noise Control, Mississauga, ON *For over 40 years Kinetics Noise Control and Vibron, have been successfully helping our customers solve their noise and vibration problems in the most economical way possible. Kinetics offers a complete line of standard products and the ability to custom engineer solutions for all your noise and vibration concerns.*	***Conference Break Spnosor*** Contact: Richard Anthony Phone: 905 670 4922 Email: ranthony@vibron.com Web: www.kineticsnoise.com/vibron1.html
Durisol Inc., Mississauga, ON *Produce noise barrier walls in highway, railroad, mass transit, airport, residential and commercial applications and acoustic facing panels that can all be custom designed for architectural and structural requirements.*	***Conference Break Sponsor*** Contact: Michael Rock Phone: 905 521 0999 Email: noisebarriers@durisol.com Web: www.durisol.com

The Canadian Acoustical Association
l'Association Canadienne d'Acoustique

Effects Of Vibration On Human Systems: A Neurophysiological Perspective

B. J. Martin, D. Adamo
Center for Ergonomics, Department of Industrial and Operations Engineering
The University of Michigan,1205 Beal Avenue, Ann Arbor, MI 48109-2117, U.S.A.

1. INTRODUCTION

Musculoskeletal disorders resulting from vibration exposure have been documented since Ramazzini indicated a relationship between vibration and health. Nevertheless, the complexity of the reactions of the musculoskeletal system is not clearly understood. This complexity stems not only from biomechanical events and physiological effects but also from the interference of vibration with the functioning of sensorimotor system. Such interference has been shown to alter central and peripheral sensory feedbacks involved in the control of muscle contraction, posture, movement, movement coordination and fatigue. These perturbations have contributed significantly to the understanding of proprioception, exteroception and their respective role in motor control. However, little attempt has been made to link the response of neurophysiological mechanisms and health outcomes. This review presents an overview of the sensory and motor responses associated with human vibration and points to the likely contribution of vibration-induced alteration of sensory motor functions to disorders.

2. KINESTHETIC ILLUSION

The early work of Goodwin et al. (1972) and following studies have demonstrated that tendon vibration applied to a static limb induces kinesthetic illusions of movement whose characteristics in term of direction, magnitude and velocity are a function of the muscles vibrated and vibration frequency. The illusion of movement is in the direction compatible with the elongation of the vibrated muscle (Goodwin et al. 1972) and the magnitude and velocity of the perceived joint rotation increase with vibration frequency (Sittig et al. 1985). Furthermore, when vibration is applied simultaneously to antagonist muscles, the direction of the illusory movement is a function of the unbalance between the respective frequencies (Gilhodes et al. 1986).

3. MOVEMENT CONTROL AND COORDINATION

Tendon vibration applied to the moving limb increases the aiming error. Undershooting occurs when vibration is applied to the antagonist muscle, while vibration of the agonist muscle does not affect target attainment (Capaday and Cooke, 1983). These results obtained in shortening and lengthening contractions (Inglis et al. 1991) indicate that sensory information from the lengthening muscle is important for perception and control of limb position and movement. Furthermore, movement sequences such as a combination of elbow rotation and hand opening can be disrupted by tendon vibration (Cordo et al. 1995). This alteration of motor coordination was found to be dependent on the vibration frequency and the timing of vibration application (before, at, or after the initiation of the movement).

4. POSTURAL RESPONSES

Various alterations of postural control are associated with vibration of the foot sole (Kavounoudias et al. 1999), legs (Martin et al. 1980), hand (Roll et al. 1986; Martin et al. 1992), neck (Wierzbicka et al. 1998) and extra-ocular muscles (Roll and Roll 1988). These alterations demonstrate that sensory information from all body areas contribute to balance and body orientation in space, which indicates that human vibration exposure profoundly modifies motor behavior in a broad manner.

5. EYE-HAND-HEAD COORDINATION

Aiming errors can be induced by neck (Biguer et al. 1988), or hand vibration (Martin et al. 1997). The latter also contribute to an alteration of eye movements. These errors are associated with an alteration of visual perception and proprioceptive information. They also confirm the contribution of hand proprioception to eye-hand coordination.

6. POST VIBRATION RESPONSES

Motor unit activity and thus increase in muscle tension remain for tenth of seconds after short duration vibration exposure (Ribot-Ciscar et al. 1996). These post effects have mainly a central origin involving a change in the processing of proprioceptive information. Some further evidence of a central effect is illustrated by long lasting modification of postural sway following neck vibration (Wierzbicka et al. 1998).

7. REFLEXES

Monosynaptic proprioceptive reflexes, involved in the adjustment of muscle tension are inhibited by tendon or segmental vibration while tonic responses, the so called tonic vibration reflex and antagonist vibration reflex can develop in the agonist or antagonist muscles with associated kinesthetic illusions, respectively (Calvin-Figuiere et al. 1999). Increase in muscle tension is also induced by whole hand vibration.

8. FORCE CONTROL, FATIGUE COMPENSATION OR ENHANCEMENT

It is well known that force exertion increases under hand vibration exposure, even when visual feedback is provided. In addition, the decrease in voluntary exertion resulting from fatigue can be compensated by short term vibration or exacerbated by long term vibration (Bongiovanni and Hagbarth, 1990, Adamo et al. 2001)

9. MECHANISMS

These effects are proprioceptive and exteroceptive consequences of the vibration-induced changes in the firing rate of muscle spindles, as evidenced by microneurographic recordings (Burke et al. 1976; Roll and Vedel, 1982). Changes in the sensory messages and their significance modify the gain of the sensorimotor loops at central and peripheral levels, which result in a) changes in motor commands and the general pattern of muscle activity, b) an increase in muscle load, and c) a forced drive of some motor units. These mechanisms contribute to an increased muscle tension and exacerbated fatigue. Hence, they are most likely to lead directly and indirectly to tissue disorders.

10. REFERENCES

Adamo D, Kim PS, Khodaee M, Johnsson P, Martin BJ. Vibration-induced muscle fatigue: a contribution to musculoskeletal injury. Proceedings HAV 2001, Nancy, France. 2001.

Biguer B, Donaldson ML, Hein A, Jeannerod M. Neck muscle vibration modifies the representation of visual motion and direction in man. Brain. 1988; III: 1405-1424.

Bongiovanni LG, Hagbarth KE. Tonic vibration reflexes elicited during fatigue from maximal voluntary contractions in man. J Physiol. 1990; 423:1-14.

Burke D, Hagbarth K, Lofstedt L, Wallin BG. The responses of human muscle spindle endings to vibration of non-contracting muscles. J. Physiol. 1976; 261:673-693.

Calvin-Figuiere S, Romaiguere P, Gilhodes J, Roll J. Antagonist motor responses correlate with kinesthetic illusions induced by tendon vibration. Exp. Brain Res. 1999; 124:342-350.

Capaday C, Cooke JD. Vibration-induced changes in movement-related EMG activity in humans. . Exp. Brain Res. 1983; 52:139-146.

Cordo P, Gurfinkel VS, Bevan L, Kerr GK. Proprioceptive consequences of tendon vibration during movement. J. neurophysiol. 1995; 74:1675-1688.

Gilhodes JC, Roll JP, Tardy-Gervet MF. Perceptual and motor effects of agonist-antagonist muscle vibration in man. Exp. Brain Res. 1986; 61:395-402.

Goodwin GM, McCloskey DI, Matthews PBC. The contribution of muscle afferents to kinaesthesia shown by vibration induced illusions of movement and by the effects of paralysing joint afferents. Brain. 1972; 95:705-748.

Inglis JT, Frank JS Inglis B. The effect of muscle vibration on human position sense during movements controlled by lengthening muscle contraction. Exp. Brain Res. 1991; 84:631-634.

Kavounoudias A, Roll R, Roll J. Specific whole-body shifts induced by frequency-modulated vibrations of human planter soles. Neuroscience Letters. 1999; 266:181-184.

Martin BJ, Gauthier GM, Roll JP, Hugon M, and Harley F. Effects of Whole-body Vibration on Standing Posture in Man. *Aviat. Space and Environ. Med.* 51(8):778-787, 1980.

Martin BJ, Saltzman J, Elders G. Effects of hand vibration frequency and duration on eye-hand coordination in pointing task. Proceedings of the IEA 97. Tempere, Finland 1997.

Martin BJ, Fletcher l, Park H. Effects of hand vibration on postural control and stability. Proceedings of NACOB II. Chicago, USA. 1992; 149-150.

Ribot-Ciscar E, Roll JP, Gilhodes JC. Human motor unit activity during post-vibratory and imitative voluntary muscle contractions. Brain Research. 1996; 716:84-90.

Roll JP, Roll R. From eye to foot. In: Amblard B, Berthoz A, Clarac F (eds) Roll in Posture and Gait. Elsevier, Amsterdam, 1988; 155-164.

Roll JP, Vedel JP. Kinaesthetic roles of muscle afferents in man, studied by tendon vibration and microneurography. Exp. Brain Res. 1982; 47:177-190.

Roll JP, Vedel JP, Gilhodes JC, Ribot E. Proprioceptive sensory coding of motor activities in man. In: Ron S, Schmid R, Jeannerod M (eds) Sensory plasticity: theoretical, experimental and clinical aspects. Inserm, Paris, 1986; 140: 283-304.

Sittig AC, Denier van der Gon JJ, Gielen CCAM. Separate control of arm position and velocity demonstrated by vibration of muscle tendon in man. Exp. Brain Res. 1985; 67:33-40.

Wierzbicka MM, Gilhodes JC, Roll JP. Vibration-induced postural posteffects. J. Neurophysiol. 1998; 79:143-150.

Repetitive Impacts From Manual Hammering: Physiologic Effects On The Hand-Arm System

D.R. Peterson and M.G. Cherniack
Biodynamics Laboratory, University of Connecticut School of Medicine, Farmington, CT 06030-6210

1. INTRODUCTION

Repetitive impact from both percussive and power tools is frequently encountered in industry. It is widely recognized that dose effect models derived from oscillatory motion may significantly underestimate impact related effects. Research on translating laboratory measurements from individual impact hand tools into human health effects is underdeveloped (SUGGS, 1982; ISO/CD 15694, 2000). Results derived from detailed dynamic measurements (i.e., forces and angles measured at high sampling rates at at point of impact rather than accumulated and averaged for the entire work cycle) have yielded measurable quantities. These are in concept that were both closely related to potential human health risks and are significantly differentiable between a sample of representative commercial hammers (PETERSON and CHERNIACK, 2001). Table 1 summarizes the observed differences of each biomechanical factor obtained from preliminary data investigations on these types of observations. Vibration analyses from these experiments showed that while the importance of vibration measured at the wrist has high importancebeen recognized because of transmission to important arm structures, but it did not differ substantially between the hammers tested. Vibration at the hammer handle was widely different between tools, but its importance is obviated by the absence of differential transmission to the hand and arm (PETERSON and CHERNIACK, 2001). On the other hand, the highest levels of energy transfer were mapped at the fingertips. This may have important health consequences because of the proximity of important neurological and neurovascular organelles.

The accelerations of the bony structures of the hand at point of impact are more likely to correspond with actual exposures than measurements that are accumulated and averaged for the entire work cycle. An even more critical consideration may be a preferential distribution of effect in the hand, particularly at the fingertip with its density of neuro-afferents and neurovascular structures. The purpose of this study was the determination of the distribution of transmitted vibration (vibration mapping) over the entire hand during a manual hammering task. Vibration mapping provides a more physiologic representation of how energy is transmitted to the hand during the tool usage than is possible from temporal and spatial cumulative models.

2. METHODS

Vibration mapping was determined from individual trials on subjects performing a standardized hammering task. A set of four uni-axial accelerometers were placed perpendicular to the longitudinal axis of, and bisected the lengths of the distal, middle, and proximal phalanges, and the metacarpal of a particular finger. The set of accelerometers were limited to one finger only for each experimental run. (Note that the thumb only required the use of three accelerometers.) In these experiments, we have used conventional commercial hammers - a specific anti-vibration model, as well as all-steel, graphite, fiberglas, and wood models - to provide single impact force mapping.

3. RESULTS

Vibration mapping on the right hand was determined by averaging the observed peak accelerations for each accelerometer. Results show that peak acceleration values of 27.0 to 34.0 m/s^2 were observed on the distal phalanges while values from 20 to 26.9 m/s^2 were observed on the middle phalanges. Peak acceleration values from 16 to 19.9 m/s^2 were observed on the metacarpal and proximal phalanges from digits 1, 4 and 5, and values from 12 to 15.9 m/s^2 were observed on the proximal phalanges from digits 2 and 3.

As was expected, vibrations were observed to be higher in the distal phalanges when compared the metacarpals. The peak acceleration values on the metacarpals were observed to be greater than the proximal phalanxes. This contrast may be due to variations in grip forces during the use of the hammer, or if the subject did not operate the tool consistently. It is necessary to study more subjects in order to prove that the values of these accelerations are consistently distributed.

4. DISCUSSION AND CONCLUSIONS

The observed values are potentially influenced by several factors. The subject is free to grip the tool at various locations about the hammer handle. Changes in these grip locations, as well as the strength of the grip, can affect vibration transmission. Missing the nail and hitting the wood board can also affect vibration transmission. Also, each accelerometer needs to be secured in the right position above the pha-

lanx. Poorly mounted accelerometers can promote sensor and sensor wire movement and introduce erroneous artifacts within the measurements, especially at the time of hammer and nail contact.
The distribution of the transmitted vibration over the hand was greatest for the distal phalanges of the hand. The metacarpals showed a greater or equal value of vibration than the proximal phalanges, which is possibly a factor of grip.

Further investigation of vibration mapping should include measures of grip force to accompany the measures of vibration in order to understand better the distribution of vibration transmission during a hammering task. Current and intended investigations of the effects of impact on mechanoreceptors and receptor mediated blood flow in the fingertips are warranted, given the high levels of energy transfer to the glabrous pad of the fingertip.

5. REFERENCES

INTERNATIONAL STANDARDIZATION ORGANIZATION, ISO/CD 15694 Committee Draft. Mechanical vibration and shock - Measurement and evaluation of isolated shocks transmitted from hand-held and hand-guided machines to the hand-arm system, 2000.

SUGGS C.W., Vibration of manual tool handles, In BRAMMER A.J., TAYLOR W., eds., Vibration Effects on the Hand and Arm in Industry, John Wiley & Sons, New York, 1982, pp.253-257.

PETERSON D.R., CHERNIACK, M.G., Vibration, grip force, muscle activity, and upper extremity movement of a manual hammering task, Proceedings for the International Congress on Hand-arm Vibration, Nancy, France, June 2001.

Table 1: Biomechanical factors and observed differences within the measured data among tested hammers.

Biomechanical Factors (Measured Quantities)	Location of Measurement	Observed Differences
Vibration (RMS Acceleration)	Hammer Shank Just Prior to Handle (Tool)	Substantial
	Between the Syloids of the Radius and Ulna (Wrist)	No
	Ratio (Wrist/Tool)	No
Muscle Activity (%MVC sEMG)	Extensor Carpi Ulnaris	Moderate
	Flexor Carpi Ulnaris	Moderate – No
	Number of Muscle Contractions	No
Exherted Grip Force (RMS Pounds Force)	Distal Phalanges of Digits 2-5, Thenar, and Hyperthenar	Very Substantial
Range of Motion (Degrees)	Ulnar Deviation	Moderate – No
	Radial Deviation	Moderate – No
	Overall Range	Moderate – No
Strike Force	Estimated Hammer Strike	Substantial

Vibrotactile Perception Thresholds: The Tactile Equivalent Of Audiometry

A.J. Brammer and J.E. Piercy
Institute for Microstructural Sciences, National Research Council, Ottawa, Ontario K1A 0R6, Canada

1. INTRODUCTION

Grasping, holding and controlling an object in the hands is part of everyday experience at work, at home and in many leisure activities. These functions together with tactile exploration of surface features and textures by the fingers are critically dependent on the sensory input, which is mediated by populations of mechanoreceptors. Disturbances in sensory acuity, such as occurs in some peripheral neuropathies, from repeated flexing of the wrist, or from use of vibrating hand-held tools, can influence hand function.

For over a century, the perception of vibration has been employed as a test of sensory function. As methods of stimulation and test procedures have become more refined, it has become apparent that the vibrotactile perception threshold (VPT) depends on details of the measurement procedure.(Maeda et al.) The lack of broadly accepted methods for determining VPTs, together with a lack of appreciation of the need to establish the acuity of specific mechanoreceptor populations, appears to have impeded acceptance in clinical medicine of this modality for quantitative sensory testing.

Efforts to rectify this situation have been underway for several years, principally within the International Organization for Standardization (ISO), building on research conducted at several laboratories including those of the National Research Council. The purpose of this paper is to summarize the information that has led to international acceptance of two, closely-related methods of measurement together with normative threshold values that may be used to identify changes from the VPTs of healthy persons. It is to be expected that the publication of standards for the measurement and assessment of VPTs will rekindle interest in, and the development of, products designed to be used in an analogous manner to audiometric instruments for determining hearing thresholds.

2. MECHANORECEPTOR PROPERTIES

The tactile performance of the hand is known to depend on neural activity in four populations of specialized nerve endings, which are commonly described by their response to mechanical indentation of the skin surface, namely: SAI - slowly adapting, type 1; SAII - slowly adapting, type 2; FAI - fast adapting, type 1, and; FAII - fast adapting, type 2.(Johannson et al., 1983) The acuity of SAI receptors is primarily responsible for the resolution of the spatial features of a surface, such as ridges or edges, while the acuity of FAI and FAII receptors is primarily responsible for distinguishing surface texture, such as silk from sandpaper, and for detecting the motion of objects in contact with the skin. The SAII receptors signal skin stretch. It is also known that the process of holding an object in the hand is controlled by the detection of micro-slips by the FAI and FAII receptors.(Srinivasan et al.)

This information has been derived from neural action potentials produced by single tactile units in response to externally applied skin displacements. When sinusoidal displacements of different magnitudes and frequencies are applied to single units of the four mechanoreceptor populations in the fingertips, the frequency ranges of maximum neural activity may be established.(Johansson et al., 1982) It is possible from the results of these experiments to define contours expressing the same rate of neuronal discharge per stimulus cycle, which have been shown in animal studies to characterize the physiological response. If the onset of a given rate of neuronal activity is combined with knowledge of the innervation density of different mechanoreceptor populations, an estimate for the threshold of the perceived response to a stimulus at the fingertip may be obtained. Contours of physiologically-based "perception" thresholds so derived are shown in Fig. 1 as a function of frequency, by solid lines of different width for the SAI, FAI, and FAII receptors. The neuronal thresholds have been constructed from the data of Johannson et al. (1982) by defining contours corresponding to one action potential per two stimulus cycles, and have been adjusted for the relative numbers of receptive units per unit skin area at the fingertip.(see Johansson et al., 1983) Note that each mechanoreceptor population responds to less stimulus than the other populations in certain contiguous, but different, frequency ranges. Appropriate stimulation at specific frequencies should thus result in vibrotactile perception being mediated by a *single* mechanoreceptor population, namely that requiring least stimulus.

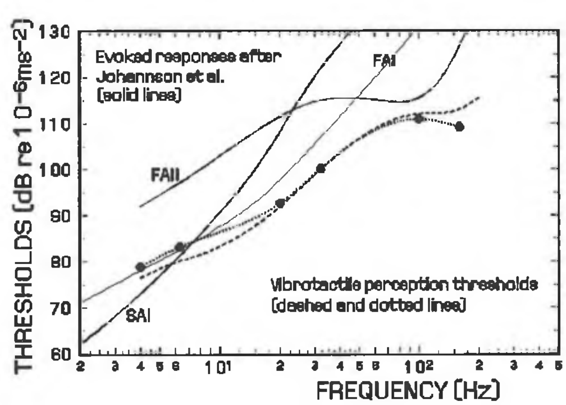

Figure1: Evoked responses and VPTs in healthy subjects

3. DETERMINATION OF VPTs

There have been two studies that attempt to mimic the essential characteristics of the stimulation conditions employed for the physiological experiments described in the previous section, in order to determine psychophysically the VPTs mediated by individual receptor populations. The thresholds obtained at the fingertips of healthy persons are shown by the dashed and the dotted lines in Fig. 1 (Löfvenberg et al., and Brammer et al., respectively).

From these studies, of the parameters most influencing the VPT at the fingertip, the indentation of the skin surface by the stimulating probe or, equivalently, the static force with which the probe contacts the skin, would appear to be the most important. Also, support is required for the forearm and hand to reduce motion between the subject and stimulator caused by environmental vibration or natural physiological processes, such as hand tremor, blood pulsation and breathing.(Piercy et al.) In addition, the rate of stimulus magnitude change within the psychophysical algorithm needs to be restricted to avoid forward masking. (Morioka) Of lesser importance is the probe diameter (a 3 mm, and a 6 mm, diameter probe was used in the two psychophysical studies cited) and the presence, or absence, of a surround, i.e., a static annular plate around the probe to support the fingertip being stimulated.(Verrillo et al.)

The essential requirements are specified in a recent international standard, ISO 13091-1 (2001), where contact conditions are provided for determining VPTs at the fingertips either with, or without, a surround.

4. DISCUSSION AND CONCLUSIONS

The extent to which the provisions of the international standard unify the VPTs recorded using alternate measurement methods may be inferred from an examination of the thresholds for healthy persons obtained in studies employing apparatus and procedures complying with, or almost complying with, its requirements. There have been four studies conducted with a surround, and two without a surround, that may be included in such an analysis (see Table 1). The mean VPTs reported at frequencies common to most studies can be seen from the Table to be similar in magnitude. Indeed, the variability in mean VPTs obtained using nominally the same method (involving a 6 mm probe and 10 mm surround) appears to be as great as the differences in thresholds between the different methods (identified in column 1). Moreover, this similarity remains, and the agreement between studies is improved, after adjusting the results to a common age for the subjects and indentation for the stimulating probe, and for differences between the algorithms used to calculate the VPT. A detailed report of this analysis will be published elsewhere.

It would thus appear that when measurements are performed according to the international standard: 1) essentially apparatus independent VPTs can be obtained, and; 2) a single set of normative values may be constructed for males.

5. REFERENCES

Bovenzi M, et al. Occup. Environ. Med. **54**, 577-587 (1997).

Brammer AJ, et al. J. Acoust. Soc. Am. **93**, 2361 (1993).

ISO 13091-1 Mechanical vibration - Vibrotactile perception thresholds for the assessment of nerve dysfunction - Part 1: Methods of measurement at the fingertips (ISO, Geneva 2001).

Johannson RS, et al., Brain Res. **244**, 17-25 (1982).

Johannson RS, et al. Trends in Neurosci. **6**, 27-32 (1983).

Lindsell CJ, et al. Int. Arch. Occup. Environ. Health **72**, 377-386 (1999).

Löfvenberg J, et al. Brain Res. **301**, 65-72 (1984).

Maeda S, et al. Ergon. **37**, 1391-1406 (1994).

Morioka M. Personal communication, 2001.

Piercy JE, et al. Scand. J. Work Environ. Health **12**, 417-419 (1986).

Srinivasan MA, et al. J. Neurophysiol. **63**, 1323-1332 (1990).

Verrillo RT, et al. Percept. Psychophys. **11**, 117-120 (1972).

Wild P, et al. (submitted for publication).

Table 1: Mean values of VPTs for healthy males reported in studies using methods in, or close to those in, ISO 13091-1.

Probe/Surround (mm/mm)	Source	Mean Age (years)	Mean VPT (dB re 10^{-6} ms^{-2}) 16-20 Hz	31.5 Hz	125 Hz
6/10	Bovenzi et al.,1997	30.1	94.4	101.8	106.8
6/10	Lindsell et al., 1999	36		102.9	108.6
6/10	Maeda et al., 1994	28.8	91.6	100.7	103.9
6/10	Wild et al., 1999	30		99.8	107.5
6/no surround	L)fvenberg et al., 1984	~25	92.0	100.0	113.0
3/no surround	Brammer et al., 1993	30	92.7	100.2	110.1

Design Of Antivibration Gloves

Douglas D. Reynolds
Center for Mechanical & Environmental Systems Technology, University of Nevada, Las Vegas, Nevada, USA

1. INTRODUCTION

Repetitive trauma associated with excessive vibration directed into the hands and arms is a significant health problem in U.S. industry. It is estimated that between two to four million workers are exposed to on-the-job hand-arm vibration in the U.S. and that around 50% of these workers either have or will develop symptoms associated with hand-arm vibration syndrome (HAVS). HAVS is associated with the destruction of the small blood vessels and with nerve damage in the fingers. HAVS is caused by excessive vibration directed into the hands from vibrating hand tools and vibration-intensive work processes. Symptoms associated with HAVS usually show up as a combination of finger blanching, particularly in response to cold, and progressive finger numbness.(1) In advanced stages, HAVS can result in the loss of tactile discrimination and manipulative dexterity.(1) When the level of vibration exposure to the hands is excessively high, symptoms associated with HAVS can appear within as little as one year's time.(2)

One method of reducing vibration energy into the hand and arm is to use protective clothing, in particular antivibration gloves. NIOSH publication 89-106 states that strategies for reducing hand-arm vibration in the U.S. shall be supplemented by the "use of antivibration clothing, mittens, gloves, and equipment."(4) The NIOSH publication further states that the vibration-damping material in an antivibration glove must:

"provide adequate damping with minimal thickness so that the dexterity required for safe and efficient tool operation will not be reduced, and

have adequate damping characteristics over the vibration frequency spectrum associated with HAVS."

The International Organization for Standardization adopted ISO Standard 10819 to define the performance criteria and related test procedures that must be met and used to classify a glove as an antivibration glove.(5) An antivibration glove must:

have an average ISO weighted transmissibility of less than 1, $\underline{TR}_M < 1$, in the mid frequency range from 16-400 Hz and of less than 0.6, $\underline{TR}_H < 0.6$, in the high frequency range from 100-1,600 Hz;

be a full-fingered glove that has the same vibration protection in the palm and fingers.

2. ERGONOMIC REQUIREMENTS FOR GLOVE DESIGN

The ergonomic effects of a tool on the hand include hand posture, grip strength, push force, tactile feedback, and temperature. The design of an antivibration glove must address these issues. Five ergonomic factors must be considered in the design of an antivibration glove. Paying proper attention to these factors increases the effectiveness of the glove in reducing vibration while making the glove comfortable to wear.

The thickness of the vibration-damping material placed in a glove to reduce vibration must be relatively thin. Placing vibration-damping material in the palm and the finger and thumb stalls of a glove increases the effective diameter of a tool handle when clasped while wearing the glove. Placing a material with too great a thickness in a glove can make the glove feel bulky and uncomfortable when clasping a hand tool or work piece. This can also make proper control of a tool difficult to maintain. A larger diameter handle requires a greater grip force to clasp the handle with the same grip effort, as compared to a smaller diameter handle. This increases muscle fatigue and the intracompartment pressure in the carpal tunnel in the wrist.(6) Increased muscle fatigue and intracompartment pressure in the carpal tunnel raises the risk of developing carpal tunnel syndrome.(7) Both HAVS and carpal tunnel syndrome must be considered when designing an antivibration glove. Increasing the thickness of the vibration-damping material in a glove usually increases the effectiveness of the glove in reducing vibration. However, thicker material can cause a glove to feel bulky and be uncomfortable. It can also increase the risk of developing carpal tunnel syndrome when using the glove over an extended time period. Material placed in the finger and thumb stalls of a glove should have a thickness less than 4.6 mm (0.18 in.) and in the palm area less than 6.4 mm (0.25 in.).

Vibration-damping materials placed in a glove should be flexible and pliable, and they should not interfere with tactile feedback. These materials should easily conform to the natural flex-lines in the palm and fingers. This allows the worker to easily maintain control of his tool or work piece. Vibration-damping materials should minimize the reduction in tactile feedback associated with their use. To properly perform work operations, an operator must be able to feel his tool and/or work piece.

The vibration-damping material must cover the full palm area and all of the digits of the fingers and thumb. Vibration from a tool or work piece enters the hand at the palm, fingers and thumb. The primary damage associated with HAVS occurs in the fingers and thumb. Thus, to protect the fingers and thumb, all of the digits of the fingers and thumb must be isolated from the tool or work piece.

An antivibration glove must have an opposed thumb. A wing thumb is often used in a glove because it simplifies the manufacturing of the glove. When a glove that contains vibration-damping material and that has a wing thumb is used to clasp a tool handle, the material in the thumb stall rotates to the outside surface of the thumb. This places the thumb in direct contact with the tool handle, exposing it to vibration. Using an opposed thumb will prevent this. When a glove with an opposed thumb is used to clasp a tool handle, the vibration-damping material always stays properly positioned between the thumb and handle.

An antivibration glove should be loose fitting. Vibration-damping material that is placed in an antivibration glove can make the glove feel tight and stiff, particularly in the finger and thumb stalls. This usually reduces manipulative dexterity. Over-sizing a glove to accommodate vibration-damping material will increase manipulative dexterity. It is particularly important to over-size the finger and thumb stalls

3. GLOVE WITH AN AIR BLADDER VIBRATION-DAMPING ELEMENT

A thin layer of air placed between a vibrating handle or work piece and the hand is the most efficient means of attenuating vibration into the hand. A thin layer of air can be achieved with an air bladder that is made by welding two layers of thin-film thermoplastic material together with a quilted pattern of weld points and with weld lines that correspond to the natural flex-lines of the hand. An air bladder made by this process is thin, pliable, and flexible. This allows the bladder to naturally conform to the palm and fingers when clasping a handle or work piece. The air bladder for each hand has a bulb inflator. The inflator is connected to the air bladder by means of a flexible tube that allows the inflator to be placed on the backside of the glove. The air bladder is placed in a pocket in the glove between the palm of the hand, fingers and thumb and the outside shell of the glove. A thin cotton or Lycra material is placed between the air bladder and the hand to prevent the hand from sweating. The outside shell of the glove can be leather, Kevlar, or any other durable material.

A worker who wears a glove with an air bladder can easily maintain control of his tool or work piece. Tactile feedback is received through the air bladder while it provides good vibration protection. A worker who wears a glove with an air bladder can always feel what he is doing. Gloves with an air bladder are made with an opposed thumb. This allows the thumb portion of the bladder to remain between the thumb and tool handle when the handle is clasped by the hand.

Compared to other glove vibration-damping materials, air is essentially massless. Thus, a glove with an air bladder is light and comfortable to wear. To provide the same vibration protection as an air bladder, every other glove vibration-damping material will require a material thickness that will make the glove uncomfortable to wear and use. Also, gloves with a thicker layer of vibration damping material will increase the potential for developing carpal tunnel syndrome with prolonged use.

4. REFERENCES

Pelmear, P. L., Taylor, W., and Wasserman, D. E., *Hand-Arm Vibration, A Comprehensive Guide for Occupational Health Professionals*, 1992, Van Nostrand Reinhold.

ISO Standard 5349: *Mechanical vibration - Guidelines for the measurement and the assessment of human exposure to hand-transmitted vibration*, 1986, International Organization for Standardization, Geneva, Switzerland.

***NIOSH Report: MUSCULOSKELETAL DISORDERS (MSDS) AND WORK PLACE FACTORS – A critical Review of Epidemiologic Evidence for Work Related Musculoskeletal Disorders of the Neck, Upper Extremity, and Low Back*, 1997, DHHS (NIOSH) Publication No. 97-141, National Institute for Occupational Safety and Health, 4676, Columbia Parkway, Cincinnati, Ohio, USA.**

***NIOSH Criteria for a Recommended Standard: Occupational Exposure to Hand-Arm Vibration*, 1989, DHHS (NIOSH) Publication No. 89-106, National Institute for Occupational Safety and Health, 4676, Columbia Parkway, Cincinnati, Ohio, USA.**

ISO Standard 10819: *Mechanical vibration and shock - Hand-arm vibration - Method for the measurement and evaluation of the vibration transmissibility of gloves at the palm of the hand*, 1996, International Organization for Standardization, Geneva, Switzerland.

Radwin, R. G., Armstrong, T. J., and Chaffin, D. B., *Power Hand Tool Vibration Effects on Grip Exertions*, 1987, Ergonomics, 30(5), 833-855.

Szabo, R. M. and Chidgey, L. K., *Stress Carpal Tunnel Pressure in Patients with Carpal Tunnel Syndrome Normal Patients*, 1989, Journal of Hand Surgery, 14A, 624-627.

AN INTERLABORATORY EVALUATION OF THE VIBRATION TRANSMISSIBILITY OF GLOVES FOLLOWING THE ISO 10819 TEST METHOD

Paul-Émile Boileau*, Subhash Rakheja and Jérôme Boutin***

**IRSST, 505 De Maisonneuve West, Montréal (Québec) H3A 3C2, Canada*

***CONCAVE Research Centre, Concordia University, 1455, De Maisonneuve West, Montréal, (Québec) H3G 1M8, Canada*

1. INTRODUCTION

Numerous studies have dealt with the difficulties associated with the application of the ISO 10819 test method for evaluating the vibration transmissibility of gloves at the palm of the hand (GRIFFIN, 1998; HEWITT, 1997). The most widely recognized difficulties relate to lack of repeatability caused by performing tests with human subjects, the difficulty in correctly aligning the hand-held adapter to measure the vibration transmitted inside the glove, the complexities associated with the experimental set-up design needed to monitor and control the grip and feed forces and generation of complex vibration excitations defined by M- and H-spectra.

In a previous study involving three different European laboratories (HEWITT, 1997), the reproducibility of the standard test for anti-vibration gloves, as defined in the ISO 10819 standard, had been shown to be adequate under the medium frequency excitation (M-spectrum) but inadequate under the high frequency excitation (H-spectrum). Although the factors leading to these discrepancies could not be clearly identified, it has been suggested (O'BOYLE and GRIFFIN, 2001) that increasing the number of subjects and the number of tests per subject could perhaps contribute to reduce the observed variability. In an effort to identify the sources of variations, this study presents the results of testing four different gloves in three different laboratories (two North American and one European), where some variations to the ISO 10819 test protocol are introduced by certain laboratories, specifically by increasing the number of test subjects and test trials and by providing control for hand-held adapter orientation.

2. MEASUREMENTS

2.1 Gloves

Four types of gloves were incorporated as part of the round-robin tests of the three laboratories. There were three large size right hand gloves of each type, originating from the same batch. The gloves contained a variety of different materials : elastomer matrix for glove 1, two-layer foam and viscoelastic material for glove 2, two-layer cushioning material for glove 3 and air membrane for glove 4. All except glove 3 were CE marked, denoting their compliance with the European Union Directive for personal protective equipment.

2.2 Glove Vibration Transmissibility Measurements

The basic evaluation procedure defined in the ISO 10819 standard was followed by the different laboratories. According to this Standard, the mean corrected frequency-weighted transmissibility of the gloves, $\overline{\mathrm{TR}}_s$, must be reported under both medium frequency (s=M) and high frequency (s=H) random spectra covering the ranges 31.5 to 200 Hz and 200 to 1000 Hz, respectively. Mathematically, TR_s represents the ratio of frequency-weighted rms acceleration measured inside the glove, a_{wg}, to that measured on the handle, a_{wh}, divided by the overall frequency-weighted transmissibility of the adapter, TR_a, measured with the ungloved hand :

$$TR_s = \frac{a_{wg}}{a_{wh} \cdot TR_a} \qquad (1)$$

In the above, the frequency weighting to be applied is that defined in the ISO 5349-1 standard. According to the ISO 10819 standard, the mean values of TR_s under each spectral class must be established for 3 subjects with hand size between 7 and 9, each performing 2 trials. The overall mean M- or H- spectrum transmissibility $\overline{TR}_M$ or $\overline{TR}_H$ for a glove is thus obtained from the average of six corrected transmissibilities. During the tests, the grip force must be maintained at 30 ± 5 N and the push force at 50 ± 8 N. The criteria for an antivibration glove are : $\overline{TR}_M < 1.0$ and $\overline{TR}_H < 0.6$.

2.3 Round-Robin Tests

The gloves were tested in three laboratories. All used a vibration shaker system with feedback control mechanism to generate the required excitation spectra. Laboratories 2 and 3 used an identical shaker system with a similar handle design involving two parts to enable grip force measurement. Laboratory 1 used a different shaker system with a handle machined from a single solid piece of aluminium. Both laboratories 1 and 2 measured push force from a force plate supporting the subjects. Laboratory 3 used a load cell inserted between the handle and the shaker head to measure push force. Laboratories 1 and 3 applied the frequency weighting defined in ISO 5349-1 :2001 in reporting the transmissibility values, while laboratory 2 used the weighting defined in the earlier version of that Standard. Furthermore, the results reported by laboratory 2 involved a mathematical correction to account for adapter misalignment. Both laboratories 1 and 2 performed the measurements with 3 subjects, laboratory 2 requesting 3 trials per subject but retaining only the two closest measures. In contrast, laboratory 3 performed the measurements with 5 subjects, each realizing 5 tests, while the results were grouped to comply with the ISO 10819 requirements and later compared with the overall mean.

Table 1. Mean overall frequency-weighted glove transmissibility measured under M spectrum.

GLOVE #	Lab.#1	Lab.#2	Lab.#3 (1)	Lab.#3 (2)	Lab.#3 (3)	Lab.#3 (4)	Lab.#3 (5)	Lab.#3 (6)	Lab.#3 (all)
1	0.92 (0.05)	0.86 (0.04)	0.84 (0.04)	0.85 (0.03)	0.84 (0.04)	0.78 (0.07)	0.80 (0.04)	0.80 (0.09)	0.82 (0.06)
2	0.94 (0.06)	0.90 (0.03)	0.88 (0.07)	0.86 (0.08)	0.87 (0.07)	0.90 (0.06)	0.87 (0.08)	0.90 (0.07)	0.89 (0.06)
3	0.91 (0.03)	0.86 (0.03)	0.78 (0.08)	0.75 (0.10)	0.76 (0.12)	0.85 (0.04)	0.84 (0.05)	0.85 (0.04)	0.80 (0.10)
4	0.94 (0.02)	0.85 (0.05)	0.81 (0.05)	0.82 (0.05)	0.79 (0.07)	0.80 (0.04)	0.80 (0.03)	0.80 (0.04)	0.81 (0.04)

Table 2. Mean overall frequency-weighted glove transmissibility measured under H spectrum.

GLOVE #	Lab.#1	Lab.#2	Lab.#3 (1)	Lab.#3 (2)	Lab.#3 (3)	Lab.#3 (4)	Lab.#3 (5)	Lab.#3 (6)	Lab.#3 (all)
1	0.63 (0.03)	0.61 (0.04)	0.63 (0.06)	0.61 (0.04)	0.64 (0.04)	0.58 (0.08)	0.55 (0.03)	0.56 (0.07)	0.59 (0.06)
2	0.82 (0.03)	0.78 (0.06)	0.81 (0.09)	0.75 (0.17)	0.78 (0.13)	0.80 (0.07)	0.74 (0.15)	0.77 (0.12)	0.80 (0.11)
3	0.77 (0.04)	0.66 (0.12)	0.62 (0.03)	0.61 (0.06)	0.60 (0.06)	0.69 (0.05)	0.69 (0.02)	0.70 (0.04)	0.65 (0.06)
4	0.75 (0.05)	0.58 (0.06)	0.53 (0.09)	0.50 (0.10)	0.51 (0.11)	0.53 (0.09)	0.51 (0.11)	0.52 (0.12)	0.54 (0.08)

3. RESULTS

The mean overall frequency weighted transmissibility of the gloves reported by different laboratories under M and H spectra are reported in Tables 1 and 2, respectively, where the standard deviations are indicated in parentheses. All of these values represent the mean of 6 measurements carried out with 3 different subjects, with the exception of the last column reported for laboratory 3 which presents the mean and standard error based on 25 values (i.e. 5 subjects x 5 trials per subject). In addition, six sets of results are reported for this laboratory by grouping the 25 data sets (5 subjects x 5 trials) in groups of six (3 subjects x 2 trials).

While closest agreement between the 3 laboratories is observed for glove #2, gloves #3 and #4 lead to the largest differences. Laboratory #1 is found to consistently report values which are higher than those from the other two laboratories, which tend to provide mean values that are in better agreement, although the standard error on the mean often appears to be higher particularly under the H spectrum. In general the overall mean values reported by laboratory #3 based on 25 measurements tend to agree reasonably well with those based on 6 measurements, suggesting that increasing the number of subjects and test trials will not necessarily improve the reliability of the measured glove performance.

4. CONCLUSION

The degree of agreement on the mean values of transmissibility reported by the different laboratories was found to be influenced by the type of glove being tested, the excitation spectrum being used and the combination of subject and test trial being considered. The laboratory whose results differed the most from that of the other two laboratories also presented the smallest values for the standard deviation. For certain gloves, the large variability observed between the different laboratories suggest that improvement to the Standard test is desirable.

REFERENCES

GRIFFIN, M.J., Evaluating the effectiveness of gloves in reducing the hazards of hand-transmitted vibration. Occup Environ Med., 1998, 55, pp.340-348.

HEWITT, S., An interlaboratory evaluation of the reproducibility of the ISO 10819 test for anti-vibration gloves. Proc. UK Group Meeting on Human Response to Vibration, U. of Southampton, Sept 1997, pp. 447-457.

INTERNATIONAL STANDARDS ORGANIZATION, ISO 10819 Standard. Mechanical vibration and shock-Hand-arm vibration-Method for the measurement and evaluation of the vibration transmissibility of gloves at the palm of the hand, 1996.

INTERNATIONAL STANDARDS ORGANIZATION, ISO 5349-1 Standard. Mechanical vibration – Measurement and evaluation of human exposure to hand-transmitted vibration Part 1 : General requirements, 2001.

O'BOYLE, M., and GRIFFIN, M.J., Inter-subject variability in the measurement of the vibration transmissibility of gloves according to current standards. 9th Int. Conf. On Hand-Arm Vibration, Nancy, France, June 2001.

The Evaluation Of Human Spinal Response To Vibration With Mechanical Shocks Of 0.5 To 4 G Amplitude

James Morrison (1) and Dan Robinson (2)
(1) School of Kinesiology, Simon Fraser University, Burnaby, BC, V5A 1S6
(2) Robinson Ergonomics Inc., 3000 Surf Crescent, Coquitlam, BC, V3C 3S8

1. INTRODUCTION

Mechanical shocks are a component of occupational whole-body vibration (WBV) exposure that may increase the risk of adverse health effects. While research has focused on the human response to WBV and to the very large impacts that occur during falls or vehicle crashes, very few studies have examined the response to low amplitude mechanical shocks (Robinson et al., 1993; Cameron et al., 1996). The ability to relate mechanical shock exposure to potential health effects depends, in part, on the ability to represent the human sensitivity to different characteristics of the motion.

Frequency weighting of the seat acceleration time history is utilized by the International Organization for Standardization (ISO 2631-1, 1997) to represent the human sensitivity to whole-body vibration. The Wk frequency weighting filter is used to represent the human response to vertical vibration. Payne (1992) and the Air Standardization Coordinating Committee (ASCC, 1982) proposed the use of the Dynamic Response Index (DRI) to represent the biodynamic response to vertical shocks of 1 to 20 g. The DRI is based on a second order linear system, initially defined by a natural frequency of 8.4 Hz and critical damping ratio of 0.224, but later revised to 11.9 Hz and 0.35 (Payne, 1992).

A series of experiments were designed to evaluate the human response to vertical mechanical shocks of varying amplitude, frequency content, and direction. This paper outlines some of the main characteristics of the human response to single mechanical shocks, and compares the measured biodynamic response to mechanical shocks with the estimation of human response afforded by the frequency weighting of ISO 2631-1 (1997) and the DRI (Payne, 1992).

2. METHODS

Experiments were conducted using the Multi-Axis Ride Simulator at the U.S. Army Aeromedical Research Laboratory, Fort Rucker, Alabama. Ten male volunteers were exposed to a variety of individual mechanical shocks ranging in amplitude from 0.5 to 4.0 g, in frequency from 2 to 20 Hz, in the +z (vertical) direction. Shock frequency was defined as the inverse of the time period of the biphasic shock waveform, where the shock waveform was presented as a damped sinusoid consisting of a single time period.

Acceleration was measured at the seat using three single axis Entran accelerometers (± 25 g) within a flexible epoxy seat pad that was securely taped to the seat cushion between the subject and the cushion. Acceleration at the spine was measured using Entran miniature accelerometers (± 25 g) attached to the skin over the thoracic and lumbar spinous process (at T3 and L4) by a small square of two-sided adhesive tape. Movement of the accelerometer and skin relative to the underlying bone was corrected using a transfer function derived from single perturbations of the accelerometer-skin system. Additional details of the experimental methods are contained in Cameron et al. (1996).

The Wk frequency weighting was applied to the measured z-axis seat acceleration using the transfer functions mathematically defined by Annex A of ISO 2631-1 (1997). The frequency response characteristics of the DRI were applied to the measured seat acceleration as a frequency weighting filter defined by the second order linear system parameters, fn=11.9 Hz and c = 0.35.

The ratio of peak acceleration response to peak acceleration input of the mechanical shock was calculated for the experimental data, the Wk filter, and the DRI model. This information was used to compare the predicted responses with the measured spinal response.

3. RESPONSE TO MECHANICAL SHOCKS

The main characteristics of the human response to individual vertical shocks with amplitudes greater than 1 g ($9.81\ m \cdot s^{-2}$) are illustrated in Figure 1. Results at the thoracic and lumbar vertebrae were similar. The acceleration data demonstrate two distinct events that influence the response at the lumbar spine: the initial mechanical shock and a secondary impact. The initial shock causes uncoupling of the seat and occupant, despite use of a seat belt, due to the phase lag in the response. When the uncoupling is reversed, there is a secondary impact. Both the initial shock and the secondary impact generate a significant response at the lumbar and thoracic vertebrae and have the potential to contribute to health effects.

While the human body tends to act as a low pass filter at low levels of vibration and shock, the body transmits higher frequency components as the magnitude of shocks increase above 2 g. This is visually evident in the response as higher frequency spikes superimposed on the lower frequency response (Figure 1).

In contrast, the Wk frequency weightings result in a response that more closely resembles the input acceleration at the seat than the response in the lumbar spine (Figure 1).

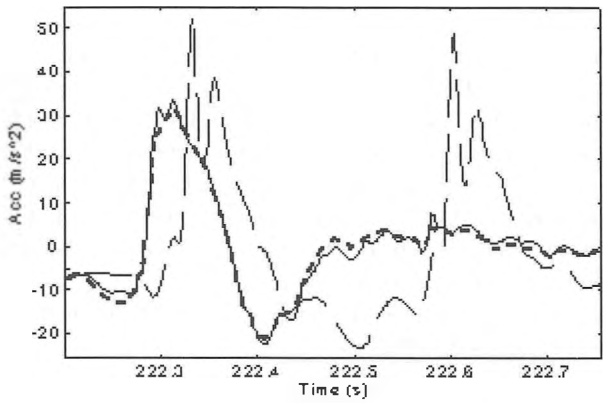

Figure 1. Acceleration (m×s^{-2}) measured at the seat (solid) and lumbar spine (long dash) and Wk frequency weighted acceleration (short bold dash) for a +4 g, 5 Hz z-axis mechanical shock.

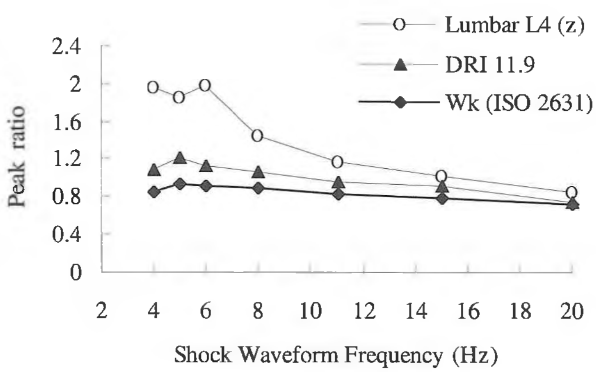

Figure 2. Ratio of measured (Lumbar L4) and estimated (11.9 Hz DRI and Wk filter) peak response acceleration to peak acceleration at the seat for 4 g, z-axis mechanical shocks.

Both the Wk filter and the DRI underestimate the measured response at all frequencies, and fail to predict the spinal response to the secondary impact (Figures 1 and 2).

These results suggest that the human spinal response in the z-axis represents a non-linear system, with the non-linear effects being dependent on both the amplitude and frequency (or period) of the shock waveform.

4. CONCLUSIONS

As shock amplitude and period increases in the z-axis, the human by transmission of higher frequency components and a response to both the initial shock and a secondary impact.

The nonlinear characteristics of the measured response to z-axis (vertical) mechanical shocks are not well represented by the frequency weighting filters of ISO 2631-1 (1997) or by linear system models such as the DRI. The DRI proposed by Payne (1992) has a natural frequency and damping coefficient that are not supported by the measured response data in these experiments. Both the DRI and the Wk filter underestimate the measured spinal response and fail to account for the response to the secondary impact.

An alternative approach is required if the human spinal response characteristics are to be adequately represented in evaluation of exposure to mechanical shock.

5. REFERENCES

ASCC (1982) Human tolerance to repeated shock. ASCC Advisory Publication 61/25, Air Standardization Coordinating Committee.

Cameron, B., Morrison, J., Robinson, D., Vukusic, A., Martin, S., Roddan, G., Albano, J. (1996) Development of a standard for the health hazard assessment of mechanical shock and repeated impact in army vehicles – Phase 4 – Experimental Phase. U.S. Army Aeromedical Research Laboratory, Contract Report No. CR-96-1.

ISO 2631-1 (1997) Mechanical vibration and shock – Evaluation of human exposure to whole-body vibration – Part 1: General Requirements. International Organization for Staardization, Geneva, Switzerland.

Payne, P. (1992) A unification of the ASCC and ISO ride comfort methodologies. Working Paper 377-3-R2, Payne Associates, Severna Park, Md, USA.

Robinson, D., Village, J., Roddan G., Remedios, B., Morrison, J., and Brammer, A. (1993) The effect of mechanical shock frequency and amplitude on spinal transmission and internal pressure. Canadian Acoustics. Vol. 21, pp. 141-142.

Investigating The Applicability Of Biodynamic Models To Account For Whole-Body Dynamics On Automotive Seats

S. Rakheja* and P.-É. Boileau**

**CONCAVE Research Centre, Concordia University, 1455, De Maisonneuve West, Montréal, (Québec) H3G 1M8, Canada*
***IRSST, 505 De Maisonneuve West, Montréal (Québec) H3A 3C2, Canada*

1. INTRODUCTION

Automotive seating comfort is strongly influenced by the perception of whole-body vibration, which is related to body posture, static and dynamic properties of the seat, and nature of vibration. The dynamics of the coupled seat-body system is highly complex due to nonlinear response of the seat cushion and the human body to vibration input. The assessment of vibration related comfort performance of automotive seats are thus mostly achieved through laboratory or field experiments involving representative subjects sample and test conditions. This approach, however, raises some ethical concerns associated with vibration exposure of human subjects, and complexities due to inter- and intra-subject variations. In view of the above and significant contributions of the occupant, considerable efforts have been made to develop analytical models of seats and the occupants (PATTEN, 1998; GRIFFIN, 1990). A review of reported seated occupant models suggests that most of these models are derived from biodynamic response measured under excitations and conditions that do not represent automobile driving [ISO/FDIS 5982, 2001]. The validity of these models for automotive seats is thus doubtful. In this study, different occupant-seat models are explored for vibration comfort analyses of automotive seats. A nonlinear model of a seat cushion and its support mechanism is developed on the basis of measured static and dynamic characteristics. Subsequently, analyses and experiments are performed to examine the applicability of some selected linear occupant models.

2. AUTOMOTIVE SEAT MODELING

The static and dynamic properties of a polyurethane foam (PUF) cushion and its support depend upon the material, construction, seated body weight and nature of vibration. An automotive seat cushion is thus characterized in the laboratory under different preloads, representing seated weights of 5^{th} percentile female to 95^{th} percentile male population, and displacement excitations ranging from 2.5 mm to 19 mm at frequencies upto 15 Hz, using a force indentor recommended in SAE J1051 (1988).

The measured force-deflection data revealed non-linear visco-elastic behavior arising mostly from non-linear stress-relaxation and stress-strain properties of PUF. A constant static stiffness value corresponding to a selected preload could be evaluated assuming small variations around a selected preload. The dynamic stiffness coefficient of a seat, however, differs from its static value. The dynamic stiffness constants are computed from mean force-deflection data measured under sinusoidal excitations of varying amplitudes in the vicinity of a selected preload (Fig. 1). The results suggested that dynamic stiffness is similar to the static value at low frequencies but increases considerably with increase in excitation frequency and decreases with increase in excitation amplitude. The damping properties of the PUF cushion are also derived from the measured data using the principle of energy similarity. The results showed high damping at low frequencies, which decreased rapidly with increase in frequency. The results also showed almost insignificant influence of excitation amplitude.

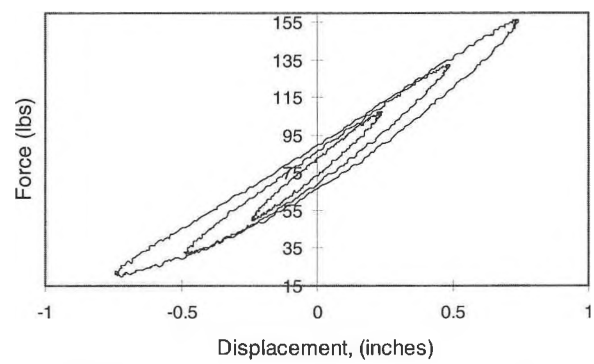

Fig. 1: Dynamic force-deflection of a seat cushion under different excitation amplitudes at 1.5 Hz.

A nonlinear model of the seat is developed on the basis of dynamic stiffness and damping coefficients as functions of excitation and seated body weight. The vibration transmission characteristics of the seat with a passive load are measured in the laboratory and the data is used to validate the seat model and the test methodology. The model results agreed very well with measured data in 0.5-4.5 Hz frequency range. Considerable deviation between the model results and measured data, however, was observed at higher frequencies, which was attributed to hopping of the passive load on the seat.

3. OCCUPANT-SEAT MODELLING

Three different occupant-seat models are derived upon integrating selected biodynamic models of seated occupants to the validated cushion model. The linear occupant models included a single-DOF model (GRIFFIN, 1990), a two-DOF model (SUGGS and STIKELEATHER, 1970) and a four-DOF model (BOILEAU, 1995). These models were derived from the biodynamic responses of subjects in the mass ranges of 58-81 kg, 57-85 kg and 58-90 kg, respectively.

4. MEASUREMENTS

The vibration transmission characteristics of the seat with 6 male human subjects were investigated in the laboratory under sinusoidal and road-measured excitations. The subjects mass ranged from 68 to 80 kg (mean mass of 73 kg). Each subject was seated with feet supported on the vibrating platform and hands on a steering wheel.

5. RESULTS

The acceleration transmissibility characteristics of the seat model employing three different seated occupant models, evaluated under sinusoidal excitations, are illustrated in Fig. 2, together with measured mean and envelope curves. It should be noted that the total masses of models considered are comparable with the mean seated mass of the test subjects (73% of mean body mass). The measured data, attained with human subjects, exhibits considerable attenuation of base vibration at frequencies above 4 Hz, while the resonant frequency of the coupled system lies near 3 Hz. The responses attained with three occupant models differ considerably among themselves and from the measured data. The seat with single-DOF occupant model yields better agreement with the measured mean transmissibility at frequencies close to and below resonace frequency. At frequencies higher than 3.3 Hz, however, the single-DOF model underestimates the measured response by as much as 50%. The responses of the seat-occupant model employing two- and four-DOF occupant models differ considerably from the mean measured response in the entire frequency range.

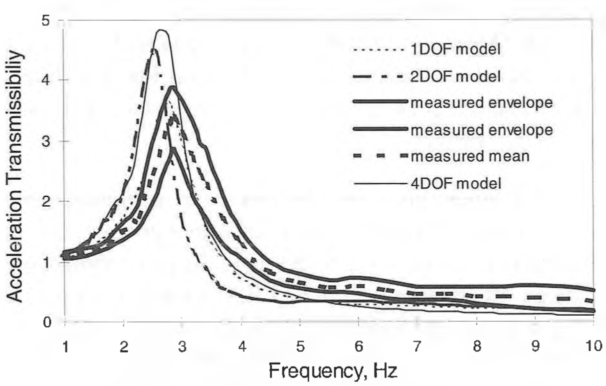

Fig. 2 : Comparison of computed and measured acceleration transmissibility of the seat-occupant system.

The responses of the seat-occupant models were also evaluated under road-measured excitation. The comparisons with mean laboratory measured data further revealed considerable differences between them, irrespective of occupant model employed. Figure 3 shows, as an example, a comparison of PSD of acceleration response of seat- model with a single-DOF occupant model with the mean measured data. In the low frequency range (below 2 Hz), all the three models demonstrated good agreement with the measured response, which is most likely attributed to negligible contributions of occupant dynamics in this range. In the 2-5 Hz range, responses of all models deviated from measured mean response. The models yielded considerable errors in near the resonannce frequency in the 3-3.5 Hz band.

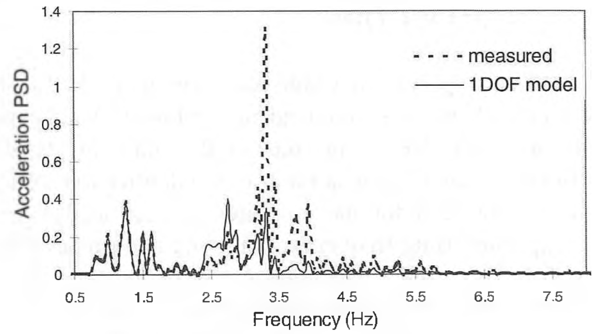

Fig. 3 : Comparison of acceleration PSD of seat model with single-DOF occupant model with mean measured response

6. CONCLUSION

From the study, it is concluded that the response characteristics of reported seated occupant models, when applied to automotive seats, differ considerably among themselves and from the measured data. The combined seat-occupant models yield considerable errors in magnitude responses and resonant frequency of the coupled system, specifically under random excitations. Under deterministic excitations, all the models yield poor estimation of vibration attenuation performance of automotive seats, while that involving the single-DOF occupant model yields somewhat better estimate of the response near the resonant frequency.

REFERENCES

BOILEAU, P.-E., A study of secondary suspension and human driver response to whole-body vehicular vibration and shock, Ph.D. Thesis, Concordia University, 1995.

GRIFFIN, M.J., Handbook of human vibration, Academic Press, 1990.

INTERNATIONAL STANDARDS ORGANIZATION ISO/FDIS 5982, Mechanical Driving Point Impedance and Transmissibility of the Human body, 2001.

PATTEN, W.N., A vibration model of open celled polyurethane foam automotive seat cushions, J. of Sound and Vibration, 217(1), 1998.

SAE J1051, Force deflection measurement of cushioned components of seats for off-road work machines, 1988.

SUGGS, C.W. and STIKELEATHER, L.F., Application of a dynamic simulator in seat testing, Trans. ASAE, 1970, 13, pp. 378-381.

Characterization Of The Health Hazard Associated With Exposure To Repeated Mechanical Shock

Dan Robinson* and James Morrison**
* Robinson Ergonomics Inc., 3000 Surf Crescent, Coquitlam, BC, V3C 3S8
** School of Kinesiology, Simon Fraser University, Burnaby, BC, V5A 1S6

1. INTRODUCTION

Occupational exposure to whole-body vibration (WBV) is associated with an increased incidence of low back pain and degenerative disorders of the spine (Wikström et al., 1994). The International Organization for Standardization (ISO) provides a standard for the measurement and analysis of WBV exposure using frequency weighting and rms averaging (ISO 2631-1, 1997). Occupational WBV exposure often involves repeated mechanical shocks that are not appropriately considered by the rms method. This standard recommends the use of a running rms average to identify the maximum transient vibration value (MTVV) or a fourth power vibration dose value (VDV) to characterize exposure that includes repeated mechanical shocks. However, these methods have been criticized as lacking physiological or biomechanical origin, and no guidance is provided to relate VDV or MTVV with potential health effects.

An alternate approach has been developed based on the concept of a material fatigue process that ultimately results in tissue failure or injury. This approach differs from that of the VDV or MTVV in that exposure is related to the repeated stress levels in the lumbar spine rather than directly to the acceleration response.

Allen (1977) and Payne (1978) explored the use of simple mechanical analogues to predict spinal loading in response to mechanical shocks, and developed the Dynamic Response Index (DRI) to account for the health effects of multiple shocks. The Air Standardization Coordinating Committee (ASCC, 1982) adopted their approach as a standard.

Sandover (1986) hypothesized that dynamic loading of the vertebral end-plates and annulus could lead to material fatigue of these tissues; therefore, the Palmgren-Miner hypothesis could be applied to predict the number of cycles required to generate damage for a known stress level. Combining the approach of Allen, Payne and Sandover allows for the generation of a dose-response model that relates input acceleration at the seat to injury in the spine. The current paper describes an approach that expands on the earlier work of Allen, Payne and Sandover to allow an estimation of health risk from exposure to repeated mechanical shocks. This approach was developed on contract DAMD17-91-C-1115 for the U.S. Army Aeromedical Laboratory, Fort Rucker, Alabama, and is mathematically described in Morrison et al. (1997).

2. OVERVIEW OF APPROACH

Figure 1 provides a schematic overview of the proposed health hazard assessment approach and the flow of data between sequential models that are applied to the seat acceleration to estimate health risk.

Figure 1. Schematic of proposed health hazard assessment method.

The Human Response Model is comprised of dynamic response models for the x, y and z axes that estimate lumbar spine acceleration from seat acceleration, and regression equations based on biomechanical data that transform the lumbar spine acceleration to compressive force at the L4-L5 intervertebral joint.

The lumbar spine response in the x and y directions was modeled as a second order linear system, similar to the DRI, with a natural frequency of 2.125 Hz and critical damping ratio of 0.22. The response to z-axis shocks was found to be non-linear (Morrison and Robinson, 2001) and a recurrent neural network was used to establish a non-linear difference equation that adequately represented the measured response (Nicol et al., 1997).

Regression equations were derived from a biomechanical model that utilized measurements of spinal posture, acceleration, and internal pressure to estimate the peak compressive and shear forces acting at the L4-L5 lumbar joint and the peak acceleration response in each axis.

The Dose Model is based on the Palmgren-Miner hypothesis that the degree of material fatigue is related to the ratio of the cumulative number of stress cycles to the total number of cycles for failure at that stress level. The Dose Model calculates a sixth power root mean sum of the lumbar compressive forces (or stresses) estimated by the Human Response Model for each shock. The exponent of 6 was selected as a conservative estimate of the rate of fatigue in bone, based on a reported range of 5 to 7.7 (Sandover, 1986). The output of the Dose Model for a series of mechanical shocks is an equivalent static load that can be compared with the ultimate strength of the L4-L5 joint, as determined by material testing of cadaveric tissue (Hutton and Adams, 1982; Morrison et al., 1997).

The Injury Probability Model relates the equivalent static load (dose) to a probability function that accounts for the population variance in ultimate strength of the L4-L5 joint.

3. DISCUSSION

The proposed approach for characterizing the health hazard associated with exposure to repeated mechanical shocks is theoretically based in that it can be related to known characteristics of the human dynamic response to shocks, the physical properties of tissue at risk of injury, and population variance with respect to those properties.

An advantage of this approach is that it can be used to assess the health hazard of a single exposure to repeated shocks, intermittent exposures over a prolonged period, or a lifetime of daily exposure. Although the model is designed for a male population in the age range of 20 - 40 yr., it can be modified to account for age and gender related changes in the biomechanical properties of tissue. This approach is now being considered by ANSI and ISO working groups as a draft standard for exposure to repeated shocks.

Validation of the proposed approach requires epidemiological data that relate mechanical shock exposure to the incidence of spinal injury. At present, data required to perform this validation is limited, since most studies characterize the rms WBV rather than the occurrence of shocks. However, analysis of the predicted probability of injury has been performed for a variety of simulated shock exposures (Morrison et al., 1999). Exposure to WBV of 0.63 $m{\cdot}s^{-2}$ rms with 32 shocks of 0.3 g and 0.6 g every 5 minutes results in a probability of injury of 1% after 10 years of daily exposure. Increasing the shock amplitudes to 0.5 g and 1.0 g elevates risk of injury to 11%, while 2.0 g shocks at the same rate (rms =1.6 $m{\cdot}s^{-2}$) results in an injury risk of 95% after only 1 year. By comparison exposure to steady state WBV of 1.6 $m{\cdot}s^{-2}$ rms results in an injury risk of 52% after 10 years of daily exposure. This increase in predicted degenerative injury as WBV increases from 0.63 $m{\cdot}s^{-2}$ to 1.6 $m{\cdot}s^{-2}$ is consistent with the epidemiological literature for WBV exposure (Wikström et al., 1994). However, the further increase in injury risk due to repeated shocks is not well defined by current assessment measures.

While more complex to implement than the frequency weighting filters and VDV or MTVV of ISO 2631-1 (1997), the current power of computers allows for greater complexity in computational approaches to the analysis of exposure to repeated mechanical shock.

4. REFERENCES

Allen, G. (1977) Human tolerance of repeated shocks. Proceedings of the European Space Agency Life Sciences Research in Space, Germany, pp 343-349.

ASCC (1982) Human tolerance to repeated shock. ASCC Advisory Publication 61/25, Air Standardization Coordinating Committee.

Hutton, W., and Adams, M.A. (1982) Can the lumbar spine be crushed in heavy lifting? Spine Vol 7, No 6, pp 586-590.

ISO 2631-1 (1997) Mechanical vibration and shock – Evaluation of human exposure to whole-body vibration – Part 1: General Requirements. International Organization for Standardization, Geneva, Switzerland.

Morrison, J. et al. (1997) Development of a standard for the health hazard assessment of mechanical shock and repeated impact in army vehicles – Phase 5. U.S. Army Aeromedical Research Laboratory, Contract No. DAMD17-91-C-1115.

Morrison, J., et al. (1999) A biomechanical approach to evaluating the health effects of repeated mechanical shocks. Models for Aircrew Safety Assessment: Uses, Limitations and Requirements, NATO, RTO-MP-20, pp 24-1 to 24-8.

Nicol, J., et al. (1997) Modelling the dynamic response of the human spine to shock and vibration using a recurrent neural network. Heavy Vehicle Systems, Special Series, International Journal of Vehicle Design, Vol. 4, Nos 2-4, pp. 145-165.

Payne, P. (1978) Method to quantify ride comfort and allowable accelerations. Aviation Space and Environmental Medicine, Vol. 49, pp 262-269.

Sandover, J. (1986) Vehicle vibration and back pain. AGARD conference proceedings No. 378, NATO, pp 13-1 – 13-8.

Wikström, B-O., et al. (1994) Health effects of long-term occupational exposure to whole-body vibration: A review. International Journal of Industrial Ergonomics, Vol. 14, pp 273-292.

Sound Transmission Loss of Insulating Complex Structures

Sebastian Ghinet and Noureddine Atalla
Department of Mechanical Engineering, Université de Sherbrooke, Boul. Université, Sherbrooke, Quebec, Canada J1K 2R1

1. INTRODUCTION

Analytical and numerical modeling of the structural vibration and acoustic phenomena are essential tools in the design work of aeronautical, automotive or architectural fields. Being easier to use and faster, the analytical models are sometimes preferred to the numerical models. In spite of these qualities, the use of the analytical models is limited to the study of simple geometrical configuration; For instance, the wave approach used in the context of laterally infinite structure is very difficult to extend and implement for complex structures.

In this paper the Transfer Matrix Method (TMM) is extended to handle the transmission loss of finite stiffened and orthotropic structures lined by porous materials in a multi-layered configuration. The effects of curvature, stiffeners and heterogeneity are considered. The developed model is easily adaptable to multi-layer configurations. Moreover, the condition of fast convergence towards the solution remains a priority.

2. THE EFFECT OF THE FINITE SIZE STRUCTURE

In a recent paper [1], the radiation efficiency and the transmission index of laterally finite plane structures are evaluated by a spatial windowing method. The authors [1] show that the transmission index of the finite size structure τ_{finite} can be expressed according to the transmission index of the infinite structure $\tau_{infinite}$ corrected by a factor :

$$\tau_{finite}(\theta, \varphi) = \tau_{infinite}(\theta, \varphi)\,[\sigma\,(k_0 \sin\theta, \varphi)\cos\theta]^2\,; \qquad (1)$$

where, θ is the plane wave incidence angle, φ the propagation direction of the structural wave, k_0 the acoustic wave number and σ the non-resonant radiation efficiency. The non-resonant radiation efficiency does not depend on the properties of the structure but only on its side dimensions. The transmission index of a laterally finite multi-layered structure can be estimated using the same correct factor $[\sigma\,(k_0 \sin\theta, \varphi)\cos\theta]^2$. Thus for a given triplet ($k_0 \sin\theta$, φ) the radiation efficiency must be evaluated. This evaluation necessitates a triple integrals on θ, φ and k. This process is numerically expensive which makes the method less attractive.

In the following a variant approach for calculating the non-resonant radiation efficiency is presented. This method is based on a direct semi-analytical evaluation of the radiation impedance of the structure. The radiation efficiency of a structure is defined as the ratio of the averaged sound power radiated by the structure and the sound power radiated by a piston having the same surface and same quadratic velocity as the structure. Lets consider the radiation efficiency of the finite baffled plate structure as:

$$\sigma = \frac{\Re e(Z)}{\rho_0 c_0 S}\,; \qquad (2)$$

where, ρ_0 is the air density and c_0 the sound speed in air; S is the plate aria and Z the radiation impedance given by:

$$Z = j\rho_0\omega \int_0^a\int_0^b\int_0^a\int_0^b W_n(x,y)G(x,y,x',y')W_n^*(x',y')dxdydx'dy'\,; \qquad (3)$$

where, a and b are respectively the length and the width of the piston, W_n is the displacement field of the plate and G the Green function expressed as:

$$W_n = e^{-j(k_p x\cos\varphi + k_p y \sin\varphi)}\,; \qquad (4)$$

$$G(x,y,x',y') = \frac{e^{-jk_0 R}}{2\pi R}\,; \qquad (5)$$

where, $R = \sqrt{(x-x')^2 + (y-y')^2}$ and k_p is the structural wave number.

After three different changes of variables one can write the radiation impedance as:

$$Z_{mnpq} = j\rho_0\omega \frac{ab^2}{4\pi}\int_{-1}^{1}\int_{-1}^{1}(1-u)(1-u')K(u+1,u'+1)F_n(u+1,u'+1)dudu'\,; \qquad (6)$$

where,

$$K(u,u') = \frac{e^{-j\frac{k_0 a}{2}\left[u^2+\frac{u'^2}{r^2}\right]^{1/2}}}{\left[u^2+\frac{u'^2}{r^2}\right]^{1/2}}; \tag{7}$$

and

$$F_n(u,u') = e^{-j\frac{k_p a}{2}\left[u\cos\varphi+\frac{u'}{r}\sin\varphi\right]}. \tag{8}$$

The expression of the radiation impedance (6) is now easily integrated using Gauss numerical integration scheme.

3. CURVATURE EFFECT

To model the effect of curvature the model of Donnell for shells is used [2]. In this context, the displacement field of the shell respects the assumptions of Love-Kirchhoff but takes account of the effect of curvature (radius of the cylinder R). Using these assumptions and the method of minimum potential energy the dynamic equilibrium equations of the shell are found. The nontrivial solution to this equations system leads to the dispersion relation (9), while the particular solution allows the writing of the acoustical impedance of the shell (10) :

$$k_s = \frac{m_s\omega^2}{D}\sqrt[4]{1-\frac{\omega_r^2}{\omega^2}\cos^4\varphi} \tag{9}$$

$$Z_s = jm_s\omega\left[\frac{k_s^4}{k_p^4}-\frac{k_0^4}{k_p^4}\cos^4\theta\right] \tag{10}$$

where, k_s is the structural wave number of the shell, m_s is the mass per unit area of the shell, ω_r the ring frequency of the shell, ω the circular frequency and k_p the wave number of the plate having the same side dimensions and thickness as the shell ($R\to\infty$). The relation (10) is similar to the acoustical impedance proposed by Koval [3] when the shell internal pressure and the external airflow excitation are neglected.

4. RESULTS AND CONCLUSIONS

The case of a finite (L_x=1.4m, L_y=1.1m, h=15mm) gypsum plate (E=2.5GN/m^2; ρ=690kg/m^3; ν=0.1; η=5%) is considered in order to valid the new approach. The structural averaged radiation efficiency is computed firstly by the Leppington [4] model and compared to the new approach (figure 1); the same results are obtained in both cases.

The second case presented (figure 2) show the transmission loss of an aluminum plate (L_x=1.4m; L_y=1.1m; h=1.1mm; E=70GN/m^2; ρ=2700kg/m^3; ν=0.33; η=1%). The two models are compared with the experimental data and the law mass. Note that, for the transmission loss computation by the new approach, just the radiating field are windowed.

ACKNOWLEDGEMENTS

The authors would like to thank NSERC, IRSST and Bombardier Aerospace for their financial support.

BIBLIOGRAPHY

1. M. Villot, C. Guigou, L. Gagliardini " Predicting the acoustical radiation of finite size multi-layered structures by applying spatial windowing on infinite structures ", *Journal of Sound and Vibration*, Vol. 245, No. 3, Aug 2001, pp. 433-455.
2. A.W. Leissa "Vibration of shells", NASA SP-288, 1973.
3. L.R. Koval "Effect of air flow, panel curvature, and internal pressurization on field-incidence transmission loss", JASA, Vol. 59, No. 6, June 1976.
4. F.G. Leppington "The acoustic radiation efficiency of rectangular panels", Proceedings of the Royal Society of London, A 382, 245-271 (1982)

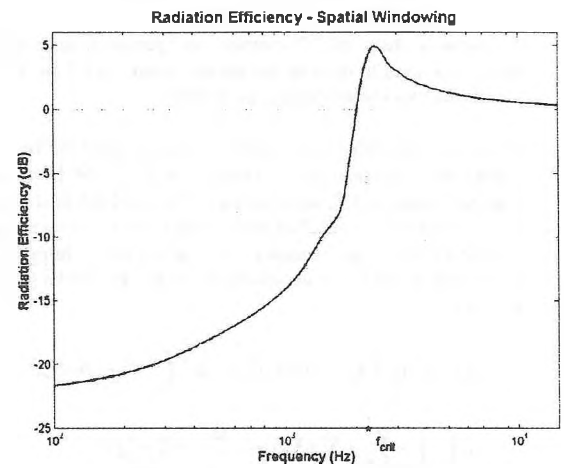

Figure 1. Radiation Efficiency for a simple gypsum plate [1] (—Leppington model, - - - Presented approach)

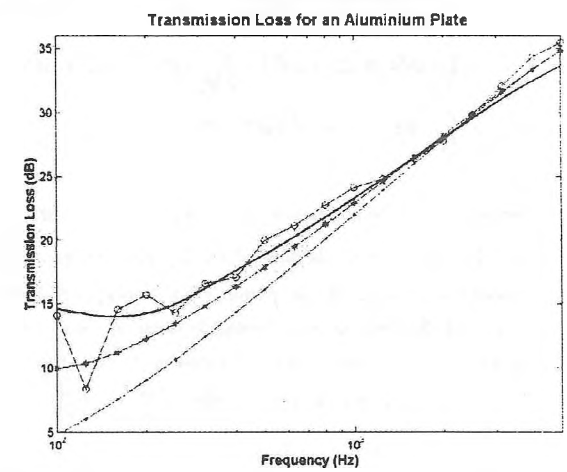

Figure 2. Transmission Loss for an aluminum plate [1]: —o— Experimental Data, — Villot and all. model, —*—New approach, —•— Infinite plate – non windowed)

The Vibro-acoustics of a Plate-Backed cavity with Non-Homogeneous Porous Materials

C. K. Amedin*, N. Atalla* and F. Sgard**
*Department of Mechanical Engineering, Université de Sherbrooke, Boul. Université, Sherbrooke, Quebec, Canada J1K 2R1
** LASH, Entpe, Rue Maurice Audin 69518 Vaulx-en-Velin, Cedex, France

1. Introduction

Various studies are performed recently to improve the acoustic performance of porous materials, which is very poor in low frequencies. Most of these studies investigate 3-D complex configurations with the finite element method. The present study presents results which indicate that use of heterogeneous material is a probable way to increase the acoustic performance. A heterogeneous material can be obtained by inclusion of elastic patches or air pockets in a homogeneous porous material. Accurate models are presented to take account of various domains (porous, fluid and elastic), and multilayer configurations are used to illustrate the advantages of a heterogeneous porous material.

2. Theoretical background

To allow a study of 3D complex configurations, finite element models are used to describe the porous, elastic and fluid domains which make up a heterogeneous multilayer.

The model associated to the porous media is based on the mixed displacement-pressure (u, p) formulation [1, 2] of Biot's poro-elasticity equations [3], which considers the solid and fluid phase of a porous material. A modified weak integral form of these equations is used to depict the boundary terms in a suitable form for the application of the coupling conditions with other media [4]. This modified form is:

$$\begin{aligned}
&\int_{\Omega_p} \underline{\underline{\hat{\sigma}}}^S(\underline{u}) : \underline{\underline{\varepsilon}}^S(\delta \underline{u})\, d\Omega - \omega^2 \int_{\Omega_p} \tilde{\rho}\, \underline{u} \cdot \delta \underline{u}\, d\Omega \\
&+ \int_{\Omega_p} \left[\frac{\phi^2}{\omega^2 \tilde{\rho}_{22}} \underline{\nabla} p \underline{\nabla} \delta p - \frac{\phi^2}{\tilde{R}} p \delta p \right] d\Omega \\
&- \int_{\Omega_p} \frac{\phi^2 \rho_0}{\tilde{\rho}_{22}} \delta(\underline{\nabla} p \cdot \underline{u})\, d\Omega \\
&- \int_{\Omega_p} \phi \delta(p \cdot \mathrm{div}\underline{u})\, d\Omega - \int_{\partial\Omega_p} (\underline{\underline{\tilde{\sigma}}}^t \cdot \underline{n}) \cdot (\delta \underline{u})\, dS \\
&- \int_{\partial\Omega_p} \phi (U_n - u_n) \delta p\, dS = 0
\end{aligned}$$

where Ω_p is the porous domain, $\delta\Omega_p$ is the boundary surface of Ω_p, $\underline{u}$ and p are the solid phase displacement vector and the interstitial pressure of the porous-elastic medium, respectively; $\delta \underline{u}$ and δp refer to their admissible variation, respectively; $\underline{n}$ denotes the unit normal vector external to the bounding surface; $\underline{\underline{\varepsilon}}^S$ is the strain tensor of the solid phase; $\underline{\underline{\tilde{\sigma}}}^S$ and $\underline{\underline{\tilde{\sigma}}}^t$ are the *in vacuo* stress tensor and the total stress tensor of the material, respectively; U_n and u_n refer to the normal component of the solid and fluid macroscopic displacement vectors, respectively; h stands for the porosity of the material; ρ_0 is the air density, and $\tilde{\rho}$ and $\tilde{\rho}_{22}$ are specific mass coefficients [3]; $\tilde{R}$ refers to the bulk modulus of the air occupying a fraction ϕ of a unit volume aggregate; and ω is the angular frequency. In this weak form, the boundary terms are written in terms of the total stress tensor and the net flow. These terms are always continuous at the boundary which simplifies the coupling of porous domain with fluid or elastic domain.

The model associated to the elastic domain is based on the following weak integral form:

$$\begin{aligned}
&\int_{\Omega_e} \left(\underline{\underline{\sigma}}^e(\underline{u}^e) : \underline{\underline{\varepsilon}}^e(\delta \underline{u}^e)\, d\Omega - \rho_s \omega^2 \underline{u}^e \cdot \delta \underline{u}^e \right) d\Omega \\
&- \int_{\partial\Omega_e} \delta \underline{u}^e \cdot (\underline{\underline{\sigma}}^e(\underline{u}^e) \cdot \underline{n})\, dS = 0
\end{aligned}$$

where $\underline{\underline{\sigma}}^e$ and $\underline{\underline{\varepsilon}}^e$ are the structure stress and strain tensors; Ω_e, and $\delta\Omega_e$ are the structural domain and its boundary; ρ_S is the structure density; $\underline{u}^e$ is the structural displacement vector, and $\delta \underline{u}^e$ refers to an arbitrary admissible variation of $\underline{u}^e$. The volume integral of the weak form represents the sum of the work done by internal and inertial forms, and the surface integral is the virtual work done by external forces applied on the surface. This weak form is also associated to a septum (screen), if the stiffness term is neglected.

For a fluid domain, the finite element formulation is based on the following weak integral form:

$$\begin{aligned}
&\int_{\Omega_f} \left(\frac{1}{\rho_0 \omega^2} \underline{\nabla} p \underline{\nabla} \delta p - \frac{1}{\rho_0 c_0^2} p \delta p \right) d\Omega \\
&- \frac{1}{\rho_0 \omega^2} \int_{\partial\Omega_f} \frac{\partial p}{\partial n} \delta p\, dS = 0
\end{aligned}$$

where Ω_f and $\delta\Omega_f$ refer to the fluid domain and its boundary; p is the acoustic pressure in the fluid medium, and δp refers to an arbitrary admissible variation of p; ρ_0 and c_0 are the fluid medium density and the sound speed in the medium, respectively. The volume integral of the weak form represents the sum of the work done by internal and inertial forms, and the surface integral is the virtual work due to an imposed motion on the surface.

These different weak integral forms are used to build an accurate finite elements code to predict and analyze the acoustic performance of multilayers composed from elastic, porous and fluid domains. Various vibro-acoustics indicators cans be calculated for this analyze. Examples include the dissipated powers by domain, and quadratic pressure or quadratic velocity.

3. Results

Multilayer configurations are proposed here to show the acoustic performance of a heterogeneous porous material. The basic configuration consists of a plastic foam coated aluminum plate backed by an air filled cavity. The studied configurations are variant of this basic configuration, by addition of air pockets or elastic patches in the porous layer. Each configuration can be excited by a normal , oblique wave plane, or by a diffuse field, The mean quadratic pressure in the cavity is used as an acoustic indicator. The plate is in 5 mm thick, the foam is a 5.08 cm thick and the cavity is 50 cm deep. The lateral dimensions of the multilayers are 80 cm and 60 cm.

Figures 1 compares the mean quadratic pressure in the cavity, between the basic configuration and configurations where air pockets are randomly distributed in the porous layer. The configurations are excited by an oblique plane wave. It is noted that there is no significant reduction of the mean quadratic pressure in the cavity, when air pockets occupy 10 % or 20 % of the porous volume. Reduction is perceptible only at frequencies greater than 350 Hz. However, these cases are interesting because they indicate that a diminution of the weight (by insertion of air pocket) do not alter the acoustic performance.

Figures 2 illustrates the comparison between the basic configuration and others configurations where elastic patches are randomly included in the homogeneous domain, with an oblique plane wave excitation. In these cases, a significant reduction of the mean pressure is noted at low frequencies. It appears that insertion of 3 % of lead gives better acoustic efficiency that 20 % of aluminum. The result is particularly interesting since 3 % of lead is equivalent to 17 kg/m2 of mass added to the basic configuration, while 20 % of aluminum gives 27 kg/m2 of added mass. Nevertheless, it is still preliminary to say if the obtained improvement justifies the added mass.

Conclusion

The effects of insertion of air pocket or elastic patches in a homogeneous porous domain are studied in this project. The different domains are modeled by using of accurate finite elements methods. The study reveals that the addition of air pockets doesn't deteriorate the acoustic performance, but leads to a reduction of the weight of the configuration. On the other hand, an increase of the acoustic performance is obtained by insertion of elastic patches, but this comes with an increase of the configuration weight.

References

[1] R. Panneton and N. Atalla, «An efficient finite element scheme for solving the three dimensional poroelasticity problem in acoustics», J. Acoust. Soc. Am. 101, 3287--3298 (1997).

[2] N. Atalla, R. Panneton, and P. Debergue, «A mixed displacement-pressure formulation for poro-elastic materials», J. Acoust. Soc. Am. 104, 1444--1452 (1998).

[3] J.-F. Allard, «Propagation of sound in porous media, Modelling sound absorbing materials», New York, London: Elseivier Application Science (1993).

[4] N. Atalla, M.A. Hamdi, R. Panneton, "Enhanced weak integral formulation for the mixed (u,p) poroelastic equations", J. Acoust. Soc. Amer., 109(6), 3065-3068, 2001.

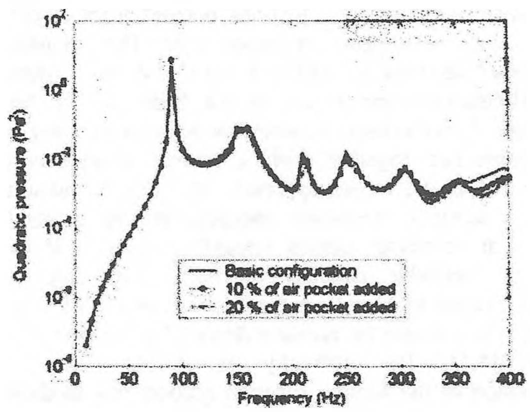

Figure 1. Effects of inclusion of air pocket s in homogeneous porous domain.

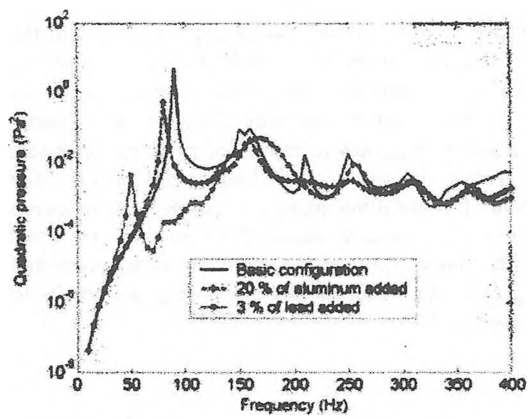

Figure 2. Effects of inclusion of elastic patches in homogeneous porous domain.

Eigenfrequency Extraction Based on Boundary Element Method

Z. Zhang and S. T. Raveendra
Global Product Development Division, Collins & Aikman Corporation, Plymouth, Michigan 48170, USA.

1. INTRODUCTION

Acousitc eigenfrequencies are important in many applications. A widely used computational simulation technique for the analysis of acoustic problems is boundary element method. However, the use of the boundary element method for the extraction of eigenfrequencies is not as widespread since the techniques available are not very effective for the solution of problems with complex geometry and boundary conditions.

In general, two approaches are used for the extraction of acoustic eigenfrequencies by boundary elment method. In the first approach, a determinant search method (DSM) is used to solve a system of equations derived from forced response analysis integral equation [1,2]. The solution process based on DSM is inefficient and also difficult when the eigenfrequencies are closely spaced. Subsequently, the computational inefficiency is somewhat reduced by using a DSM approached together with a matrix interpolation technique [3]. In the second approach, an integral equation is derived using a frequency independent fundamental solution. The resulting domain integral is eliminated by using the particular solution of the inhomogeneous differential equation based on the approximation of the forcing function within the acoustic domain by interpolation functions [4,5]. The difficulty associated with the approximation of the forcing function renders this method not so useful in the solution of problems with complex geometry.

An alternative approach is developed here by recasting the nonlinear acoustic eigenvalue problem to a standard eigenvalue form through the linear interpolation of boundary element system matrices. That is, the system matrix at a given frequency is expressed in terms of system matrices at two closed spaced frequencies using liner interpolation. The resulting matrix equation is then solved by using readilly available standard eigenvalue extraction routines. The applicability of the technique is demonstrated by solving example problems and comparing the results to alternative solutions.

2. FORMULATION

The indirect boundary integral equation for a homogeneous acoustical cavity with rigid enclosing surface Γ is [6]:

$$0 = \int_{\Gamma} \frac{\partial^2 G}{\partial n_x \partial n_y} \mu^y d\Gamma_y$$

where G is the fundamental solution and μ is the double layer potential. The solution to the above equation can be obtained through the minimization of a functional deroved using variational approach. The resulting sytstem of equations at a frequency f can be expressed in matrix form as

$$[A]\{\mu\} = 0$$

The matrix $[A]$ can be interpolated within a suitable frequency interval in terms of matrices at the end frequencies of this interval. Suppose that the two current end frequencies are f_a and f_b ($f_a < f_b$) and the corresponding system matrices are $[A_a]$ and $[A_b]$, respectively. The linear interpolation between these two frequencies results in the following relations:

$$[A(f)] = [B] - f^* [C] \qquad (f_a \le f \le f_b)$$

where,

$$[B] = \frac{f_b[A_a] - f_a[A_b]}{f_b - f_a}, \quad [C] = \frac{[A_a] - [A_b]}{f_b - f_a}$$

Thus, the eigenvalue problem becomes:

$$\{[B] - f^* [C]\}\{\mu\} = \{0\}$$

where f is the eigenvalue. The eigenvalues are extracted from the above equation using QZ algorithm [7].

3. EXAMPLES

Two example problems are used to illustrate the applicability of the technique developed in the previous section. First, the eigenfrequencies of an acoustical cavity within a generic passenger car cabin are computed. The boundary element mesh of the cavity is shown in Figure 1. The eigenvalues extracted from the present approach (COMET/BEM) are compared to alternatively computed eigenvalues (COMET/FEM) [7] in Table 1. The results from both approaches are in good agreement, although one additional eigenfreuency is found in the present approach. Next, the acoustic eigenfrequencies of a simplified aircabin are computed numerically. The boundary element model for the generic aircabin is shown in Figure 2. The comparison of the eigenfrequencies obtained using two numerical methods (COMET/BEM and COMET/FEM) is shown in Table 2. Again, excellent correlation between the reults is observed.

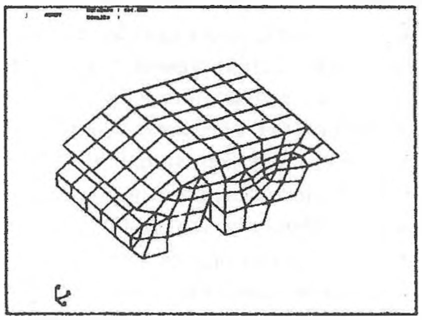

Figure 1. Boundary element model of a generic car cabin

Table 1. Comparison of the car cabin acoustic eigenfrequencies obtained using two numerical methods

COMET/FEM (Hz)	COMET/BEM (Hz)
53.042	52.199
87.167	85.335
102.036	99.931
109.144	108.041
130.818	126.994
139.690	137.373
157.198	153.349
168.645	164.820
–	172.249
182.873	180.735
189.840	186.198
190.410	194.763

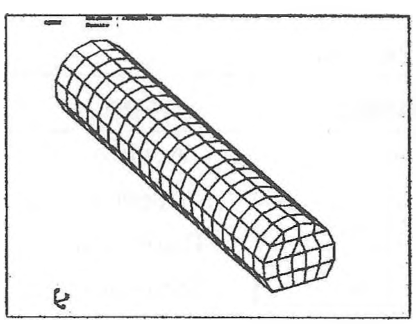

Figure 2. Boundary element model of a simplified aircabin

Table 2. Comparison of the aircabin acoustic eigenfrequencies obtained using two numerical methods

COMET/FEM (Hz)	COMET/BEM (Hz)
11.436	10.612
22.890	22.298
34.379	34.084
45.922	45.232
57.535	57.428
65.623	65.084
66.612	66.323
69.236	68.800
69.501	69.076
74.084	73.931
77.003	75.830
77.849	76.826
80.095	79.483
80.334	81.072
84.374	84.023
87.276	86.055
89.740	89.533
92.978	93.031
95.394	93.723
96.124	95.278

REFERERENCES

[1] G. DeMey, 'Calculation of eigenvalues of the Helmholtz equation by an integral equation method, Int. J. Numer. Methods Eng., 10, 55-667, 1976.

[2] G. Tai and R. P. Shaw, Helmholtz equation eigenvalues for arbitrary domains, J. Acoustc. Soc. Am.,56, 796-804, 1979.

[3] S. T. Raveendra, A Technique for extracting natural frequencies of acoustical cavities, Noise-CON98, Ypsilanti, Michigan, 643-648, 1998.

[4] P. K. Banerjee, S. Ahmad and H. C. Wang, 'A new BEM formulation of the acoustic eigenfrequency analysis, Int. J. Numer. Methods Eng., 26, 1299-1309, 1988.

[5] S. T. Raveendra and P. K. Banerjee, Polynomial particular solutions based on boundary element analysis of acoustic eigenfrequency problems, Int. J. Numer. Methods Eng., 35, 1787-1802, 1992.

[6] S. T. Raveendra , An efficient indirect boundary element technique for multi-frequency acoustic analysis, Int. J. Numer. Methods Eng., 44, 59-76, 1999.

[7] G. Golub and C. Van Loan, Matrix Computations, The Johns Hopkins University Press, Baltimore, Third Edition, 1996.

[8] COMET/Acoustics User Document, Version 5.0, Collins & Aikman Corporation, Plymouth, Michigan, 2001.

On the Use of the Auditory Pathway for Comprehending Complex Engineering Concepts

Hans Kunov
Institute of Biomaterials and Biomedical Engineering, and The Edward S. Rogers Department of Electrical and Computer Engineering, University of Toronto

Introduction

The auditory pathway constitutes an underused means of learning in the classroom. For a number of years, I have used appropriately designed sound files in an acoustics course, and found the effect on student learning very positive. Acoustics is, of course, a "natural" for the use of sound files, and students reported that the experience was both enjoyable and very useful.

Given this, albeit subjective, success, we speculated that the auditory system could be engaged more effectively in the learning of concepts not directly associated with acoustics. I wanted to test this in a rigorous way, and designed an experiment that would allow us to answer that question.

Hypothesis

In order to gain more qualitative information, we tested the following hypothesis:

The use of appropriate auditory/visual demonstrations improves the comprehension of a number of important signal processing concepts.

Methodology

Eight 20-minute long modules were developed on separate (and not interrelated) topics. The eight modules were chosen such that half were more theoretical, and half were more advanced. Sliced differently, half were on an introductory level, and half advanced. Finally half were natural candidates for acoustic demonstrations, the other half not. Each of the eight modules is a unique combination of those three dimensions see Table 1 below.

Volunteers were recruited from the undergraduate population in the engineering faculty, and were asked to sign a consent form, approved by the University's Ethics Review Board. The recruitment lecture explained the purpose and method of the experiment, and contained a sample module. During the following four weeks, a rigid presentation schedule was followed: In a given week, a set of two modules was presented during one lecture on two occasions. On the first occasion, Module A was presented with sound files, and Module B without. On the second occasion, A was without sound files, and B with sound. Otherwise the modules were identical. A given student would attend only one of the two lectures in a given week. Questions from the class, relating to the material, during and after the presentations were discouraged. After each module, a simple four-question multiple-choice quiz was administered. Each question had five alternative choices. Chance performance is therefore 20%. Answer sheets requested information about previous exposure to the material taught in the module, and the student's year and program of study.

The fifth and last set of lectures consisted of a retention quiz of all eight modules in the same format that was used in the preceding four weeks, plus a brief entertaining module on auditory illusions, included to ensure good attendance.

Results

The experiment ran in September and October 2000. A total of 33 students attended the two recruitment lectures, and an average of 11.1 students attended each of the eight sessions. The sessions were scheduled for Tuesdays and Thursdays 12:00 noon to 1:00 p.m., and light refreshments were available at all sessions.

Table 1: Modules can be classified along three dimensions

Module	Level	A priory suitability	Type
Convolution	Introductory	Not natural for acoustics	Applied
Fourier	Introductory	Natural for acoustics	Applied
Sampling	Introductory	Natural for acoustics	Theoretical
Taylor	Introductory	Not natural for acoustics	Theoretical
Dispersion	Advanced	Not natural for acoustics	Theoretical
FIR vs. IIR	Advanced	Natural for acoustics	Theoretical
Quantization	Advanced	Not natural for acoustics	Applied
ModulationTransfer Fct.	Advanced	Natural for acoustics	Applied

Quiz		Retention test	
No sound	With sound	No sound	With sound
0.713	0.755	0.611	0.583

Table 2: Overall performance (all modules taken together): Average mark out of 1.00, chance performance = 0.200

The overall result is shown in Table 2. Here the average mark is shown for all modules taken together. We notice that in the quiz at the end of the teaching module, sound files have a moderate positive effect: The average mark went from 0.713 to 0.755. On the other hand, the average mark was slightly lower (0.583 vs. 0.611) in the retention test for those students exposed to sound files.

The data was also broken down according to the classification shown in Table 1 above. The result is shown in the bar graph in Figure 1.

In order to determine the effect of sound files on retention, we subtracted the average scores on the retention tests from the average scores on the quiz administered immediately after the module was taught. The result is shown in Figure 2.

Conclusion

The results shown here do not support the hypothesis that learning is enhanced by the introduction of relevant sound files, although there is a slightly positive correlation between student performance immediately after the material was taught and the presentation of appropriate sound files. Retention seems to actually suffer from the presence of

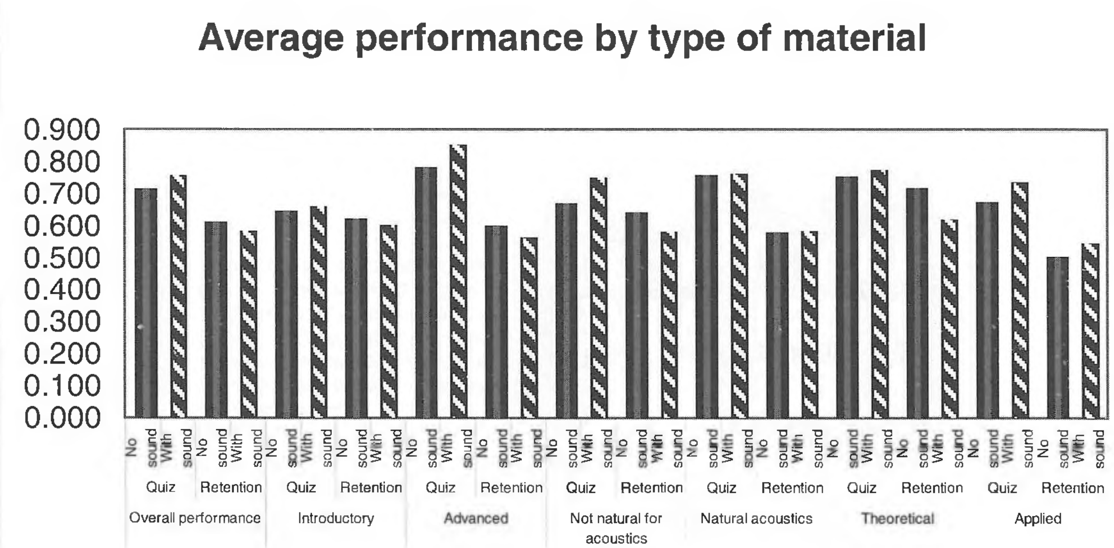

Figure 1: Performance on different classes of material, by quiz vs. retention test, and no sound vs. with sound

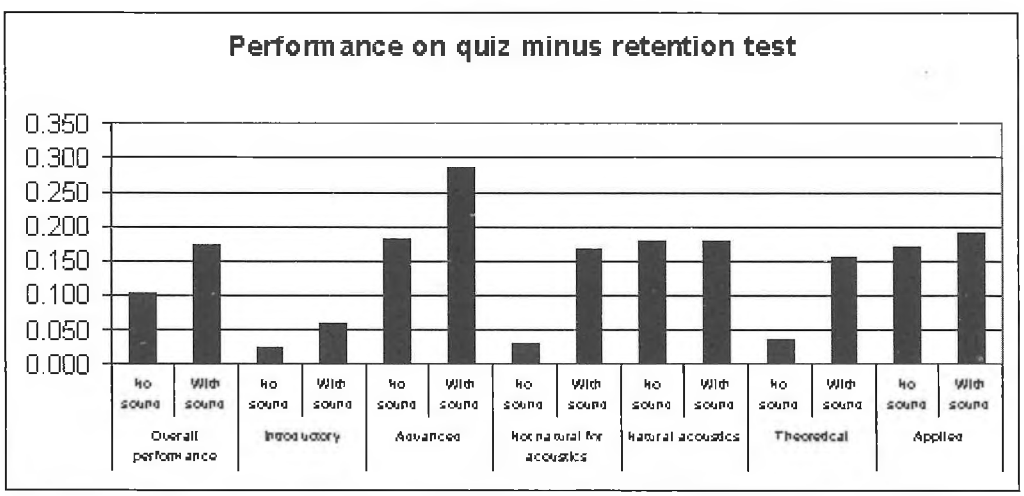

Figure 2: Effect of sound files on retention: Average quiz mark minus average retention test mark on different caluses of material.

sound files. This is a surprising outcome, given the intuitive appeal of sound files in teaching complex concepts, as well as the written comments provided by students throughout the experiment.

We were exceptionally careful to avoid undue bias in the work, including being fully aware of the effect on "professorial enthusiasm" in the classroom.

Bibliography

URL: http://www.ecf.utoronto.ca/~p2k/

Note

The University of Toronto Ethics Review Board approved the research reported in this paper.

Acknowledgements

This work was supported by a grant from the Academic Priorities Fund, and the Edwards S. Rogers Department of Electrical and Computer Engineering, University of Toronto. The following undergraduate students made substantial contributions to the work: Linda Chan, Anthony Fong, Raeid Ishoop, Cumily Lai, Alan Poon, Adam Robson, Vanda Tong. Katrine Jørgensen helped with the data analysis.


ENGINE TEST FACILITY


ECKOUSTIC FUNCTIONAL PANELS

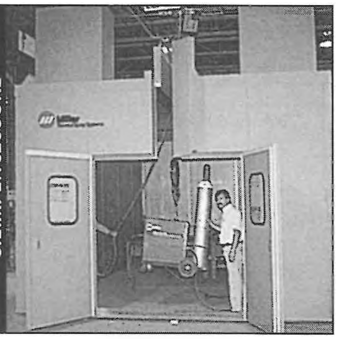
O.E.M. ENCLOSURE

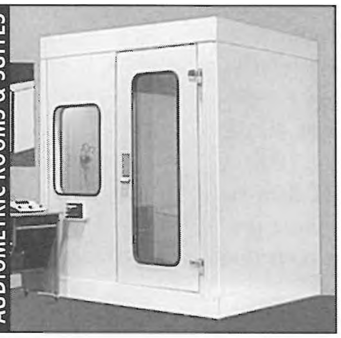
AUDIOMETRIC ROOMS & SUITES

SOUND SOLUTIONS FOR THE FUTURE


ARCHITECTURAL ACOUSTICS

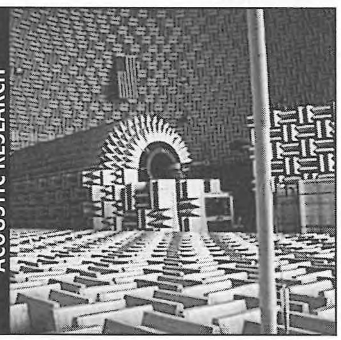
ACOUSTIC RESEARCH

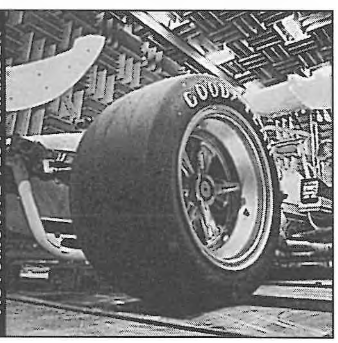
AUTOMOTIVE TEST CHAMBER

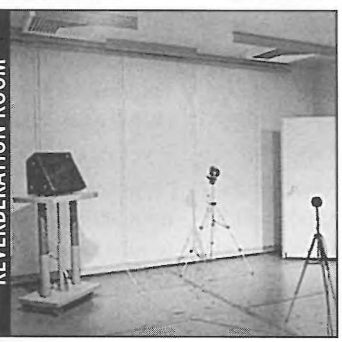
REVERBERATION ROOM

LOUDNESS ENCODING AT THE AUDITORY NERVE

[a]Elad Sagi, [ab]Kenneth H. Norwich and [c]Hans Kunov
Sensory Communications Group, Institute of Biomaterials and Biomedical Engineering
Departments of [a]Physiology and [b]Physics and [c]Department of Computer and Electrical Engineering, University of Toronto

The 'sone' scale developed by Stevens (1956) describes the rate at which loudness grows with sound level. Using a method of magnitude estimation, human participants were required to quantify the loudness of a stimulus tone relative to a reference tone of some fixed level and frequency (or frequencies). For example, a 1 kHz reference tone at 40 dB SPL was assigned an arbitrarily scaled value of, say, 100. A 1 kHz stimulus tone deemed twice as loud would then be assigned a value of 200. After all stimulus tones were presented, the assigned values were then normalized such that the reference tone was given a value of 1 'sone'.

A full logarithmic plot of loudness (in sones) against sound level (in dB) yields a curve that is linear over much of its extent. The slope of the linear portion of this curve gives the loudness exponent, n, which describes the rate at which loudness grows with sound level. That is, the relationship between loudness, L, and sound level, I, is approximately

$$L \propto I^n \tag{1}$$

where sound level is represented here as a linear measure.

The loudness exponent, n, is characteristic of the stimulus frequency (or frequencies) used for experimentation and varies from about 0.3 for 1 kHz tones to greater than 0.4 for pure tones of higher and lower frequencies. Whereas the 'Loudness function' in Equation (1) holds true for the human perceiver, we are interested in the extent to which this relationship is reflected at the auditory nerve.

In response to a tone stimulus of constant sound level, the stereocilia of a given inner hair cell within the cochlea become deflected resulting in a depolarization of the cell's receptor potential followed by the release of neurotransmitter. Approximately 20 auditory nerve fibers synapse onto this hair cell, each of which produce action potentials at a rate proportional to the amount of neurotransmitter release (Slepecky, 2000). The initial rate of neural firing, however, does not persist. For the duration of the stimulus, the neural response peaks immediately after onset of the tone and is followed by a component that adapts rapidly to a steady state.

As the sound level of the stimulus tone is increased, both the onset and steady state firing rates will become larger, but tend to saturate at higher intensities depending on the spontaneous rate of the nerve fiber. This feature is demonstrated in Figure 1, adapted from Smith (1979). Firing rate was measured from a single fiber of the auditory nerve in the Mongolian gerbil in response to a 50 Hz narrow-band stimulus of constant sound level centered around the characteristic frequency of the fiber at 1.86 kHz.

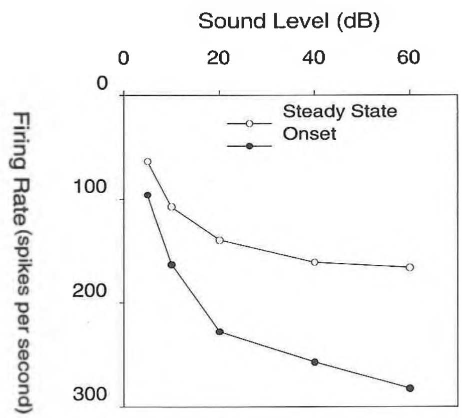

Figure 1

Neither the onset nor the steady state firing rate displays the necessary growth with sound level that would be characteristic of the loudness function. Similarly, Relkin and Doucet (1997) found that a gross measure of neural firing in the form of a perstimulus compound action potential taken from the chinchilla auditory nerve also does not demonstrate the required growth. That is, loudness is not simply proportional to the auditory nerve spike count.

Individual units of the mammalian auditory nerve fall into three categories, depending on their spontaneous firing rate. Units of high, medium and low spontaneous rates respond to low, medium and high sound levels respectively (Liberman, 1978). Hence, one might suggest that sound level is coded by the recruitment of subgroups of fibers in response to increasing sound levels. Nevertheless, if loudness were to be preserved amongst these fibers, each fiber would be required to encode the psychophysical growth of loudness, regardless of the limited dynamic range per fiber.

We propose that in each fiber of the auditory nerve, the loudness of a tone can be represented as an information such that the greater the loudness, the greater the information. Within information theory, information is defined as the difference between the stimulus uncertainty and the stimulus equivocation.

Consider a pure tone stimulus of 'constant' sound level acting on the inner hair cell. On a moment-by-moment basis, the square of the peak amplitude will fluctuate by an amount ΔI about the mean sound level I. That is, the hair cell is presented with a normal distribution of sound level values with a mean of I dB and standard deviation of ΔI dB.

Similarly, the inner hair cell is by no means exact in its ability to detect the instantaneous sound level and will make errors, say by an amount σ dB.

Taken together, ΔI and σ determine the stimulus uncertainty and the stimulus equivocation respectively. Hence, one can calculate the information on a moment-by-moment basis simulating the process through which the inner hair cell samples the stimulus level. Figure 2 is a representative example of the information (in natural units [n.u.]) calculated as a function of the number of trials (or samples) for this process. Characteristically, the information rises to a peak and subsequently falls to an asymptotic value. For a given value of ΔI, the peak and asymptotic values are completely determined by σ.

We propose that the calculated information is proportional to the firing rate one would observe in a single auditory nerve fiber in response to a constant sound level. Hence, the ratio of onset to steady state firing should equal the ratio of peak to asymptotic information.

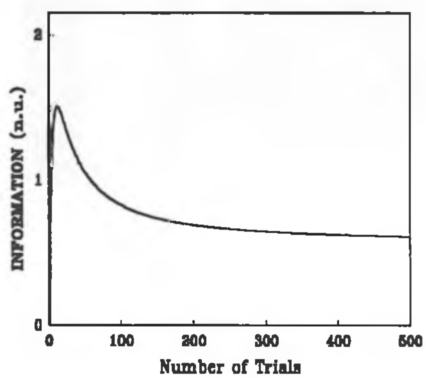

Figure 2

By way of example, let us use the data from Figure 1. At each stimulus level, one can calculate the ratio of onset to steady state firing rate. Using these ratios, one can generate the corresponding information curves.

First, however, we must define the value of ΔI. We suggested above that the hair cell is presented with a stimulus uncertainty measurable in decibels. We simply assume here that $\Delta I = I/2$ dB corresponding to a square root law in linear space.

Using this relationship, one can now determine the values of σ required to generate information curves such that the ratio of peak to asymptotic information corresponds to the ratio of onset to steady state firing rate at stimulus level.

Figure 3 represents a full logarithmic plot of variance, i.e. σ^2, against ΔI (already a logarithmic measure). Notably, the slope of the straight line is measured at 0.34 corresponding to the loudness exponent of Equation 1.

Hence, in every auditory nerve fiber, the loudness becomes encoded in the error intrinsic to the fiber as it samples the sound level of the stimulus tone.

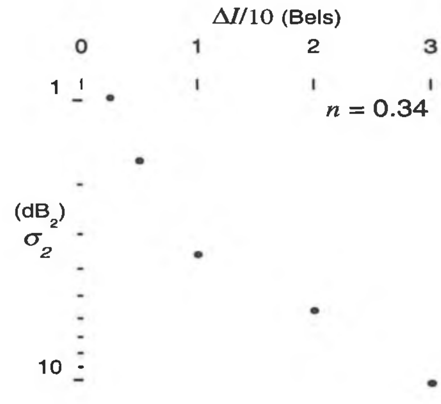

Figure 3

Liberman, M. C., (1978). Auditory-nerve response from cats raised in a low-noise chamber. *Journal of the Acoustical Society of America*, **63**, 442-455.

Relkin, E. M. & Doucet, J. R. (1997). Is loudness simply proportional to the auditory nerve spike count? *Journal of the Acoustical Society of America*, **101**, 2735-2740.

Slepecky, N. B., Galsky, M. D., Swartzentruber-Martin, H., Savage, J. (2000). Study of afferent nerve terminals and fibers in the gerbil cochlea: distribution by size. *Hearing Research*, **144**, 124-134.

Smith, R. L. (1979). Adaptation, saturation, and physiological masking in single auditory-nerve fibers. *Journal of the Acoustical Society of America*, **65**, 166-178.

Stevens, S. S. (1956). The direct estimation of sensory magnitudes-loudness. *American Journal of Psychology*, **69**, 1-25.

Modelling The Mechanics Of The Coupling Between The Incus And Stapes In The Middle Ear

Siah T. Heng and W. Robert J. Funnell
Depts. BioMedical Engineering & Otolaryngology, McGill University, Montréal, QC, Canada H3A 2B4

1. INTRODUCTION

The middle ear contains of a chain of three small bones or ossicles (Figure 1): the malleus, the incus and the stapes. Between the long process of the incus and the lenticular process is a tiny bony bridge (pedicle). Although many studies have been done on the mechanics of the ossicles, little is currently known about the function and mechanical behaviour of the pedicle. Therefore, a simple finite-element model which includes the pedicle and the incudostapedial joint was created and used for a preliminary analysis of the mechanics of the coupling between the incus and the stapes.
The model consists of the end of the long process of the incus, the pedicle, the lenticular plate, the joint gap, the joint capsule, and the head of the stapes. The shape and dimensions of the model were based on histological sections of a cat middle ear. Possible values for the Young's moduli of the joint, joint capsule and pedicle were tested under simple static loading conditions to investigate the interaction between the pedicle and the joint.

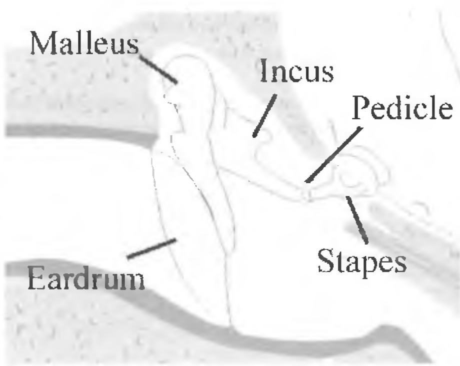

Figure 1: The human middle ear

2. FINITE-ELEMENT MODEL

2.1 Model Geometry

The simple representation of the pedicle and the incudostapedial joint was constructed with several hexahedra as shown in Figure 2(a) and (b). The dimensions of each structure were carefully approximated from the histological sections of a cat middle ear, and are shown in Figure 2(c) and (d). Figure 3 shows two histological sections from different cats. Practically, it is very difficult to keep the tiny pedicle or the incudostapedial joint intact in histological sections.

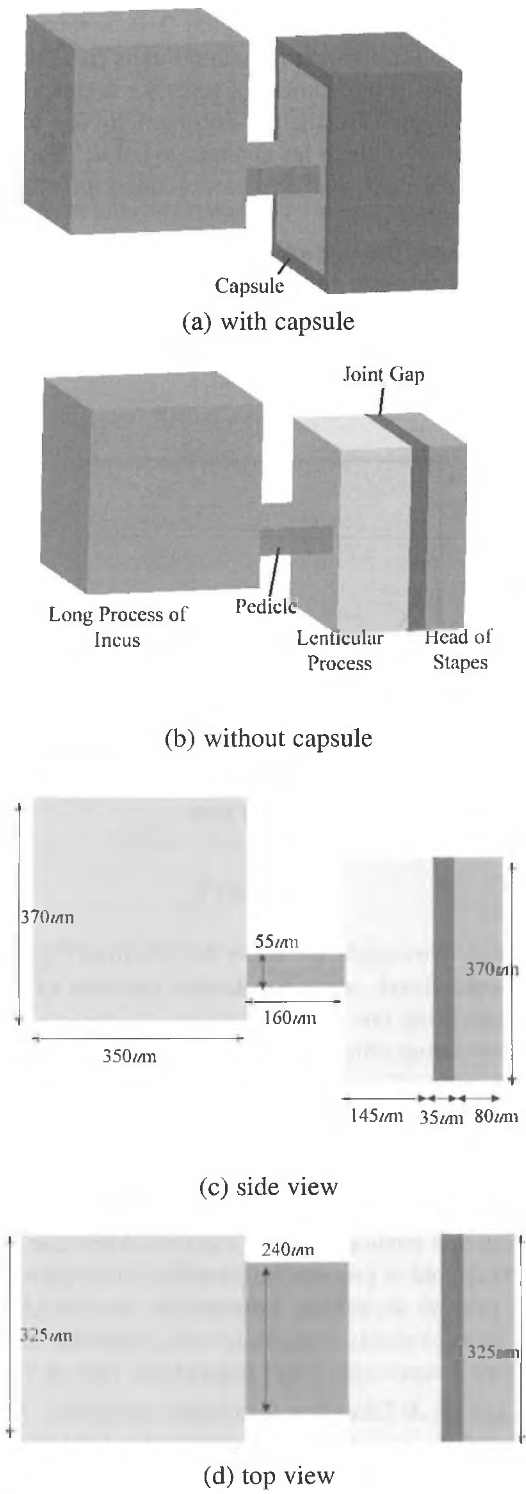

Figure 2: Shape and dimensions of the finite-element model

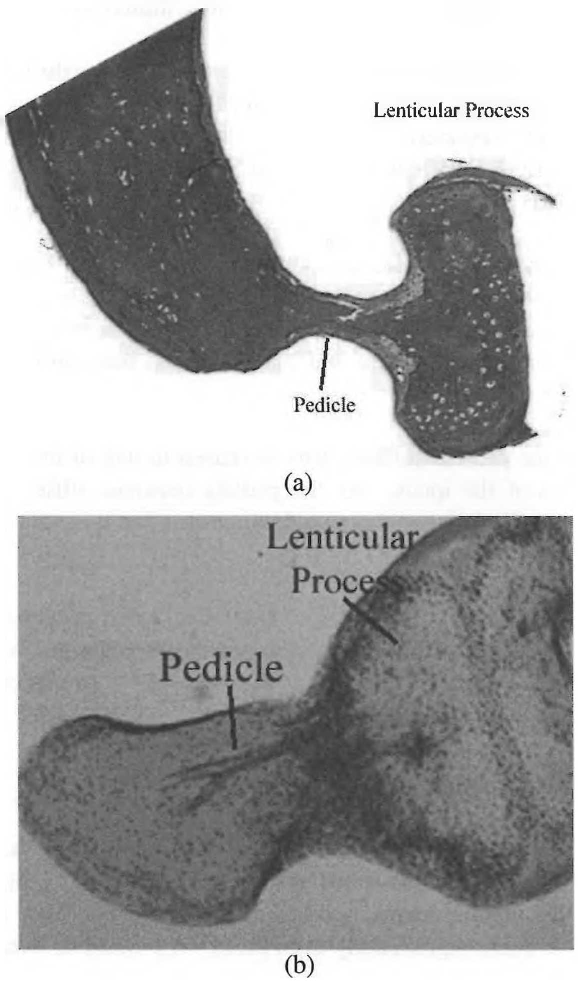

Figure 3: Part of the histological sections of cat middle ear with pedicle in (a) side view; (b) top view.

2.2 Material Properties

The material properties of the model are assumed to be linearly elastic, uniform (i.e., the same in all locations) and isotropic (i.e., the same in all directions). Viscoelastic properties of the biological materials will be ignored in this model for simplicity. The linearity assumption is generally true for small strains under normal hearing conditions.

The material stiffness is expressed as a Young's modulus. Poisson's ratio has been taken to be 0.3.

Pedicle

Evidence from the serial histological sections of the pedicle suggests that it is most likely to be a continuation of bone from the long process of the incus to the lenticular plate. The estimates for Young's modulus for bone may vary from 1 G to 20 G, depending on the nature of the bone, the direction of measurement, and the part of the bone. In this model, a stiffness modulus of 5 GPa is adopted for the pedicle, as measured from small bone specimens directly beneath joint cartilage (Mente and Lewis, 1994).

Joint Gap

The incudostapedial joint is a synovial joint, in which the load is transferred from a cartilage layer on one bone to a cartilage layer on the other bone, either through direct contact, through a thin film of synovial fluid between the layers, or by a mixture of both.

As shown in Figure 2(b), the contacting region in the incudostapedial joint is modelled by a 35-μm-thick articular cartilage. This is based on the assumption that the two articulating surfaces are (at least partially) in direct contact during acoustic vibration. A stiffness modulus of 10 MPa is a fair estimate for cartilage in healthy joint (Elices, 2000), and is adopted for the joint gap in the model.

Capsule

Another key structure in the model is the incudostapedial joint capsule that completely encloses the joint. Figure 2(a) shows that the joint capsule is modelled by introducing an extra 30-μm-thick outer layer surrounding the joint model. To be consistent with the real anatomy of the synovial capsule as observed in the histological sections, only the two ends of the capsule are attached to the bone.

The outer layers of the capsule consist of dense fibrous connective tissue and capsule ligament, which dominate the capsule mechanical properties. Therefore it is possible to apply the value of Young's modulus for capsule ligament to the capsule directly. In this model, a rough estimate of 50 MPa is used as the Young's modulus of the capsule.

Others

The long process of the incus is given a Young's modulus of 12 GPa, corresponding to stiff compact bone. The lenticular process and the head of the stapes may regarded as composite materials, mainly consisting of calcified cartilage ($E \approx 0.32$ GPa) and subchondral bone ($E \approx 5$ GPa) (Mente and Lewis, 1994). Hence an intermediate value of 1 GPa is used as the Young's modulus for the two structures.

2.3 Meshing Considerations

One important question that needs to be addressed in finite-element modelling is how many elements are enough for accurate simulation results while keeping reasonable computational time. In the 3-D tetrahedral representation of the model, most of the major substructures, such as the pedicle and the joint contact region, were first tested in simple convergence tests that involved both compressive and shearing loads. Then an optimal resolution was decided upon for each substructure. In the model presented here, a discrepancy of 15-30% between the simulation results and the analytical results is considered to be within the "acceptable" range based on the rationale that 15-30% is relatively small compared with the uncertainties of the Young's moduli of each substructure.

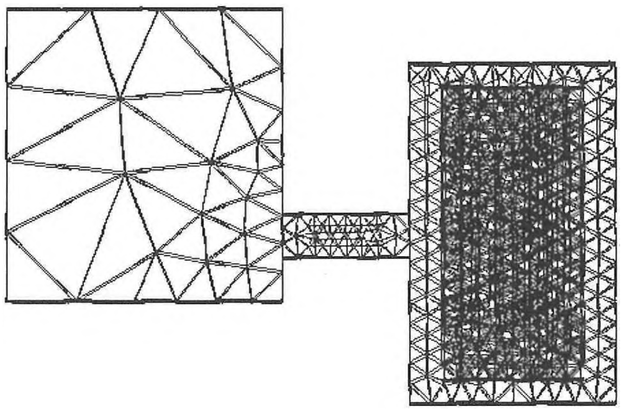

Figure 4: Side view of the model

Another way of reducing the number of elements is to use longer and thinner tetrahedral elements. However, the quality of the mesh will be affected, as the tetrahedral elements should ideally be equilateral for the best simulation results. A poorly meshed model is very likely to reduce the accuracy of the finite-element simulation results. Hence it is important not to over-stretch the elements. Generally, reducing the quality of the mesh can be accomplished by changing the settings in the mesh generation programme or by stretching the geometry of the model after the mesh generation.

3. RESULTS

The simulated load was a uniform static pressure applied on the long process of the incus. A few simulation results are shown in Figure 5. As the displacements of the ossicles are on the order of nm, the simulated deformations presented here were scaled up so that the displacements can be seen.

One way to evaluate the results is to compare the relative contributions of the pedicle and incudostapedial joint to the displacements of the long process of the incus. If there is a significant bending of the pedicle while the incudostapedial joint appears to be relatively rigid, then it suggests that the presence of the pedicle has an effect on the mechanics of the ossicles.

Since the values for the Young's moduli are uncertain, we have explored a range of possible values. In Figure 5(a) the Young's modulus of each substructure in the model was set to the value given in Section 2. In this case, there is a comparatively large bending at the pedicle.

In (b) the Young's modulus of the joint gap was reduced from 10 MPa to 5 MPa, and the result is similar to (a).

In (c) the Young's modulus of the capsule was reduced to 20 MPa, which is the value used for the eardrum in a previous model (Funnell, 1978). Again, lowering the stiffness of the capsule does not make much difference to the results compared with (a).

In (d) the Young's moduli of the joint gap and the capsule were both reduced, to values of 5 MPa and 20 MPa respectively. As the joint becomes more flexible, there is more deformation at the joint and relatively less bending of the pedicle.

In (e) the pedicle stiffness was increased to that of the long process of the incus. As the pedicle becomes stiffer, the degree of bending at the pedicle decreases but it is still significant in this case.

In (f) the Young's modulus of the pedicle was reduced to 3 GPa, which is the value estimated for subchondral bone specimens from a human tibia (Murray, 1984). In this case the pedicle bending becomes quite large.

4. DISCUSSION

The results presented here suggest that load transmission from the incus to the stapes is affected by both the pedicle and the incudostapedial joint. For this model, at least, the pedicle bends significantly even though it is made of bone.

Due to the similarity of the cat and human middle ears, the model and the simulation results presented here can serve as a guide for the modelling and mechanics of the human middle ear. Validation of the results could be accomplished by making experimental measurements on the pedicle and the incudostapedial joint in a preparation with, for example, a disarticulated incus and a fixated stapes. The present model can be incorporated into a complete middle-ear model in order to provide more insight into the significance of the pedicle in hearing.

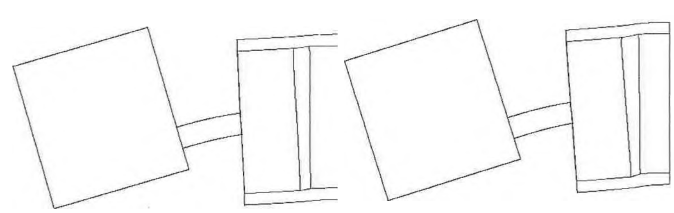

(a) p=5 G; j=10 M; c=50 M (b) p=5 G; j=5 M; c=50 M

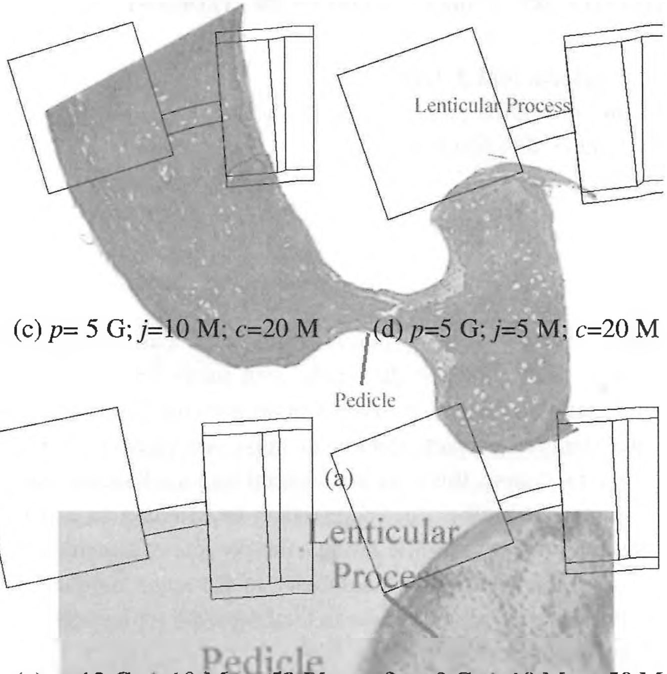

(c) p= 5 G; j=10 M; c=20 M (d) p=5 G; j=5 M; c=20 M

(e) p=12 G; j=10 M; c=50 M (f) p=3 G; j=10 M; c=50 M

Figure 5: Results of the finite-element analysis. The Young's moduli (measured in Pa) of the pedicle, joint gap and the capsule are represented as p, j and c, respectively.

ACKNOWLEDGEMENTS

This work was supported by the Canadian Institutes of Health Research and the Natural Sciences & Engineering Research Council (Canada). The histological sections were kindly provided by M. McKee of McGill University (Figure 3a) and S. M. Khanna of Columbia University (Figure 3b).

REFERENCES

Elices M (2000), "Structural Biological Materials". Pergamon, Amsterdam, xv+361 pp.

Funnell WRJ and Laszlo CA (1978), "Modeling of the cat eardrum as a thin shell using the finite-element method", J. Acoust. Soc. Am. 63: 1461-1467

Mente PL and Lewis JL (1994), "Elastic modulus of calcified cartilage is an order of magnitude less than that of subchondral bone", J. Orthop. Res. 12: 637

Murray RP, Hayes WC, Edwards WT, Harry JD (1984), "Mechanical properties of the subchondral plate and the metaphyseal shell", Trans. Orthop. Res. Soc. 9: 197

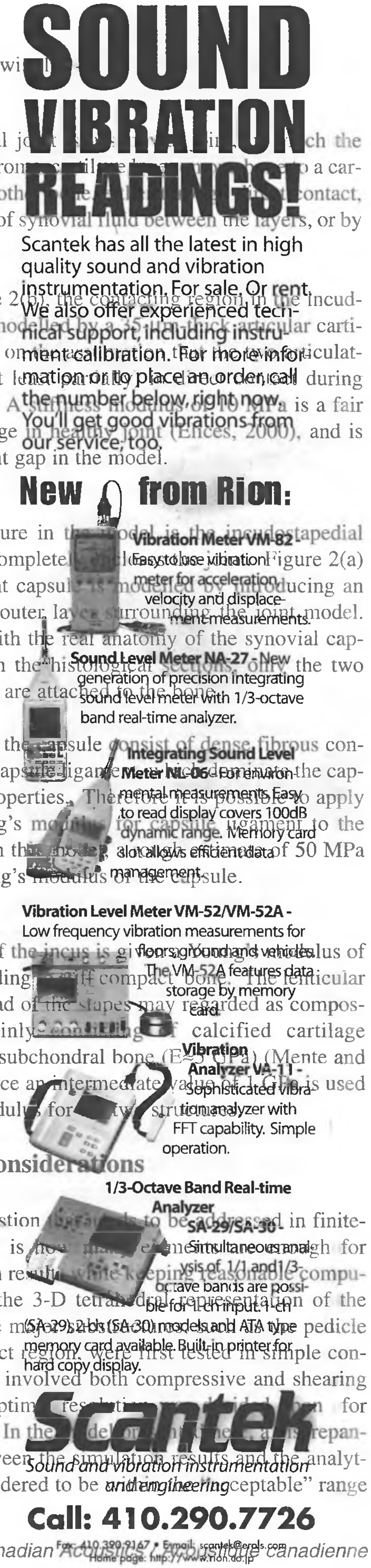

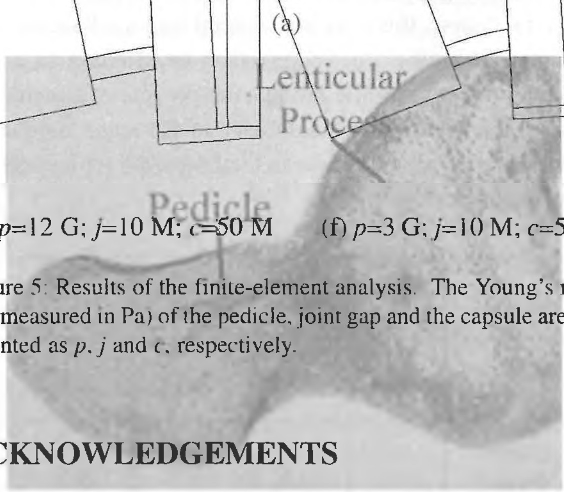

(a)

(b)

Figure 3: Part of the histological sections of cat middle ear with pedicle in (a) side view; (b) top view.

2.2 Material Properties

The material properties of the model are assumed to be linearly elastic, uniform (i.e., the same in all locations) and isotropic (i.e., the same in all directions). Viscoelastic properties of the biological materials will be ignored in this model for simplicity. The linearity assumption is generally true for small strains under normal hearing conditions.

The membrane stiffness [illegible] Young's modulus [illegible] Poisson's ratio has been taken to be 0.3.

Pedicle

Evidence from the serial histological sections of the pedicle suggests that it is most likely to be a continuation of bone from the long process of the incus to the lenticular plate. The estimates for Young's modulus for bone may vary from 1 G to 20 G, depending on the nature of the bone, the direction of measurement, and the part of the bone. In this model, a stiffness modulus of 5 GPa is adopted for the pedicle, as measured from small bone specimens directly beneath joint cartilage (Mente and Lewi[illegible]

Joint Gap

The incudostapedial jo[illegible]ch the load is transferred from [illegible] a cartilage layer on the oth[illegible] contact, through a thin film of synovial fluid between the layers, or by a mixture of both.

As shown in Figure 2(b), the contacting region in the incudostapedial joint is modelled by a 35-µm-thick articular cartilage. This is based on [illegible] the two articulating surfaces are (at le[illegible] during acoustic vibration. A stiffness modulus of 10 MPa is a fair estimate for cartilage in healthy joint (Elices, 2000), and is adopted for the joint gap in the model.

Capsule

Another key structure in the model is the incudostapedial joint capsule that complete[illegible] Figure 2(a) shows that the joint capsul[illegible] modelled by introducing an extra 30-µm-thick outer layer surrounding the joint model. To be consistent with the real anatomy of the synovial capsule as observed in the histological sections, only the two ends of the capsule are attached to the bone.

The outer layers of the capsule consist of dense fibrous connective tissue and capsule ligament, which dominate the capsule mechanical properties. Therefore it is possible to apply the value of Young's modulus for capsule ligament to the capsule directly. In this model, a rough estimate of 50 MPa is used as the Young's modulus of the capsule.

Others

The long process of the incus is gi[illegible] modulus of 12 GPa, corresponding [illegible] compact bone. The lenticular process and the head of the stapes may regarded as composite materials, mainly [illegible] calcified cartilage (E≈0.32 GPa) and subchondral bone (E≈5 GPa) (Mente and Lewis, 1994). Hence an intermediate value of 1 GPa is used as the Young's modul[illegible] for [illegible] structures.

2.3 Meshing Considerations

One important question [illegible] to be addressed in finite-element modelling is how many elements are enough for accurate simulation results while keeping reasonable computational time. In the 3-D tetrahedral representation of the model, most of the major substructures, such as the pedicle and the joint contact region, were first tested in simple convergence tests that involved both compressive and shearing loads. Then an optim[illegible] for each substructure. In the [illegible] discrepancy of 15-30% between the simulation results and the analytical results is considered to be [illegible]ceptable" range

Participation Rates in Noisy Leisure Activities By Three Samples of Students

M. F. Cheesman, L. Ciona, S. Mendoza, and J. Grew

National Centre for Audiology and School of Communication Sciences and Disorders
University of Western Ontario, London, ON N6G 1H1

The risk of acquiring a noise-induced hearing loss is a function of the intensity level of the noise exposure, the duration of the exposure, and the pattern of exposure. Noise exposures associated with leisure or recreational activities, many of which may exceed 80 dB(A), have the potential to cause hearing loss because of their high sound levels[1]. However, the typical duration and pattern of exposure to such leisure and recreational activities has not been documented and therefore the actual hearing risk associated with participation in such activities is unknown.

An increased incidence of high-frequency hearing loss in young adults has been attributed to noise exposure from such leisure activities[2,3], however the rate and pattern of participation by youth in noisy activities is unknown. Recreational activities of youth, particularly those activities that use high fidelity, high intensity sound delivery systems such as personal stereo systems and movie theatres, impulse noises such as fireworks and hunting rifles, and high powered motorized vehicles such as motocross bikes and drag race cars, have been implicated as potentially damaging to the human auditory system.[1] The present research was an initial attempt to quantify the participation by Canadian teens and young adults in noisy leisure activities in terms of participation rates, hours per activity, and frequency of participation as well as the number of noisy activities in which youth participate.

Method

The participation of three samples of students in noisy leisure activities was examined using a cued-recall questionnaire format. Three hundred and forty-six students completed a questionnaire during the summer months of July and August. The respondents were students from a high school (n=55), a community college (n=101), and a university (n=122). The questionnaires were administered by telephone for the high school students, and in person for the post-secondary students. The questionnaires elicited information about participation rates and participation durations for 32 activities that have been identified as capable of producing sound levels of 80 dB(A) or greater. For each activity, respondents were asked if they participated in the activity over the past seven days and, if so, the total duration of their participation.

Results and Discussion

Most students reported participating in at least one noisy leisure activity during the week, with many reporting that they had participated in five or more activities. The mean total duration of participation in noisy activities was 20.7 hours. Of course, this does not account for simultaneous participation in multiple activities, such as listening to a personal stereo system while riding a motorcycle or mowing the lawn. Table 1 provides a summary of the mean number of activities reported and the mean total duration for each of the three student samples.

	high school	college	university	all
number of activities	6.6	5.3	4.2	5.1
total duration (hrs)	24.4	20.2	19.5	20.7

Table 1. Mean number of activities and total duration of participation in noisy leisure activities for the three student groups for the one week reporting period.

High school students reported participating in more activities than the older students and for longer total duration. This pattern may be related to the age of the student groups, but may also be affected by the summer school attendance of the college and university students, who may have had less leisure time. A more valid comparison might be made during the winter and spring months, when all students were in full-time attendance in educational programs.

Table 2 contains a summary of participation rates and participation durations for a selection of the 32 leisure activities included on the questionnaire. Only activities in which at least one group had >6% participation has been included. Music-related activities, such as listening to music via headphones and speakers, were the most commonly reported activity in all three samples. The older students, in college and university, had higher attendance rates at pubs and bars than the high school students. Other activities, such as vacuuming and lawn mowing, differed between the student groups, perhaps as a result of the living situation of the students (more dorms and apartments for older students and parental homes for high school students).

References

1. W. W. Clark, Otolaryngology-Head and Neck Surgery 106 (1992) 669-676.
2. R. E. M. Lees, J. H. Roberts, and Z. Wald, Canadian Journal of Public Health 76 (1985) 171-173.
3. D. H. Kirkwood, Hear, J. 45 (1992) 13-23.

[The support of NSERC and Unitron Industries is gratefully acknowledged.]

	high school		college		university	
sample size (n)	55		101		113	
age range (years)	14-19		18-30		18-29	
music via speakers	94.5 %	**6.7 h**	83.2 %	**7.2 h**	89.4 %	**7.8 h**
attend movie	60.0	**2.1**	34.7	**2.4**	32.7	**2.6**
vacuum	56.4	**0.8**	50.5	**0.9**	29.2	**0.8**
lawn mower	49.1	**2.5**	28.7	**1.7**	7.1	**2.8**
music via headphones	43.6	**2.8**	22.8	**5.6**	31.0	**5.0**
sports events	43.6	**3.5**	26.7	**3.0**	17.7	**3.7**
boom car	41.8	**1.6**	44.0	**5.2**	23.0	**4.7**
loud restaurant	34.5	**1.7**	25.0	**2.3**	28.3	**2.7**
farm equipment	20.0	**7.0**	8.9	**3.0**	0	-
ATV	18.2	**1.4**	8.9	**2.5**	0.9	**0.5**
clubs/disco/bar	18.2	**4.2**	53.5	**5.6**	58.4	**5.7**
drag race	18.2	**3.5**	5.0	**10.2**	0	-
rock concert	18.2	**3.0**	8.9	**3.1**	15.9	**2.9**
power tools	16.4	**4.9**	18.8	**2.4**	2.7	**0.4**
motor bikes	16.4	**1.3**	7.9	**1.5**	1.8	**3.0**
jet ski	14.5	**3.0**	8.9	**2.6**	2.7	**1.3**
attend dance	12.7	**2.9**	7.0	**2.6**	15.9	**4.1**
arcade	10.9	**3.9**	6.9	**1.1**	6.2	**2.2**
model plane/cars	3.6	**1.8**	8.9	**6.4**	4.4	**5.2**
fitness class	3.6	**0.9**	20.8	**4.3**	21.2	**4.2**
carnival/midway	0	-	4.0	**5.8**	6.2	**3.1**
other	25.5	**17.7**	15.8	**9.1**	9.7	**7.2**

Table 2. Participation Rates (in percent) and mean number of hours (in bold) for selected activities.

CAA Student Travel Subsidy and Student Presentation Award Application Form
DEADLINE FOR RECEIPT 1, August, 2001

Procedure

- Complete and submit this application at the same time as the abstract to the Technical Chair of the Conference. Both must be received on or before deadline listed above.
- By 31 August 1999, the CAA Secretary will notify you of the Travel Subsidy funding that you can expect to receive.
- Subsidy cheques will be mailed directly to you within 30 days of the end of the Conference

Eligibility Requirements

In order to be eligible for the Travel Subsidy you must meet the following requirements:
1. Full-time student at a Canadian University;
2. Student Member in good standing of the Association;
3. Distance traveled to the Conference must exceed 150 km (one way);
4. Submit a summary paper for publication in the Proceedings Issue of Canadian Acoustics with the applicant as the first author;
5. Present an oral paper at the Conference. Due to limited funding, a travel subsidy can only be given to the presenter of the paper even though there may be more than one student authors.

Section A: All applicants must complete this section

Name of Student:______________________________

Address:______________________________
(where the cheque is to be sent)

Title of the proposed paper:______________________________

Is the paper to be judged in the Student Presentation Award(s) [Yes/No]:______________________________

Name and Location of the University: ______________, ______________

Faculty and Degree Being Sought: ______________, ______________

Section B: Complete this section only if you are applying for the CAA Student Travel Subsidy

I hereby apply for a travel subsidy from the CAA

Proposed Method of Transport to conference:______________________________
Brief description of the route and method of transportation (e.g., bus, train, air, etc.)

Estimated Cost of Transportation:______________________________
Provide least expensive transportation cost.

Date of Departure to, and Return from the Conference: ______________. ______________

Other Sources of Travel Funding:______________________________
List other sources of travel funding and the amount

Signature of Applicant	**Signature of University Supervisor**
______________________________	______________________________
I certify that the Information provided above is correct	I certify that the applicant is a full time student
______________________________	______________________________
Print Name	Print Name

Subvention de l'ACA pour les Frais de Déplacement des Etudiants et Prix Récompensant les Présentations d'Etudiants - Formulaire d'Inscription
DATE LIMITE DE RÉCPTION, 1 AOUT 2001

Procédure

- Compléter le formulaire et le soumettre en même temps que le sommaire au Président Technique de la Conférence. Tous deux doivent être reçus avant la date limite indiquée ci-dessus.
- Le Secrétariat de l'ACA vous enverra une note avant le 31 Août 1999 indiquant la Subvention que vous êtes susceptible de recevoir.
- Les chèques de Subvention vous seront directement envoyés dans les 30 jours suivant la fin de la Conférence.

Conditions d'Eligibilité

1. Pour avoir droit à la Subvention pour les Frais de Déplacement, vous devez remplir les conditions uivantes:
2. Etre étudiant à temps plein dans une Université Canadienne;
3. Etre Membre de l'ACA;
4. La distance parcourue jusqu'à la Conférence doit être supérieure à 150km (aller simple);
5. Soumettre un sommaire en vue de sa publication dans les actes d'Acoustique Canadienne, l'étudiant doit être le premier auteur du som maire;
6. Présenter une communication orale pendant la conférence. En raison du financement limité, une Subvention pour les Frais de Déplacement ne peut être attribuée qu'à l'étudiant présentant la communication même si plusieurs étudiants sont auteurs du sommaire.

Section A: Tous les candidats doivent remplir cette section

Nom de l'étudiant:______________________________

Adresse: ______________________________
(où le chèque doit être envoyé)

Titre de la communication proposée: ______________________________

La communication est elle inscrite au concours pour le Prix Récompensant les Communications d'Etudiants [Oui/Non]: __________

Nom et adresse de l'université: ______________________________

Faculté et niveau d'étude en cours: ______________________________

Section B: Compléter cette section si vous postulez pour une Subvention des Frais de Déplacement
Je postule par le présent document à une Subvention de l'ACA pour des Frais de Déplacement

Moyen de Transport proposé pour se rendre a la conférence: ______________________________
Brève description du trajet et du moyen de transport (i.e bus,train,avion etc.)

Coût estimé du Transport: ______________________________
Fournir le coût de transport le moins élevé
Date de Départ pour la Conférence et de Retour: ______________________________

Autres sources de financement pour le transport:______________________________
donner la liste des sources de financement et leur montant

Signature du candidat	**Signature du superviseur**
______________________________	______________________________
Je certifie que les informations fournies ci dessus sont correctes	Je certifie que le signataire est un étudiant à temps plein
______________________________	______________________________
Nom	**Nom**

Acoustic Attenuation Performance Of Double Expansion Chamber Silencers With Inter-Connecting Tube

Zhenlin Ji
Silex Inc., 6659 Ordan Drive, Mississauga, Ontario L5T 1K6

1. INTRODUCTION

The multi-chamber reactive silencers are widely used to reduce the engine exhaust noise, due to their broadband high noise attenuation. The one-dimensional analytical approach, which assumes plane wave propagation in the axial direction in silencers, is a classical method for the prediction of silencer's acoustic attenuation performance. However, The one-dimensional theory cannot account for the effect of multi-dimensional waves inside the silencers on the acoustic attenuation performance. The experimental and one-dimensional analytical studies on the double chamber silencers [1] demonstrated that a multi-dimensional approach is required for the accurate prediction of acoustic attenuation performance of the silencers at higher frequencies, while the simple one-dimensional theory provides reasonable predictions at lower frequencies. The objective of this study is to apply the three-dimensional boundary element method (BEM) to predict the acoustic attenuation performance of double expansion chamber silencers with inter-connecting tube and to investigate the effect of geometry with respect to the acoustic attenuation of these configurations.

2. FORMULATION

To employ the boundary element method for the prediction of the acoustic attenuation performance of double chamber silencers with inter-connecting tube, a multidomain approach is needed due to the presence of singular boundaries [2, 3]. The silencer considered here is divided into five substructures as shown in Figure 1: inlet tube, inlet expansion chamber, inter-connecting tube, outlet expansion chamber, and outlet tube. For each substructure, the BEM gives [2, 3]

$$[H^j]\{P^j\} = \rho_0 c_0 [G^j]\{V^j\},$$
(1)

where $[H^j]$ and $[G^j]$ are the coefficient matrices; $\{P^j\}$ and $\{V^j\}$ are the vectors of acoustic pressure and outward normal particle velocity at boundary nodes, respectively, for the substructure j; $\rho_0 c_0$ is the characteristic impedance of the medium. The boundaries are grouped into the inlet, outlet and rigid wall represented by the subscripts i, o and w, respectively. Equation (1) combined with the rigid wall boundary condition $V_w = 0$, yields

$$\begin{Bmatrix} P_i^j \\ P_o^j \end{Bmatrix} = \rho_0 c_0 \begin{bmatrix} T_{11}^j & T_{12}^j \\ T_{21}^j & T_{22}^j \end{bmatrix} \begin{Bmatrix} V_i^j \\ V_o^j \end{Bmatrix},$$
(2)

For two series substructures, the resultant impedance matrix can be derived by the continuity conditions of acoustic pressure and particle velocity on the interface as

$$[T^R] = \begin{bmatrix} T_{11}^1 - T_{12}^1(T_{11}^2 + T_{22}^1)^{-1}T_{21}^1 & T_{12}^1(T_{11}^2 + T_{22}^1)^{-1}T_{12}^2 \\ T_{21}^2(T_{11}^2 + T_{22}^1)^{-1}T_{21}^1 & T_{22}^2 - T_{21}^2(T_{11}^2 + T_{22}^1)^{-1}T_{12}^2 \end{bmatrix}$$
(3)

Finally, combining all substructures yields

$$\begin{Bmatrix} P_i \\ P_o \end{Bmatrix} = \rho_0 c_0 \begin{bmatrix} Q_{11} & Q_{12} \\ Q_{21} & Q_{22} \end{bmatrix} \begin{Bmatrix} V_i \\ V_o \end{Bmatrix},$$
(4)

which defines the impedance matrix between the inlet and outlet of silencer. The four-pole parameters and the transmission loss calculation procedure are identical to those used earlier [3] and will not be elaborated here.

3. RESULTS AND DISCUSSION

For all configurations, the present study considers D=18" for the chamber diameter, d=6" for the inlet/outlet and inter-connecting tube diameters, and c=550 m/s for the speed of sound. For the silencers with chambers of equal lengths, Figure 2 compares the transmission loss for three different inter-connecting tube lengths. Increasing the length of inter-connecting tube shifts the resonance peaks to lower frequencies. The effect of unequal lengths of inter-connecting tube extended into two chambers is examined next by keeping the overall length of inter-connecting tube and fixing all other parameters, and the transmission loss results are shown in Figure 3. The longer extension in a chamber leads a lower resonance frequency and a lower attenuation dome after the resonance. An observation for the silencers with chambers of equal lengths is found that the troughs in the transmission loss are located at $kL_{S1} = kL_{S2} = n\pi$, and were not changed by the lengths of inter-connecting tube in the chambers. The effect of unequal lengths of chambers by fixing the lengths of silencer and inter-connecting tube and changing the location of bulkhead is shown in Figure 4. The first low attenuation dome is independent on the locations of inter-connecting tube and bulkhead, while the attenuation behavior is complex above the first pass frequency for fixed overall lengths of silencer and inter-connecting tube. Figure 5 compares the transmission loss of silencers without and with inlet/outlet extensions. The inlet and outlet extensions contribute also resonance peaks in the plane wave region. The lengths of extended inlet and outlet tubes into chambers may be chosen that the resonances are located at the troughs of the silencer with no inlet/outlet extensions leading a desirable high acoustic attenuation. An example is illustrated in Figure 5 also. This behavior demonstrates the advantage of extended inlet and outlet in the silencer design.

4. CONCLUSIONS

A three-dimensional substructure boundary element technique is employed to predict the acoustic attenuation performance of double expansion chamber silencer with inter-connecting tube. The effect of the lengths of inter-connecting tube and expansion chambers, as well as the extensions of inlet and outlet tubes is investigated. The double expansion chamber silencers exhibit a very low attenuation dome at lower frequencies, and the combination of the broadband domes and resonance peaks above the first pass frequency and below the plane wave cut-off frequency. The pass frequency of the first low attenuation dome is dependent on the lengths of silencer and inter-connecting tube for a given expansion ratio. The resonance frequencies decrease as the extended lengths of tubes into the expansion chambers are increased. By choosing the lengths of extended inlet/outlet tubes to match the resonances with troughs of the silencers without extensions an excellent acoustic attenuation may be obtained. Above the plane cut-off frequency the attenuation behavior is complex.

REFERENCES

1. D. D. Davis, G. M. Stokes, D. Moore and G. L. Stevens 1954 *NACA TN 1192*. Theoretical and experimental investigations of mufflers with comments on engine exhaust muffler design.
2. C. Y. R. Cheng and A. F. Seybert 1991 *Journal of Sound and Vibration* 151, 119-129. A multidomain boundary element solution for silencer and muffler performance prediction.
3. Z. L. Ji, Q. Ma and Z. H. Zhang 1994 *Journal of Sound and Vibration* 173, 57-71. Application of the boundary element method to predicting acoustic performance of expansion chamber mufflers with mean flow.

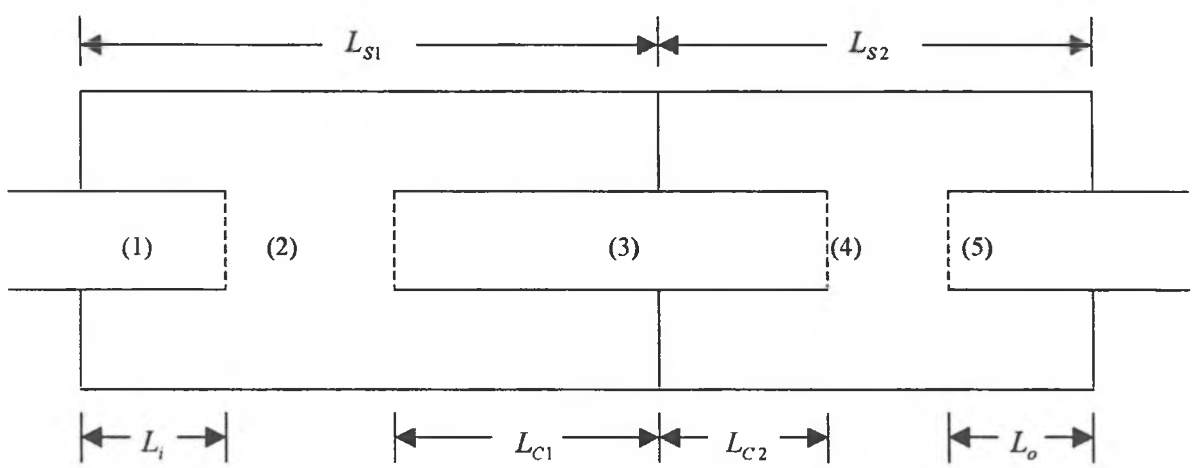

Figure 1. Double expansion chamber silencer with inter-connecting tube.

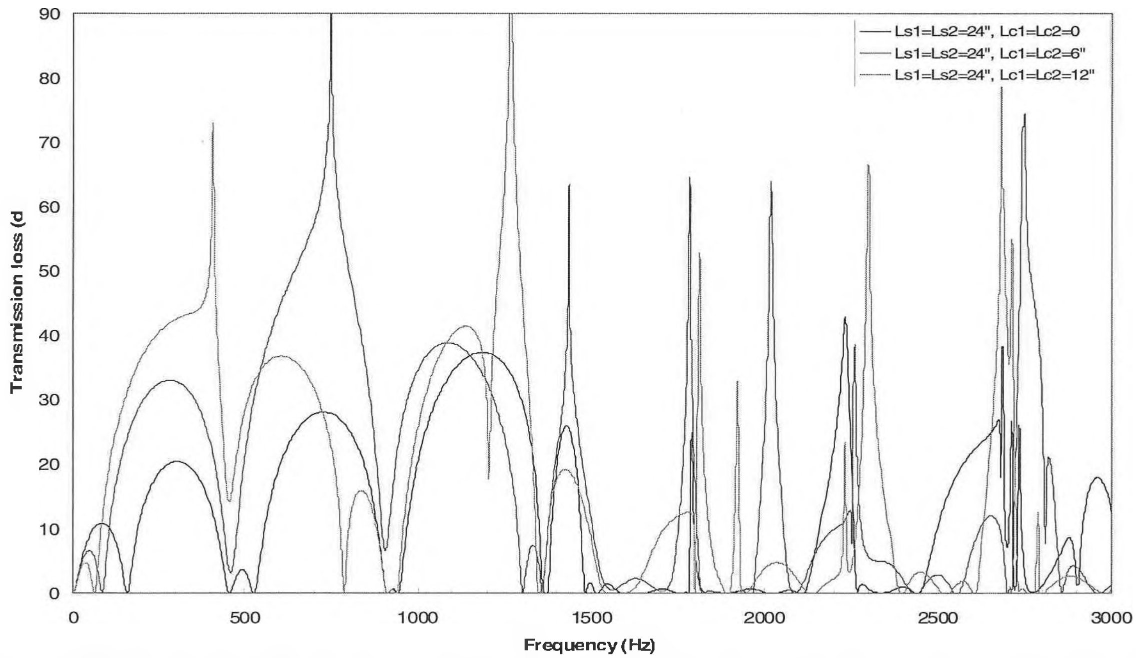

Figure 2. Effect of the length of inter-connecting tube on the acoustic attenuation performance of double expansion chamber silencers.

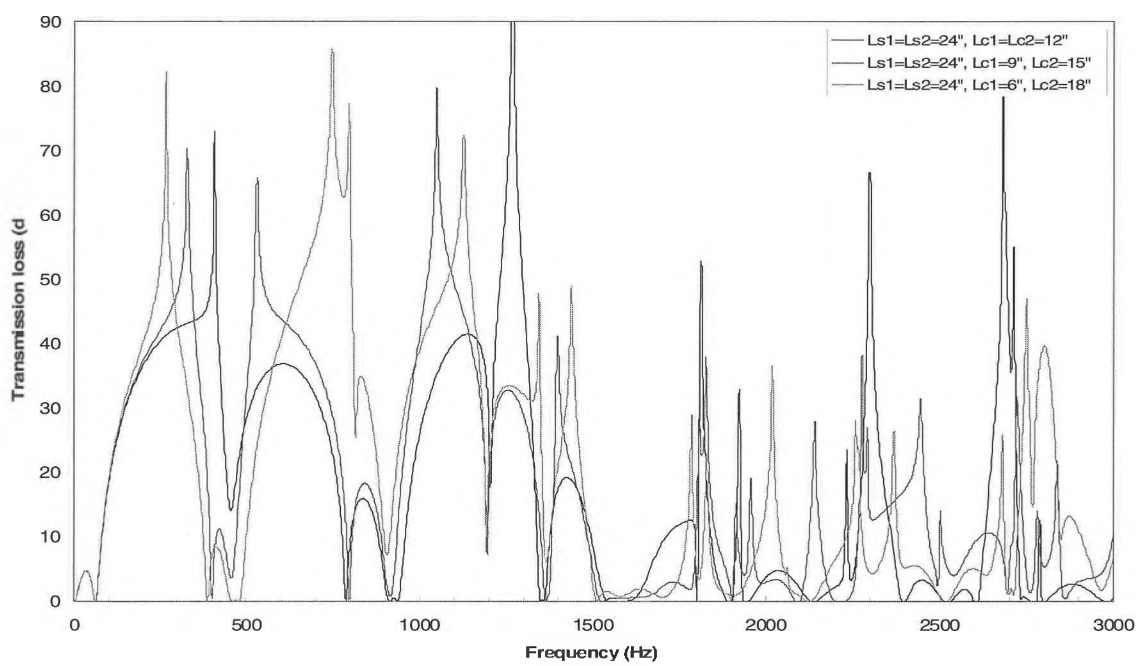

Figure 3. Effect of the extended lengths of inter-connecting tube into chambers on the acoustic attenuation performance of double expansion chamber silencers.

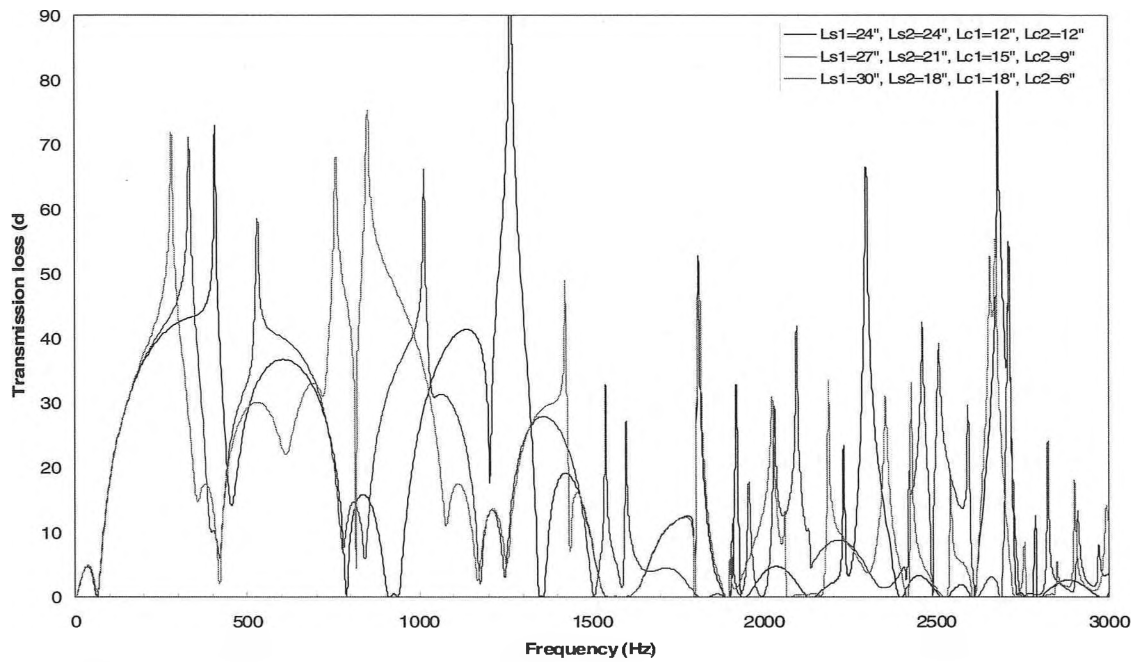

Figure 4. Effect of the lengths of expansion chambers on the acoustic attenuation performance of double expansion chamber silencers.

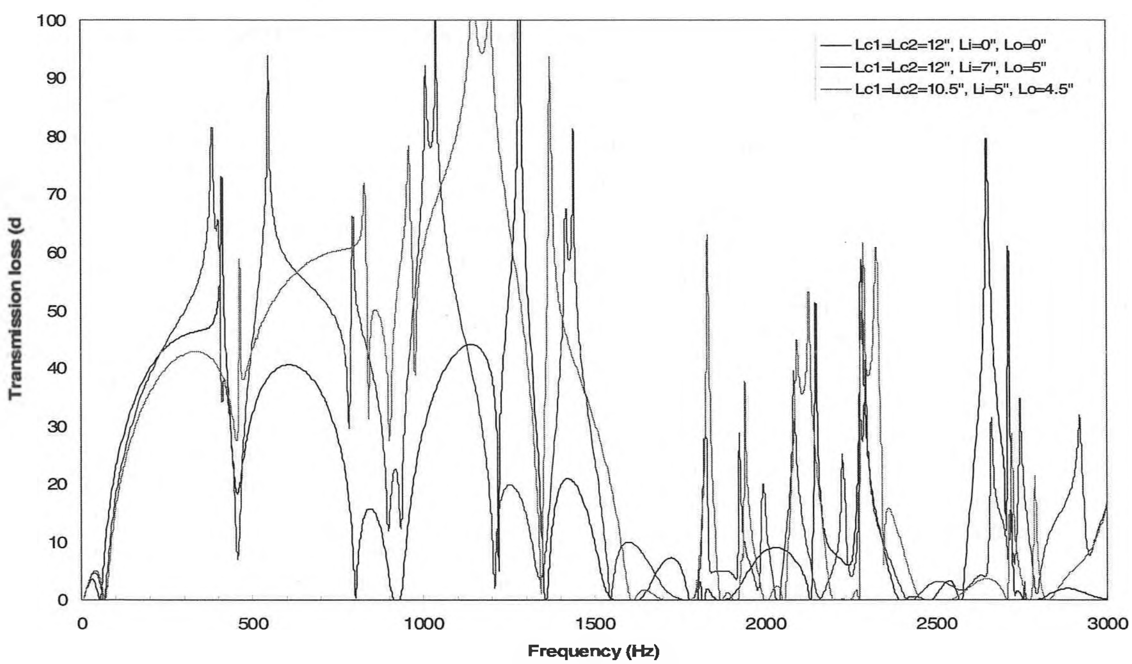

Figure 5. Effect of the inlet and outlet extensions on the acoustic attenuation performance of double expansion chamber silencers.

The Effects Of Safety Gear Worn In Combination And Hearing Loss On Earmuff Attenuation And Speech Understanding

Sharon M. Abel*, Andrea Sass-Kortsak and Aneta Kielar
Depts. of Otolaryngology and Public Health Sciences, University of Toronto, Toronto, Ontario M5S 1A1

1.0 INTRODUCTION

This study was designed to determine whether the wearing of other safety gear in combination would decrease the sound attenuation of hearing protective ear muffs. Preliminary results showed that, in young normal-hearing listeners, the wearing of safety glasses and a half mask respirator significantly decreased the attenuation provided by a Class A earmuff[1], particularly in the low frequencies.[2] This was due to leakage of sound under the ear cup.[3] A question of interest was the interactive effect of the hearing status of the listener. In previous studies we had demonstrated that, while the amount of sound attenuation achieved was not affected by hearing loss, speech understanding was compromised by the wearing of conventional muffs and plugs.[4,5] We hypothesized that a decrease in attenuation due to the wearing of devices in combination might improve speech understanding in the hearing-impaired listener.

2.0 METHODS AND MATERIALS

2.1 Experimental Design

The design of the experiment has been previously described.[2] To assess the effects of hearing loss, the results were compared for two groups of 24 subjects, aged 40-68 years, with normal hearing and moderate bilateral high-tone hearing loss, respectively. Half of each group were males and half females. Subjects were each tested with the ears unoccluded (UN), and subsequently with Class A earmuffs attached to a hard hat (M), the muffs in combination with safety glasses (MG), the muffs in combination with an air-purifying half-mask respirator (MR), and with the muffs in combination with both the glasses and respirator (MGR). The muff on hard hat was always fit by one of the experimenters (SMA) with the goal of optimizing the attenuation of the muff. In each listening condition diffuse field hearing thresholds were measured in quiet for eight one-third octave noise bands with centre frequencies ranging from 0.25 to 8 kHz. Consonant discrimination was assessed in quiet (75 dB SPL) and in a background of 80 dB SPL speech spectrum noise.

2.1 Subjects

All subjects were fluent in English and had been screened for a history of medical disorders which might signify a central auditory processing deficit or compromise sustained attention and the ability to understand instructions. In the normal-hearing group, headphone hearing thresholds at 0.5 and 4 kHz were less than 15 dB HL on average.[6] In the hearing-impaired group, thresholds ranged from -0.5 to 26.5 dB HL at 0.5 kHz, and 21.5 to 55.5 dB HL at 4 kHz (better ear).

2.2 Apparatus

The apparatus has previously described in detail.[7] The testing was carried out in a semi-reverberant sound proof booth that met the requirements for hearing protector testing.[8]

2.4 Procedure

Hearing thresholds were measured once in each ear for each of the eight one-third octave band frequencies, using a variation of Bekesy tracking.[6] Consonant discrimination was tested by means of the Four Alternative Auditory Feature Test (FAAF).[9] For a detailed description of both protocols, see Abel et al., 2000[2].

3.0 RESULTS AND DISCUSSION

Fig. 1 shows the mean attenuation achieved as a function of stimulus frequency for each of the four protected listening conditions. Attenuation scores were derived by subtracting the unoccluded from the protected hearing threshold at each frequency, within subject. The results for the two groups are shown separately. Data from male and female subgroups have been averaged. An ANOVA and post hoc comparisons applied to these data indicated that there was no effect of hearing status. Overall, females achieved 3-dB less attenuation than males. Regardless of protector condition, attenuation increased significantly as frequency increased from 0.25 to 1 kHz and then remained constant. The least attenuation was achieved with the muff in combination with the glasses and respirator and the greatest attenuation was achieved with the muff alone. The muff/respirator and muff/glasses combinations fell midway between and were not different from each other. The range in attenuation across these conditions was greatest at 0.25 and 0.5 kHz (9 dB) and least at 2 and 3.15 kHz (3-4 dB). For the muff alone, values were lower than the manufacturer's specifications. However, the difference was no greater than 6 dB at any frequency.

An ANOVA and post hoc comparisons on the results of the FAAF test showed that there was no effect of gender. Scores for the impaired group were significantly lower than those for the normal group. For the normal listeners, there was no difference between unoccluded and protected scores. In contrast, for the hearing-impaired, protected scores were significantly lower than the unoccluded scores, by 22% in both quiet and noise. Protector combination was not a significant factor, likely because the wearing of other safety gear had its impact below the speech frequency range. Both groups performed more poorly in noise than in quiet. In the unoccluded condition, mean scores declined by 25% for both groups. In the protected conditions, mean scores declined by 18% and 27% in the normal and impaired groups, respectively.

Conclusions: Decrements in attenuation due to the wearing other safety gear in combination with hearing protective ear muffs were no different for normal and hearing-impaired listeners. As in previous studies, in the normal group, consonant discrimination was unaffected by the wearing of protectors. The hearing-impaired showed significant deficits. There was no additional affect of wearing other safety gear in combination.

ACKNOWLEDGMENTS

Supported by the Workplace Safety and Insurance Board and an Isabel Silverman CISEPO Senior Scientist Award (SMA).

References

1. CSA (1994). CSA Z94.2-94 "Hearing protectors" (Canad. Standards Assoc., Rexdale, Ont. Canada).

2. Abel, S.M., Sass-Kortsak, A. and Bruce, S. (2000). "The effect on sound attenuation provided by earmuffs of other safety gear worn in combination." Canad. Acoust. 28(3), 150-151.

3. Wagstaff, A.S., Tvete, O., and Ludvigsen, B. (1996). "The effect of a headset leakage on speech intelligibility in helicopter noise." Aviat. Space & Environ. Med. 67, 1034-1038.

4. Abel, S.M., Alberti, P.W., Haythornthwaite, C. and Riko, K. (1982). "Speech intelligibility in noise: Effects of fluency and hearing protector type." J. Acoust. Soc. Am. 71, 708-715.

5. Abel, S.M., Armstrong, N.M. and Giguère, C. (1993). "Auditory perception with level-dependent hearing protectors: The effects of age and hearing loss." Scand. Audiol. 22(2), 71-85.

6. Yantis, P.A. (1985). "Puretone air-conduction testing," in *Handbook of Clinical Audiology*, 3rd ed., edited by J. Katz (Williams & Wilkins, Baltimore), pp. 153-169.

7. Giguère, C. and Abel, S.M. (1990). "A multi-purpose facility for research on hearing protection." Appl. Acoust. 31, 295-311.

8. ANSI (1984). ANSI S12.6-1984 "Method for the measurement of the real-ear attenuation of hearing protectors" (Am National Standards Inst., New York).

9. Foster, J.R. and Haggard, M.P. (1979). "FAAF–An efficient analytical test of speech perception," in Proc. of the Inst. Of Acoustics, MRC Inst. of Hearing Research, Nottingham, England, pp. 9-12.

* Present address: DCIEM, 1133 Sheppard Ave. W., P.O. Box 2000, Toronto, Ont. M3M 3B9.

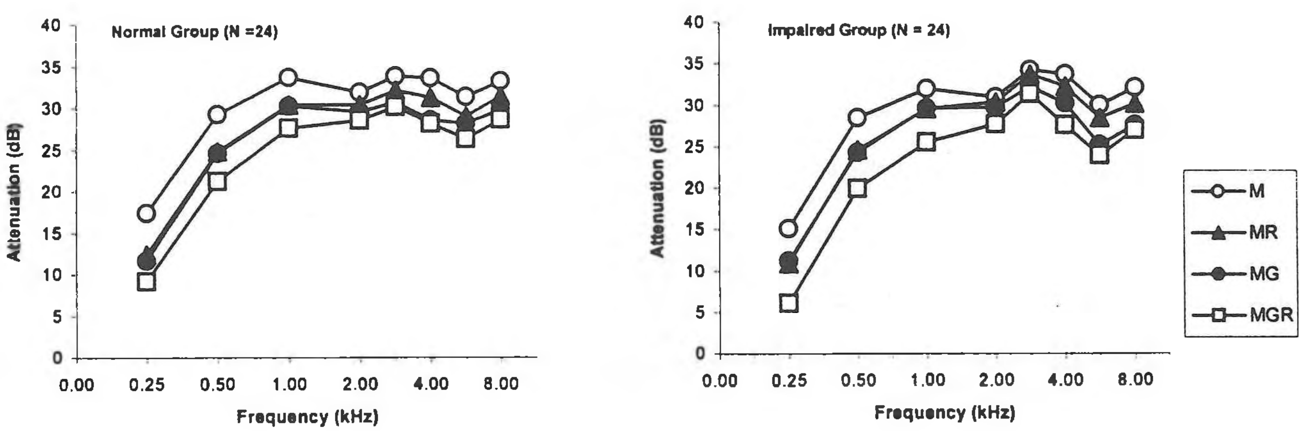

Figure 1. Attenuation as a function of frequency. Efects of ear condition and hearing status.

Testing Of ANR (Active Noise Reduction) Headsets

Alberto Behar
IBBME, University of Toronto, alberto.behar@utoronto.ca

1 INTRODUCTION

ANR is a technique by which a signal of equal characteristics but with opposite phase is injected to neutralize the original one. Although patented in the early 30th, it was only in 1957 that it was adapted to earmuffs. And it was only in the last 20 or so years that the technique started to be applied outside of the research labs for practical applications.

The main advantage of the use of ANR headsets is the increase of the attenuation at frequencies below 1KHz. There is no significant reduction of the risk of hearing losses at those frequencies. However, due to the forward masking phenomenon, a reduction of the sound level at low frequencies results in an improvement in intelligibility and the consequent ease in oral communications. Therefore, the two main applications of those headsets is in communications and in comfort.

A typical ANR includes a microphones, processor and speakers under each of the cups. A communication headset also includes means to inject the audio signal and a noise excluding microphone. The "comfort" headset, found mainly in executive classes of airlines does not include those means.

There are two main characteristics that can be measured in an ANR headset. They are the attenuation ad different frequencies and the intelligibility as perceived by the wearer under different circumstances (types of noise and sound levels). Although testing of those characteristics is something manufacturers as well as authorities are interested in, there are still no test methods standardized or even recognized. Right now, in Canada, researches are underway (at the DCIEM and the NRC among others) trying to design a testing protocol that could be universally accepted.

The Sensory Communications group at the University of Toronto is presently studying a method that uses an Acoustical Test Fixture (ATF or Artificial Head) and allows for the measurement of Insertion Loss (IL). The attenuation could be, eventually calculated using the IL values.
At the present, we are interested in the repeatability from consecutive measurements on the same protector, between protectors of the same type, as well as comparison between protectors of different types and from different manufacturers.

2 MATERIALS AND METHOD

The protectors we are presently testing are:

a) one "comfort" supra-aural (Supra-aural are muffs that seat on top of the pinna, those providing limited attenuation even at high frequencies.)
b) two "comfort" circumaural (Circumaural muffs cover completely the pinna providing excellent high frequency attenuation), and
c) one flying helmet

Protectors are mounted on the ATF, that is a mannequin with one instrumented ear. Features of the mannequin include circumaural area, pinna and auditory canal fabricated with simulated skin and tissue which retains the correct dynamic mass and textural properties of human flesh. The auditory canal is terminated in Zwislocki type DB100 coupler and B&K type 4134 microphone that simulate the acoustical impedance of human ears. Measurements were performed on the left ear of the ATF, the only ear that is instrumented.

The measurements were performed in a IAC Double walled, double room Audiometric Cabin. The pink noise signal used for the tests was generated by a General Radio Random Noise Generator Type 1382, amplified by two Rotel Stereo Integrated Amplifiers Type RA-930AX (50W) and fed into the cabin via four Mirage Speakers Type M-90is and four horn loaded piezoelectric loudspeakers Motorola type KSN1016. The resulting signals where detected by the microphone in the ATF and analyzed by a B&K Dual Channel Real-time Frequency Analyzer Type 2144. Measurements were performed in 1/3-octave bands at the frequencies between 20 and 8,000 Hz.

Each series of measurements consisted in the IL measurements of one protector repeated three times. To do so, first, the sound level (SL_1) of the open ear was measured at each of the test bands. Then, the muff was donned on the head with the ANR switched off and the sound level (SL_2) of the passive mode was measured. Finally, the ANR was switched on and the sound level (SL_3) of the totally protected ear was measured again. The series were repeated three times. Each time the headset was donned and taken away.

3. RESULTS

Some preliminary results from tests on are shown in Figures 1 and 2.

Figure 1 shows results from a series of three tests of the supra-aural muff.

Figure 1A shows the IL of the muff in "passive" mode (difference of SL without and with the muff, with the electronics off). Shown are the results of the three tests as well as the mean IL.

Figure 1B shows results of the active IL (difference of SL with the electronics off and on).

Figure 1C shows the total IL (difference of SL without and with the muff on, with the electronics on).

Figure 2 shows results from a series of three tests of the circumaural muff.

Figures 2A, 2B and 2C shows the results from the same tests as in 1A, 1B and 1C

Figure 1A. Supra-aural, three tests, PASSIVE IL

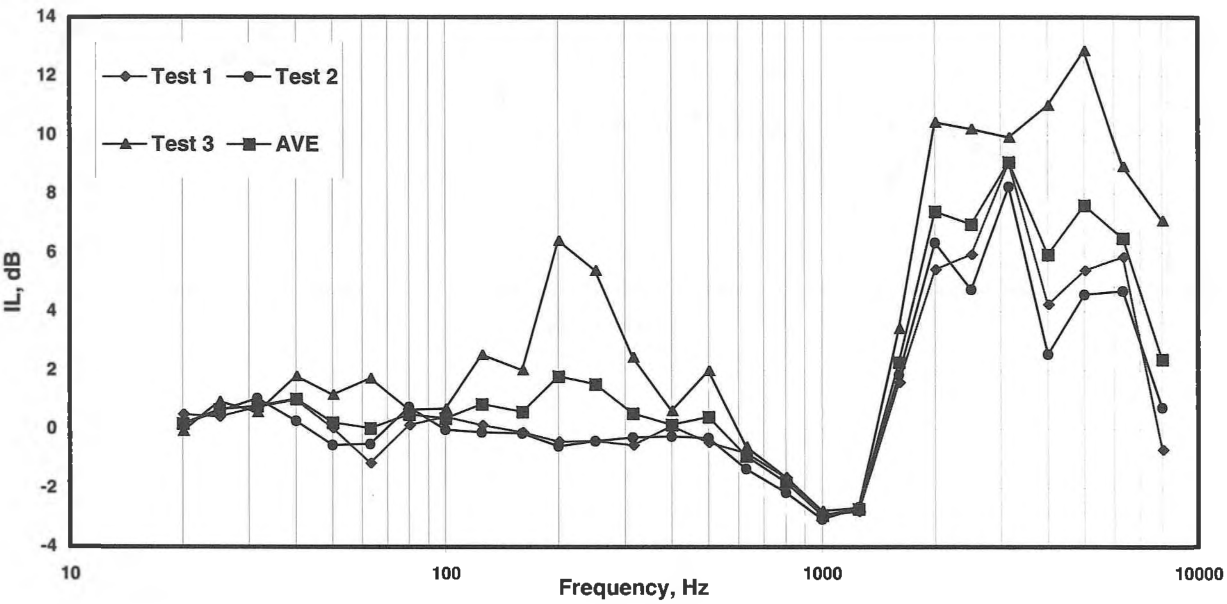

Figure 1B. Supra-aural, three tests ACTIVE IL

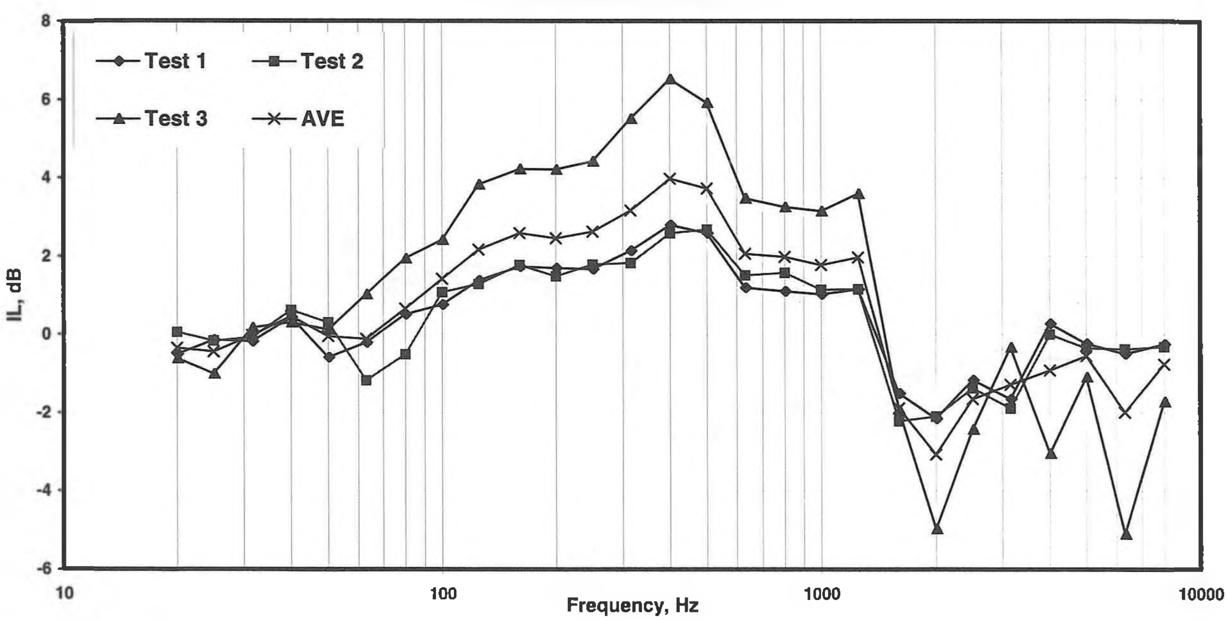

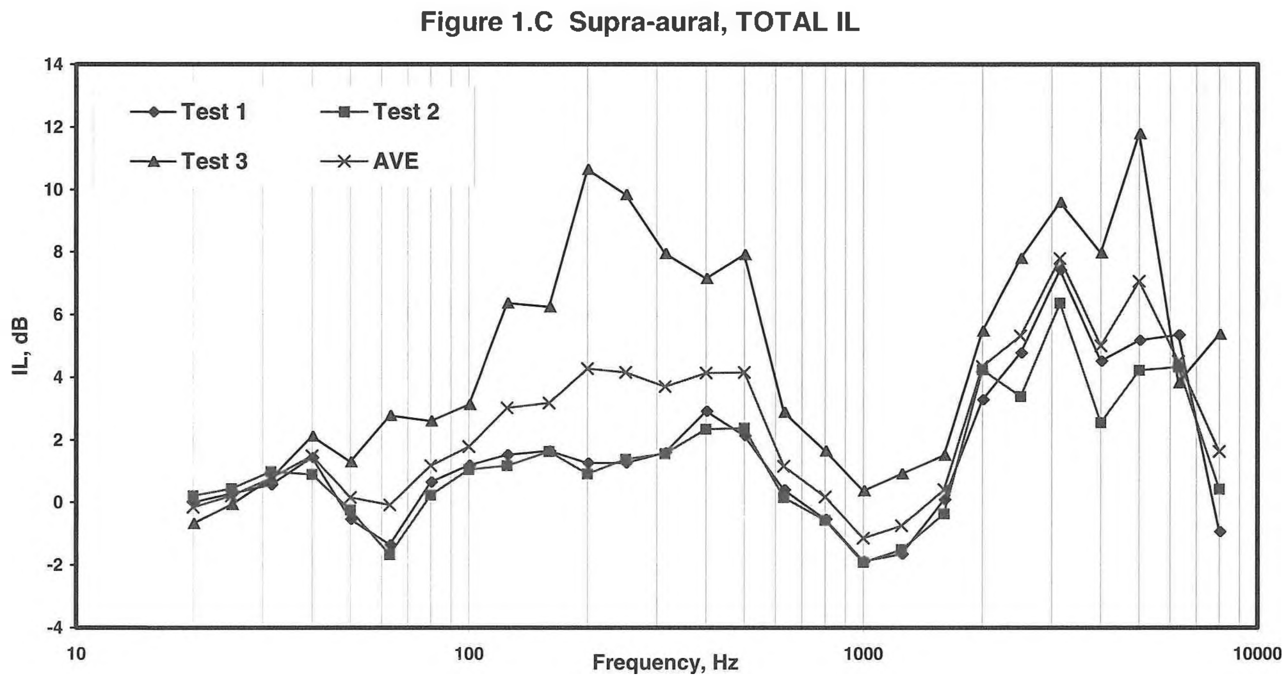
Figure 1.C Supra-aural, TOTAL IL
Test 1
Test 2
Test 3
AVE
IL, dB
Frequency, Hz
14
12
10
8
6
4
2
0
-2
-4
10
100
1000
10000

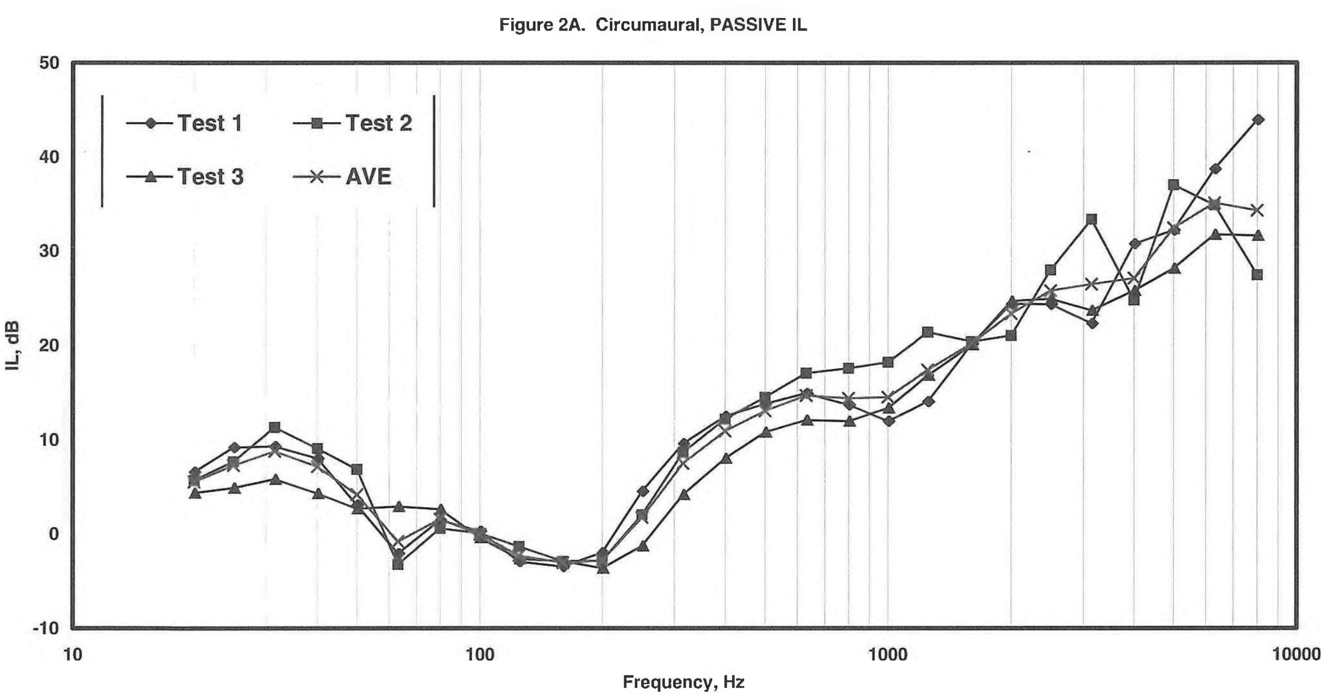
Figure 2A. Circumaural, PASSIVE IL
Test 1
Test 2
Test 3
AVE
IL, dB
Frequency, Hz
50
40
30
20
10
0
-10
10
100
1000
10000

Figure 2B. Circumaural, ACTIVE IL,

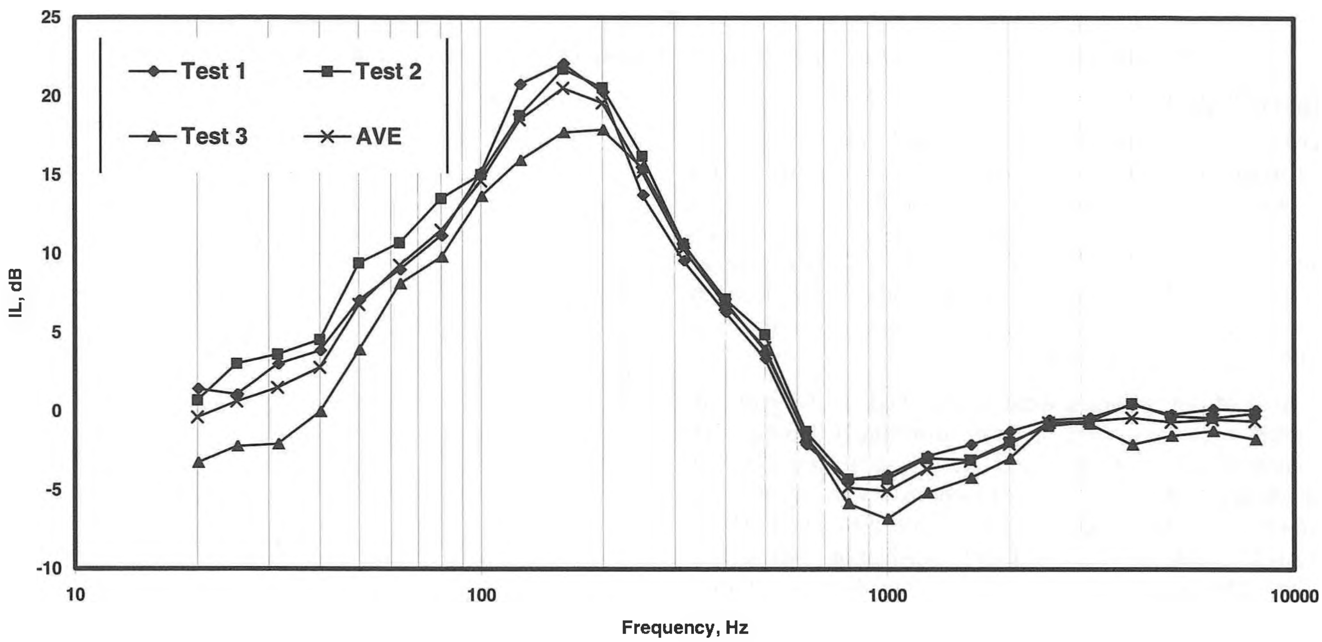

Figure 2C. Circumaural, TOTAL IL,

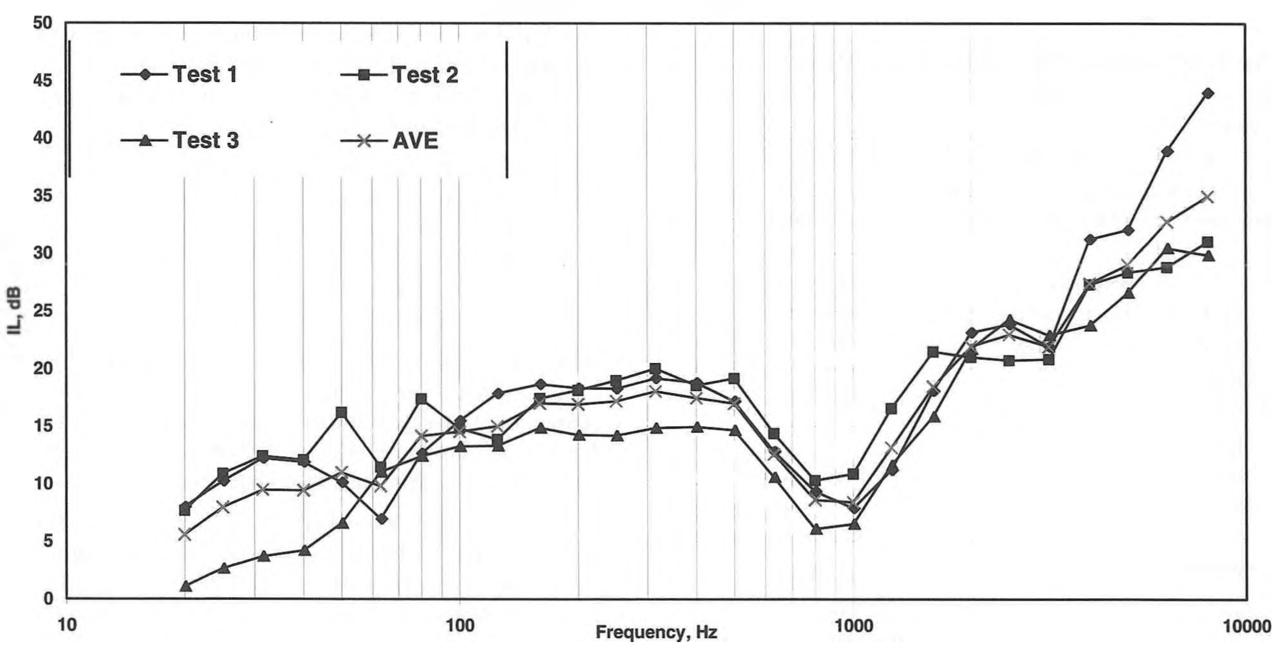

ACCEPTABLE PARTY WALL SOUND INSULATION CRITERIA

J.S. Bradley

Institute for Research in Construction, National Research Council, Montreal Rd. Ottawa, K1A 0R6

Introduction

This paper present the results of analyses of aggregate response data from a field survey of the sound insulation of walls separating multiple unit housing in 3 Canadian cities. The survey included extensive face-to-face interviews in subjects' homes as well as complete sound transmission loss measurements of party walls between homes and ambient noise measurements in each home over a complete 24 hour period.

A total of 600 subjects were interviewed in 300 pairs of homes. Homes were equally distributed among the combinations of owners and renters, row housing and apartments and 3 cities (Toronto, Vancouver and Montreal). Subjects were first approached by letter asking them to participate in a building satisfaction survey and were subsequently interviewed in their homes. Initial questions obtained spontaneous responses without any mention of sound insulation or noise. Subsequent questions gathered directly elicited responses concerning whether they heard various sounds and how annoying they were. For most survey questions, responses were in the form of 7-point response scales. The survey procedure was essentially the same as that found to be successful in a smaller pilot study.

In this paper only the apparent STC ratings (i.e. including possible flanking paths) of the walls will be presented. They varied from 38 to 60 with a mean of 49.8. Data were aggregated into 8 groups by apparent STC rating.

The Importance of Sound Insulation

Direct questions about noise or sound insulation can potentially bias results by sensitizing subjects to the importance of sound insulation between homes. The initial questions were intended to avoid this problem by obtaining spontaneous responses related to the importance of sound insulation. For example, when subjects were asked if they would like to move from their present home, the percentage saying yes significantly decreased with increasing measured STC of their party wall. (See Figure 1). Of the people saying they would like to move in each of the 8 STC groups, 94 to 100 % of them gave a noise related reason. Sound insulation is clearly a major cause of people wanting to move and noise problems appear to be an almost ubiquitous reason for wanting to move.

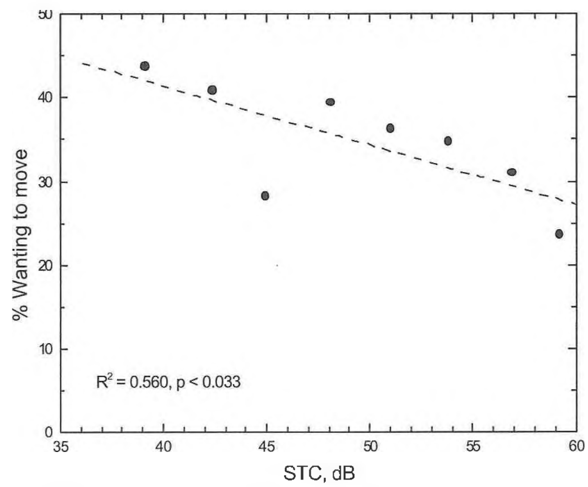

Figure 1. Percentage wanting to move versus STC.

Response	R^2	p
Percentage wanting to move.	0.560	0.033
How satisfied with your building?	0.832	0.002
How considerate are your neighbours?	0.857	0.001
How often awakened due to noise from neighbours?	0.602	0.024
Subjective rating of sound insulation.	0.921	0.000

Table I. Relationships with measured STC values. (R^2 is coefficient of determination, p is probability of the result occurring by chance).

When subjects were asked how satisfied they were with the building in which they lived, the responses were significantly related to measured STC values (see Table I) and subjects with better sound insulation were more satisfied with their building.

Subjects' responses concerning how considerate their neighbours were, were also significantly related to measured STC values. That is, subjects with lower sound insulation tended to blame their neighbours as being less considerate. Poor sound insulation between homes is thus seen to be a potential cause of social disruption.

When asked how often they were awakened by noises from neighbours in their building, their responses were again significantly related to measured STC values (See Table I). Thus the quality of resident's sleep is related to the amount of sound insulation between their homes.

When subjects were asked to rate the sound insulation between them and their neighbours, their responses were significantly related to measured STC values as shown in Figure 2. Subjects are aware of the quality of the sound insulation; it is important to them, and it affects their quality of life.

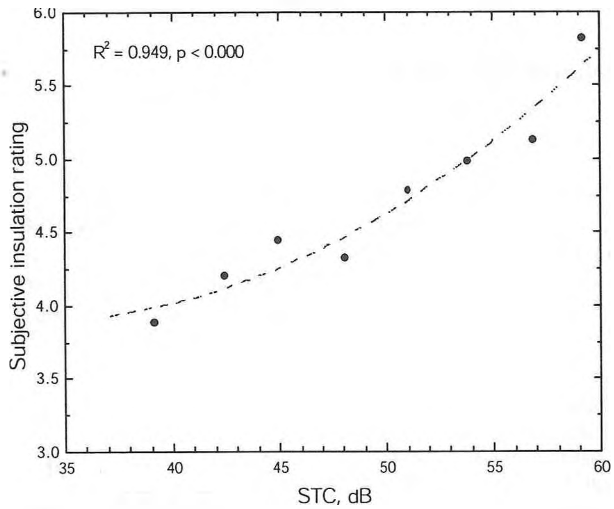

Figure 2. Subjective rating of sound insulation vs. STC.

Deriving Goals for Better Sound Insulation

The questionnaire included many items that asked directly how often they heard specific sounds and how annoying they were. They concerned sounds from neighbours either side, sounds of neighbour's voices, sounds of neighbour's radios and televisions, and music related sounds from their neighbours. A factor analysis of the responses simply suggested that each pair of responses concerning hearing and being annoyed by a particular type of sound were related. Thus in the following analyses the averages of each pair of responses is considered.

Figure 3 plots the average responses to questions asking about sounds from their neighbours either side of them. These included responses to questions asking how often they heard these noises and how annoying they were.

Similar plots were produced for responses concerning sounds of neighbour's voices, sounds of neighbour's radio and TV and music related sounds. The best-fit regression lines to these average responses are compared in Figure 4.

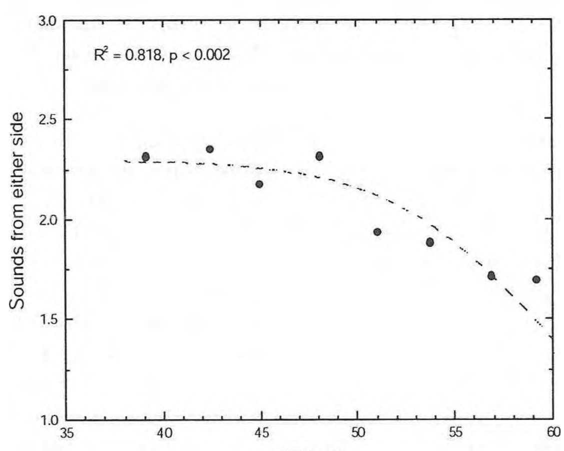

Figure 3. Responses concerning sounds from neighbours either side versus STC.

The R^2 values for these plots varied from 0.772 to 0.944 and all indicated significant relationships. All of these responses show similar patterns. For lower STC values, the responses do not vary with STC but for higher STC values they systematically decrease with increasing STC. Disturbance from neighbour's noises depends, not only on the amount of sound insulation, but also on how noisy their neighbours are and how frequently they make noise. For lower STC values, the sound insulation was not as effective and the average frequency of hearing neighbours simply depends on how often the neighbours are noisy. It is only above about STC 50 that these responses decrease systematically with increasing sound insulation. Therefore sound insulation of greater than STC 50 is required to decrease the disturbance that these noises cause.

If one compares the point at which each curve starts decreasing with increasing STC value, one can estimate where sound insulation starts influencing subjects' perceptions of various types of sounds. For voice sounds, this point is a little less than STC 50. For radio and television sounds as well as more general sounds from neighbours either side, the critical point is about STC 50. However, for music related sounds, the sound insulation must be greater than about STC 55 to reduce its impact on residents. These differences are consistent with the likely strength and the potential disturbance of these sounds.

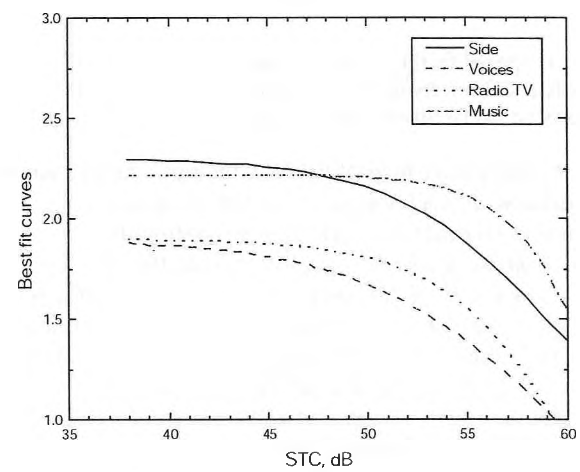

Figure 4. Regression fits to average responses vs. STC.

Conclusions

For most types of sound, the benefits of sound insulation only occur for STC ratings substantially above STC 50. For music related sounds, the sound insulation becomes more effective for STC values well over STC 55. Responses are close to 1 for an STC of 60 indicating that at this point residents would not hear these sounds from their neighbours 'at all' and they were 'not at all annoyed' by them. An effective STC of 55 is therefore recommended as a realistic goal and STC 60 as a more ideal goal for party wall sound insulation.

Flanking Sound Transmission in Wood-Framed Construction

T. R. T. Nightingale, R. E. Halliwell and J. D. Quirt
Institute for Research in Construction, National Research Council, Montreal Road, Ottawa, K1A 0R

1. INTRODUCTION

This paper presents selected results from a research project to study sound and fire resistance of wall/floor junctions intended for multi-family residential buildings. A consortium - CMHC, Forintek Canada, Gypsum Manufacturers Canada, IRC/NRCC, New Home Warranty (Ontario, Alberta, B.C. & Yukon), Ontario Ministry of Housing, Owens Corning Inc., Roxul Inc., and Canadian Home Builders' Association - supported the project.

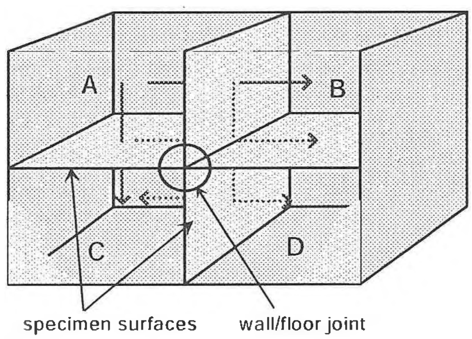

Figure 1: Special facility for the measurements. Party wall assembly and floor divide the space into 4 rooms. Structural transmission via facility surfaces is suppressed.

First, it is necessary to establish terminology. ***Direct*** sound transmission between rooms A and B is by airborne transmission through the party wall separating the two rooms. ***Flanking*** transmission involves all the other transmitted sound energy, which includes other source room surfaces such as the floor, is transmitted by structure-borne paths, and is radiated into the receiving room from various surfaces. The ***Apparent Sound Transmission Loss*** combines the sound energy transmitted directly through the partition and via all flanking paths.

This paper presents only the apparent airborne sound transmission loss between Rooms A and B. Other results - including impact sound transmission, airborne sound transmission between all pairs of rooms, acoustic intensity from various surfaces, and non-standard tests - are given in Report IRC-IR-754.

Measurements were made according to ASTM E336, except that in most cases the sound transmission includes direct transmission through the party wall separating the rooms, plus flanking transmission involving the wood joist floor system. Typical wall and floor constructions are shown in Figure 2. Two wall types were used, both with two rows of wood 2x4 studs. The basic wall has one layer of 5/8" Type-X gypsum board on each face and glass fiber batts filling the inter-stud cavities of one row of studs. The superior wall has 2 layers of 5/8" Type-X gypsum board on each face and has glass fiber batts filling cavities of both rows of studs.

Figure 2:
Wall and floor specimen details for the basic wall with floor joists parallel to the party wall. For clarity, the insulation batts in the stud and joist cavities are not shown.

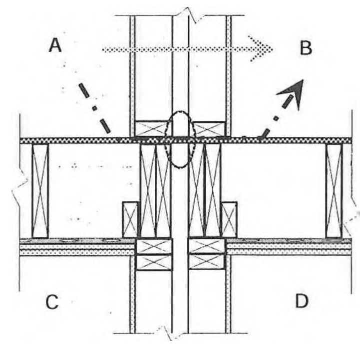

The floors had wood 2x10 joists, with joists parallel to the party wall (as in Fig 2), or perpendicular to the wall with each set of joists supported on one row of studs. Changing joist orientation had little effect on FSTC for this wall/floor combination. The sub-floor membrane was 5/8" oriented strand board (OSB) for most specimens. Substituting plywood caused negligible change.

2. TRANSMISSION AT FLOOR /WALL JUNCTION

The most important detail for flanking was continuity of the OSB or plywood sub-floor across the floor-wall junction. This slows fire spread (a focus of this project), but is also commonly used where seismic resistance or wind loads are of concern. This provided the main structure-borne path.

Previous papers examined the effect of changes in the floor/wall junction to reduce vibration transmission while maintaining adequate fire resistance. The continuous OSB sub-floor gives only apparent FSTC 52 even with the superior wall. Thin sheet steel (on top of the OSB sub-floor, bridging the gap) gives apparent FSTC 57, as does 1" thick gypsum board (filling the gap between the rows of studs across the junction). The best case, FSTC 66, has a gap in the OSB to eliminate the structure-borne vibration; batt or semi-rigid insulation material in the gap handles fire resistance. All these junction details resist fire spread, but some would not provide enough shear bracing for structural performance, especially where seismic loading or high winds are an issue.

This paper focuses on modifying floor systems to reduce the effect of vibration transmission via the continuous subfloor membrane across the floor-wall junction

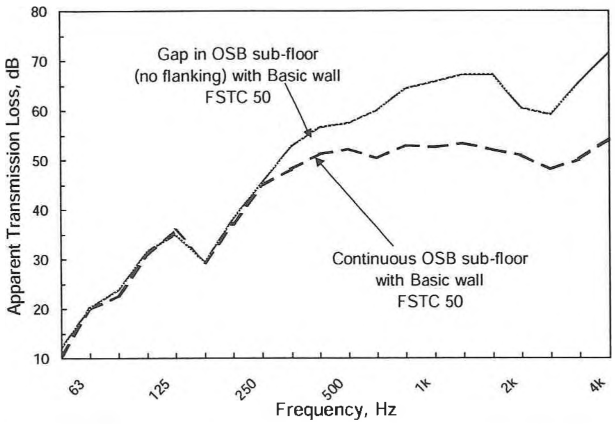

Figure 3: Effect of flanking transmission via the continuous OSB sub-floor in the case with the basic party wall.

The upper (solid) curve in Figure 3 is the apparent sound transmission loss when the flanking path across the wall is eliminated, by cutting the OSB membrane at the party wall between the two rows of studs. The dashed curve shows the lower apparent sound transmission loss when the OSB layer is continuous across the junction. Above 250 Hz, the transmission from one floor surface to the other becomes dominant, and limits the apparent TL. This onset of flanking effects above a characteristic frequency is typical of flanking effects in wood-framed construction. Below about 250 Hz, the flanking path has negligible effect. Changing to the superior wall (not shown), one observes essentially the same apparent sound transmission loss above 250Hz where the floor-floor flanking transmission dominates, because the floor systems are identical. At lower frequencies where direct transmission through the party wall is dominant, the apparent TL increases by about 10 dB with the superior wall, but apparent FSTC increases only from 50 to 52.

3. THE FLOOR/FLOOR PATH

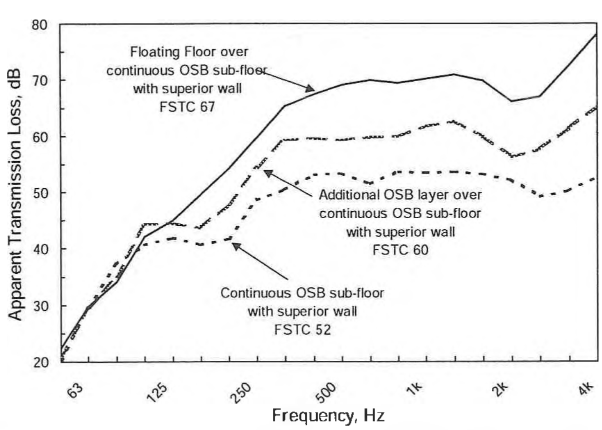

Figure 4: Apparent TL with the superior party wall and various treatments over a continuous OSB sub-floor.

A large improvement can be introduced by treatments over the sub-floor surface, as shown in Figure 4. Improving the sub-floor, by adding a second layer of 16mm OSB stapled on top of the sub-floor within each room (but not across the wall junction) increased apparent FSTC from 52 to 60. This both increases the mass/unit area of the exposed surface (reducing radiation) and introduces an impedance change at the junction (reducing vibration transmission). When an engineered floating floor system (18mm wood chipboard supported on 40mm rock wool material) was added over the continuous OSB sub-floor, FSTC increased to 67, with apparent TL limited over most of the range by direct transmission through the party wall.

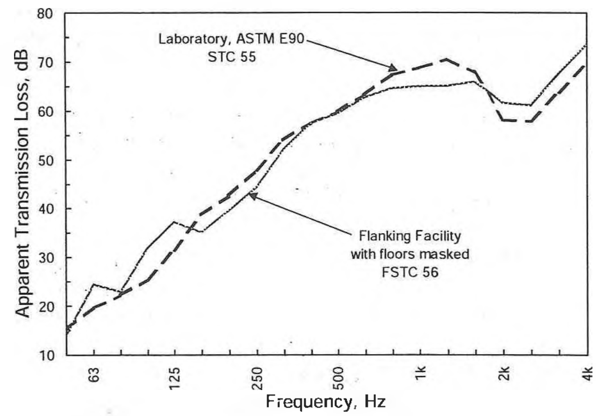

Figure 5: Comparison of laboratory and field TL for basic wall.

Preceding slides have shown that transmission via flanking paths can significantly reduce the apparent sound transmission loss. The comparison in Figure 5 emphasizes the flip side - there is little change due to different transmission through the wall itself. The result here is typical - when a wall system is built with identical materials and construction practice, the laboratory result deviates only slightly from the field performance with the flanking paths suppressed. At low frequencies, results from the flanking facility fluctuate around those from the laboratory, presumably due to modal response of the smaller rooms in the field situation. At frequencies above 2kHz (i.e. above coincidence) laboratory results are generally lower, presumably indicating lower damping. Because edge conditions and room sizes in the flanking facility are expected to resemble common field conditions, similar deviations are probable in the field.

4. SUMMARY

Overall, the key message is that the lower apparent TL observed in the field is often due to flanking. It is *apparent* sound transmission that determines the sound perceived by occupants of adjacent apartments. Flanking effects can significantly lower the apparent sound transmission loss, and cannot be effectively offset by improving the nominal separation (A-B party wall in this case). However, details to control the flanking paths can be developed, to provide a basis for effective designs and retrofit improvements.

In-Situ Sound Insulation Measurement when a Room is Very Absorptive

Trevor R. T. Nightingale and Robin E. Halliwell
Institute for Research in Construction, National Research Council, Montreal Road, Ottawa, K1A 0R

INTRODUCTION

When a noise source is placed in a room the resulting acoustic energy will be contained in two fields, reverberant and direct. The relative magnitude depends primarily on the amount of absorption, room dimensions, and distance from the source. Transmission loss test methods (ASTM E90, E336, ISO 140) assume that the energy density of the reverberant field will dominate. Consequently, laboratory test chambers are large and have little absorption to ensure that the reverberant field dominates, and the sampling positions are located away from sources. Unfortunately, for in-situ measurements there may be significant absorption in the rooms that may cause a marked deviation from these idealized conditions. This paper investigates the sensitivity of the ASTM E336 to absorption in either the source or receiving room and its effect on the number of microphones needed to sample the resulting field.

MEASUREMENT METHOD AND METRIC

The metric used by most European objective based building codes is the weighted apparent sound reduction index (R'_w ISO 140-4), a single number rating derived from sound pressure level difference measurements made without suppressing flanking and normalized to the area of the separating partition and the receiving room reverberation time (RT). A similar result is obtained when ASTM E336 is applied without suppressing flanking paths. In this summary paper the resulting measure is referred to as the "apparent transmission loss", (ATL) and is computed using,

$$ATL = 10Log\left[\frac{1}{N}\sum_{i=1}^{N}10^{\frac{P_{source,i}}{10}}\right] - 10Log\left[\frac{1}{N}\sum_{i=1}^{N}10^{\frac{P_{receive,i}}{10}}\right] + 10Log\left[\frac{S}{0.161V\cdot N}\sum_{i=1}^{N}RT_{60}\right] \quad (1)$$

where P is the resulting sound pressure level (SPL) at the i^{th} sampling position, N is the number of positions in the room, S is the area of the separating element, while V and RT_{60} are volume and the reverberation time of the receiving room, respectively.

Measurements were made using the four-room Flanking Transmission Facility at the NRC/IRC in which realistic sound transmission paths in multifamily dwellings, including flanking, between rooms can be evaluated under controlled conditions. Each room (volume 35-50 m^3) had three incoherent sources below 1.2 kHz and one above this. Nine microphone positions satisfying the ASTM E336 location requirements sampled the SPL.

The ATL was measured in both directions between the three possible room pairs: horizontally separated by a partition wall, vertically separated by a floor, and diagonally where there was no common element (in this special case the normalization area was set to 10m^2). These measurements were made for three absorption conditions, Minimum, Partial, and Maximum. Sheets of 50-mm thick open cell foam were placed on room surfaces not involved in a transmission path. This allowed for coverage on three room surfaces, each orthogonal to the others.

Figure 1 shows that the Partial condition has a receiving room RT that is typically within one standard deviation of the mean value measured in 300 Canadian multifamily dwellings[1]. The maximum condition represents an extreme case.

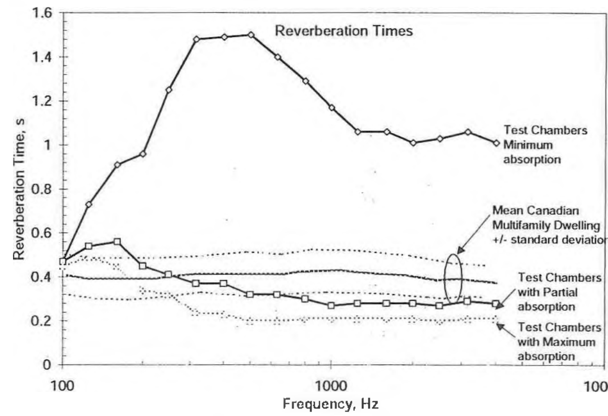

Figure 1: RT for the three absorption conditions examined in this study and the mean for 300 Canadian multifamily dwellings.

MEASURED RESULTS

When all nine microphone positions are used to sample the source and receiving room the mean change in measured ATL (averaged for the three possible room pairs) relative to the case when there is Minimum absorption is typically less than 2.5 dB as shown in Figure 2.

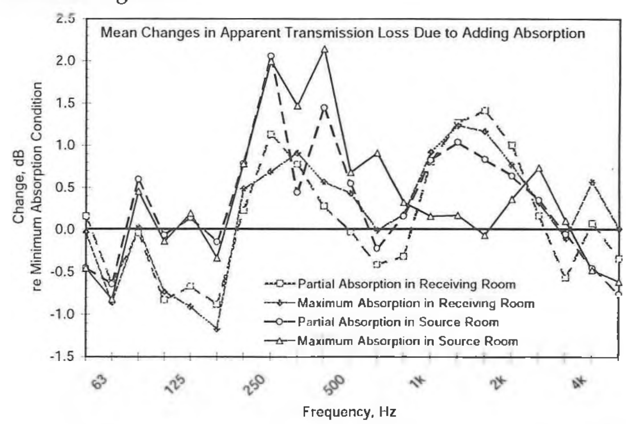

Figure 2: Change in measured ATL due to adding absorption to either the receiving room or source room.

Below about 200 Hz adding the absorption to either the source or receiving rooms had minimal effect which is consistent with the change in the RT which was not as large as in the mid and high frequencies. A significant change occurred in the frequency range, 250-500 Hz, especially when absorption was added to the source room. A physical explanation for this is not known. However, there was also a significant change in this range when absorption was added to the receiving room so it is speculated that this is related to room dimensions which tended to be similar in two of the three orthogonal directions. Above 500 Hz the change due to adding absorption was typically less than 1.5 dB. If ASTM E413 were applied the resulting change in the single number rating would be typically 1 with a maximum change of 1.

ASTM and ISO test methods use the concept of energy balance to express the power transmitted into the receiving room in terms of the resulting SPL (which is assumed to be reverberant) and the room absorption. If the receiving room does not satisfy the necessary conditions then the resulting receiving room SPL will not vary as -10Log(A) where A is the receiving room absorption in m^2. Figure 3, shows that although the correct trends are observed there is a greater change in the absorption correction term than the receiving room SPL. This may indicate the presence of a strong direct field the magnitude of which does not depend on the room absorption.

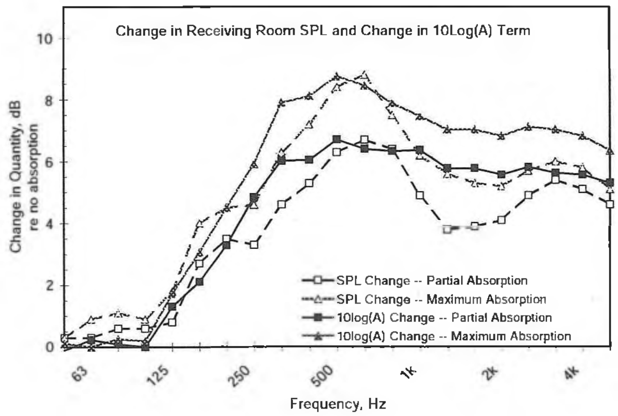

Figure 3: Change in receive SPL and absorption correction term.

SENSITIVITY TO ROOM SAMPLING

To investigate the sensitivity of the measurements to the number of sampling positions, mean values for each quantity were computed using a sub set of 2 through 8 positions of the original nine. The mean values for each possible set of positions were then compared to the mean value for the full set of nine and a standard deviation (STD) computed which was then band averaged, using,

$$STD = \sqrt{\frac{1}{5N-1}\sum_{j=1}^{5}\sum_{i=1}^{N}\left(X_{mean\,all\,nine,\,j} - X_{subset\,value,\,i,\,j}\right)^2} \quad (2)$$

where i is the index to the sampling position and j is the index to the five frequency bands from 125 to 400 Hz, and N is the total number of sampling positions. The Schroeder frequency with Minimum absorption is approximately 400 Hz.

In general, Figure 4 shows that the uncertainty (expressed as STD) increases with increasing absorption and/or with reducing the number of sampling positions. The STD of the absorption correction term is an order of magnitude lower than that for the receive or source SPL. It shoud be noted that the measurements below 1.2 kHz were made using three incoherent sources and reducing the number will increase uncertainty in SPL estimates.

DISCUSSION AND CONCLUSIONS

Since the overall accuracy of the ATL will be determined by the sum of all the uncertainties, the uncertainty of the room correction term, 10Log(A), was insignificant relative to those for the SPL. The change in estimates of the mean SPL proved to be sensitive to the number of sampling positions when the room had significant absorption. Increasing the amount of absorption increased the uncertainty. Thus, the results indicate that measurements in rooms having absorption typical of furnished multifamily dwellings are possible if the room volumes are adequately sampled.

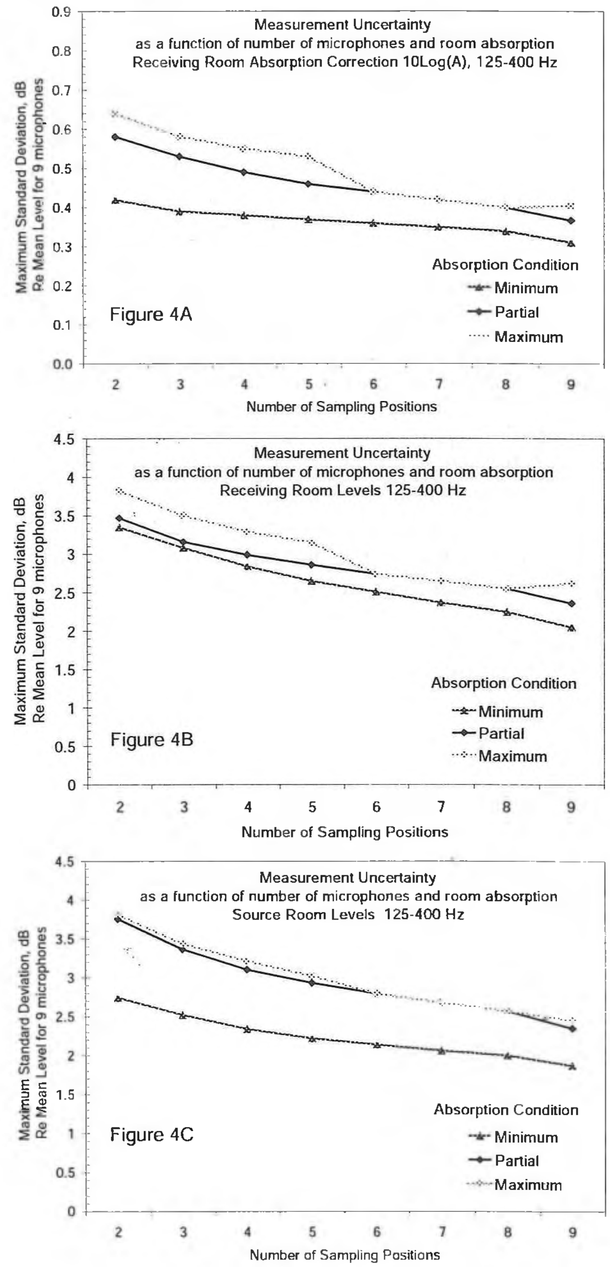

Figure 4: Uncertainty in measures as a function of absorption conditions and number of sampling positions.

REFERENCES

1.) J.S. Bradley, "Acoustical measurements in some Canadian homes," Canadian Acoustics, Vol. 14, No. 4, 1986, pp. 19-21, 24-25.

Sound Transmission through Gypsum Board Walls - Effect of Shear membranes and Framing Details

T. R. T. Nightingale, R. E. Halliwell and J. D. Quirt
Institute for Research in Construction, National Research Council, Montreal Road, Ottawa, K1A 0R

1. INTRODUCTION

This paper focuses on trends observed in the sound transmission results from a research project that studied both sound and fire resistance of wall assemblies intended for multi-family residential buildings. The National Research Council led the consortium project, with support from CMHC, Canadian Wood Council, Forintek Canada, Gypsum Manufacturers Canada, Ontario Min. of Housing, Owens Corning, Roxul, and Can. Home Builders' Assoc.

The series of 70 wall assemblies were all load-bearing constructions with gypsum board surfaces, but they varied in other details. Approximately half had framing of 16-20 gauge steel; the others were framed with wood studs plus a shear-bracing layer to increase the racking strength of the wall. To provide a basis for assessing the range of constructions in common use, the study included typical variations of component materials, as indicated in Figure 1.

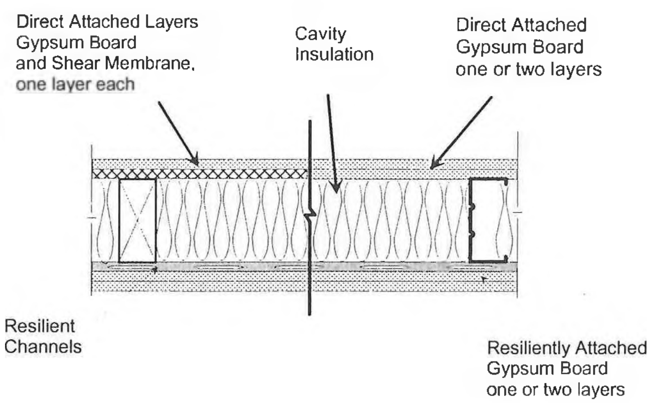

Figure 1: Horizontal cross-section through the wall assemblies.

Assemblies are identified in captions using a short hand coding for components. For surfaces, 'n' layers of Gypsum board 'xx' mm thick is denoted: **nGxx**. Corresponding codes for Oriented Strand Board and Plywood are **OSBxx** and **PLYxx** respectively. For framing members 'xx' mm deep spaced 'ss' mm apart on centre, **WSxx(ss), SSxx(ss),** and **RCxx(ss)** denote Wood Studs, Steel Studs, and Resilient metal Channels. Insulation in inter-stud cavities is denoted **GFBxx, MFBxx, or CFLxx** for Glass Fibre Batts, Rock Fibre Batts, or Cellulose Fibre 'xx' mm thick. For this key, all dimensions are rounded to the nearest mm; for example 12.7 mm gypsum board is listed as G13.

The discussion of factors controlling the sound transmission loss (TL) focuses first on factors controlling airborne transmission, and subsequently on structure-related aspects.

2. FACTORS FOR AIRBORNE TRANSMISSION

Density of the surface layers is the single most important parameter. As shown in Figure 2, the typical improvement in transmission loss (and STC) is 4-5 dB when the number of layers of gypsum board (and hence the mass) is doubled on one side of the wall. Similar changes are observed with both wood and steel studs.

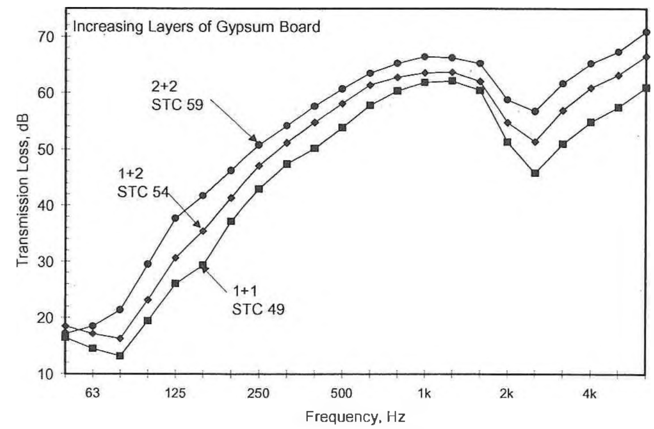

Figure 2: Adding layers of gypsum board to wall construction nG16_SS92(406)_GFB92_RC13(610)_mG16.

Adding cavity absorption improves the TL above 80 Hz, but the effect is smaller at the low frequencies that control STC for these walls. The type of insulation has a slight influence. Data in Figure 3 suggest that for frequencies above 400 Hz,

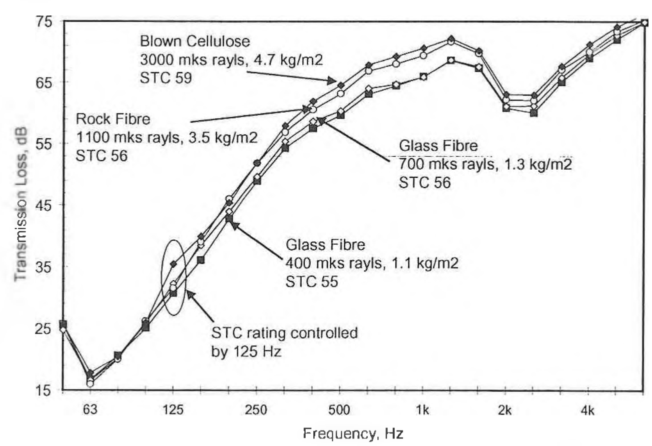

Figure 3: Varying the cavity insulation for wall constructions G16_OSB13_WS89(406)_xxx89_RC13(610)_2G16.

the airflow resistance of the fibrous insulation in the cavity controls the ranking of the walls' transmission loss. The additional mass and any damping introduced by heavier fibrous materials in contact with the surfaces may also contribute. At low frequencies (where the STC tends to be determined and reproducibility is worse) the trend is much less clear. For the few cases with partly-filled cavities, the TL is lower than those shown in Figure 3, but the type of insulation seems less significant.

3. EFFECT OF STRUCTURAL ELEMENTS

Structural elements affect both structure-borne transmission and airborne transmission (via panel boundary conditions).

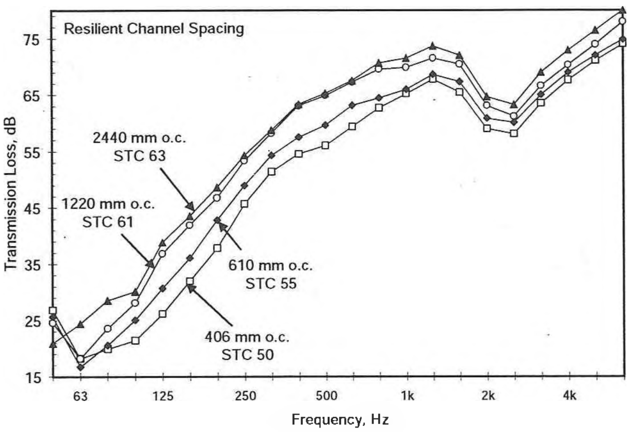

Figure 4: Changing resilient channel spacing in constructions G16_OSB13_WS89(406)_GFB89_RC13(xxx)_2G16.

Resilient metal channels are used to reduce structural transmission in these walls. As shown in Figure 4, the TL rises with greater inter-channel spacing (or equivalently, with fewer channels) approaching a limit as the structural transmission becomes negligible at very large spacing.

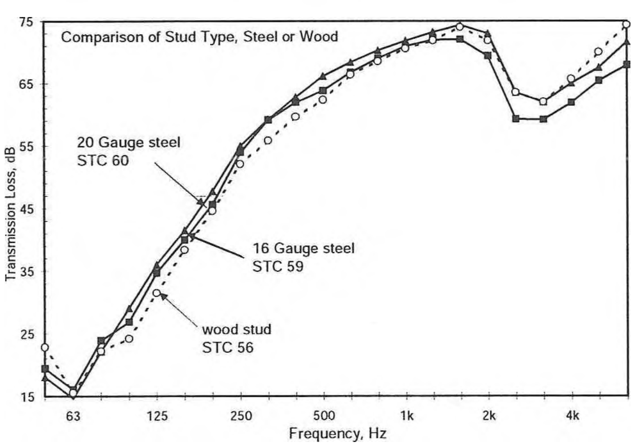

Figure 5: Effect of changing stud type, in wall constructions 2G13_stud(406)_MFB90_RC13(xxx)_2G13.

Because these steel studs are more compliant than wood studs of the same nominal depth, they give slightly greater TL at the lower frequencies, as shown in Figure 5. Regression analysis confirms this trend in STC versus stud type. The lower TL for 16 Gauge steel framing above 1 kHz is unexplained, and may be due to a construction anomaly.

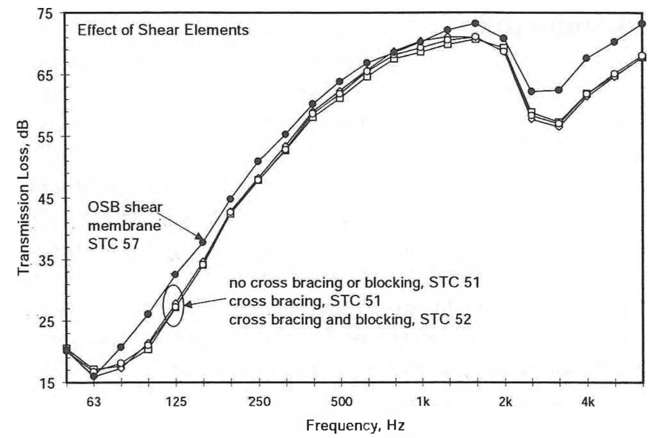

Figure 6: Adding shear bracing to 20 gauge steel-framed wall G13_SS92(406)_MFB90_RC13(404)_2G13.

A major focus of this project was the effect of shear bracing on sound transmission. Figure 6 shows that blocking and/or cross-bracing straps have little effect on TL of these steel-framed walls. Adding an OSB layer gives the highest TL, mainly due to increased surface weight.

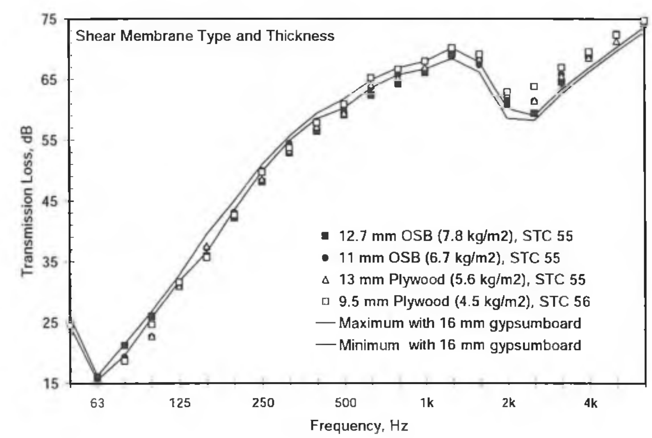

Figure 7: Replacing G16 with shear membrane in wood-framed wall G16_xx_WS89(406)_GFB89_RC13(404)_2G16.

Adding a shear membrane to a wood-framed wall also increases the TL. As shown in Figure 7, the four walls with wood-based shear membranes have quite similar TL. When the plywood or OSB layer is replaced with gypsum board (11 kg/m^2), the TL changes slightly. The increase in surface weight should increase TL by ~2 dB at all frequencies, if behavior matched that in Figure 2. This expected increase is apparent below 500 Hz, but at higher frequencies specimens with the (lighter) shear membranes consistently exhibit higher TL, presumably due to typical stiffness and damping.

The Attenuation of Aircraft Noise by Wood Stud Walls

J. S. Bradley and J. A. Birta
Institute for Research in Construction, National Research Council, Montreal Road, Ottawa, K1A 0R6

Introduction

This paper presents measurements of the effects of: the mass of surface layers, stud size and spacing, structural breaks, and cavity insulation, on the sound transmission loss of exterior wood stud walls. Modern Canadian constructions tend to be more air-tight and to have thicker walls with greater thermal insulation than previously. This investigation of the acoustical properties of such modern wall constructions is part of a larger project to measure exterior building façade components [1] and to develop a computer based procedure for the design of the sound insulation of buildings exposed to aircraft noise.

Measurements were made according to the ASTM E90 procedure but with the frequency range of measurements extended from 50 to 5k Hz. The overall performance of the walls was rated using the ASTM Outdoor-Indoor Transmission Class (OITC).

Key Features of Acoustical Characteristics

Figure 1 illustrates the measured sound transmission loss (TL) versus frequency for two walls that illustrate the important characteristics that are key to understanding the parameters that most influence their overall sound insulation. One wall was the base wall from which many of the comparisons in this study were based. It consisted of a single 13 mm layer of directly attached gypsum board on the interior of 140 mm wood studs at a 406 mm spacing and with glass fibre thermal insulation filling the stud cavities. The exterior surface was vinyl siding on Oriented Strand Board (OSB) sheathing. The other wall was similar except that the interior surface was a double layer of gypsum board mounted on resilient channels. These results show the obvious improvements due to the addition of the structural break created by the use of the resilient channels.

For the results of both walls shown in Figure 1, the dip in the 2.5k to 3.1k Hz region is the well-known coincidence dip, due to the coincidence between the velocity of the incident sound and the bending waves in the gypsum board and OSB panels. However, the low frequency dips more strongly influence overall indoor sound levels for these walls and are therefore more important. For the base wall, without resilient channels, the dip at 125 Hz is the primary structural resonance of the ribbed panel system formed by the surface layers rigidly attached to the stud system [2]. When resilient channels are added to create a structural break, this primary structural resonance no longer exists. However, the two surface layers are then effectively coupled by the stiffness of the air cavity and a mass-air-mass resonance occurs in the 63 Hz band for this wall. The frequency of this resonance is determined by the masses of the surface layers and the stiffness of the contained air and is further modified by the additional stiffness of the resilient channels. Both of these resonances limit the overall performance of the respective walls and have the most important influence on the A-weighted indoor aircraft noise levels.

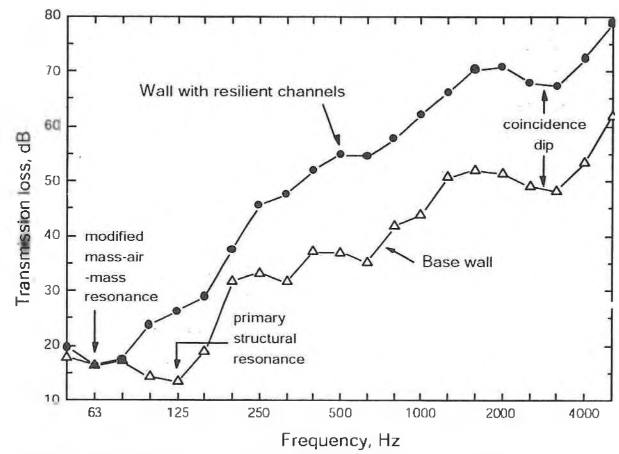

Figure 1. Key characteristics influencing the sound insulation of wood stud walls

Mass of the surface layers

Figure 2 illustrates examples of the effects of varied surface mass for walls without structural breaks. For most changes the increase in OITC rating is approximately 10 times the logarithm of the ratio of the surface masses. Adding brick cladding resulted in a larger increase than this because there was also a 16 mm air gap (with occasional ties) between the exterior sheathing and the brick. All results are limited by the primary structural resonance of the wood stud wall.

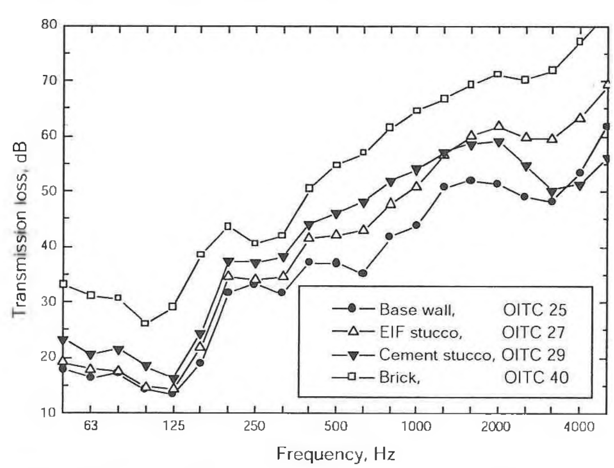

Figure 2. Adding heavier surface layers to the base wall.

Stud Size and Spacing

Increasing the stud spacing and/or the stud size lowers the frequency of the primary structural resonance and hence improves the overall sound insulation of the walls. Figure 3 shows that the effect of stud size is most significant for larger stud spacings. Increasing the stud spacing from 305 to 406 and to 610 mm decreased the frequency of the resonance dip from 200 to 125 and to 80 Hz and would also decrease A-weighted indoor sound levels (not shown).

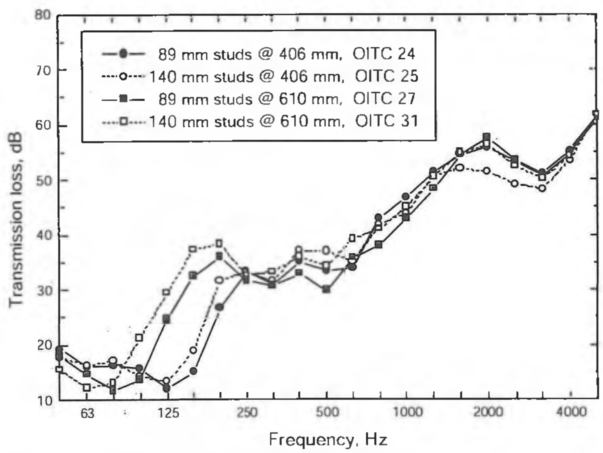

Figure 3. Varied stud size and spacing.

Structural Breaks

Structural breaks were achieved by either attaching the gypsum board using resilient channels or by using staggered stud constructions. Figure 4 illustrates that adding resilient channels eliminates the primary structural resonance at about 125 Hz, but introduces a modified mass-air-mass resonance that limits the low frequency sound insulation. Adding mass to the surfaces of the walls with resilient channels further improves the TL values.

The results in Figure 5 for staggered stud walls show that these walls can be more effective at the important lower frequencies. Adding mass to the surface layers systematically lowers the mass-air-mass resonance and improves the overall OITC rating for these walls. When resilient channels were added to staggered stud walls, the TL values improved above 400 Hz. Stud spacing was not important in walls where there was a structural break.

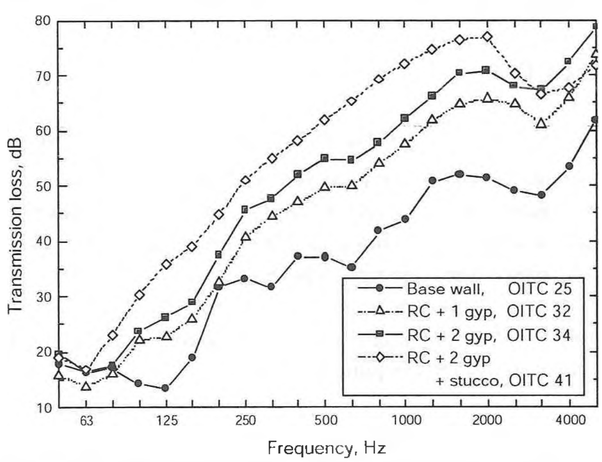

Figure 4. Effects of adding resilient channels (RC).

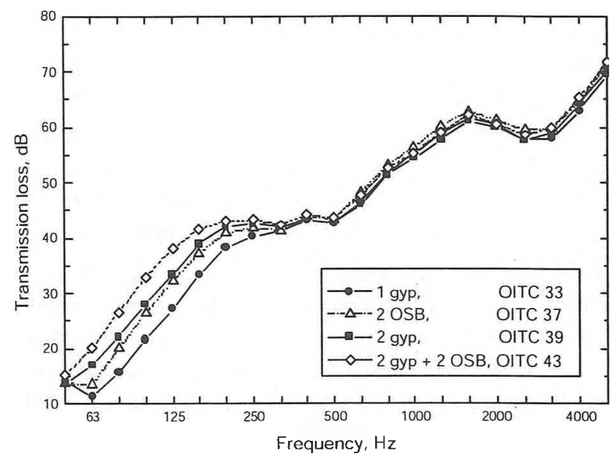

Figure 5. Staggered stud walls.

Cavity Thermal Insulation

The effects of three types of thermal insulation in the stud space were compared in a wall having vinyl siding and OSB sheathing on the exterior and with two layers of gypsum board attached with resilient channels as the interior surface. Varied insulation led to changes in OITC values of 1 or 2 points but these were partially due to the rounding up of the values to integers in the OITC procedure and to the particular wall construction used.

Conclusions

The overall sound insulation of wood stud exterior walls is limited by poor performance at the low frequencies due to one of 2 types of low frequency resonance. It is therefore very important to concentrate on improving the low frequency sound transmission loss to achieve better overall sound insulation.

Acknowledgements

This work was jointly funded by the Department of National Defence, Transport Canada and the National Research Council with additional support from Vancouver International Airport.

References

1. Bradley, J.S. and Birta, J.A., "Laboratory Measurements of the Sound Insulation of Building Façade Elements", Institute for Research in Construction Internal Report IR-818, October 2000.

2. Lin, G-F and Garrelick, J.M., "Sound Transmission Through Periodically Framed Parallel Plates", J. Acoust. Soc. Am., Vol. 61, No. 4, pp. 1014-1018, (1977).

F2/F1 Vowel Quadrilateral Area In Young Children With And Without Dysarthria

Carolyn M. Higgins and Megan M. Hodge

Department of Speech Pathology and Audiology, 2-70 Corbett Hall, University of Alberta, Edmonton, Alberta, T6G 2G4

INTRODUCTION

Previous studies have examined the formant frequencies of vowels produced by children with normal speech development[1,2,3,4]. As expected from acoustic theory, these studies have found that formant frequencies of vowels decrease as a child's age, and vocal tract size, increases. Formant frequencies appear to reach adult values around the age of 12 or 13 years[4]. Kent[5] identified vowel area as one of several acoustic correlates of speech intelligibility. One method of estimating vowel area is to use coordinates of the first (F1) and second (F2) formants of the four point vowels (high front, low front, low back, and high back) to plot a quadrilateral and then determine its planar area.

Using reported formant values[1,2,3,4] it can be shown that the F2/F1 vowel quadrilateral area decreases in size as age increases, that is, when F1 by F2 vowel area is determined using formant frequency values expressed in Hz, intertalker comparisons of vowel are size are confounded by differences in vocal tract size[6]. Differences between acoustic vowel measures produced by individuals with and without dysarthria have also been reported[7,8]. Nearey[9] predicted that a $\log_n$ Hz scale would normalize vocal tract size differences when comparing formant frequency values. Therefore it was of interest to determine if use of a $\log_n$ Hz scale would eliminate the effect of vocal tract size on vowel area across a broad age range of talkers and also be sensitive to potentially smaller vowel areas of dysarthric individuals.

The objectives were to:

1) Extend the results of previous work by testing hypotheses about the effect of age (vocal tract size) on vowel area, expressed in Hz and $\log_n$ Hz scales. It was predicted that a $\log_n$ Hz scale would eliminate the effect of vocal tract size differences on vowel area that are evident in the Hz scale.
2) Test the hypothesis that vowel areas of children with dysarthria would be significantly smaller than those of age-matched peers with normal speech production.
3) Examine the relationship between speech intelligibility and vowel area in age-matched children with and without dysarthria.

METHODS

2.1 Subjects

Recordings produced by six 3 year-old children, six 5 year-old children and six young women, all with normal speech development, and six 5 year-old children with dysarthria were analyzed for this study. Of the children with dysarthria, three were diagnosed with a lower motor neuron impairment and three were diagnosed with central nervous system impairment. Identification rates obtained from normal adults listeners for the vowels in the recorded words used in this study were high for the normally speaking children (Mean = 94.7%; SD = 3.1%), and lower for the dysarthric children (Mean = 70.7%; SD = 16.8%).

2.2 Audio Recordings

Digital audio recordings from the subjects' productions of a subset of 24 words from Form 1: Word Test of Children's Speech (W-TOCS)[10] were measured. Six words were used for each of the point vowels /i/, /æ/, /a/ and /u/ for Western Canadian English.

2.3 Formant Measurement

F1 and F2 values were estimated for each vowel token from wideband spectrograms generated using CSpeech 4.0[11]. A 30 ms window within the vowel was isolated for measurement. This section was taken from a point in the vowel judged to be the most stable. F1 and F2 values in Hz for each vowel token were converted into $\log_n$ Hz and then averaged for each vowel for each subject. F2/F1 planar area for each subject's vowel quadrilateral was calculated in Hz and $\log_n$ Hz scales.

RESULTS

Mean vowel areas in Hz and $\log_n$ Hz scales for each subject group are shown in Table 1. As predicted, for the Hz scale, vowel quadrilateral areas for adult women were smaller than those of children. Older children (5 years) had smaller vowel areas than younger children (3 years). A one-way ANOVA revealed a significant age effect ($F=22.241$, $p=.0001$). Post-hoc analysis revealed significant differences between all age group pairs.

When formant measures were converted to the $\log_n$ Hz scale, a significant difference in vowel quadrilateral area was also found between subject groups ($F= 9.318$, $p=.0023$). Post-hoc analysis revealed that vowel area, calculated in

$\log_n Hz^2$, was significantly larger in three year-olds than in the women ($p=.0024$) but that there was not a significant difference between the 5 year-olds and the 3 year-olds ($p=.0813$) or between the women and the 5 year-olds ($p=.2100$).

Results of a one-way ANOVA demonstrated that the dysarthric children had significantly smaller vowel quadrilateral areas, calculated in $\log_n Hz^2$, than their age-matched, normally speaking peers ($F=5.275$, $p=.0445$).

Vowel quadrilateral areas in $\log_n Hz^2$ for the 5 year-old children with and without dysarthria were correlated with their single word intelligibility scores on the complete W-TOCS. Results showed a moderately strong positive correlation between vowel area and intelligibility scores ($r = .71$).

Table 1. Mean F2/F1 vowel quadrilateral areas in Hz^2 and $\log_n Hz^2$ for subject groups.

	3 year-olds	5 year-olds	Women	Children (Dysarthria)
Hz^2	1078736	748862	468055	527487
(SD)	(94522)	(226980)	(123190)	(122869)
$\log_n Hz^2$	.624	.444	.301	.294
(SD)	(.13)	(.16)	(.09)	(.06)

4. CONCLUSIONS

Vowel area, when measured in Hz^2 and $\log_n Hz^2$, decreases in size as age increases, suggesting that a $\log_n$ Hz scale does not normalize age differences in F2 by F1 vowel area. However, factors other than vocal tract size, such as articulatory differences, might account for age differences in acoustic space.

Vowel areas of children with dysarthria are smaller than those of their age-matched peers.

There is a moderately strong positive correlation between intelligibility scores on the W-TOCS and vowel quadrilateral area, expressed in $\log_n Hz^2$.

Future research will address whether using only vowels that have been identified accurately will reduce differences in vowel quadrilateral area found between children with and without dysarthria.

REFERENCES

Eguchi, S.Hirsh, I.J. (1969). Development of speech sounds in children. Acta Oto-Laryngologica.Supplement, 257, 1-51.

Hodge, M.M. (1989). A comparison of spectral-temporal measures across speaker age: Implications for an acoustic characterization of speech maturation. Unpublished doctoral dissertation, University of Wisconsin-Madison.

Hillenbrand, J., Getty, L.A., Clark, M.J., & Wheeler, K. (1995). Acoustic characteristics of American English vowels. The Journal of the Acoustical Society of America, 97(5 pt1), 3099-3111.

Lee, S. Potamianos, A., Narayanan, S. (1999). Acoustics of children's speech: Developmental changes of temporal and spectral parameters. The Journal of the Acoustical Society of America, 105(3), 1155-1168.

Kent, R., Kent, J., Weismer, G. & Duffy, J. (1998). Selected acoustic measures for various aspects and components of normal and disordered speech production. Presented at the Annual Convention of the American Speech-Language Hearing Association, San Antonio, TX.

Fant, G. (1973). Speech sounds and features. Boston, MA: MIT Press.

Hodge, M. (1999). Relationship between F2/F1 vowel quadrilateral area and speech intelligibility in a child with progressive dysarthria. Canadian Acoustics, 27(3), 84-85.

Doyle, P.C., Raade, A.S., St.Pierre, A., Desai, S. (1995). Fundamental frequency and acoustic variability associated with production of sustained vowels by speakers with hypokinetic dysarthria. Journal of Medical Speech-Language Pathology, 3(1), 41-50.

Nearey, T.M. Applications of Generalized Linear Modeling to vowel data, Proceedings, 1992 International Conference on Spoken Language Processing, 583-586.

Hodge, M.M. (1996). Speech Intelligibility measures of young children with dysarthria. Presented at the Conference on Motor Speech, Ameila Island Plantation, FL.

Milenkovic, P.H., Read, C. (1992). CSpeech 4.0, Laboratory Version [Computer Program], Department of Electrical and Computer Engineering, University of Wisconsin, Madison, WI.

The Relation Of Vocal Emotions And Gender To Convey Urgency Of Verbal Auditory Warnings

G. Robert Arrabito
DCIEM, 1133 Sheppard Ave. W., P.O. Box 2000, Toronto, ON M3M 3B9

INTRODUCTION

One approach for attracting the attention of the aircrew to a dangerous situation and suggesting corrective action is to present a verbal warning. At present, to the best of the author's knowledge, voice messages in the cockpit of aircraft used by the Canadian Forces (CF) are spoken in a monotone voice, and the gender of the voice is male (except in the CF-118 and the AUP Hercules). The author's recent review of military standards pertaining to aircrew station warning signals revealed no rationale for the use of a neutral voice style, and the annunciator's gender was not specified.

Previous findings (1) have shown that subjects can elicit higher ratings of "carefulness" by responding to a female talker speaking in an emotional vocal style compared to a monotone voice. These results may have implications for voice warnings in the cockpit of high performance jets particularly when fast reaction time to auditory warnings is necessary, such as when performing combat maneuvers. In these instances, quicker response to an auditory warning may result in crash avoidance.

The present on-going study was undertaken to examine methods for improving aircrew reaction time to verbal auditory warnings. The "attention getting" of verbal auditory warnings that differed in both vocal style and gender was measured, while subjects were performing a visual tracking task.

METHOD

Subjects. To date 26 females and 26 males participated.

Stimuli. The stimuli were six verbal auditory warnings (Bingo, Caution, Climb, Gear, Lock, and Warning) presently used in the cockpit of some aircraft. Each warning was spoken by a female and male talker in an emotional, monotone, and whisper vocal style. These 36 warning combinations were digitally stored as single channel sound files on the hard disk of the host computer.

Apparatus. Testing took place in an IAC sound booth. The booth contained the host computer, monitor, 6-button response box (one button for each of the six warning names), and chair.

Procedure. Subjects were individually tested in the sound booth. The subject's task was to perform a visual tracking task; when a verbal auditory warning was presented over headphones he/she was to identify the spoken word by depressing the corresponding labeled button on the response box. Following a training session, the subject performed 72 tracking trials. Half of the 72 trials, selected at random, contained 1 cycle of a random ordering of the 36 warning combinations. The same visual tracking task was used in all 72 trials. The duration of each trial was 75 seconds. Half of the subjects were instructed to emphasize the auditory task, while the others were instructed to emphasize the tracking task.

RESULTS AND DISCUSSION

Data collection is presently on-going and thus the reported data constitute a preliminary analysis and are subject to change pending the outcome of the study. Subjects correctly identified the name of the warning in 97.3% of the 1872 trials.

A between- (instructional manipulation having two levels) and within-subjects (vocal style having three levels, talker having two levels, and warning having six levels) ANOVA on subjects' response times (RT) revealed that instructional manipulation and talker both had significant main effects on subject RT ($p < 0.03$). A Tukey pairwise comparison ($p < 0.05$) revealed that the auditory instructional manipulation, and the female talker yielded significantly quicker mean responses. The female talker significantly improved RT by 45 ms. This reduction in RT is approaching a practical significance of 60 ms, a time frame which may imply crash avoidance for a fighter pilot performing a nap-of-the-earth maneuver (2). The emotional voice style yielded the quickest mean RT but this did not significantly differ from the other two vocal styles.

In summary, the preliminary results of the present on-going study are encouraging. The final results may yield recommendations for improving aircrew reaction time to verbal auditory warnings, with the implication that accidents may be avoided.

REFERENCES

Barzegar, R.S., and Wogalter, M.S. (1998). Intended carefulness for voiced warning signal words. *Proc. Hum. Factors and Ergonomics Soc. 42nd Annual Meeting*, 1068-1072.

Haas, E.C., and Casali, J.G. (1995). Perceived urgency of and response time to multi-tone and frequency-modulated warning signals in broadband noise. *Ergonomics*, **38**, 2313-2326.

Age-related effects on temporal processing speed in the inferior colliculus (IC)

Julie R Mendelson, H Jin Lee* and Tasneem Wallani****
*Department of Speech-Language Pathology - **Institute of Medical Science
University of Toronto, 6 Queen's Park Cres. W., Toronto, Ontario, M5S 3H2

Difficulty in understanding speech is one of the most common problems afflicting the elderly population. One factor that may contribute to this is a deterioration in the ability to process dynamic aspects of speech such as the formant transitions (components of speech in which frequency and amplitude vary over time). Underlying this deterioration may be an age-related decline in temporal processing speed in the central auditory system. A number of investigators have suggested that processing speed deteriorates with age. For the aging auditory system, this deterioration may be manifest as a deficit in processing time-varying sounds that contain rapidly changing sounds, such as the formant transitions. Thus, if temporal processing speed deteriorates with age, then our ability to recognize speech could be seriously affected.

A stimulus which lends itself well to studying this type of processing is the frequency modulated (FM) sweep which, in many respects, resembles formant transitions found in a variety of communication signals. We have recently shown that auditory cortical cells recorded from young animals responded best to fast FM sweeps while those recorded from aged animals preferred slower sweeps (Mendelson & Ricketts, 2001). These results suggest that there is a difference in temporal processing speed at the level of the cortex. The next question we asked was whether or not this aging effect was exclusive to the cortex or if it was apparent in subcortical structures such as in the inferior colliculus (IC), an important auditory integration centre in the central auditory system.

METHODS

Experiments were conducted on 18 young (3-4 months) and 12 old (24-30 months) male Long Evans hooded rats. Rats were anaesthetized and maintained at a surgical level of anesthesia throughout the experiment. Animals were placed in a modified head holder and a craniotomy performed over the occipital cortex overlying the IC. Earphones connected to speculate were placed within 3 mm of the tympanic membranes. All extracellular single unit recordings were conducted in a sound attenuating chamber. Following the recording of a unit, a lesion was made (6 mA for 6 sec) for histological verification.

Rats were initially stimulated monaurally through the contralateral ear with pure tone burst stimuli (100 ms duration with a 10 ms rise/decay time, 700 msec interstimulus interval) to determine characteristic frequency (CF) and threshold. Following this, linear FM sweeps ranging from 150 Hz to 45.0 kHz (upward-directed) and 45.0 kHz to 150 Hz (downward-directed) at speeds of 0.8, 0.3, 0.05 and 0.03 KHz/msec were presented at 30 dB above threshold. All stimuli were generated and data collected by a Macintosh computer using the MALab system.

RESULTS

A total of 131 units were examined of which 68 were recorded from young animals and 63 from old animals. The average CF for cells recorded from young animals was 12.3 kHz (range: 2.0-20.5 kHz) and 12.3 kHz (range: 2.0-21.0 kHz) for aged animals. With the exception of 4 units from young rats and 3 units from old rats, all units showed FM speed and/or direction selectivity. These seven units were subsequently eliminated from further analysis.

There was no significant difference between the two age groups for threshold intensity of CF (Young = 49.34 + 1.17 dB; Old = 51.57 $\pm$ 1.01dB: p = 0.15), first spike response latency at threshold CF (Young = 25.46 $\pm$ 1.47 ms; Old= 24.34 $\pm$ 1.58 ms: p = 0.61), or Q_{10dB} value (Young = 1.97 $\pm$ 0.17; Old = 1.88 $\pm$ 0.44: p = 0.85).

Figure 1A shows the comparison of the distribution of preferred speed responses for young and old animals. There was no significant difference in speed preference between the two age groups (c^2 3 d.f.= 3.34, p = 0.43). The majority of units recorded from both age groups preferred the fast and medium speeds while relatively few cells preferred the slower speeds.

For direction selectivity, again there was no significant difference between the two groups of animals (c^2 2 d.f.= 0.064, p=0.97). The majority of cells in both groups were nondirection-selective (Fig. 1B).

For both age groups, preferred speed was independent of CF (Young: r = 0.198, p > 0.05; Old: r = -0.080, p > 0.05). However, for direction selectivity, there was a significant correlation with CF for young (r = -0.338, p < 0.02) but not aged animals.

DISCUSSION

The results from the present study indicate that aging does not seem to affect FM speed selectivity at the level of the IC. Recently, Palombi et al., (2001) found no age-related effect in responses to sinusoidal amplitude modulate stimuli. Collectively, these studies suggest that the locus for an age-related effect in temporal processing speed occurs higher up in the auditory pathway. While we know that temporal processing speed is affected by age at the level of the auditory cortex (Mendelson & Ricketts, 2001), it is unclear if, and to what extent, this function may be affected at the thalamic level which lies between the IC and the cortex. Studies are currently underway to ascertain if there is an age-related effect on processing speed in the medial geniculate nucleus.

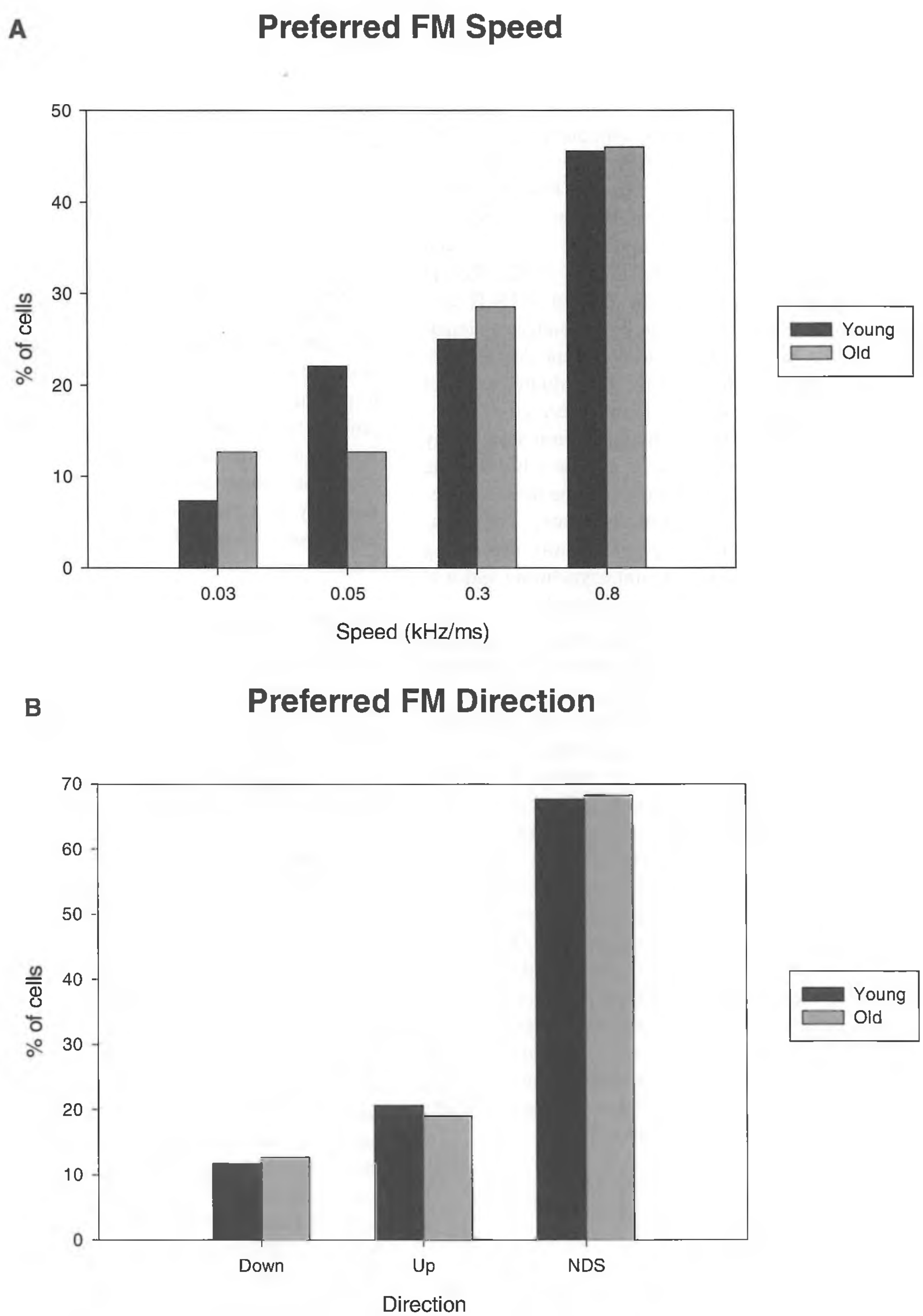

Figure 1. Distribution of preferred speed (1A) and preferred direction (1B) responses for old animals. For preferred speed, the majority of cells (75% or 47/63) preferred the fast and medium speeds. For preferred direction, 68 % of the cells were nondirection-selective.

Temporally Jittered Speech Produces PI-PB Rollover in Young Normal-Hearing Listeners

Terence T. Miranda and M. Kathy Pichora-Fuller
The University of British Columbia, 5804 Fairview Avenue, Vancouver, BC, V6T 1Z3

1. INTRODUCTION

In general, elderly listeners, even those with audiograms in the normal range, have great difficulty when trying to understand language spoken in background noise (e.g., CHABA, 1988). One possible explanation for their poor performance is the existence of an auditory temporal processing deficit such as neural asynchrony (e.g., Pichora-Fuller & Schneider, 1992). Recent studies in our lab have used temporally jittered SPIN-R sentences to test young, normal hearing adults in a range of signal-to-noise (S/N) ratios (e.g., Pichora-Fuller, Schneider, Pass & Brown, submitted). One conclusion from these studies was that the external jitter introduced into the stimuli seemed to simulate, in young normals, the increased internal neural asynchrony hypothesized to exist in the elderly. It is also possible that the results of Pichora-Fuller et al (submitted) may be due to something other than the simulation of neural asynchrony. For example, the jitter may be simulating a type of auditory processing deficit other than, or in addition to, neural asynchrony and it is this other deficit that is behind the pattern of results.

This study uses a different approach to help answer the question of whether or not temporal jitter simulates neural asynchrony in young, normal hearing listeners. The question is addressed by temporally jittering word discrimination lists and presenting them to young adults with normal hearing to see if they will show performance-intensity phonetically balanced (PI-PB) rollover. PI-PB rollover occurs when word discrimination scores decrease with increases in presentation level. There exists substantial clinical and theoretical evidence to suggest that neural PI-PB rollover (e.g., the type found in acoustic neuroma cases) is due to increased neural asynchrony in the auditory system. Results from a number of studies (e.g., Jerger and Jerger, 1971; Meyer and Mishler 1985) provide clinical evidence suggesting a connection between the measure of PI-PB rollover and the existence of neural asynchrony in both the acoustic neuroma and elderly populations. A theoretical link between PI-PB rollover and neural asynchrony can be established using the Average Localized Synchronized Rate (ALSR) computational model of Young and Sachs (1979).

2. METHODS

2.1 Participants

Sixteen young listeners (mean = 27.3 years, SD = 3.5 years), eleven females and five males, were tested. All were native English speakers, had normal middle ear function, and had bilateral pure-tone air-conduction thresholds at 0.25, 0.5, 1, 2, 4, and 8 kHz less than or equal to 20 dB HL. Each participant gave informed consent and received remuneration of $10 following completion of each experimental session.

2.2 Design

Each participant attended two sessions of 1 hour each. The sessions were separated by at least one week to reduce the effects of practice. Uncomfortable listening level (UCL) for speech was determined for each participant and PI-PB functions were created by measuring speech discrimination scores at 40, 55, 65, and (UCL-5) dB HL in each of three conditions: one intact and two different jittered conditions. Participants were randomly assigned to one of four groups, with four participants per group. Experimental conditions (e.g., word list presentation, intensity presentation) were counterbalanced between and within groups. Speech discrimination was tested in the intact and first jitter condition using 50-word lists of Northwestern University Auditory Test No. 6 (NU6). The second jitter condition was tested using 50-word Central Institute for the Deaf (CID) W22 lists.

2.3 Procedures

Digitized CD recordings of all stimuli were fed from a JVC XL-Z232 compact disc player, into a Grason-Stadler GSI-16 audiometer and then into TDH-50P headphones (left ear only). In order to prevent crossover, speech noise was delivered to the right ear at an effective masking level. All equipment was calibrated to ANSI 3.6 1969/ISO 389 1975 standards.

2.4 Stimuli

The intact NU6 and W22 word lists were purchased on a commercial CD recording (Auditec of St. Louis). Each target word and the accompanying carrier phrase was extracted from the original CD, redigitized at a sampling rate of 20 kHz and saved as a *.SND file on a PC hard drive. These soundfiles were used to produce a jittered version of the word discrimination lists. A Fast Fourier Transform (FFT) was used to separate the incoming signal into its component frequencies. For the first jitter condition, the speech (NU6 lists) was then divided into two bands, one above and the other below 1.2 kHz. For the second jitter condition, the speech (W22 lists) was divided into four bands, one above 1.2 kHz, and three below 1.2 kHz (0-.4, .4-.8, and .8-1.2 kHz). For both jitter conditions, only the components below 1.2 kHz were jittered. Jittering was accomplished using in-house software (Jaeger, 2000). Using our method, the sequence of amplitude values in the soundfile is altered by shifting them by delay values. The delay value applied to each sample is determined using a low-pass (LP), band-limited white noise model. Such a noise has amplitude values that are normally distributed with a mean of 0 and a specified standard deviation (SD). Bandwidth (BW) represents the upper cut-off frequency of the LP band-limited noise. The higher the BW value, the more rapid are the changes in amplitude of the noise. The larger the SD, the greater the range of the delay values that can be used in jittering the signal. For each data point in the digitized sound file, the program selects a delay value by referring to a noise generated with an experimenter-specified SD and BW, determining the amplitude value of the noise at the corresponding point in time, and then converting this amplitude into a delay value. The delay value determines the position (in time) of the sample in the original file whose amplitude value is to be substituted in for the data point under consideration. For both jitter conditions, the specified values for jittering were SD = 0.50 msec and BW = 0.5 kHz. In the first jitter condition, all signal components below 1.2 kHz were jittered using one noise exemplar. In the second jitter condition, each of the three bands below 1.2 kHz was jittered using a unique noise exemplar; therefore, at any given sample point, the delay value applied to one band was independent of the delay value applied to the other two bands. After jittering, the jittered low-frequency band(s) and the intact high-frequency band were recombined, re-sampled at 44.1 kHz, saved as *.WAV files, and written back to CD, with a different CD for each of the three conditions. The 1.0 kHz calibration tone was saved to each CD and used for calibration.

3. RESULTS

Speech discrimination scores were measured for each of the 16 participants using intact NU6, jittered NU6 and jittered W22 word lists presented at four levels, 40, 55, 65, and (UCL-5) dB HL, denoted respectively as Level 1, Level 2, Level 3 and Level 4. These results are summarized in Figure 1. While the scores for the intact lists remain high as presentation level increases, scores for the jittered lists decline as presentation level increases. For each PI-PB function (one per condition, 3 per participant, 48 in total), rollover was calculated (Rollover = PBmax – PBmin, where PBmin is the lowest score obtained at an intensity greater than the intensity at which PBmax is observed). Figure #1 clearly shows that the average amount of rollover obtained in the jittered conditions is substantially greater than the rollover in the intact condition. This is confirmed by an ANOVA with group as a between-subjects factor and jitter condition as a within-subjects factor. There was no significant main effect of group on rollover [$F(3,12)=0.42$, $p=0.75$], but there was a significant main effect of jitter condition [$F(2,24)=27.91$, $p<0.001$]. A Student Newman-Keuls test confirmed that rollover in the intact condition was significantly ($p<0.001$) less than in the jitter conditions which did not differ significantly from each other.

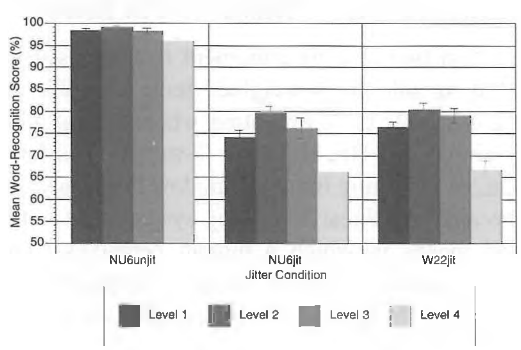

4. CONCLUSIONS

Because the participants in the present study had ipsilateral acoustic reflexes within the normal range and did not exhibit rollover when intact speech was presented, natural mechanical and neural bases for the rollover are ruled out. Thus, the rollover that was observed must be attributed to the simulation of neural asynchrony that involved externally jittering the signal. Importantly, the simulated asynchrony disproportionately disrupted speech discrimination at high presentation levels, thereby ruling out the possibility that the jittering simply degraded the signal in a level-independent fashion. In contrast, other kinds of signal degradation, such as low-pass filtering, would be expected to yield better scores at high presentation levels than at lower levels. Consistent with the clinical and theoretical considerations presented in the introduction, the results of the present study support the hypothesis that PI-PB rollover is due to disruptions of synchrony coding. Furthermore, the present findings support the theoretical notion that synchrony coding plays an important role in the perception of high-level speech. The lack of difference between the two jitter conditions suggests that various types of asynchrony could produce PI-PB rollover and further research will be required to determine how to characterize the exact nature of the asynchrony found in particular pathologies or individual cases.

5. REFERENCES

CHABA: Committee on Hearing, Bioacoustics, and Biomechanics, Working Group on Speech Understanding and Aging. (1988). Speech understanding and aging. JASA, 83: 859-895.

Jaeger CP. (2000). Jitter14.exe [computer program]. Vancouver: CJA Consulting.

Jerger J, Jerger S. (1971). Diagnostic significance of PB word functions. Arch Otolaryngol 93:573-580.

Meyer DH, Mishler ET. (1985). Rollover measurements with Auditec NU-6 word lists. J Speech Hear Disord 50:351-356.

Pichora-Fuller MK, Schneider BA. (1992). The effect of interaural delay of the masker on masking-level differences in young and old adults. JASA, 91(4): 2129-2135.

Pichora-Fuller MK, Schneider BA, Pass HE, Brown S. (Submitted). Temporal jitter disrupts speech intelligibility and memory.

Young ED, Sachs MB. (1979). Representation of steady-state vowels in the temporal aspects of the discharge patterns of auditory-nerve fibers. JASA, 66:1381-1403.

Quantifying Receptor Annoyance From Low Frequency Industrial Noise In The Environment

David C. DeGagne and Will Remmer
Alberta Energy & Utilities Board, 640 Fifth Avenue S.W., Calgary AB, T2P 3G4

1 INTRODUCTION

The Alberta Energy & Utilities Board has been conducting research for several years in an attempt to quantify annoyance levels from Low Frequency Noise (LFN). With this information it will then be possible to begin deliberations on a low frequency adjustment to be implemented into the next EUB Noise Control Directive. Currently the EUB Interim Directive ID 99-8 uses A-weighted energy equivalent (L_{Aeq}) to measure the sound intensity level that in turn determines if a facility is in compliance. It has long been believed that the use of the A-weighted scale does not accurately address the impact of low frequency noise (LFN) from industrial operations on nearby residents. The A-weighted scale ignores a large proportion of sound that is in the low frequency range, typically below 200 Hz. Therefore, in some situations, sound pressure levels emanating from industrial facilities measured at a resident location will not register as an A-weighted energy equivalent (L_{Aeq}) value that exceeds the regulatory requirements yet will contain a significant LFN component (which is known to be the source of annoyance) that is essentially discounted by the A-weighting metric.

2 IMPACTS OF LFN

LFN produces masking effects in the medium and higher frequency ranges. Speech sounds are strongly modified by amplitude. Conversation is disturbed although speech remains intelligible. The masking property of LFN cannot be addressed using the current A-weighting scale. For example a low frequency component measures 50 dB at 50 Hz on the linear scale (dB). When this is translated to the dBA scale it measures 20 dBA. This in turn will have little effect on augmenting the L_{Aeq} level. The 50 Hz band will have a greater effect when masking of sounds is taken into consideration than the dBA scale represents.

As mentioned previously, the purpose of the research is to establish the need to address LFN specifically within the Noise Control Directive. This research has focused primarily on physical and mental health issues related to LFN and the differential response to LFN between genders. As industry grows larger, the effects of noise grow more and more out of control. At the same time, peoples' expectancies for their quality of life increase. When these two facts coincide, the issues related to LFN problems grow exponentially.

The fundamental characteristic of LFN is that of "intrusiveness." After much research, it has been suggested that LFN contributes to annoyance responses by:

- creating a sensation of pressure in the ear,
- periodically masking effects on medium and high frequency sound with a strong modulation effect that can disturb normal conversation, and
- by creating secondary vibrating effects typically experienced within homes.

Analysis of documented noise complaints would seem to be consistent with the above suggestions. With continuous exposure to LFN, behavioral dysfunction such as task performance deterioration, reduced wakefulness, sleep disturbance, headaches, and irritation, can occur.

LFN does not need to be considered "loud" in order for it to cause such forms of annoyance and irritation. One significant characteristic of LFN is that it is found to be more difficult to ignore than higher frequency noise. Individuals suffering from LFN annoyance have been known to describe it as

> omnipresent - impossible to ignore - worse indoors (due to the effects of vibration) - unable to locate, and difficult to tune out.

Unlike high frequency noise, LFN is difficult to suppress. Closing doors and windows in attempt to diminish the effects of LFN make the noise worse, due to the propagation characteristics of LFN and the low-pass filtering effect of structures. Individuals often become irrational and anxious as attempts to control LFN fail, serving only to increase the individual's awareness of the noise.

There is quite a significant difference between genders in their response to loudness. Experiments conducted by N. Broner and H. G. Leventhall concluded that males tend to react to loudness with a significantly higher response than females do. The annoyance response remains similar between genders, although males seem to be less sensitive to low noise levels and more sensitive to high noise levels than females.

3 ALTERNATE MEASUREMENT TECHNIQUES

In this section two new measurement techniques using C-weighted along side the A-weighted scale is explored. C-weighting is similar to A-weighting when dealing with frequencies above 200 Hz. However C-weighing is far more sensitive to A-weighting for detecting low frequency sounds. This is because it's linear weighting system does not try to mimic the means in which a human perceives sound, it weights all frequencies equally, with the exception for infrasound, less than 16 Hz, and ultrasound, 8000 Hz and higher.

The first technique is slightly more lenient with respect to current regulatory requirements and would leave the majority of gas plants and compressor stations in compliance. However, a few facilities that do have serious problems with LFN would certainly be affected if this new metric were incorporated into the next iteration of the Noise Control Directive. The second technique takes a more stringent approach to addressing LFN. It incorporates the same method of locating the presence of LFN however requires that a 1/3 octave band spectrum analysis be performed.

3.1 TECHNIQUE #1

The first technique calculates the difference in dBC L_{eq} and dBA L_{eq} values resulting from a comprehensive sound survey. The magnitude of difference between the two scales of measurement can determine if a low frequency component likely exists.

Our research suggests that a difference equal to or greater than 20 dB between the dBC L_{eq} and dBA L_{eq} values can be considered abnormal in comparison with the Internationally Standardized Weighting Curves for sound level meters. C-weighted and A-weighted measurements, according to these curves, begin to deviate at a frequency around the 300 Hz band increasing to a spread of 10 dB at 200 Hz and nearly 30 dB at 50 Hz. Field measurements taken at residences (under representative conditions as defined by the Noise Control Directive) that result in differences between C and A-weighted sound pressure values greater than 20 dB correlate strongly with complaints where the expressed symptoms have been consistent with typical LFN annoyance. Most of the residents where the dBC L_{eq} minus dBA L_{eq} value is less than 20 dB are able to more readily accept the remnants of industrial noise that is in compliance with the current regulatory requirements.

Usually where the value of dBC L_{eq} minus dBA L_{eq} exceeds 20 dB, a linear spectrum bar graph will display a pronounced tonal component somewhere between the 16 Hz to 200 Hz band range. This tonal component should be present to verify that a LFN situation may exist. The properties of the tonal component should be that on either side of the pronounced tone there should be at least a 5 dB difference in adjacent bands. Research suggests that without the presence of a distinct tonal component LFN may contribute to the noise environment but should not cause excessive annoyance to the average individual.

3.2 TECHNIQUE #2

The second technique is quite similar to the first except takes a more rigorous approach. The advantage of this technique is that more cases of LFN will be routinely identified reducing the likelihood of missing a genuine concern. The disadvantage of course is the probability that some cases of LFN will result where the matter could have been solved with a less technical approach.

Technique #2 consists of using a difference of 15 dB from the dBC minus dBA readings and conducting a full frequency spectrum analysis. Many researchers say that with a difference of 15 dB between readings there is usually a LFN issue present. This technique differs from the first because in this case all 1/3 octave bands are examined particularly those in the low frequency range. The amplitude for the spectrum analysis should always be in linear units (dB LL_{eq}). The shape of the spectrum graph becomes of interest because the level of annoyance associated to LFN is directly related to the magnitude in which frequencies differ from one another. In most situations a decreasing slope of the spectral graph will be observed. If the difference between adjacent octave bands is more than 9 dB or the difference between 1/3 octave bands is more than 3 dB consecutively for at least four (4) 1/3 octave band widths an increased annoyance with LFN will likely be expressed. Research with pink noise has confirmed that annoyance levels are generally reduced where sound pressure levels at each frequency decrease at a rate of less than 3 dB/octave band.

As in the first case a tonal component must also be present in the low frequency portion of the spectrum. To qualify the tonal component must be pronounced in the graph and have at least a 5 dB difference with adjacent bandwidths. With industrial facility noise measured at the receptor location, usually some distance away, the low frequency component dominates the spectrum. If the transition in the spectrum from low frequencies to high frequencies is not gradual, then LFN is often noticed by nearby residents in the sound environment even though sound pressure levels are below the 40 dBA L_{eq} permissible limit for most rural residences.

4. VALIDATION OF TECHNIQUES

The first technique was tested using two sets of comprehensive survey data. The first survey to be analyzed was from data collected at Residence "A" at a survey conducted on July 13-14, 1999. Results are as follows; the noise level during the nighttime period was 42.1 dBA L_{eq} and 64.0 dBC L_{eq}. The difference between dBC and dBA is 21.9 dB.

This is over the 20 dB difference that the first method suggests for when a LFN component may exist. The spectrum analysis (Fig 1) showed a pronounced tonal component in the low frequency range at 63 Hz. The difference with the adjacent bands is 16.3 dB, between 50 Hz. AND 13.3 dB between 80 Hz 1/3 octave band. At 63 Hz the band is pronounced in the spectrum. This satisfies the spectrum analysis criteria clearly demonstrating a low frequency tonal component at 63 Hz.

A second set of data was analyzed again using the first technique. The data was gathered on the night of June 15-16,

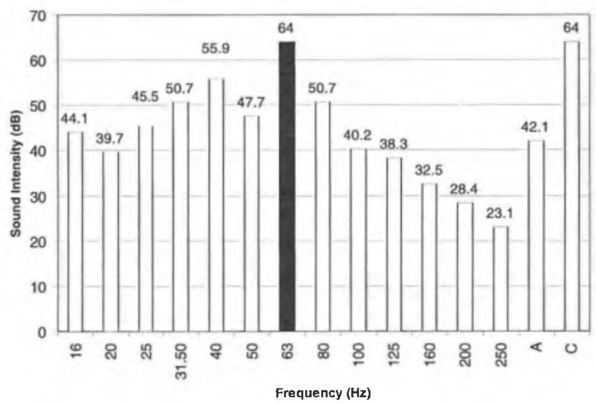

Figure 1. Low Frequency Spectrum (Isolated) LLeq Residence "A" - Nighttime Period

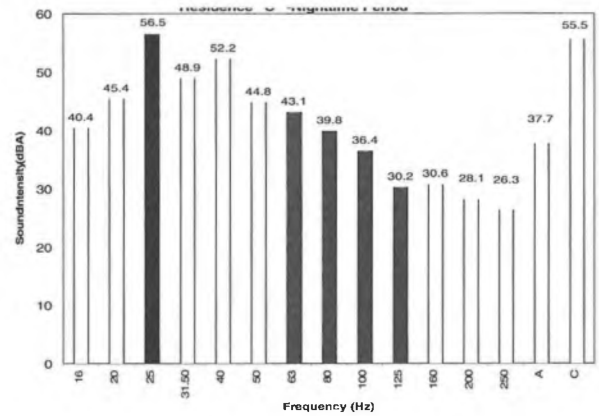

Figure 3. Low Frequency Spectrum (Isolated) LLeq Residence "C" - Nighttime Period

2000 at the Residence "B". The sound level readings were 60.3 dBC L_{eq} and 40.0 dBA L_{eq} respectively. The difference between the two readings is 20.3 dB. A spectrum analysis (Fig 2) shows that there is no pronounced tonal component. The resident confirmed in an interview that they did not experience any of the symptoms associated with LFN. Standard noise control measures at the industrial facility addressed the problem by reducing the sound pressure level at the residence to within the regulatory limits.

An Analysis using the second technique was preformed for a survey conducted on the night of June 6-7,2000 at Residence "C". In this case one of the residents complained of noise affecting sleep patterns due to its constant presence in and around the home. This technique looks at data where the difference between dBC L_{eq} and dBA L_{eq} is >15 dB. Also a full spectrum analysis is preformed to determine if LFN is a major factor of the noise. The sound pressure level readings were 55.5 dBC L_{eq} and 37.7 dBA L_{eq}. The difference of dBC and dBA was 17.8 dB. While the full spectrum analysis confirmed a low frequency tonal component, the 1/3 octave band analysis (Fig 3) was able to show a decrease of more than 3 dB for four successive octave bands between 63 Hz to 125 Hz with an overall difference in sound pressure levels of 12.9 dB which is above the 9 dB limit for technique #2.

Residence "D" was also assessed using the second technique. Data gathered on August 1-2, 2000 showed measured readings of 56.4 dBC L_{eq} and 39.9 dBA L_{eq} , a difference of 16.5 dB. Spectrum analysis (Fig 4) was preformed using the prescribed method.

Analysis showed that although the difference between dBC and dBA reading is greater than the 15 dB limit and between the 40 Hz to 80 Hz bands the decrease is greater than 3 decibels per band there was not a tonal component present. In this case LFN was not identified strictly using only the results of technique #2. Unless the residents complained about excessive annoyance consistent with LFN descriptors, the industrial operator would need only demonstrate compliance with the regulatory requirements as they currently exist and not take extraordinary steps to address a specific tonal component

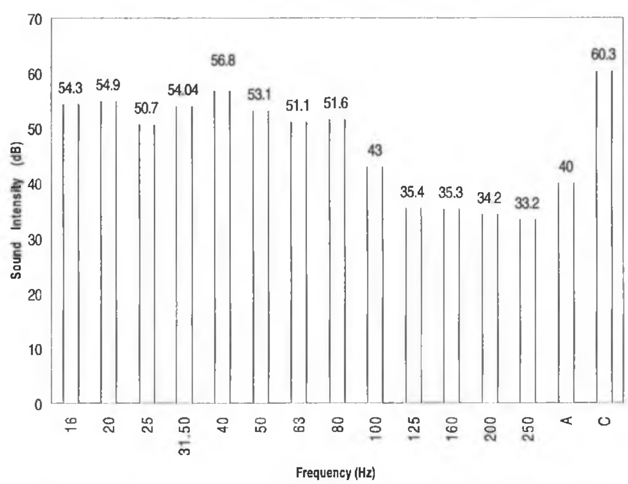

Figure 2. Low Frequency Spectrum (Isolated) LLeq Residence "B" - Nighttime Period

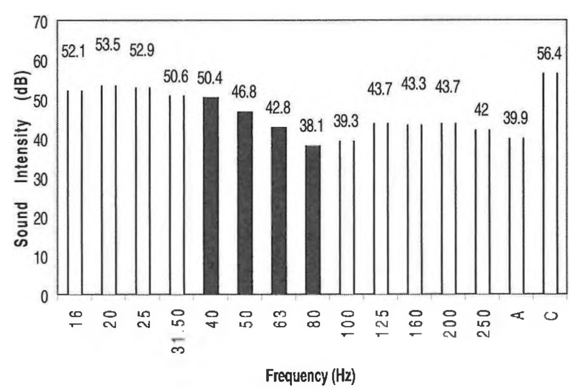

Figure 4. Low Frequency Spectrum (Isolated) LLeq Residence "D" - Nighttime Period

5. DISCUSSION OF RESULTS

The previous section tested the methods that have been proposed. The result from the first method shows that a difference of >20 dB between dBC L_{eq} and dBA L_{eq} requires a LFN assessment to be performed. In the first example the difference was above 20 dB and a tonal component in the low frequency range exists. A written evaluation of the noise should also support this claim. In the second example the difference was also above 20 dB however there was not a tonal component present. From talking to the residents from the second example and evaluating the situation first hand it could be concluded that LFN did not play a major role.

The results when using the second technique of detecting LFN also proved that a difference of >15 dB between dBC L_{eq} and dBA L_{eq} along with an appropriate spectrum analysis confirming a tonal component can yield valid results regarding the presence of LFN. Again if one of the criteria is lacking the impact on nearby residents to industrial noise should be minimal if regulatory compliance requirements are met.

It has been proposed tentatively (Lambert & Vallet, 1994) that when the difference between dBC and dBA is 10 dB or more a penalty of 5 dBA should be added for an Leq that is <60 dBA. If this difference of 10 dB were put into the next intern directive almost all facilities would be over this margin. The use of 10 dB cannot be considered unless all facilities find better methods of eliminating low frequency noise. The use of 20 dB difference would be a more realistic number to be used at the present time. Method one uses a simple procedure to find if LFN is a factor in the noise environment. With the use of method two many more facilities would require a LFN assessment to be performed. This method should be implemented once the first method is firmly established and found too lax for assessing LFN.

An improvement to technique #1 would be to perform a complete spectrum analysis in the low frequency range to identify a significant tonal component that could cause a significant amount of annoyance. This is due to the fact that the threshold of hearing for humans below 31.5 Hz must have a sound intensity >60 dB in order to be audible. This could lead to only tonal components above 31.5 Hz to be used in the determination of a tonal component if the 1/3 octave band frequency analysis is used to satisfy the criteria from the first method. This may prove problematic to regulators and industry as a large tonal component in one of the bands below 31.5 Hz, could result in severe vibrations or harmonics with a dwelling causing annoyance to the resident.

An improvement to technique #2 could be determining whether the margin of 3 dB per 1/3 octave band decrease is too small when analyzing free field data. Some references state that if the hearing threshold for 50% of the population has been exceeded in the low frequency range then LFN must be reduced [2]. However others state that if a decrease of over 7.4 dB/octave band is present then a LFN problem exits [3]. The mentioned value of 9.0 dB/octave band or 3 dB per 1/3 octave band was arrived at rather arbitrarily because it was believed that 7.4 dB/octave band was too small of a decrease for analyzing field data and it would be too hard for existing facilities to meet this standard. Further research would have to be conducted using data from the field and other references so that representative spectrum values may be established.

6. CONCLUSIONS

Low frequency noise is an issue that must be resolved to improve the current system of noise impact assessments and complaint resolution in Alberta. European standards such as those used by the Dutch Noise Annoyance Foundation are having some success in identifying LFN problem areas. In Alberta's case if technique #1 was implemented into the regulatory requirements, the major cases where LFN is a serious problem will be addressed. This is a reasonable first step in the improvement of regulating LFN related to industrial facilities. Technique #2 on the other hand would likely affect a much larger number of facilities. Using the second technique would be too onerous on regulators and industry alike. More research must be conducted to verify the validity of technique #2 using a variety of objective data to determine if it may have some role in the future.

The authors' believe that Technique #1 be considered in the next review of the Noise Control Directive as a means for addressing low frequency noise. The authors are also of the opinion that implementing such an approach into the regulations will not be overly punitive to industry in achieving compliance or complex for regulators to administer.

The outcome will hopefully result in a reduction of LFN issues with an added benefit of improved relationships between rural residents, industrial operators trying to meet regulatory requirements as well as being responsible neighbours, and regulators who want fair, balanced and enforceable policy.

9. REFERENCES

1 'Guide 38, Noise Control Directive User Guide', Alberta Energy and Utilities Board (November 1999)

2 G.P. van den Berg, W. Passchier-Vermeer, 'Assessment of Low Frequency Noise Complaints.' Science Shop for Physics, (Jan, 2000)

3 W. Tempest, 'Infrasound and Low Frequency Vibration', Academic Press Inc. (1976)

4 M. Tesarz, A. Kjellberb, U. Landstrom, K. Holmberg, 'Subjective Response Patterns Related to Low Frequency Noise', (August, 1997)

5 D. DeGagne, M. Hamm 'The Current State Of Quantifying Receptor Annoyance Related To Low Frequency Noise In The Environment' (April, 2000)

6 B. Berglund, Lindvall T., 'Community Noise', Archives of the center for sensory Research, 1995, 2(1), 1-195. www.nonoise.org

7 'Noise Control Regulations-Oregon Administrative Rules', Chapter 340, Division 35 – Department of Environmental Quality

8 Marsh A., 'Low Frequency Noise' UWA, 1999, University of Western Australia

Perceived Urgency Of Non-Verbal Auditory Alarms In The CH146 Griffon Helicopter

G. Robert Arrabito, Todd A. Mondor, and Kimberley J. Kent
DCIEM, 1133 Sheppard Ave. W., P.O. Box 2000, Toronto, ON M3M 3B9

INTRODUCTION

Non-verbal auditory alarms in the cockpits of aircraft are intended to alert the aircrew to a present hazard, to indicate the degree of danger of the hazard, and to suggest corrective action. When alerted by an alarm, the aircrew may continue to perform the ongoing task(s), make further observations concerning the alarmed condition, or take immediate action to address the alarmed condition. In many instances the perceived urgency conveyed by alarms is inadequate due to an incorrect mapping of the alarm's psychoacoustic parameters to the triggering situation (1). Accurate coding of urgency may increase detectability and reduce the time to address the alarmed condition.

The present research was undertaken to determine if the psychoacoustic parameters of the non-verbal auditory alarms in the CH146 Griffon helicopter convey the appropriate level of danger. Ratings and rankings of the perceived urgency of these alarms were measured.

METHOD

Subjects. Three groups of subjects participated, comprised of 25 male pilots of the CH146 Griffon helicopter, 25 female non-pilots, and 25 male non-pilots.

Stimuli. The stimuli were five non-verbal auditory alarms presently used in the CH146 Griffon helicopter. The names of these alarms are Crypto (signals encrypted radio message), ELT (emergency locator transmitter), Low Rotor (indicates rotor speed has dropped below preset RPM value), Radalt (indicates aircraft has descended below preset altitude), and Selcal (signals an in-coming call on high frequency). These alarms were digitally stored as single channel sound files on the hard disk of the host computer.

Apparatus. Testing took place in a quiet room. The room contained the host computer, monitor, keyboard, and chair.
Procedure. Subjects were individually tested in the quiet room. The subject's task was to indicate the perceived urgency of an alarm presented over headphones (i.e., to rate the importance of the heard alarm based solely on its acoustic properties). The source of the heard alarm was not revealed to the subjects. A rating scale was used to make the judgements, with 0 indicating low urgency and 100 indicating extreme urgency. Following a training session, 50 trials comprised of 10 cycles of a random ordering of the 5 alarms, were presented. Subsequently, the pilots were required to complete a questionnaire in which they were asked to rank the urgency of the CH146 Griffon helicopter alarms. The purpose of the questionnaire was to compare the perceived level of urgency with the urgency of the triggering situation.

RESULTS AND DISCUSSION

Preliminary data analysis are given. A between- (group having three levels) and within-subjects (alarm having five levels) ANOVA on subjects' median ratings of perceived urgency revealed that the only significant main effect was alarm ($p < 0.0001$). A Tukey pairwise comparison ($p < 0.05$) revealed that the means of ratings of perceived urgency for all alarms significantly differed from one another with the exception of Radalt and Crypto. The ELT alarm was perceived as the most urgent, followed by Low Rotor, and then Selcal. The Radalt and Crypto alarms were perceived as being the least urgent. Participants' ratings of perceived urgency appear to be based on the acoustic properties of the alarms. Previous research has shown that physical characteristics such as frequency composition, repetition rate, amplitude, and harmonic relation of the frequency components can significantly influence the listener's interpretation of the urgency of an auditory alarm (1).

For each alarm, a Spearman correlation was performed between the pilots' median ratings of perceived urgency and their corresponding ranks of that alarm as indicated in the questionnaire. All correlations yielded non-significant results ($p > 0.05$). These findings are in agreement with (2) who found no significant correlation between the rating of perceived urgency of auditory alarms used in hospital operating rooms when judged by practicing anaesthetists and the clinical urgency as judged by senior anaesthetists.

In summary, the five tested alarms have different levels of encoded urgency, but these are poorly mapped to the urgency levels of the triggering situations.

REFERENCES

Edworthy, J., Loxley, S., and Dennis, I. (1991). Improving auditory warning design: Relationship between warning sound parameters and perceived urgency. *Hum. Factors,* **33**, 205-231.

Finley, G.A., and Cohen, A.J. (1991). Perceived urgency and the anaesthetist: Responses to common operating room monitor alarms. *Can. J. Anaesthesia,* **38**, 958-964.

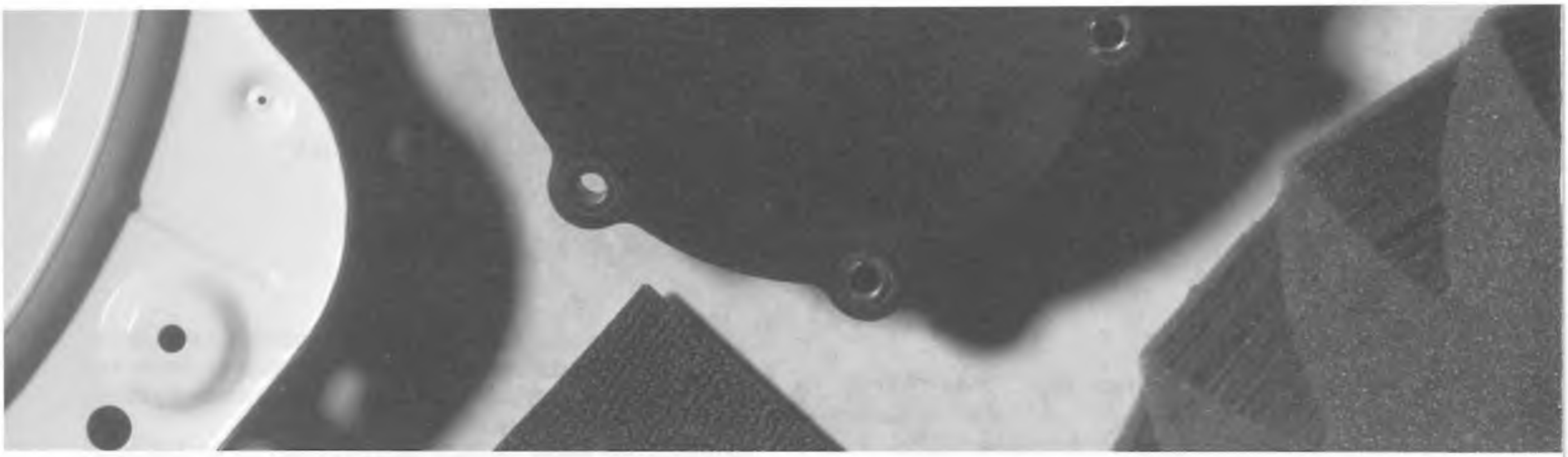

USE OF FEM/BEM TO IMPROVE HANDSFREE TELEPHONE AUDIO QUALITY

Stéphane Dedieu and Philippe Moquin
Mitel Networks, 350 Legget Drive, Kanata, Ontario, CANADA, K2K 2W7

INTRODUCTION

The telephone audio band ranges from 300 to 3400 Hz for traditional telephony and 150 to 7000 Hz for wideband audio. In spite of such a wide bandwidth numerical methods offer a valuable design tool. Previous work has investigated main factors to be taken into consideration in the model [1]. This paper presents a case study on a telephone conference unit, and will show some interesting aspects of the design process required. First some theoretical basics of the full structure/acoustic problem are presented and commented. Secondly, the Finite and Boundary element model is presented. Results are analysed and practical solutions are brought to improve the acoustic receive performance.

THEORETICAL BACKGROUND

The telephone can be considered as an elastic structure S enclosing a fluid cavity and radiating sound in the external domain. Let P_1 and P_2 be the pressure in the internal and external domain, f the force on the loudspeaker diaphragm, and U the normal diaphragm displacement field. To solve the full coupled vibro-acoustic problem a mixed variational (structure/internal fluid) and integral formulation (external fluid) is used. After discretization by finite and boundary elements, it leads to the following linear system [2]:

$$\begin{bmatrix} K-\omega^2 M+A & -C_1 & B+\dfrac{C_2}{2} \\ -C_1^t & \dfrac{H}{\rho_1\omega^2}-\dfrac{Q}{\rho_1 c^2} & 0 \\ \left(B+\dfrac{C_2}{2}\right)^t & 0 & \dfrac{D}{\rho_2\omega^2} \end{bmatrix} \begin{Bmatrix} U \\ P_1 \\ P_2 \end{Bmatrix} = \begin{Bmatrix} f \\ 0 \\ 0 \end{Bmatrix} \qquad (1)$$

Where K and M are the structural stiffness and mass matrices, A the acoustic admittance matrix, C_1 the structure/internal fluid coupling matrix, C_2 and B the structure/external fluid coupling matrices and D the external fluid admittance. H and Q are the internal fluid matrices linked to the internal compression and kinetic energies. U, P_1, P2, f are nodal displacement, pressure and force field vectors. Using the cavity and the elastic structure eigen modes, and eliminating P_1, P_2, the structure modal displacement field vector d is solution of the linear system:

$$[\mathbf{Z_m} - \mathbf{Z_{ar}} - \mathbf{C_r}\, \mathbf{Z_f^{-1}}\, \mathbf{C_r^t}] \quad \{d\} = \{g\} \qquad (2)$$

where: $\mathbf{Z_m} = \Omega_s^2 - 2\, i\omega\eta_s\Omega_s - \omega^2\, \mathbf{I}$ is the modal mechanical impedance matrix, $Z_f = \dfrac{1}{\rho_1\omega^2 c^2}[\Omega_f - 2i\omega\eta_f\Omega_f - \omega^2 I]$ and Z_{ar}, the modal acoustic impedance matrices for the internal and external fluid.

Ω_s, Ω_f are the natural angular frequencies matrices, I the identity matrix , C_r the modal structure/internal fluid coupling matrix and d and g the modal displacement field and force vectors. P_1 and P_2 can be determined depending on d.

Notice that the modal coupling matrix C_r terms do not depend on frequency but only on the geometry of the cavity and structure modeshapes. According to equation (2), when the forcing frequency is close to a cavity natural frequency, one term in Z_f^{-1} tends to infinity, so that the correspondent displacement vector d component must tend to zero. This means that close to a cavity resonance and depending on the shape of the coupling matrix C_r, the structure displacement field can be "blocked". This will likely happen when the coupling between an acoustic mode in the cavity and a structural mode is important, and may have an impact on the external frequency response.

ACOUSTIC MODEL OF A CONFERENCE UNIT

The system is a telephone conference unit with a diameter of about 16 cm and a height of 6.5 cm. The loudspeaker (64 mm diameter) has its first resonance frequency f_0 close to 260 Hz. The first step is to construct a simplified model where unnecessary details are eliminated. For example, since in normal telephony the maximum frequency is 3400 Hz, details much smaller than 10 cm are eliminated in the cavity as they are not relevant to the model. Also it has been previously shown [1] that from medium frequencies and above, the housing has little influence on the acoustic radiation compared to the loudspeaker diaphragm. The structure is meshed with shell elements, the acoustic cavity with volume finite elements and the external fluid with a layer of boundary elements. IDEAS Vibro-Acoustic with Rayon solvers were used for the simulation.

First cavity eigenfrequencies:

0 Hz
1200 Hz
2000 Hz
2300 Hz

First structure eigenfrequencies:

210 Hz
260 Hz (loudsp.)
475 Hz
640 Hz
935 Hz (loudsp.)
......

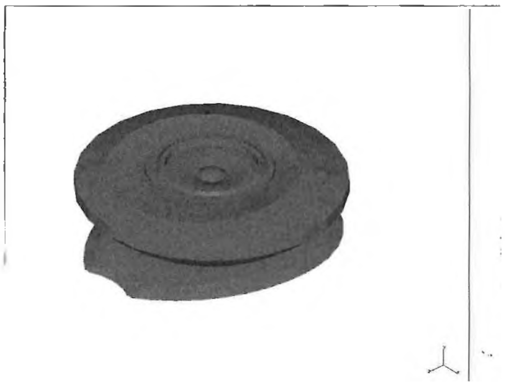

Figure 1: Description of the Conference Unit on its stand. Boundary Elements mesh. (IDEAS – Vibro-Acoustics)

Effect of acoustic modes on the loudspeaker response:
The loudspeaker's light diaphragm has a high mobility due to a low stiffness and relative low damping in this case (about 11 % for the 1st diaphragm mode f0). Therefore, more than the housing (2.7 mm thick plastic), the diaphragm is very sensitive to acoustic resonance in the cavity. After computation and as expected, recalling equation (2) above, we notice that close to cavity resonance, significant notches appeared in the sound pressure response at the receiving position (50 cm). The most critical notch appeared close to the third resonance, where the acoustic mode has an axi-symmetric shape with an antinode in the centre, at the position of the loudspeaker. As the coupling term between this cavity mode and the first diaphragm mode is important, the phenomenon described at the end of section 2 is very strong. This result was confirmed by measurement.

As manufacturing constraints prevent the use of porous material in the cavity, we decided to solve this problem by designing a cap to de-couple the loudspeaker from the housing cavity. A closed cap proved to stiffen the diaphragm, shifting up the first resonance. A cap with a leak was designed to properly "load" the diaphragm shifting down f_0.

Breathing mode:
The in-vacuum structure modal analysis exhibited a kind of housing "breathing" mode at about 1.2 kHz likely to be driven by the loudspeaker vibration. The initial design of the conference unit had only screws around the perimeter top and bottom parts. Despite the fact the housing vibration levels are much smaller than those of the diaphragm, we took no risks and decided to add a central post linking the cap and the bottom to prevent this kind of structural resonance, and avoid any buzzing noise.

MEASUREMENTS

Once plastic parts were manufactured we were able to verify our modelling predictions. We performed a measurement of the conference unit receive characteristics. Figure 2 shows the receive frequency response at 50 cm, in a semi-anechoic condition as specified in ITU P.340. We can clearly see the notches at 1.5kHz, 2.0kHz and particularly at 2.2kHz illustrating the computational prediction. Also shown is the frequency response of the system with the cap and the post as we designed using the modelling results. The frequency response is clearly improved and meets the standard for speakerphones.

CONCLUSIONS

Provided that the physics is mastered and given some simplifying assumptions, numerical modelling can be effectively used to model telephony type enclosures and provides reasonably good results even at medium frequencies and above. The major advantage is that many acoustical problems can be solved before any physical model is made. This saves money, as we do not have to modify plastic tools. It also saves significant design time, as the acoustic design is more likely to work in the first iteration as in this case.

REFERENCES

[1] Joris Brun-Berthet; *Utilisation de plans d'expérience pour choisir la modélisation acoustique d'un téléphone mains-libres, Proceedings CAA 1999, pp 102-103.*

[2] Philippe Jean; *Une méthode variationelle par équations intégrales pour la résolution de problèmes intérieurs et extérieurs de couplage élasto-acoustique*, Ph.D. Thesis, Université de Compiègne, France, 1985.

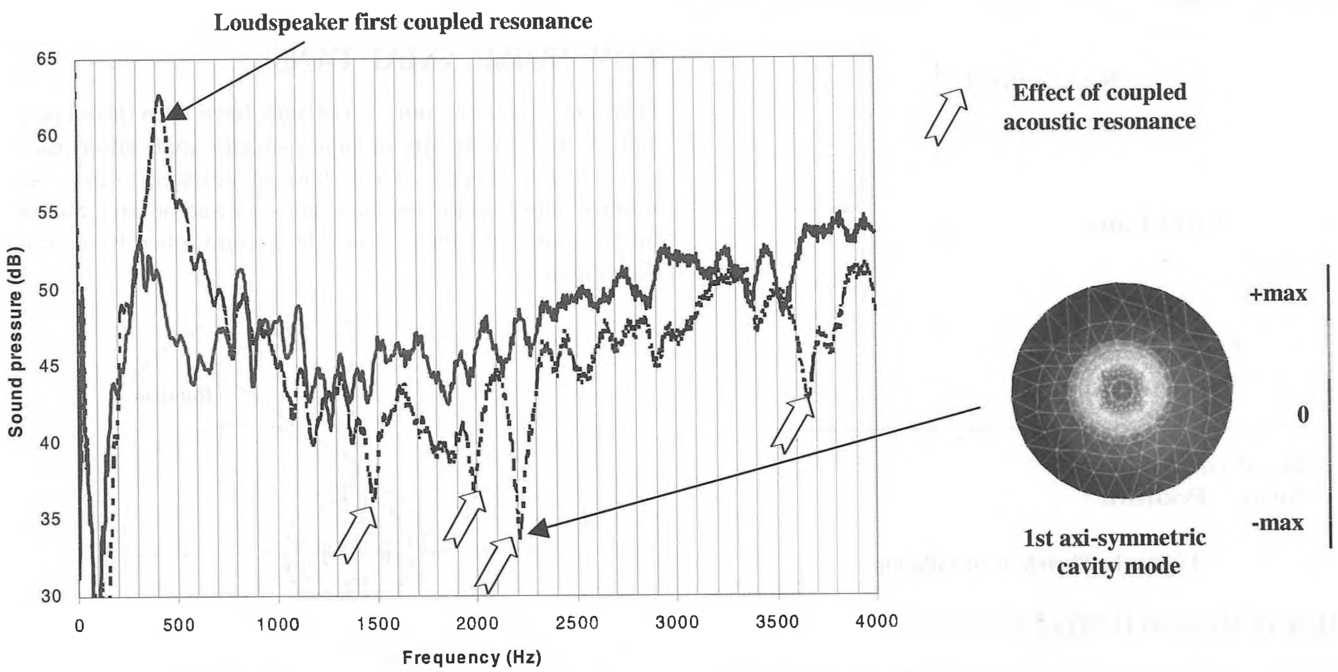

Figure 2: Measured receive response at 50 cm (Ear Reference Point-ITUP340). Initial response (dotted line) and improved response after use of a loudspeaker cap (solid line)

Case Study: The Use Of 'High-Solidity' Low Noise Axial Fans To Reduce Noise From A Rooftop Air-Handling Unit

Robert D. Stevens
HGC Engineering, 2000 Argentia Road, Plaza 1, Suite 203, Mississauga, Ontario, L5N 1P7

INTRODUCTION

Controlling the noise from axial (propeller type) condenser fans in an air-handling unit is a challenge, since these fans typically cannot accommodate the added back-pressure introduced by silencers, acoustical hoods or lined plenums. In existing installations where noise from such a unit is found to be excessive, the options for noise control are often severely limited. This paper presents a case study, in which the newer generation of 'high-solidity' low-noise axial fans were found to be an effective means of significantly reducing the noise impact of an existing rooftop air-handling unit.

PROBLEM DESCRIPTION

The air-handling unit of concern was a 15 ton heating/cooling unit, with a pair of 30" diameter propeller fans used to move outdoor air over the condenser coil. The unit was located on the roof of the podium level of the building. About 9 metres away was the residential component of the building – a multi-storey tower with with overlooking balconies (see Figure 1).

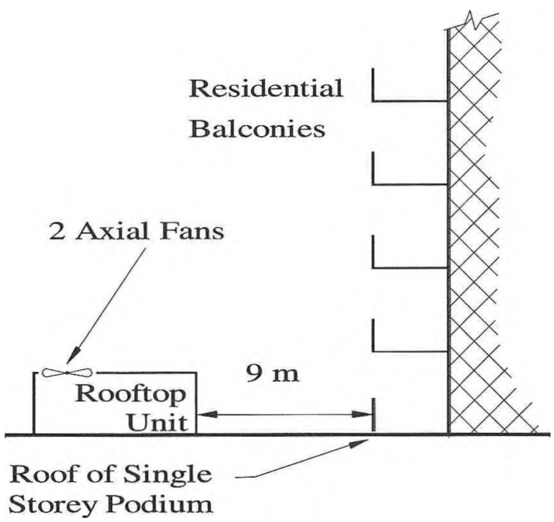

Figure 1: Sketch of Installation

MEASURED SOUND LEVELS

With the existing condenser fans operating, the sound level at the balconies was about 60 dBA. The typical nighttime ambient sound level at the balconies was 45 to 50 dBA. A noise reduction of about 15 dBA was desired.

Sound intensity methods were used to measure the overall sound power of the unit. The results are presented in octave bands, and overall dBA, in Figure 2, along with the manufacturer's published sound power levels. While there were slight differences in octave band values between the measured and published sound power levels, the overall dBA level was almost identical. An examination of the measured sound power levels indicated that virtually all of the measured sound power was attributable to the axial fans.

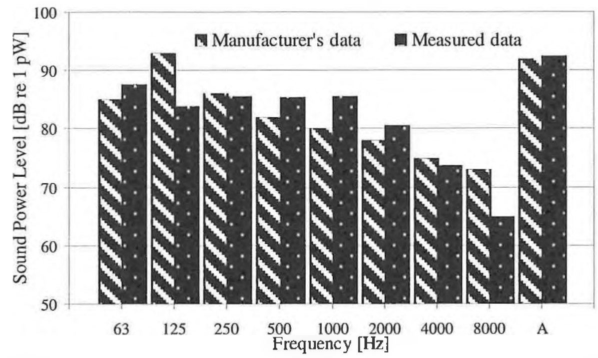

Figure 2: Sound Power Levels of Existing Rooftop Unit

LOW NOISE AXIAL FANS

In recent years, low noise axial fans have been developed, and are in use primarily in large-diameter applications such as cooling towers[1]. These fans are referred to as 'high solidity' fans because the blade area, viewed on axis, almost fully occupies the circular profile circumscribed by its tips (See Figure 3).

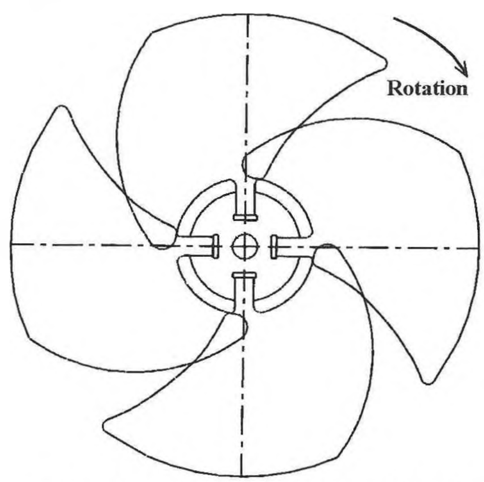

Figure 3: High Solidity Low Noise Fan

The blades are forward swept with a high pitch, and overlap each other in the axial direction. These fans achieve their noise reduction through increased efficiency, such that they can be run at about half the rotational speed of an ordinary axial fan for a given airflow and static pressure.

For this project, a manufacturer of the 'high solidity' low noise fans was contacted. Although the typical use of these fans involves sizes in excess of 28 feet in diameter, smaller diameter fans were found to be available as a special order item. A 30" diameter low noise fan blade was selected by the manufacturer to have comparable flow volume and static pressure characteristics.

NOISE REDUCTION OF NEW FANS

The pair of selected high solidity fan had a combined sound level power level of 76 dBA, overall, according to the manufacturer's published data (see Figure 4). The combined sound power of the two existing fans, as measured in-situ was 92 dBA. The resulting noise reduction possible by replacing the fans was anticipated to be 16 dBA.

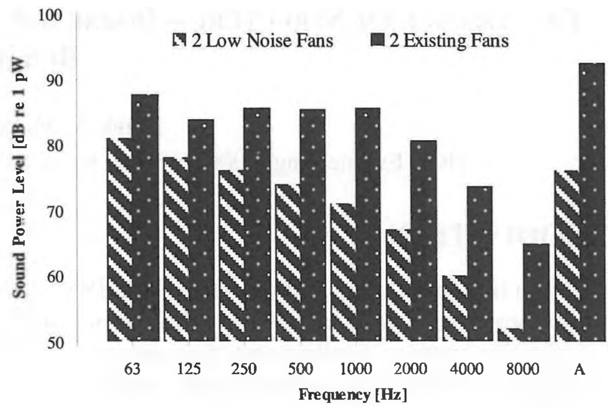

Figure 4: Published Data for Low Noise Fans vs Existing

Procurement and installation of the new fans was yet to be completed for this project, at the time of writing.

References

van der Spek, Henk F. *Advanced Low Noise Air Cooling Fans*, Presentation at the Alberta Acoustical Society "Spring Conference on Environmental and Occupational Noise. April, 2000

THE ABSENCE OF STRUCTURE – BORNE SOUND TRANSMISSION REGULATION IN THE ONTARIO BUILDING CODE

Mark A. Melo, Brian V. Chapnik
HGC Engineering, 2000 Argentia Road, Plaza 1, Suite 203, Mississauga, Ontario, L5N 1P7

INTRODUCTION

The Ontario Building Code (OBC), last revised in 1997, regulates airborne sound transmission through demising structures separating suites or dwelling units from any other areas in a building [1]. However, structure-borne sound transmission (SBST) can potentially be the most dominant sound transmission path between two spaces, yet it is not regulated in the OBC. Figure 1 illustrates the potential dominance of SBST compared to airborne sound transmission in a residential condominium unit situated above a fitness centre. The high levels of airborne sound reduction compared to the relatively low levels of vibration reduction between the fitness centre and the living room in the unit above are apparent. The tenant of this unit had concerns originating from floor impacts in the fitness centre, which were found to travel through the building structure to the unit above.

This paper outlines how SBST can propagate, describes why regulation of SBST is desirable, and suggests methods for reducing this sound transmission path in building construction.

BACKGROUND

SBST involves the transfer of vibrational energy from one structure to another through physical connections. Due to low damping of typical building components, a significant amount of the vibrational energy is not dissipated near the source of the vibration. The vibrational energy can then be transferred to any structures in direct contact, with the amplitude of the resulting vibration on the contacting element being a function of the nature of the connection between the two structures.

In multi-tenanted buildings such as residential condominiums and office buildings, there are many vibration sources. These sources can include mechanical equipment such as pumps, chillers, and boilers, and physical activities such as jumping, walking, and the moving of objects. For example, noise generated by a pump is transmitted through both the flanges and through the contained fluid into the adjacent piping. As the pipe runs and risers extend through the building, they must be supported from the structure at various locations. If these connections are rigid, then the pipe vibrations can cause the adjacent structures to vibrate at the same frequency. Depending upon the type of physical connection, the amplitude of vibration may not be significantly reduced, and the resulting vibration and/or sound radiated from the building structure may be perceptible.

The acoustical environment within a space can be significantly impacted by vibrational motion of the room surfaces. These effects may include sound intrusions caused by radiation from these surfaces and perceptible vibratory motion on the surfaces of lightweight supported objects. These effects have the potential to be disturbing to those subjected to them.

REGULATION

The OBC does not currently include any regulations to prevent significant vibration propagation throughout building structures. In Appendix A-9.11.1.1 of the OBC, the potential annoyance caused by SBST is discussed and a recommended level of impact isolation is provided. However, impact isolation is not mandated by the OBC. As a result, some buildings do not achieve a suitable level of vibration isolation, and SBST can be the dominant form of sound transmission. In addition, vibration isolation for vibrating equipment supported from the building structure is suggested, but not required. The result of the lack of regulation of SBST is that relatively simple methods of vibration isolation within building structures are commonly not incorporated into the building design by profit-minded developers.

SBST can be addressed at the source, along the path of transmission, or at the receptor. Source isolation usually involves installing a resilient layer on surfaces subject to vibrational impacts and balancing the vibrating equipment to reduce the amplitude of the oscillations. Path isolation can be achieved by ensuring that structural discontinuities or separations are present between the vibration source and receiver, installing vibration isolation between the source and the structure, and by incorporating vibration damping treatments on the transmitting structure. If these methods are not feasible, then the vibration of the receiver can be reduced by treating the radiating surfaces with a resilient layer or by vibration damping [2]. The type of vibration reduction method depends on the source of the vibration. Impact-induced vibration can successfully be dampened by altering the interaction between the source and receiver through the use of rubber, plastic, or other soft cushioning material. Noise induced by plumbing vibrations can be addressed with flexible connections and resilient pipe mountings, usually incorporating a liner, pad, or sleeve between the pipe and support structure.

Mechanical equipment isolation can be reduced through semi-rigid mounts, such as molded rubber or neoprene pads made of a resilient material, springs, or a combination of the two.

These vibration isolation methods all involve replacing a rigid connection with one that is able to successfully isolate the vibrations that would otherwise pass through it. The methods suggested are relatively easy and inexpensive to install during construction. However, if the vibration propagation characteristics of the structure and building components are not considered during design and construction, then costly retrofits may be required due to future complaints.

REFERENCES

[1] Ministry of Municipal Affairs and Housing, *Ontario Building Code 1997 containing the Building Code Act and O. Reg. 403/97*, June 1999 update.

[2] Harris, C.M. *Handbook of Noise Control*, McGraw Hill Book Company, 1979.

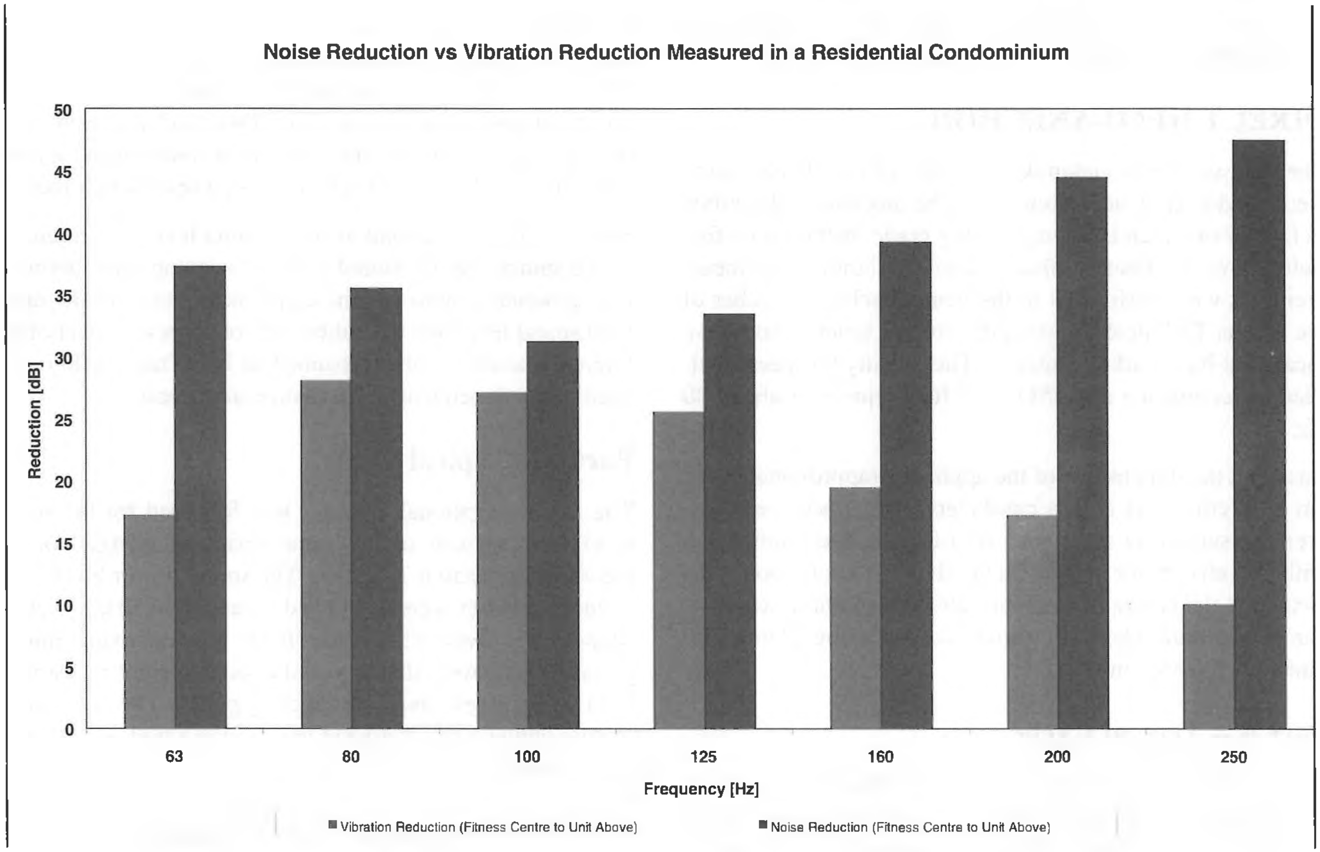

Figure 1: Noise reduction compared to vibration reduction measured between a fitness centre and the unit above. Typical sources of impacts in the fitness centre were simulated, such as the skipping of rope, the dropping of weights, and treadmill activity. Those activities did not provide sufficient signal to noise ratios in frequency bands outside of the 63 to 250 Hz range, and were excluded from the results.

Comparison Of Product Sound Level Emissions: Direct Hemi-Anechoic Versus Reference Reverberant Methods

Alex P. Lorimer
HGC Engineering, 2000 Argentia Road, Plaza 1, Suite 203, Mississauga ON L5N 1P7

INTRODUCTION

There are numerous methods of quantifying the sound level emissions from consumer products, many of which are contained in international standards. These methods are generally divided into reverberant field and "free field" (including hemi-anechoic) types. They can further be divided into direct and reference sound power determinations. This article provides an approximate statistical comparison of the results obtained by a direct hemi-anechoic method versus a reference reverberant method for a consumer product, namely a conventional household refrigerator-freezer. The statistical validity is limited by the sample size of six.

DIRECT HEMI-ANECHOIC

The measurements undertaken for this phase of the testing were conducted in accordance with the procedures described in ISO 3744 which is an engineering grade method for a free field above a reflecting plane (hemi-anechoic). The measurements were performed in the hemi-anechoic chamber of the Atoma Technical Centre, a division of Intier Automotive located in Newmarket, Ontario. This facility has been qualified in accordance with ISO 3745 for frequencies above 80 Hz.

Based on the dimensions of the appliance (approximately 75 cm x 75 cm x 164 cm), a parallelepiped defined the measurement surface at a distance of 1.0 m in each dimension with the refrigerator upright on the floor. A microphone was located at the centre of each face and at each three-way corner of the parallelepiped, above the reflecting plane (i.e., nine microphones in total).

Part A – Typical Cycle

After 24-hours of continuous typical operation to reach steady-state, sound levels averaged over 30 seconds were recorded simultaneously for all microphones at 1, 5, and 7 minutes from the beginning of a cooling cycle. The sound power was calculated as described in the standard based on the nine sound levels and the dimensions of the parallelepiped. These sound powers were then equated to sound pressures from an idealized point source at one meter over a reflecting plane. The 1, 5, and 7-minute equivalent sound levels in dBA were averaged to produce an overall sound level from a typical operating cycle.

Part B – Component Contributions

The sound level measurements were repeated in the middle of the subsequent cycle, but with the individual components operating sequentially (i.e., the compressor, then the evaporator fan, and finally the condenser fan). The same calculations were performed to arrive at 1-metre equivalent sound levels for each component. The total sound level of each unit was then calculated based upon the energy sum of the component sound levels.

REFERENCE REVERBERATION

These measurements were conducted by a laboratory associated with the product manufacturer, and as such, details on the measurement procedure were not fully disclosed. However, it is understood that the measurements were conducted in general accordance with ISO 3742 which includes determination of the sound power of a source using a comparison to a reference sound source in a reverberant room.

Specifically, a 32-second average sound level of a reference sound source was measured with a traversing microphone in a reverberant chamber. The difference between this measured sound level and the calibrated sound power level of the reference source is then assumed to be a 'test-facility constant', $\boldsymbol{K}$, independent of the source under test.

Part A – Typical Cycle

The same operational protocol was followed for the sound level measurement of the same series of refrigerators as measured in Section 2, above. The sound power levels at 1, 5, and 7-minutes were calculated by adding $\boldsymbol{K}$ to the average sound level over 32-seconds from the traversing microphone. These were then equated to equivalent 1-metre free-field sound levels above a reflecting plane. The 1, 5, and 7-minute values were averaged to produce a typical operating cycle sound level.

Part B – Component Contributions

As described in Section 2.2, the measurements were repeated with the refrigerator components operating sequentially. The 1-metre equivalent sound levels from each component were then added on an energy basis to compute the total sound level of each unit.

RESULTS

The overall 1-metre equivalent sound levels for the six refrigerator units (Part A) are presented in Table I for both the direct hemi-anechoic and reference reverberant methods.

As well, the total 1-metre equivalent sound levels for each unit are presented, based on the summation of the component sound levels (Part B).

Table I: 1 m Equivalent Sound Levels [dBA]

Unit	ISO 3744[1]		ISO 3742[2]	
	Overall[3]	Sum[4]	Overall[3]	Sum[4]
1	45.0	45.3	45.4	44.9
2	43.8	42.3	46.6	45.5
3	45.1	43.2	47.6	45.5
4	40.2	41.1	41.4	40.9
5	40.6	40.0	42.9	40.6
6	40.1	40.0	41.9	39.8
μ	42.5	42.0	44.3	42.9
R	4.9	5.3	6.2	5.7

[1] ISO 3744 is the Direct Hemi-anechoic method.
[2] ISO 3742 refers to the Reference Reverberation method.
[3] Overall is the average measured sound level of a typical cycle
[4] Sum is the total of component sound levels.

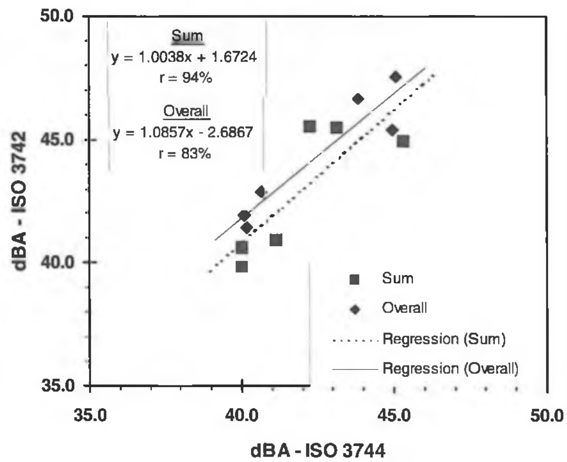

Figure 1: Method comparison with descriptor as parameter

The data indicates that the range of values is comparable for both measurement methods, and that there is a slight bias (lower) for the direct hemi-anechoic method. This bias may be partly due to the inherent property of reverberation methods of representing all of the sound power, whereas hemi-anechoic methods typically only sample the radiated sound power at discrete points.

The data sets were plotted against each other for graphical interpretation of the relationships between the two measurement methods (ISO 3744 and ISO 3742) and the two descriptors (Overall and Sum). Figures 1 and 2 present these plots, with the statistical indicators shown on the graphs.

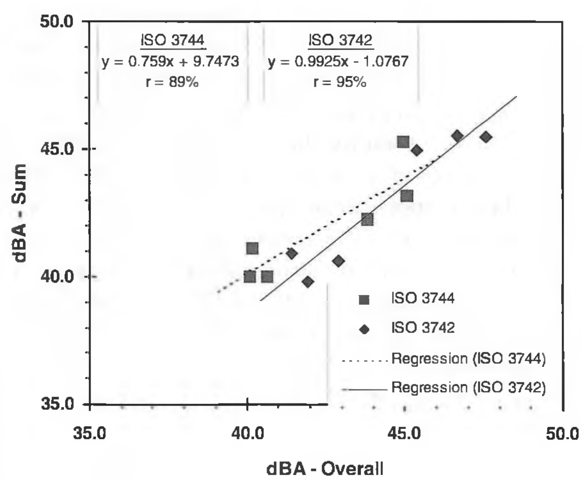

Figure 2: Descriptor comparison with methodas parameter

CONCLUSION

The foregoing indicates that despite a small negative bias for sound level data measured under free-field conditions (particularly for directional sources or components) in comparison to reverberant field measurements, the correlation is very strong. This bias could be overcome by increasing the microphone mesh density, particularly near areas with higher directional characteristics. One of the main advantages of the ISO 3744 method is that the individual sound levels at each microphone position can be used to estimate the directional characteristics of the sound source. This is not possible under the reverberant field conditions found in ISO 3742.

Sysmeas Program For Acoustical Modelling Of Muffler Systems

Jay S. Detsky (1), Brian V. Chapnik (1), and Rick McWilliam (2)
(1) HGC Engineering, Plaza One, Suite 203, 2000 Argentia Road, Mississauga, Ontario, L5N 1P7
(2) Siemens Automotive Inc., 16 Industrial Park Road, Tilbury, Ontario, N0P 2L0

1. INTRODUCTION

A computer program called SYSMEAS has been developed for Acoustical Parameter Estimation and System Modelling of muffler systems. Siemens Automotive is currently using this program as a predictive tool for the preliminary design of intake resonators. SYSMEAS is a Matlab^{TM} based program that combines both theoretical and measured data to predict various acoustical performance parameters such as insertion loss (IL) and transmission loss (TL). This paper outlines the theory behind SYSMEAS, describes the features of the program, and illustrates the accuracy of the computer model's parameter estimation.

2. THEORY

The SYSMEAS program utilises the Transfer Matrix Method as described by Munjal [1]. This method describes the input/output relationships between acoustic pressure and velocity across different types of elements. Each element is characterised by a two-by-two 'four-pole parameter' transfer matrix. These parameters are based on the element's physical and acoustical properties. The resultant system transfer matrix can then be used for the calculation of insertion and transmission losses of an acoustic muffler. In order for the model to better approximate the effects of flow on the acoustic performance of the system, an aeroacoustic formulation of the transfer matrix, also described by Munjal [1], is applied. The formulation is valid up to the cut-off frequency of the system, defined by the largest lateral dimension above which modes other than the fundamental plane wave mode begin to propagate.

The transfer matrix of each element may be derived theoretically or through measurement. Measurements of muffler components and the resulting analysis used in SYSMEAS are based on the method developed by Chung and Blaser [2]. This method uses two pairs of microphones (one pair upstream and one pair downstream of the element) to get the sound intensity on each side of the element. A minimum of two loads with known termination impedances is needed to estimate the four-pole parameters for the transfer matrix.

3. SYSMEAS PROGRAM

Matlab^{TM} was chosen as the application language for this program because of its ease with manipulating matrices. SYSMEAS runs on any PC computer with a Windows O/S and a current version of Matlab^{TM} installed. The latest version of the program operates under Matlab^{TM} Release 12.

3.1 System Design

Muffler systems designed in SYSMEAS can be comprised of any combination of ten types of elements (listed in Table I).

Table I. SYSMEAS supported element types.

Uniform straight tubes	Conical tubes	Extended-tube resonator	Concentric hole-cavity resonator	Full expansion chamber
Helmholtz resonator	Overlap tuner	Quarter-wave resonator	Simple area discontinuity	Measured element

There are also various system parameters than can be selected, including the inlet source type, outlet termination type, and fluid parameters such as the fluid temperature and flow rate. Source and termination impedances can be modelled as ideal (open, closed, or anechoic), or measured impedance data can be used. Similarly, measured source strength spectral data can be used if an estimate of absolute radiated sound pressure is required, or the source may be considered 'white'.

3.2 Analysis

Once the system has been modelled, SYSMEAS can analyse its various performance parameters. The program can estimate the TL and IL of any subset of elements as a function of frequency. The pressure at a junction between two elements or radiated into the far field can be estimated, as can the pressure distribution along any straight tube. Finally, the pressure drop across a series of elements can be calculated.

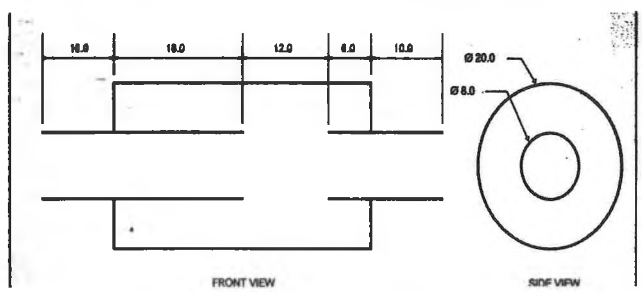

Figure 1. Dimension diagram (in cm) of expansion chamber.

3.3 Data Acquisition and Evaluation

SYSMEAS utilises a modular formulation for data acquisition. Data can be acquired directly from Matlab^{TM}-supported DSP cards, GPIB equipped analysers, or read from a variety of different file formats according to user requirements (this module may be customised for each user). After a measurement has been acquired, it is saved to a file. The element's characteristics can then be calculated from the measured data files. These characteristics are then saved in a separate element library.

3.4 Optimisation

The optimisation module allows the user to simultaneously optimise some of the parameters of theoretical elements located within the system. This optimisation uses constrained minimisation techniques. One of three different cost functions can be selected: maximisation of TL, maximisation of IL, or minimisation of radiated pressure from the system outlet. These functions are optimised over a selected frequency range.

4. RESULTS

The SYSMEAS program can be validated by comparing measured TLs for a given muffler system to the TLs predicted by SYSMEAS.

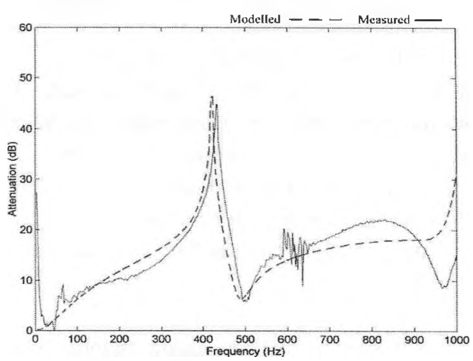

Figure 2. Transmission losses for expansion chamber.

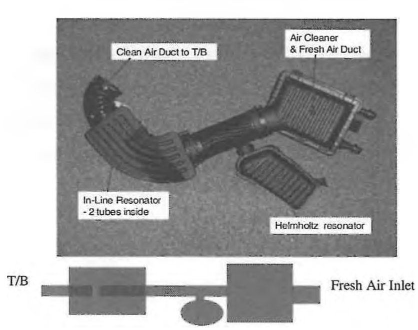

Figure 3. Daimler Chrysler LH 3.5L induction system.

A simple expansion chamber, with extended inlet and outlet tubes, was modelled and then measured to evaluate the accuracy of SYSMEAS. The dimensions of the expansion chamber are shown in Figure 1. The results of the comparison, illustrated in Figure 2, show a good correlation between theory and experiment.

A more complex muffler system was also tested. The muffler shown in Figure 3 is in current production for the Daimler Chrysler LH (Intrepid) 3.5L induction system. The measured and modelled TLs are shown in Figure 4. Again, a reasonably good correlation is shown.

REFERENCES

[1] Munjal, M.L. Acoustics of Ducts and Mufflers. New York: John Wiley & Sons (1987).

[2] Chung, J.Y. and Blaser, D.A. *Transfer function method of measuring in-duct acoustic properties*, Engineering Mechanics Department, General Motors Research Laboratories, June 5, 1980.

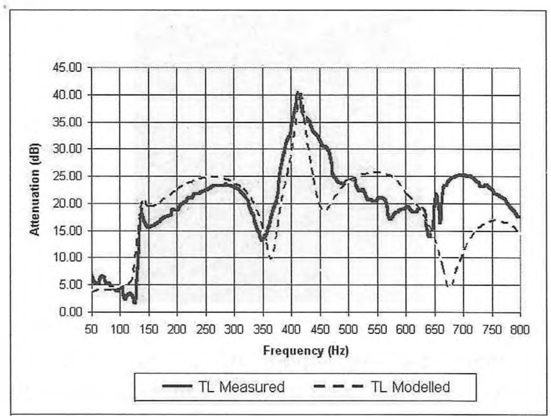

Figure 4. Transmission losses for Daimler Chrysler LH 3.5L induction system

Craftsmanship At Intier Automotive: Increasing Product Quality Through Improved Acoustical Engineering

F. Stewart and G. Paton
The Atoma Technical Center, Intier Automotive Incorporated, Magna International Newmarket, Ontario, L3Y 4X7

Craftsmanship, the hand crafted excellence of a quality product, is currently changing the focus of automotive manufacturers. As consumers attempt to differentiate brands, automotive manufacturers are spending more time perfecting the overall sensory perception of their products. Manufacturers have come to realize the need to focus on not only product performance but also on other sensory stimuli. Visual, tactile, olfactory, and the focus of this document, auditory observations, must be exploited by product engineers to ensure that their products are recognized as having craftsmanship.

The Atoma Technical Centre, a division of Intier Automotive, has responded to the need for superior auditory quality by testing automobile parts in its anechoic chamber.

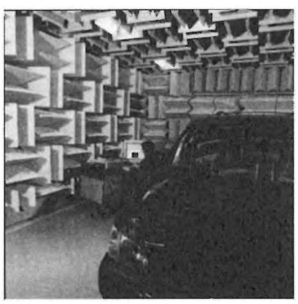

The chamber and its supporting instrumentation have enabled ATC to offer both internal and external customers the ability to evaluate the acoustical performance of the products they are developing. With the new focus on craftsmanship, the information the test centre provides allows designers to assess the sound quality of interfacing products. This attention to overall acoustic quality gives ATC's customers a competitive advantage because they no longer discover that certain products in combination produce unpleasant sounds at the production stage. Instead, customers of ATC are able to engineer their products to exhibit favourable sound qualities.

For example, during the development of door lock/unlock actuators, sound quality was defined as a product requirement. In order to achieve this, measurements were taken at the component and vehicle level. The data taken from the component level tests allowed the design engineers to isolate when peak sound levels and/or objectionable noises occurred during the door locking event and understand how this event was correlated to the sound performance in the final vehicle. With this information, it led to the development of new materials in the actuator stops and a reduction in the peak loudness experienced in the final product.

ATC offers its customers use of the anechoic chamber and its associated acoustic instrumentation. The anechoic chamber at ATC has an 80 Hz cutoff frequency that is large enough to test a 95-percentile sport utility vehicle.

This technical capability, in combination with ATC's laboratory accreditation allows customers an independent facility to test or evaluate products that require objective acoustical test reporting. Furthermore, for analysis beyond testing, ATC has professional acoustic engineers within the organization that can analyze the sound quality data and provide engineering recommendations to improve the sound quality of the particular product or system.

While the range of testing capabilities are expanding, the existing capabilities at the technical center are:

80 Hz cutoff, full vehicle hemi-anechoic chamber.
Measurement capability in a laboratory or field environment using microphone and/or binaural recording.
Measurement of sound quality, sound pressure, vibration analysis or concurrent analysis of microphones, accelerometers and other inputs such as current or voltage.
Determination of sound power from sound pressure measurements following standard ISO protocol.
Analysis capabilities such as sound quality, octave filtering, FFT, and spectral processing.

Given today's focus on value added manufacturing, the Atoma Technical Center has responded to the essential need for exceptional products that provide an overall pleasing sensory experience for the consumer. While ATC has developed an expertise in sound quality measurement and analysis in the automotive sector, the facilities and accreditation allow them to offer non-auto sector companies the professionalism and objectivity their current customers demand. If you are interested in discussing your company's requirements with the Testing Manager at Atoma Technical Centre, or touring the facility in Newmarket please call (416) 292 8662 ext. 2766.

Vibration Insulation

2 ways Regupol Regufoam

1 goal **Optimal vibration absorption and insulation of structure-borne sound using recycled rubber and foam materials.**

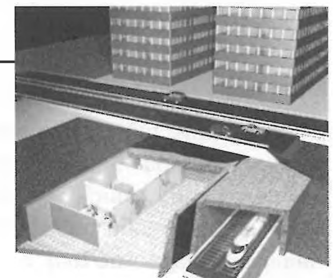

Road Construction

For rail and tunnel construction, as well as for road and bridge construction, Regupoi and Regufoam are used for vibration insulation and shockproofing.

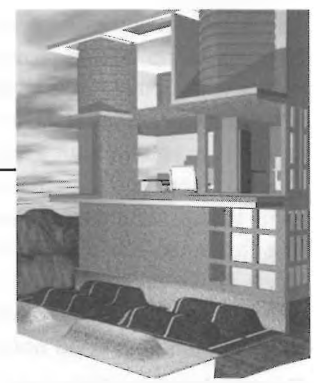

Foundations

To protect against ground vibration, Regupol and Regufoam insulate large buildings with appropriate load distribution slabs.

High-Rise Building

Whether for elevator motors, pumps, ventilation systems or block-type thermal power stations, structure-borne sound insulation and vibration absorption with Regupoi and Regufoam are simple and permanent.

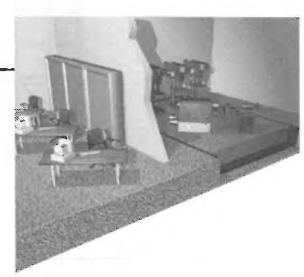

Industry

Here Regupoi and Regufoam are used for the active insulation of machines and passive insulation of floor slabs for precision measuring instruments, laboratory facilities or measuring chambers. Both sub-critical and supercritical bearings are possible.

For more information and technical data call:
Paul Downey, B. Eng.
Business Development Manager

DODGE-REGUPOL
INCORPORATED
Leaders in recycled products technology

www.regupol.com

Phone: 416.440.1094
Toll free: 800.322.1923
Fax: 416.440.0730
Email: pcd@regupol.com

Aeolian Tones in Wind Tunnels

R. Ramakrishnan, D. Van Every and M. Hess
Aiolos Engineering Corporation, 2150 Islington Avenue, Toronto, M9P 3V4

1.0 INTRODUCTION

There has been a recent trend in new wind tunnels to require very low, test section, background noise levels. This trend can been seen for the most common types of low speed wind tunnels; including automotive climatic wind tunnels, and both automotive and aerospace aero-acoustic wind tunnels. Designers of aircraft and road vehicles are striving to produce quieter designs. A quiet aero-acoustic wind tunnel is a primary tool for the investigation of aerodynamic noise.

Climatic wind tunnels are primarily used for the development of automotive engine cooling systems, HVAC systems and testing all vehicle systems under climatic extremes. Quiet climatic wind tunnels allow the test engineer to use sound as a diagnostic tool; e.g. evaluation of drivability and engine knock.

The dominant source of noise in any low speed wind tunnel is the main fan, which provides the test section air flow. To reduce test section noise to the required levels, the wind tunnel designer will first endeavor to reduce the background noise at its source with a very efficient, custom fan design. The next step will be to make extensive use of acoustic treatment in the wind tunnel circuit to attenuate the fan noise. The fan noise can thus be reduced to essentially inaudible levels in the quietest recent aero-acoustic wind tunnels. In these facilities secondary sources of noise can dominate the test section background noise spectrum.

The usual source of secondary noise is the airflow noise produced by the wind tunnel flow as it impinges on obstructions within the flow path, or by the test section jet.

There are other mechanisms, not usually experienced in most wind tunnels, which produce strong noise levels within the circuit and thereby increase the test section noise levels. Two such mechanisms will be presented in this paper. These two mechanisms will be illustrated with examples from a climatic wind tunnel and an aero-acoustic wind tunnel. Both of the example wind tunnels were provided with extensive acoustic treatment to reduce background noise levels. The noise levels produced by the secondary mechanisms were so high that test section background noise levels actually exceeded noise levels typically found in wind tunnels without any acoustic treatment. Thus the mechanisms for the production of Aeolian tones discussed in this paper can be important for any wind tunnel.

2.0 CIRCUIT DESCRIPTION

A schematic diagram of a typical wind tunnel circuit is shown in Figure 1. A wind tunnel can be either horizontal or vertical and has four legs; with the two longer legs containing the main fan and the test section. The cross-section of the legs can be either rectangular or circular. The test section leg, between Corners 1 and 4, usually has the settling chamber, for conditioning the flow, the main contraction and a diffuser downstream of the test section. Unusual noise generating mechanisms located in this leg are the main focus of this paper.

3.0 HEAT EXCHANGER AND AEOLIAN TONES

A Heat Exchanger (HE) is used in the circuit to control the air temperature of the flow. The HE is usually placed in the settling chamber as this is the region of lowest wind speed and thus lowest pressure loss. The HE consists of rows of small finned tubes, usually 6 mm to 15 mm diameter copper pipes, which span the height and width of the settling chamber. The HE may consist of between 2 to 12 rows of tubes in the flow direction. The tube rows are staggered for better heat transfer performance. The flow speeds in the settling chamber are in the range of 3 to 12 metres/sec. The wind tunnel flow passing over the HE tube banks sheds vortices

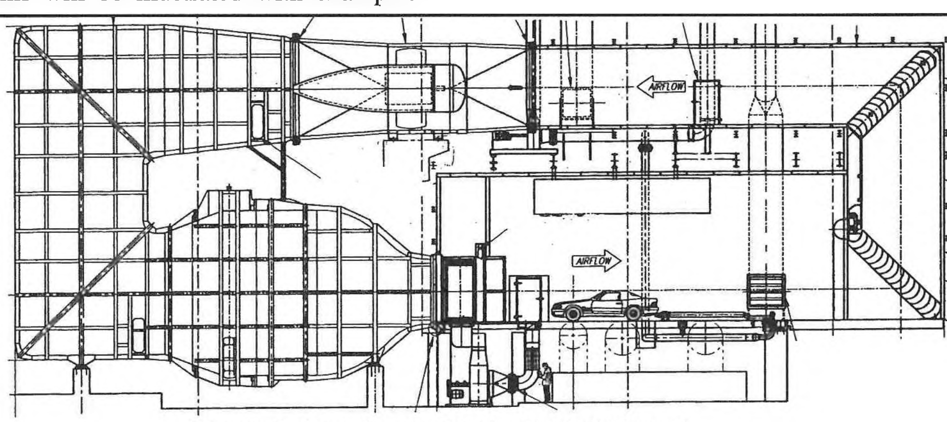

Figure 1. Details of a Typical Wind Tunnel.

with strong frequency preferences. If the shedding frequency coincides with the frequency of a room mode for the settling chamber, a very strong resonant tone may be produced. The noise that can be generated by the shedding vortices (Aeolian Tones) and possible mitigation measures will be discussed. General details of the flow-induced noise can be found in the literature. Wind Tunnel I is a recently constructed climatic wind tunnel for the automotive industry. A very strong acoustic resonance in the settling chamber was observed starting at a main fan speed of 450 rpm. This resonance was excited at a number of fan speeds between the initial 450 rpm speed and the maximum speed of 950 rpm. The resonance was not present at intermediate fan speeds between the discrete fan speeds.

When the resonance occurred the heat exchanger tubes and heat exchanger structure experienced large amplitude vibrations. Standing waves were readily observed in the settling chamber. The heat exchanger consisted of horizontal tubes and it has been shown in the available literature that this type of flow-induced resonance always excites a mode transverse to the direction of the tubes. At 450 rpm a pure vertical mode consisting of a 3 period standing wave was found (the (0,3) settling chamber mode). The narrowband noise spectra and a vertical survey which shows the mode shape is presented in Figure 2. The strongest resonances occurred when pure vertical modes were excited; i.e. the (0,3), (0,4), (0,5), (0,6) modes. As the vortex shedding frequency is directly proportional to fan speed, these strong resonances occurred at 450 rpm, 600 rpm, 750 rpm and 900 rpm. Resonances were also observed at intermediate fan speeds when a combined lateral/vertical mode was excited (e.g. (1,3) mode).

There are three basic approaches possible to solve this kind of noise problem and these are,

1. Change the boundary condition (apply acoustic treatment to the space)
2. Change the space natural frequency (e.g. position a splitter in the settling chamber)
3. Eliminate the forcing function (reduce the vortex shedding strength)

Figure 2a: Narrow Band Settling Chamber Sound Pressure Level, Fan speed = 450 rpm

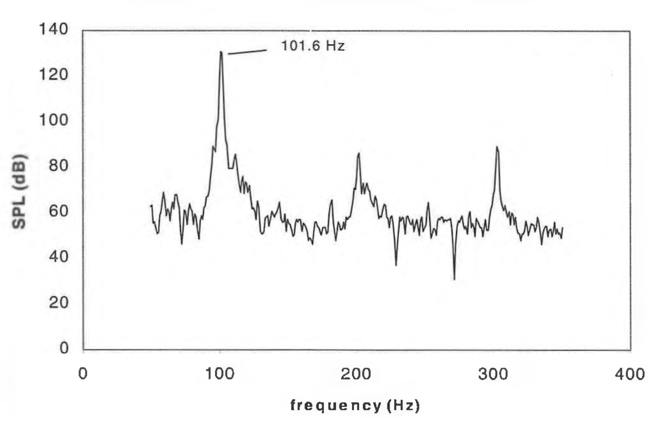

Figure 2b: Measured Peak SPL (101.6 Hz) for a Vertical Traverse, Fan speed = 450 rpm, (0,3) mode, settling chamber height = 5080 mm

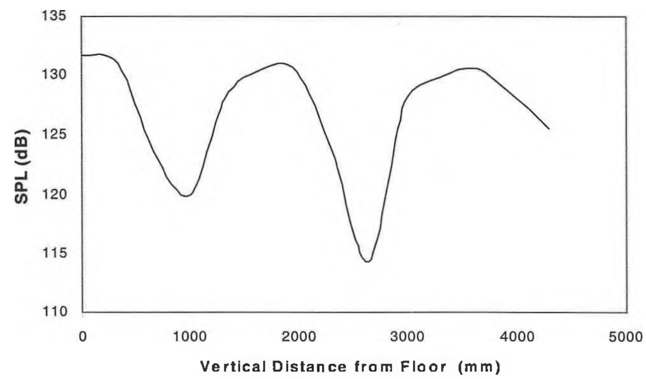

Approach 1 and Approach 2 were tried without success (unlike in other Wind Tunnels cases). Several ideas to change the vortex shedding were tried and the idea that worked was to block the flow over critical tubes in the heat exchanger array. Flow obstructions, which ran across the full width of the heat exchanger, were attached to the upstream face of the heat exchanger to cover tubes located at several pressure antinodes for the mode that was being excited. In order for a resonance to occur, the feedback from the excited settling chamber mode must be able to synchronize the vortex shedding such that all of the vortices are shed in phase. It is conjectured that the flow blocking strips disrupted tube to tube communication, at critical points in the tube array, so that the vortex shedding was not able to lock on.

The final solution, to completely eliminate the resonance, required flow blocking strips attached to the upstream face of the heat exchanger as well as extensive acoustic treatment on the floor of the settling chamber.

4.0 BOUNDARY LAYER CONTROL SYSTEM AND AEOLIAN TONES

Wind Tunnel II is a horizontal wind tunnel with a solid wall test section used for aerospace applications. The wind tunnel was being renovated to improve its testing capability for automotive racing cars, as the test section was large enough for full-scale cars. One of the main requirements of an automotive wind tunnel is the control of the floor boundary layer in the region where the test vehicle is located. Aiolos was retained to design and install a Boundary Layer Control System (BLCS) with its attendant ducts and system fan. The main specifications, in addition to the aerodynamic performance, included a low noise level in the test section for the top speed of the boundary layer system fan. The peculiar noise generated by the BLCS is described below.

The BLCS consisted of two large openings covered with perforated plates, just downstream of the nozzle. The BLCS drew air from the test section through the perforated plates and down into the rest of the suction system ducting and fan.. The covers for the openings had to be able to withstand the weight of heavy forklift vehicles. Hence, the openings were covered with 26 mm thick perforated plates supported by heavy 100 mm deep catwalk grilles. The results presented in this paper are for those cases where the BLCS was operated without the wind tunnel main fan running. Similar trends in noise the noise levels were observed with thw wind tunnel main fan operating. Only the wind-off noise data was considererd as it simplified the analysis. A strong high frequency tone was generated at higher speeds of the boundary layer fan. The tone's intensity was high enough to be audible in adjacent buildings. Typical third-octave band spectra of noise levels, measured in the test section for selected fan RPM's are shown in Figure 3. Both noise and vibration measurements were conducted for different fan speeds and the results are summarized in the following observations:

a) The onset of tonal resonance noise started at around 400 RPM of the fan and continued through to maximum fan speed.
b) The dominant frequency increased with increasing speed The resultant intensity of the noise levels also increased with wind speed.
c) Intense plate vibration levels of the support grating as well as the perforated plate, followed the same frequency trend as the noise.
d) Impact tests of the plate/grating combination showed strong resonance at the noise frequencies.

The above observations led to the following conclusions:

1. the vortex shedding frequency of the plate perforations matched with the plate natural frequencies of both the 25 mm steel plate as well as the 100 mm deep grating support; and
2. the 100 mm cavities formed within the transverse and longitudinal bars of the grating amplified the shedding vortex sound.

The steel perforated plate was replaced by a thicker polyurethane plate with the same perforation pattern. The noise levels were reduced by between 5 and 10 dB, but the tonal resonance sound was still persistent. Since the grating was the main support mechanism, no major modifications were possible. The cross bars were then covered with 6 mm foam and the 100 mm deep cavities were filled with 50 mm diameter hollow foam tubes and the strong tonal resonance attenuated substantially. Figure 3 includes the noise levels after the installation of the above two control measures.

Note: Ramani Ramakrishnan is currently at the Department of Architectural Science, Ryerson University, Toronto, Ontario, Canada.

Figure 3. Test Section Noise Levels at Different Fan Speeds
(Before modifications and after modifications)

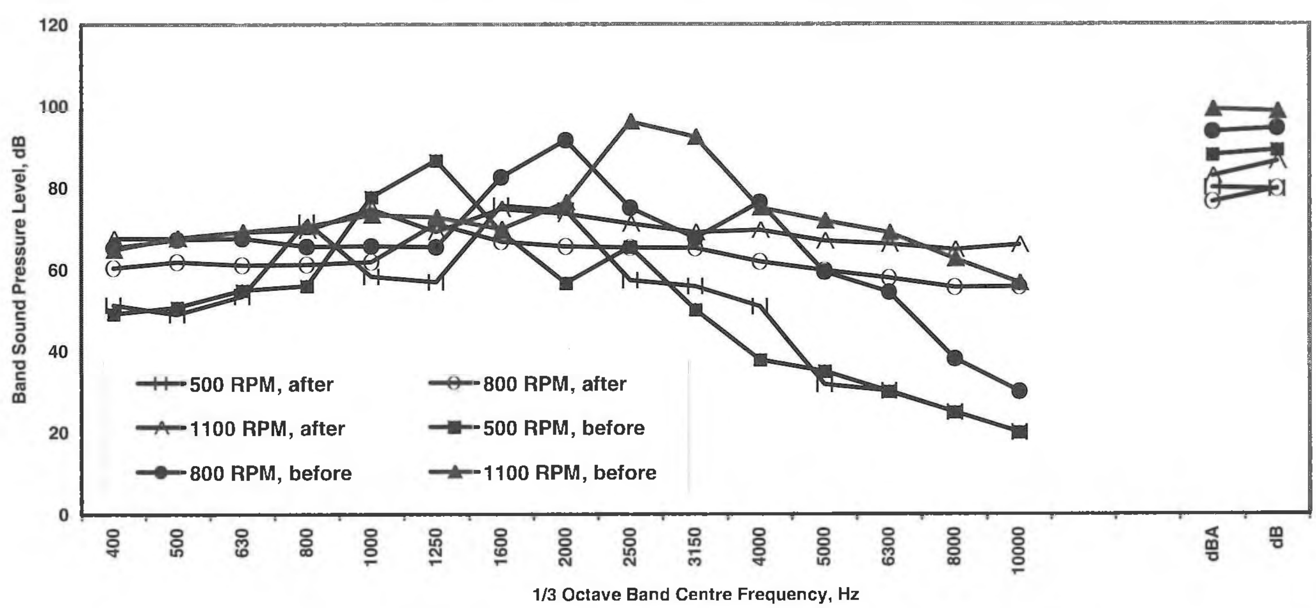

PRECISION MICROPHONES and MICROPHONE SYSTEMS

ACO Pacific, Inc.

2604 Read Ave.
Belmont, CA 94002 U.S.A.
Tel:650-595-8588 FAX:650-591-2891
e-mail: acopac@acopacific.com

Established in 1978 ACO Pacific, Inc. is chartered to serve the needs of both End-users and Equipment Manufacturers. Headquartered in the San Francisco Bay Area, ACO Pacific, Inc. has manufacturing facilities and suppliers both in California and internationally.

Our OEM relationships include Hewlett Packard, Audio Precision, SPS, DRA Labs and many other large and small instrumentation and process control manufacturers. Our End-user customers include: manufacturers of loudspeakers; computers and peripherals; heavy equipment; automobiles and automotive parts - tires, brakes, engines; universities; aerospace; and an alphabet soup of government agencies US and foreign.

ACO Pacific's Product Family

Measurement Microphones
Microphone Preamplifiers
Microphone Power Supplies
SPL Calibrators
Simple Intensity™ Sound Intensity Systems
Very Random™ Noise Generators

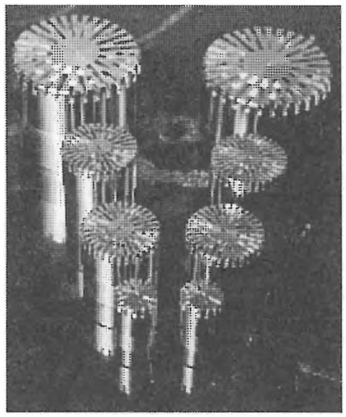

The "Alternative"

Type 1 Measurement Microphones
1, 1/2 and 1/4 Inch Models
Stainless Steel
and
Titanium Diaphragms
Quartz Insulators
Frequency Responses to 120 kHz
Noise Floors below 10 dBA
Meets or Exceeds IEC and ANSI Standards

Model 3024

Very Random™Noise Generator

Pink and White Noise, 1kHz Sine Outputs
1.6 Hz to 39 kHz (-3dB)
Portable - Battery and AC Power

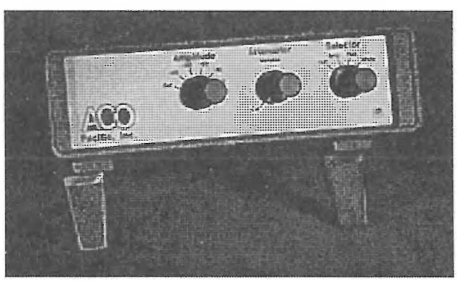

ACOustical Interface™

Precision Microphone Power Supplies
2 and 4 Channels - Gain Available
XLR and Lemo™ Connectors

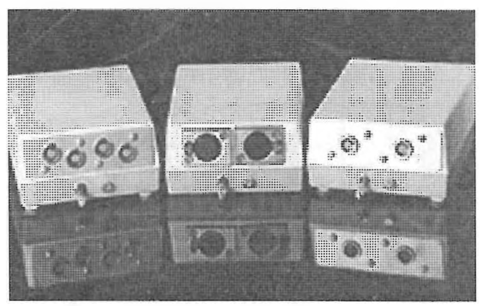

PS9200KIT

Includes: PS9200 (XLR) Power Supply
AC Adaptor
4012 Preamplifier w/CA4012-5 Cable
Selection of 1/2 Inch Type 1 Microphone
WS1 - 3 inch Windscreen
SC1 Die Cut Storage Case (SC2 optional)
Options: 511E SPL Calibrator (shown)
"G" Gain Stage

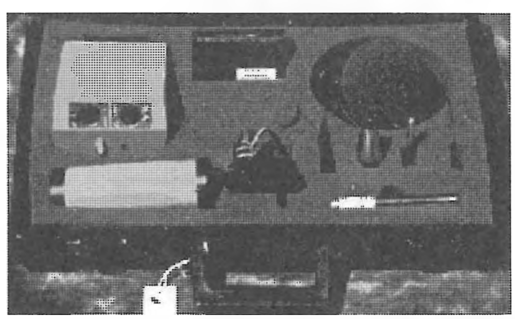

ACOustics Begins With ACO™

Uncommon Noise Signatures in a Wind Tunnel

R. Ramakrishnan, M. Rennie and S. Lau
Aiolos Engineering Corporation, 2150 Islington Avenue, Toronto, M9P 3V4

1.0 INTRODUCTION

Wind tunnel testing has become an important part of all aspects of road vehicle design. In addition to the well-known use of wind tunnels for the aerodynamic or aero-acoustic optimization of new vehicle designs, smaller wind tunnels are also used to investigate engine cooling, HVAC, and other aerodynamic integration issues. For these small, "climatic" wind tunnels, test-section acoustic noise levels are not a significant factor in the design of the wind tunnel; however, control room ambient noise levels are very often specified as part of occupational safety considerations. Limits on control room ambient noise levels are typically in the range 60 to 70 dBA over the full wind-speed range of the facility.

As a general rule, acoustic noise in a wind tunnel originates with the fan, and the bulk of the acoustic design effort for a new wind tunnel focuses on reducing the noise of the main fan. However, secondary noise sources many times stronger than the main fan may occur when the wind-tunnel flow excites resonant vibrations of an internal structure within the wind tunnel circuit. These flow-structure interactions can be complex in nature, are often not well understood, and are difficult to predict beforehand. As a result, these types of noise problems do not become apparent until the first wind-on startup of the wind tunnel, and must be rectified during the startup and commissioning phase of the facility. This paper describes an on-site investigation that was undertaken to correct a resonant tone that was eventually traced to the main fan support structure.

2.0 CIRCUIT DESCRIPTION

A schematic of the wind tunnel circuit is shown in Figure 1. The test section, where the test vehicle is located, is shown at the lower right of the figure. The control room is located next to the test section, at the same height as the test vehicle. The wind tunnel is an "overhead return" design, meaning that the return leg, which includes the main fan, is built on top of the test section. The air is guided through the wind tunnel circuit using flat-plate, circular-arc turning vanes located at each of the four corners. A heat exchanger is located in the settling chamber for temperature control. The temperature range of the facility is –40°C to +50°C.

3.0 TUNNEL NOISE LEVELS

The noise levels measured in the control room for three test-section wind speeds are plotted in Figure 2. In addition to these data, the following observations were made:

a) Strong tones were observed from a wind speed of 90 kph up to the facility maximum wind speed of 200 kph.

b) The tone frequency increased with wind speed; however, the frequency was not a linear function of wind speed.

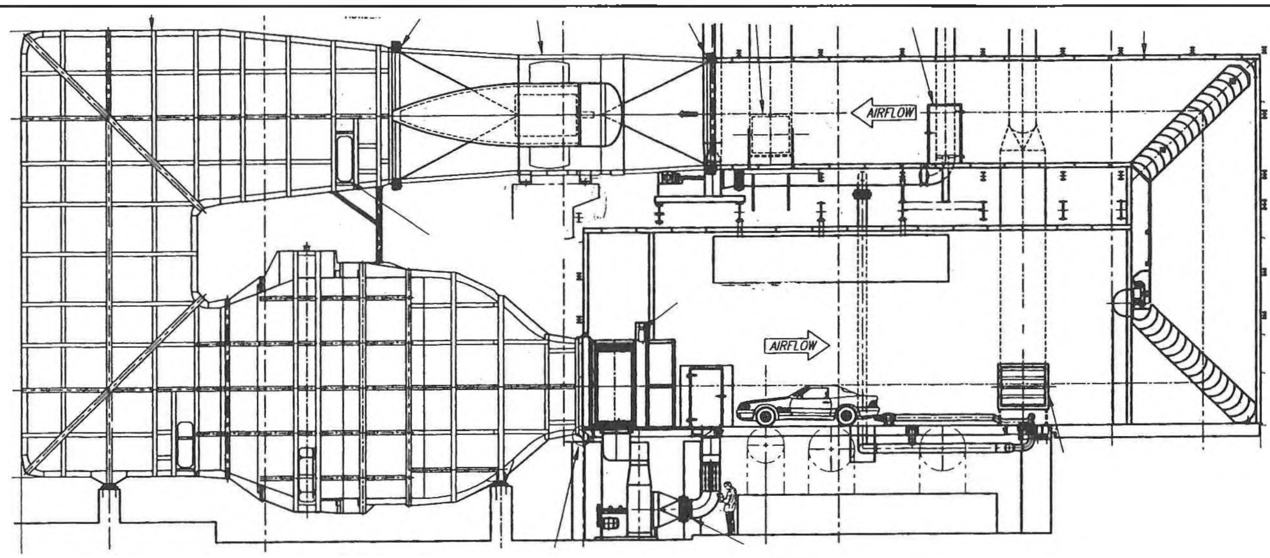

Figure 1. Typical details of a Climatic Wind Tunnel.

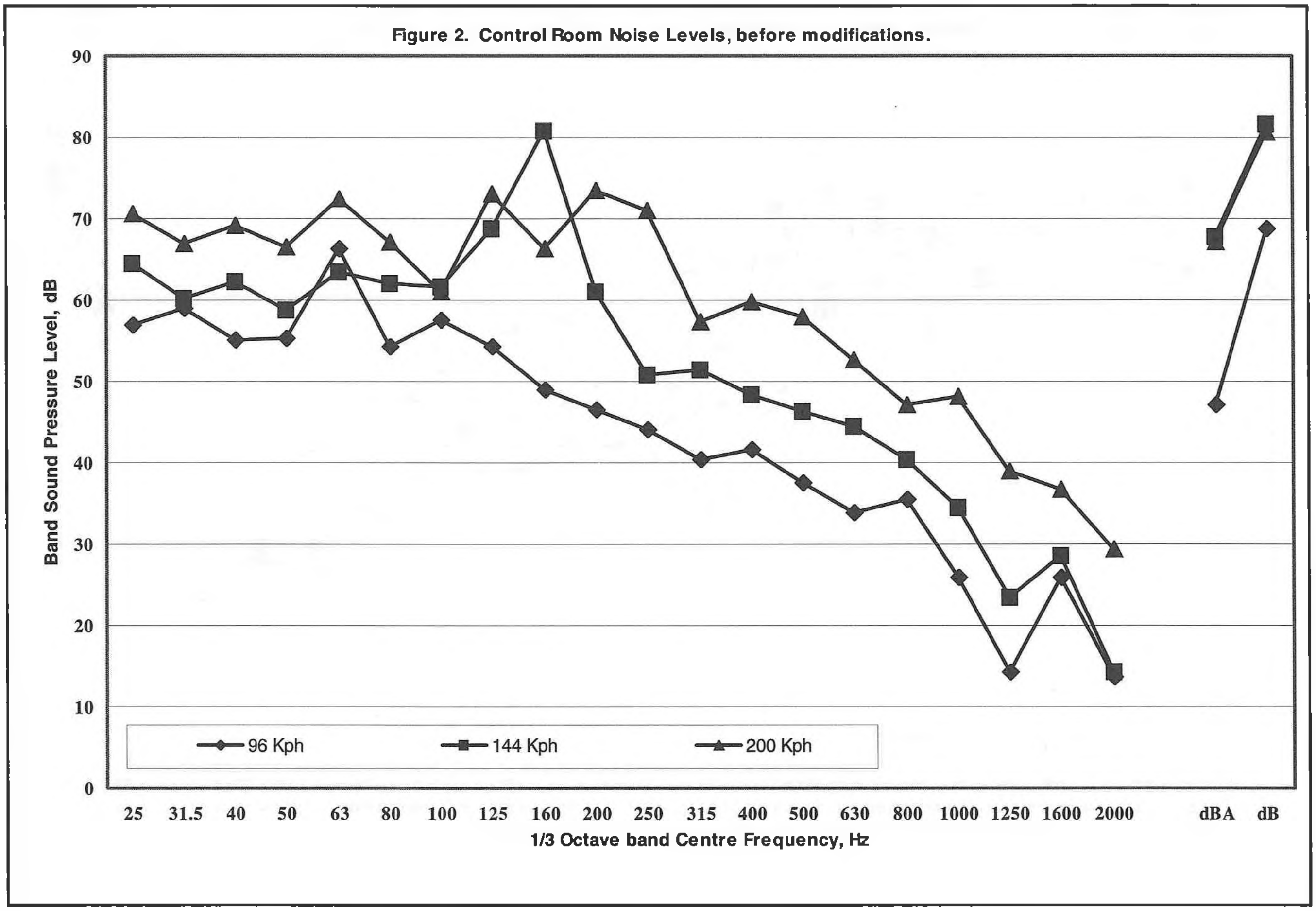
Figure 2. Control Room Noise Levels, before modifications.
Band Sound Pressure Level, dB
1/3 Octave band Centre Frequency, Hz
96 Kph
144 Kph
200 Kph
0
10
20
30
40
50
60
70
80
90
25
31.5
40
50
63
80
100
125
160
200
250
315
400
500
630
800
1000
1250
1600
2000
dBA
dB

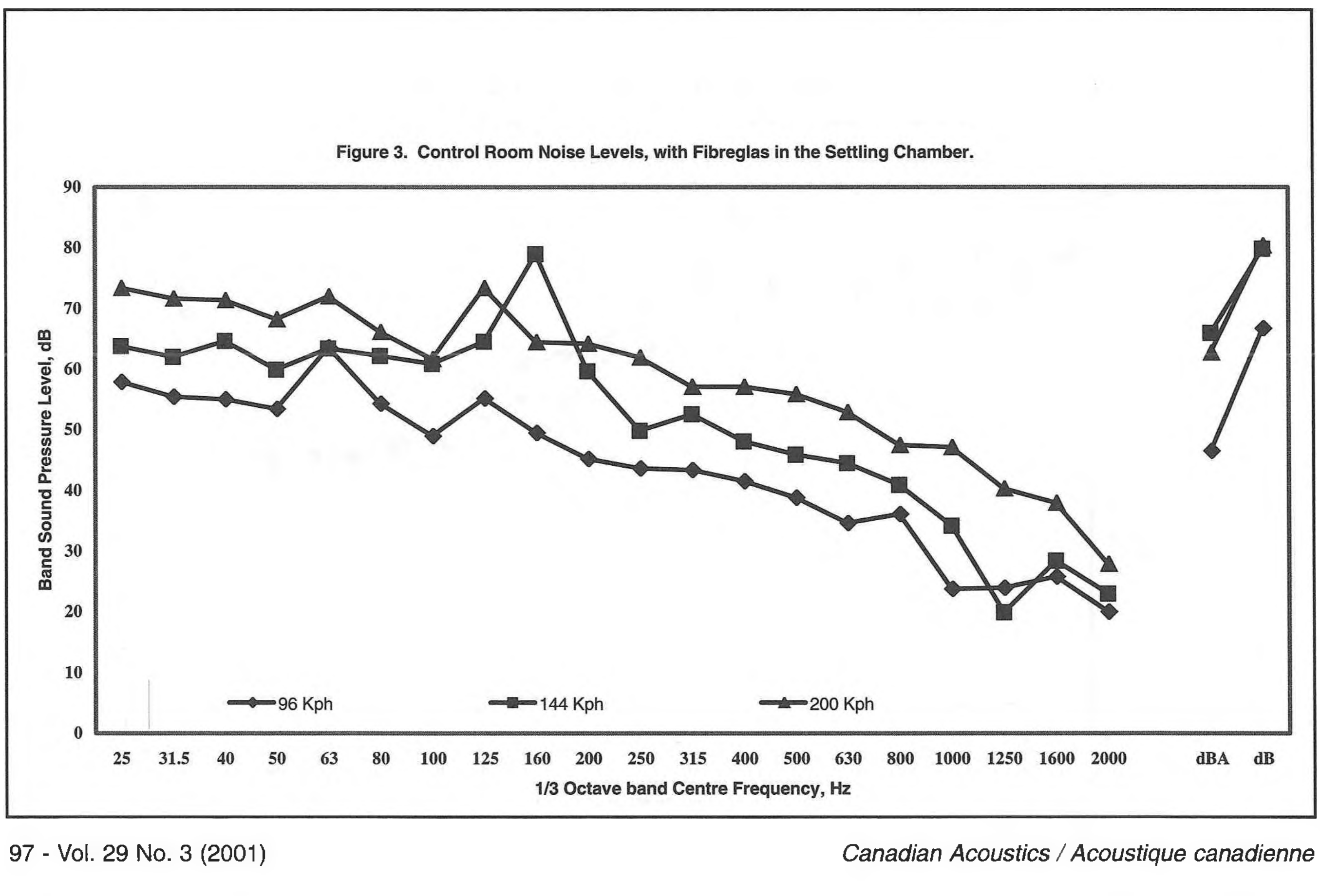
Figure 3. Control Room Noise Levels, with Fibreglas in the Settling Chamber.
Band Sound Pressure Level, dB
1/3 Octave band Centre Frequency, Hz
96 Kph
144 Kph
200 Kph
0
10
20
30
40
50
60
70
80
90
25
31.5
40
50
63
80
100
125
160
200
250
315
400
500
630
800
1000
1250
1600
2000
dBA
dB

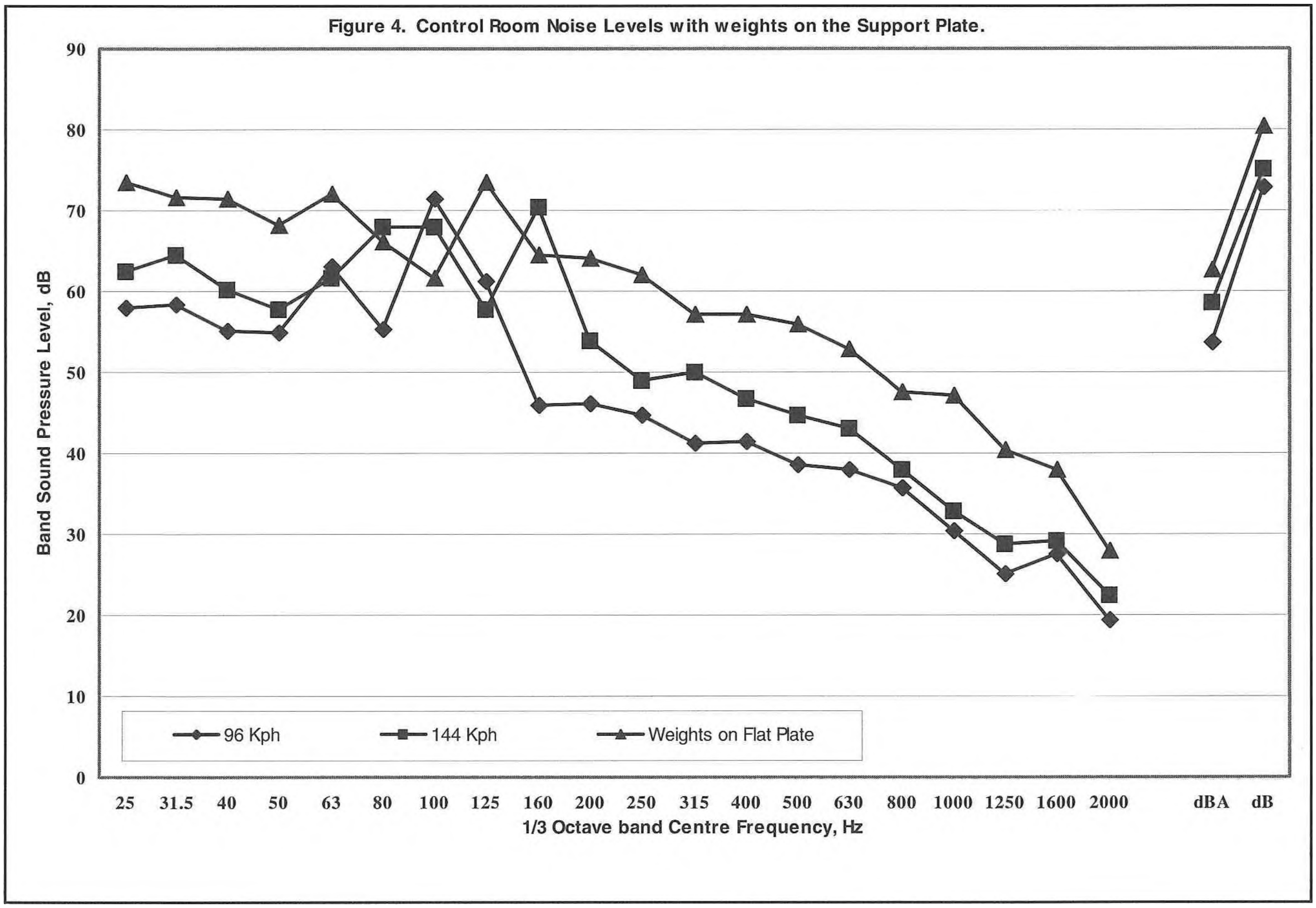

Figure 4. Control Room Noise Levels with weights on the Support Plate.
Band Sound Pressure Level, dB
0
10
20
30
40
50
60
70
80
90
96 Kph
144 Kph
Weights on Flat Plate
25 31.5 40 50 63 80 100 125 160 200 250 315 400 500 630 800 1000 1250 1600 2000 dBA dB
1/3 Octave band Centre Frequency, Hz

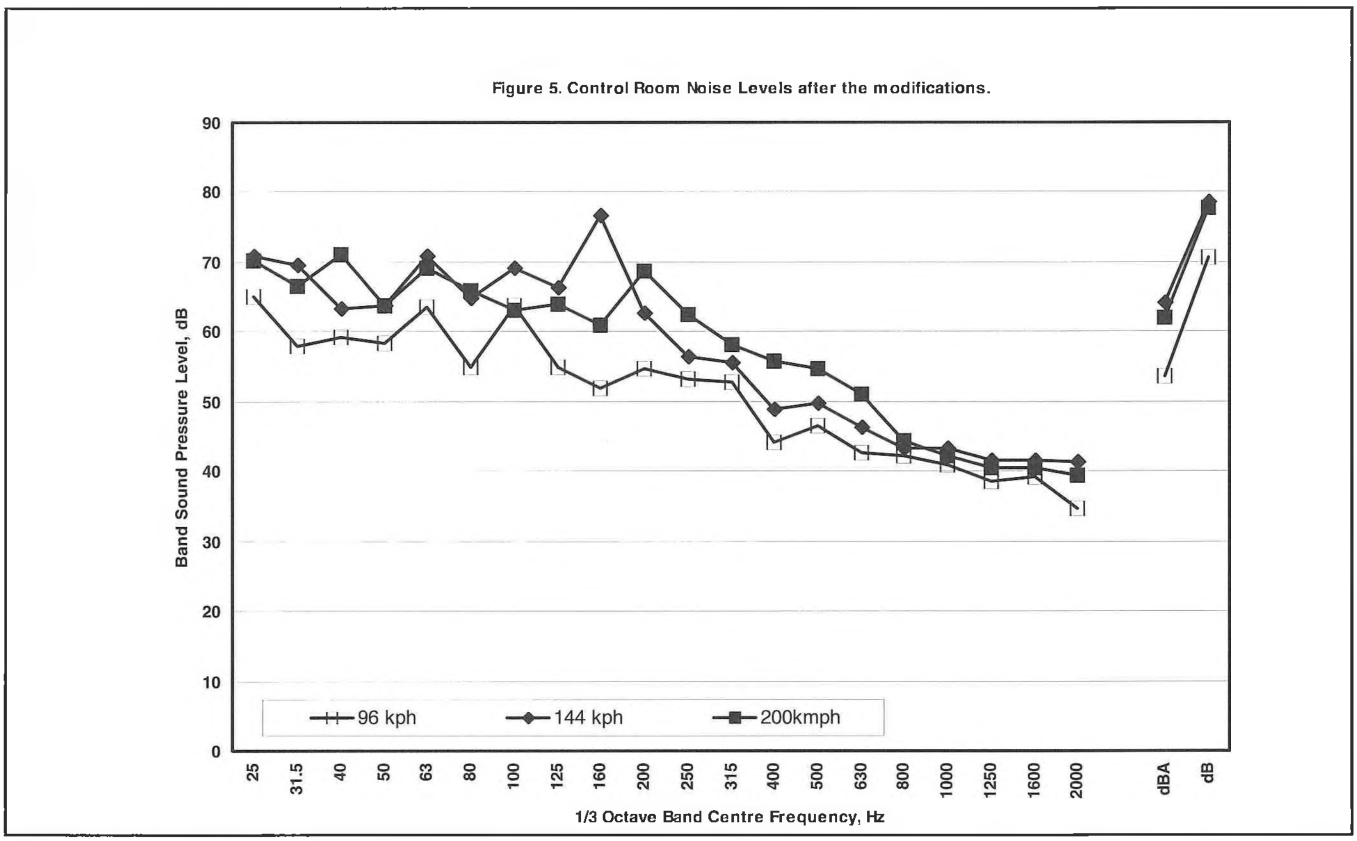

Figure 5. Control Room Noise Levels after the modifications.
Band Sound Pressure Level, dB
0
10
20
30
40
50
60
70
80
90
96 kph
144 kph
200kmph
25 31.5 40 50 63 80 100 125 160 200 250 315 400 500 630 800 1000 1250 1600 2000 dBA dB
1/3 Octave Band Centre Frequency, Hz

4.0 FURTHER INVESTIGATIONS

The following tests were undertaken to isolate the source of the acoustic tone:

1) A one-meter thick layer of fiberglass was placed on the floor of the settling chamber, and wind-on noise measurements were repeated. The purpose of this test was to check for possible flow-induced noise from the heat exchanger, or to determine whether the settling chamber was amplifying existing noise. The results of this test (Figure 3) demonstrate that the fiberglass layer had an effect at only low wind speed, indicating that the settling chamber did not significantly impact the maximum noise levels.

b) The main fan blades were re-pitched. Aerodynamic measurements indicated that, while fan performance was satisfactory, the fan blades were not pitched to the optimum blade angle. As such, due to inefficient operation, the blades may have been subject to larger-than-normal aerodynamic forces that were driving blade resonant modes. However, with the fan blades re-pitched, no effect on the tone intensity or the wind speed at which it occurred was measured.

Attention next turned to the fan structure downstream of the rotor. For this wind tunnel, the main fan had 9 rotor blades followed by 8 stators and, downstream of the stators, a further 8 flat-plate support vanes. This arrangement of stators and support vanes is unusual due to its increased susceptibility to interaction between the unsteady wake of upstream components and downstream structures; typically, fans designed for aeroacoustic wind tunnels have only a single row of stator blades that also act as support vanes.

Visual inspection of the fan structure showed, in fact, the close proximity of the stators and support vanes in 1 or 2 locations. Impact tests showed that the support vanes had natural frequencies between 70 to 250 Hz. As a simple test, C-clamps were attached to the affected support vanes so as to modify their natural frequencies; this modification was found to reduce the noise level at the tonal frequency by more than 5 dB (Figure 4). Detailed finite element analysis of the support vanes corroborated that the vanes had transverse mode shapes at the problem frequencies.

Based on the above evidence, it was concluded that the trailing edge flow leaving the stator blades and impinging on the flat support vanes was the main cause of the tonal noise problem. The fan manufacturer was apprised of these findings and the support vanes were modified with additional ribs to change their natural frequencies. The results of these changes are shown in Figure 5 for three operating speeds. The intensity of the tonal noise has reduced substantially and the control room noise levels are within the allowable tolerance of 60 dBA at all speeds.

Note: Ramani Ramakrishnan is currently at the Department of Architectural Science, Ryerson University, Toronto, Ontario, Canada.

MEASUREMENT OF STRUCTURAL INTESNTIY ON BEAM STRUCTURES

Stefan Schoenwald* and Trevor T. Nightingale**
* Fachhochschule Stututgart, Hochschule fur Technik, Schellingstrasse 24, D-70174 Stuttgart, Germany
** Institute for Research in Construction, National Research Council, Ottawa, Ontario, Canada K1A 0R6

INTRODUCTION

This paper provides a summary report of a recent project where a scanning laser vibrometer and specially developed analysis software were used to systematically investigate the optimal point spacing, and the suitability of measurement quality indicators, such as the residual intensity index, for the two and four point methods. Also, the sensitivity of the two-transducer method to near fields close to sources and discontinuities is also examined.

GOVERNING EQUATIONS

Although this paper focuses on beams, it is convenient to present the equations for a plate as they will be used in a companion paper (1) and represent a superset of those for a beam. It is assumed that the beam or plate is homogeneous, isotropic and that the dimension, d, in the direction of displacement is considerably smaller than the wavelength (i.e., $\lambda < 6d$). This allows thin beam/plate theory to be used and the intensity (W/m) transmitted by bending motion can be written in terms of the product of the forces (Q) and moments (M) with their corresponding normal velocity (ξ) or angular velocity (θ),

$$I_x = \langle Q_s \dot{\xi} \rangle_t + \langle M_x \dot{\theta}_x \rangle_t + \langle M_{xy} \dot{\theta}_y \rangle_t \quad (1)$$

where the subscript x and y denotes the direction and t denotes time. The first term of Eqn. 1 is the intensity due to shear forces and can be written using the bending stiffness B,

$$I_{x,sf} = -B \cdot \left\langle \frac{\partial}{\partial x}\left(\frac{\partial^2 \xi}{\partial x^2} + \frac{\partial^2 \xi}{\partial y^2} \right) \cdot \dot{\xi} \right\rangle_t \quad (2)$$

the second term of Eqn. 1 is the component due to bending moment and can be written as,

$$I_{x,bm} = B \cdot \left\langle \left(\frac{\partial^2 \xi}{\partial x^2} + \mu \cdot \frac{\partial^2 \xi}{\partial y^2} \right) \cdot \left(\frac{\partial \dot{\xi}}{\partial x} \right) \right\rangle_t \quad (3)$$

and third term of Eqn. 1 is the term for intensity due to twisting moment and can be written as,

$$I_{x,tm} = B \cdot (1-\mu) \cdot \left\langle \frac{\partial^2 \xi}{\partial x \partial y} \cdot \frac{\partial \dot{\xi}}{\partial y} \right\rangle_t \quad (4)$$

For a plate, intensity is transported by all three components. While for a beam, the intensity is transported by only shear forces and bending momements. The relative magnitude of the force and moment components depends on the presence or absence of discontinuities such as sources, sinks, joints, etc. In the free field, the force and the two moment components are equal.

For a beam, the challenge is to obtain accurate estimates for the spatial derivatives of the flexural displacement in Eqns 2 and 3. Assuming free field conditions, Noiseux (2) using a finite difference approximation to provide a simplified description using only the velocity signals at two points,

$$I_x = -\frac{2\sqrt{B \cdot m'}}{\Delta} \cdot \mathrm{Im}\{G_{12}\} \quad (5)$$

where G_{12} is the cross spectrum between the velocity signals measured at two points indicated by the subscript, Δ is their spacing, and m' is the material surface density.

Similarly, the third order spatial derivatives of Eqns 2 and 3 can be estimated (3) using finite difference approximations and the measured velocity at four equally spaced co-linear measurement points. The resulting equations are,

$$I_{x,sf} = \frac{B}{\omega \cdot \Delta^3} \cdot \langle \mathrm{Im}(6G_{32} - G_{31} - G_{42} + G_{12} - G_{43}) \rangle_t \quad (6)$$

$$I_{x,bm} = \frac{B}{\omega \cdot \Delta^3} \cdot \langle \mathrm{Im}(2G_{32} - G_{31} - G_{42} - G_{12} + G_{43}) \rangle_t \quad (7)$$

where ω is the angular frequency. The total intensity is the sum of the two components.

MEASUREMENT SYSTEM

The measurement system consisted of a steel beam (1000x19x4.8 mm) which had one end free and the other clamped. Viscoelastic damping compound covered 400 mm of the beam at the clamped end while the free end was excited using an electrodynamic shaker coupled via an impedance head. Assuming no twisting motion of the beam and the force is applied perfectly normal to the beam then the source appears as a point force and the injected power can be accurately estimated from the force and acceleration signals from the impedance head.

A scanning laser vibrometer (Poltytec PSV300) was used to excite the beam (using a synchronized source) and to measure the resulting velocity at a series of closely spaced points along the beam from the source to the clamped end. Since the PSV 300 system measures only a single point at a time the phase relationship between the points must be obtained using the complex transfer function between the excitation signal (force from the impedance head) and the measured velocity at each point (4). Proprietary software was written to compute the structural intensity for the two and four-point methods.

SENSITIVITY OF THE METHOD TO POINT SPACING

It has been recognised that there is an optimal spacing between measurement points and that this will be a function of the wavelength. One study has suggested an operating range of $0.15\lambda < \Delta < 0.2\lambda$ for the two-point method. However, a systematic investigation of the bias has not been conducted for either the two- or four point methods.

Figure 1 shows the error in intensity estimate as a function of the ratio of point spacing to wavelength for both the two and four-point methods. For both methods the choice of spacing between measurement points is critical to attaining an accurate intensity estimate, as there is a bias. A very small spacing causes an overestimation while a large spacing causes an underestimation. A very large spacing may also result in an incorrect estimate of the intensity direction. It is quite clear that the four-point method is considerably more sensitive to the spacing between points and produces very large errors outside a very small range centered about 0.35λ. For the two-point method there will be no bias when the spacing is 0.25λ.

NEARFIELD EFFECTS AND MEASURMENT METHODS

Figure 2 which shows the measured intensity on the beam as a function of the measurement position from the source indicates that for distances greater than 100 mm from the source, the far field, the moment and force components reported by the 4-point method of the intensity are equal. However closer to the source nearfield effects become important and the two components are not equal. This is the regime where the two-point method reports erroneous results as shown by the under then overestimation of the intensity. (The four-point method requires more points and a larger spacing so it is not possible to measure as close to a source).

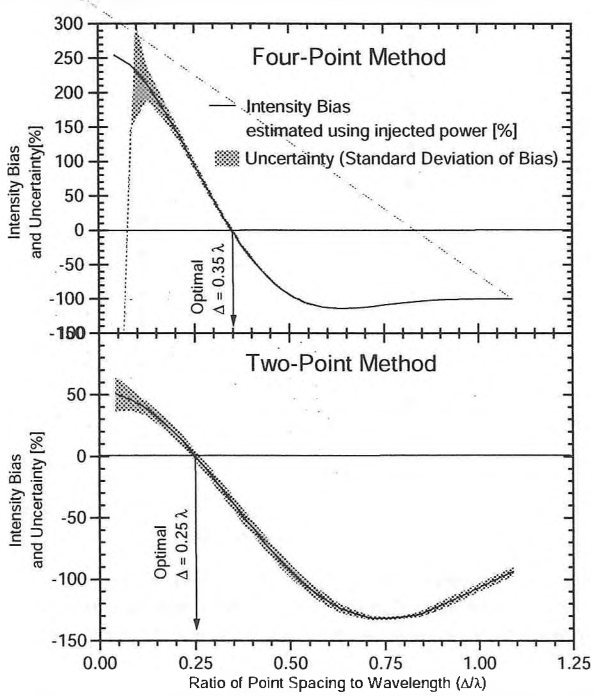

Figure 1: Bias and uncertainty in measurements as a function of the ratio of point spacing, Δ, to wavelength, λ.

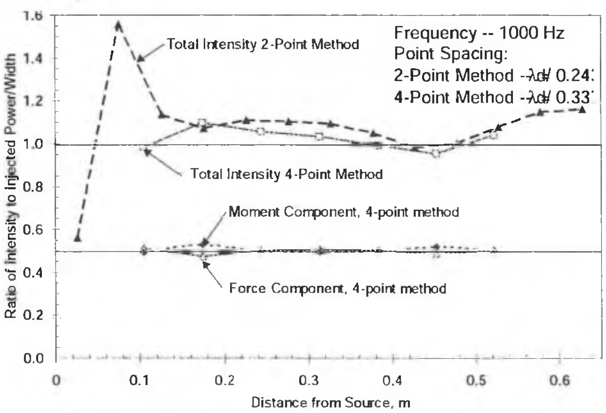

Figure 2: Ratio of intensity measured using the vibrometer and the injected intensity (power/beam width).

A MEASUREMENT FIELD QUALITY INDICATOR

For both acoustic and structural intensity measurements the ideal measurement condition is a field that consists only of a single free propagating wave. In this idealized situation there are no other sources and can be approximated by a single source in an anechoic space. For non-disipative media, the pressure/force and velocity will be in phase so the measured intensity can be written in terms of the rms velocity at the measurement point. However, when there are multiple incoherent sources there may be a very low intensity due to interference but the resulting rms velocity will be high. Accurate measurements in these situations require very precise phase information at the measurement points. The residual intensity index, R_{II}, compares the measured intensity to that predicted from the rms velocity assuming a single free propagating wave,

$$R_{II} = 10 \cdot \lg\left(\frac{|I|}{\left| 2 \cdot k \cdot \sqrt{m' \cdot B} \cdot G_{vv} \right|} \right) \tag{8}$$

and large negative values indicate a highly reverberant field one for which even small phase mismatches may cause large random errors. While values close to zero indicate ideal conditions. Figure 3 shows the magnitude of the error for a reasonably small range in R_{II}. Since changing the ratio Δ/λ introduces a bias the range was controlled ($0.23\lambda<\Delta 0.27\lambda$) keeping the bias error typically less than ±15%. (The reason for the outlying data point is not known). The error in the measurement is not very strongly correlated R_{II}, at least for the limited R_{II} range investigated here indicating that the phase matching adequate. However, there is a slight trend to increasing uncertainty with increasing R_{II}.

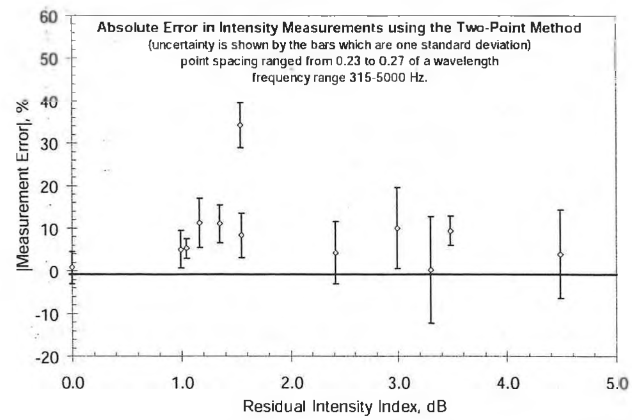

Figure 3: Error and uncertainty in the measured intensity of the two-point method as a function of the residual intensity index, R_{II}.

DISCUSSION AND CONCLUSIONS

The two-point structural intensity method provides acceptable accuracy if the measurement positions are not in the near field. In this situation the four-point method should be used. Correct selection of point spacing is critical to both methods. If an error of approximately 1dB (±30%) in the intensity can be tolerated then the point spacing should be in the following range:

Two-point $0.16\lambda < \Delta < 0.33\lambda$, with 0.25 λ being optimal;

Four-point $0.31\lambda < \Delta < 0.39\lambda$, with 0.35 λ being optimal.

The correlation between R_{II} and the measurement uncertainty was not very good. Nevertheless, it is still a useful indicator of the potential uncertainty in a measurement.

REFERENCES

(1) Stefan Schoenwald, Trevor RT Nightingale, "Measurement of Structural Intensity on Plate Structures," Canadian Acoustics Vol. 29, No.3.

(2) Noiseux, D.U., JASA, Vol. 47, No. 1, 1970, pp. 238-247.

(3) Cuscheri, J.M., Noise Control Engineering Journal, Vol. 37, No. 5, 1991, pp. 97-107.

(4) Linjama, J., Lahti, T., JSV, Vol. 153, No. 1, 1992, pp. 21-36.

Measurement of Structural Intesntiy on Plate Structures

Stefan Schoenwald* and Trevor T. Nightingale**
* Fachhochschule Stututgart, Hochschule fur Technik, Schellingstrasse 24, D-70174 Stuttgart, Germany
** Institute for Research in Construction, National Research Council, Ottawa, Ontario, Canada K1A 0R6

INTRODUCTION

This paper provides a summary report of a recent project where a scanning laser vibrometer and specially developed analysis software were used to investigate structural intensity as a tool to study power flow in plate structures. In this paper the method will be used to examine the power flow in a rib-stiffened plate system where the rib is attached using a series of local connections formed by bolts. The number of equally spaced fasteners is changed from sixteen to four to determine if structural intensity can be used to identify line and point connected regimes of the junction.

MEASUREMENT SET-UP

Both the plate, rib and method attachement are the same as those used in an earlier study of method to model plate/rib junctions. The plate and rib were fabricated from Plexiglas (density, 1191.3 kg/m^3, Young's modulus 4.59x10^9 N/m^2, and Poisson's ratio 0.289) which approximates a homogeneous and isotropic media. The plate had dimensions 2.41 x 1.25 x 0.0115 m while those of the rib were 1.225 x 0.235 x 0.0187 m. The face of the rib that attached to the plate was machined flat and fastened so that it divided the plate into two 1.2 x 1.2 m sections using four or sixteen equally spaced fasteners.

The system was excited by an electrodynamic shaker located one of two positions. First, the rib was excited normal to its surface at a location 0.535 m from the bottom of the rib and 0.165 m from the plate. For this position the junction can be viewed as being a source for both portions of the plate. Second, The lower left portion of the plate was excited approximately 0.75m from the rib and 0.35 m from the bottom of the plate. For this excitation position, the junction can be viewed as a discontinuity blocking transmission to the other portion of the plate.

MEASUREMENT METHOD

The plate surface velocity was sampled using a scanning laser vibrometer (Polytec PSV 300) using a uniform grid of approximately 8000 points. Proprietary software developed at the NRC was used to compute the structural intensity vectors using both the two-point and thirteen-point methods. Since the location of sources can be identified by the direction of the intensity vectors, this paper is primarily concerned with resolving the direction. A comparison of the vector plots obtained from the two-point method (which measures only the moment component) and the thirteen-point method (which measures both the force and moment components) is excellent, and will not be presented here due to limited space. The nearfield may potentially affect estimates of the absolute intensity for distances less than 100 mm from a source or sink. However, it should not affect estimates of direction as only the ratio of the magnitudes in the x and y direcxtions are needed.

Only a 600-mm section of the plate centered on the junction is shown in Figures 1 though 4. The vector plots and contour plots at 1000 Hz for the two-point method are shown on the left and right of the figures, respectively. The plate and rib can be considered as being thin since the transition to thick plate theory is well above 1000 Hz. Fastener locations are shown by solid dots.

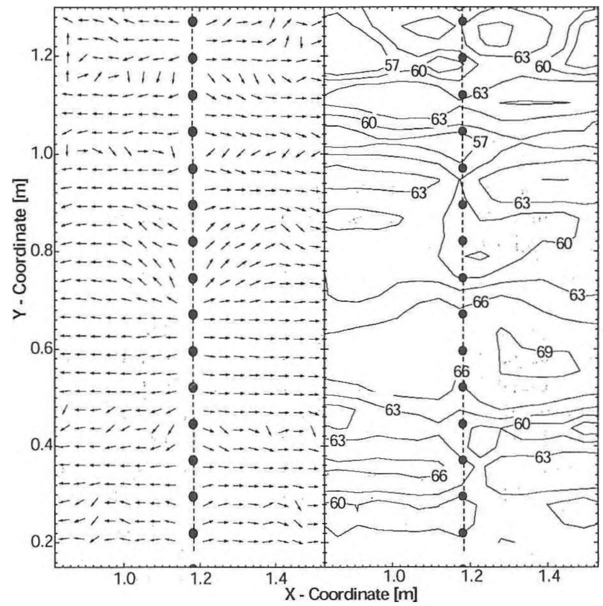

Figure 1: Measured intensity vectors (left) and contour plot (right, intensity magnitude in dB) of the Plexiglas plate due to excitation by a rib attached with sixteen bolts shown by the dots.

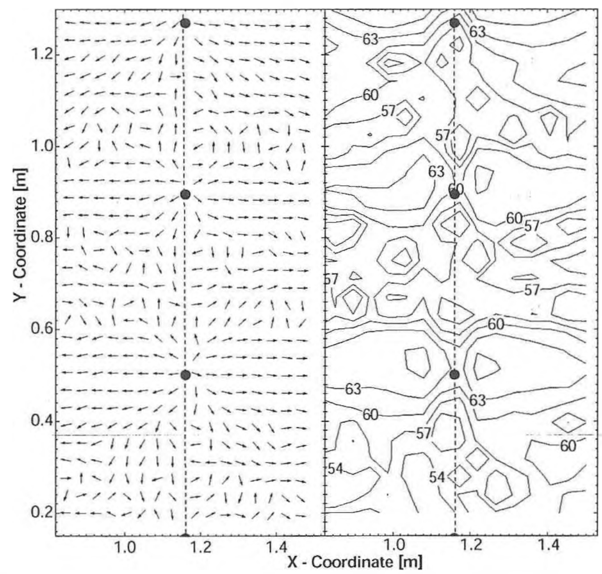

Figure 2: Measured intensity vectors (left) and contour plot (right, intensity magnitude in dB) of the Plexiglas plate due to excitation by a rib attached with four bolts shown by the dots.

MEASUREMENT RESULTS – RIB EXCITATION

Figure 1 shows the measured structural intensity of the plate when the rib is excited and attached to the plate using sixteen fasteners spaced 0.078 m on center, which is less than one-half of the wavelength at 1000 Hz. The radiation pattern is quite symmetric about the junction and at a distance of about 100 mm the almost all vectors are oriented normal to the junction axis. This behavior is typical of a line source, indicating the junction is line-connected. It is also consistent with the generally accepted rule that discretely fastened junctions behave as if they were line-connected if the fastener spacing is less than one-half of a wavelength.

Near the mid-point of the junction the vectors tend to point toward the top the plate at an angle of 45 degrees. Examining the contour plot it can be seen that the vectors are flowing from a region of high intensity to low intensity centered around the seventh and eighth fastener from the top. The cause is likely due to differences in the degree of mechanical contact or modal properties of the rib, which is exciting the junction. A detailed discussion is beyond the scope of this summary paper.

The contour plot indicates that there is significant variation in the intensity in the direction parallel to the junction while there is not nearly the same degree of change in the direction normal to the junction. This may be caused by the modes of the rib.

Figure 2 shows the results when there are only four fasteners connecting the plate and rib. In this situation the spacing between the points is 0.390 m, which is approximately twice the wavelength in the plate. The radiation pattern is quite different than that exhibited when there are sixteen fasteners, as now each fastening point appears to be independent and can be clearly identified. Midway between the fastening points the vector field is somewhat random. Here the field is a superposition of fields of approximately equal intensity from the adjacent points and they will tend to sum to near zero in the y direction. The contour plot clearly indicates high intensity near the fasteners with considerably reduced intensity between them. Also the contours tend to be closed indicating that there is attenuation with distance in the x direction, something that was not readily evident when the junction was line connected with sixteen fasteners (Figure 1).

MEASUREMENT RESULTS - PLATE EXCITATION

Figure 3 shows the measured intensity when the left portion of the plate is excited and the rib is attached using sixteen fasteners. On this portion of the plate vector orientation changes with location and the resulting vector field is somewhat regular indicating the presence of modes. On the source side, near the junction, the vectors tend to be oriented parallel to the junction axis, indicating a significant portion of the incident intensity is reflected producing a near-zero intensity flow normal to the junction, the x direction.

On the opposite side of the junction the vectors tend to be oriented normal to the junction axis as they had done when the rib was the source. The discontinuity in the intensity caused by the junction can be clearly seen in the corresponding contour plot.

Figure 4 shows the measured intensity when there are only four fasteners. Midway between the fastening points, the vector fields tend to be reasonably continuous across the junction. While close to a fastening point the vectors tend to be disordered and on the left portion of the plate (containing the source) the vectors tend to point toward the fasteners indicating that they are taking energy out of the system (i.e., sinks). Also the vectors on the left side of the plate tend to be more ordered indicating that the effective damping for this portion of the plate has increased and the direct field from the source is more prevalent. This is consistent with more energy being transmitted across the junction. The contour plots clearly indicate the fastening points are marked by regions of low intensity with regions of high intensity between them.

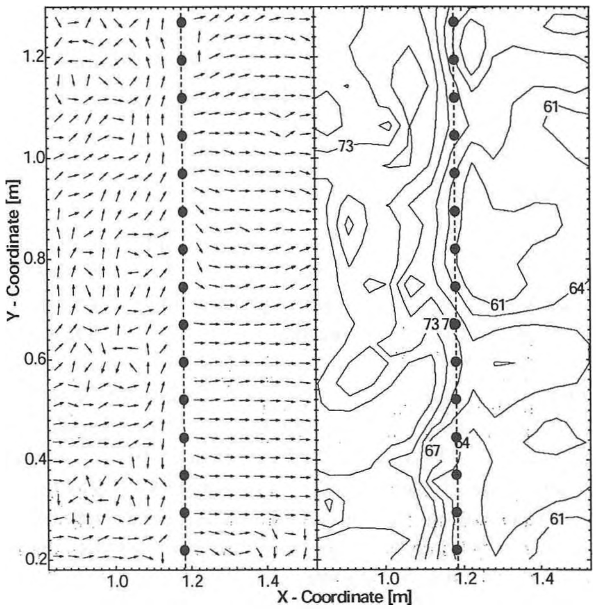

Figure 3: Measured intensity vectors (left) and contour plot (right, intensity magnitude in dB) of the Plexiglas platedue to excitation by a rib attached with sixteen bolts shown by the dots.

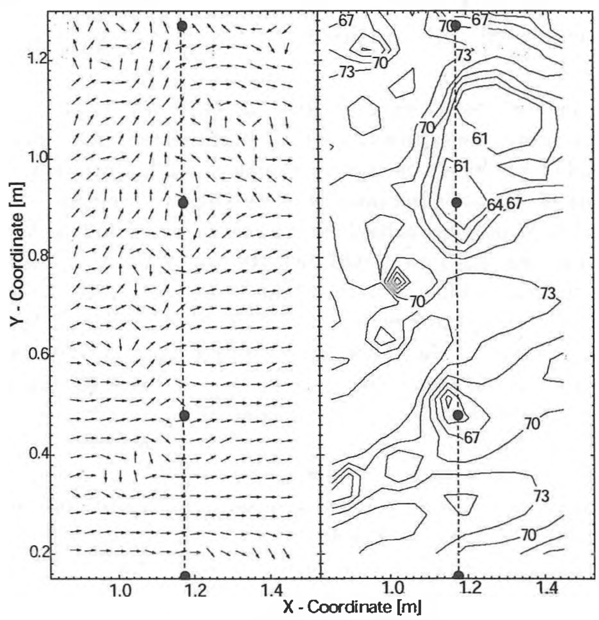

Figure 4: Measured intensity vectors (left) and contour plot (right, intensity magnitude in dB) of the Plexiglas plate resulting due to a rib attached with four bolts shown bv the dots.

CONCLSUIONS

The results show that the orientation of structural intensity vectors can be a useful tool when studying the behavior of junctions in homogenous and isotropic systems. Structural intensity vectors also showed that a plate rib junction with discrete fastening points will exhibit two types of behavior point and line-connected. An investigation of the behavior of the junction near the transition frequency is beyond the scope of this paper. Finally, energy sources are much easier to identify than sinks.

Effects of Forward/Backward Head Position on Judged Auditory Direction

M. J. Reina Lamothe and Annabel J. Cohen
Department of Psychology, University of Prince Edward Island, Charlottetown, PE C1A 4P3

INTRODUCTION

At least three factors have been shown to control judged clockwise (CW) or counterclockwise (CCW) direction of two tones each emanating from a different location on an azimuthal circumference (Cohen, Lamothe, MacIsaac, Fleming, & Lamoureux, 2001). First *proximity* of the two sources governs the judgment such that the directed vector takes the shortest distance between the two sound sources. (A similar finding in the pitch domain has been observed by Shepard, 1964). Secondly, if listeners tend to hear sounds from only the front or back hemisphere, sources of tones in the ignored hemisphere will be re-located to the mirror-imaged position in the preferred hemisphere. This common phenomenon of *front-back confusion* was early described by Toole (1970). Finally, a small but significant tendency for a *clockwise bias* causes listeners to hear tones move in a CW direction more than would be predicted by the other two factors. This last factor is particularly evident for trials containing two locations that are separated by 180-degrees, because in this case the first factor cannot provide proximity cues.

The present study focuses on the role of front-back confusion and examines specifically the listener's nearness to speakers ahead or behind. In our previous studies, the listener sat in the centre of the circle but position of the head with respect to the speakers (ahead and behind the head) was not controlled. Some listeners may have positioned their body more within one hemisphere than the other. This possibility leads to three hypotheses. First, because greater immersion of the head within one hemisphere increases the intensity of the speakers in that hemisphere, hearing of all sounds will be biased to that hemisphere. Secondly, because greater immersion within one hemisphere increases the time and intensity cue differentiation between front and back speakers, this increased differentiation will assist in creating a 360-degree acoustic space. Third, for listeners who have a location bias to one hemisphere or another when centred in an array, positioning the body in the unpreferred hemisphere and the consequent cue differentiation may correct this bias and create the 360-degree space.

In the present study, to test these hypotheses and to increase our understanding of the effect of forward/backward head position on CW and CCW auditory motion direction judgments, an experiment was conducted in which listeners made CW/CCW judgements about auditory direction in three conditions that differed in location of the listeners who were either centred within the circular array of speakers or were positioned one foot ahead of centre or one foot behind.

METHOD

Subjects. There were 4 male and 2 female subjects ranging from 18 to 21 years of age. Hearing level, tested with Digital Recordings AUDIO-CD™ was within normal limits in the range 1000 - 4000 Hz.

Apparatus. In a single-walled sound-attenuated room (Eckel), 12 small Koss speakers (12 x 8 x 8 cm) were spaced at intervals of 30- degrees around an azimuthal circumference of the largest circle (diameter = 119 cm) that could be accommodated by the room. The speakers were 1.5 m off the floor, roughly at ear level for an individual seated in the centre of the circle. Two speakers were suspended from each of three walls, however, because the room was slightly rectangular speakers on the back wall sat on a shelf. The 4 remaining speakers were supported independently on metal stands. A multiplexing switch directed an audio signal to one of the 12 speakers. The signal was a complex tone composed of 10 octaves of 22.5 Hz with an envelope that approximated a Gaussian function. Each signal was 250 ms in duration.

Procedure. Listeners were tested individually, seated within the circumference of the 12-speaker array. In a block, each listener was presented with (12 x 11 =) 132 pairs of successive tones, such that all possible successive pairs of the 12 speakers were represented. The intertone interval within a trial was 450 ms. On each trial, the listener was requested to judge the direction of the sound around his or her head represented as two choices (CW or CCW) on a computer screen. The listener clicked a mouse to make the selection and this initiated the next trial automatically. The block of trials took about 10 min. There were 3 successive blocks in a session, such that each pair was represented 3 times for a total of 396 trials. Each listener received 3 sessions (1.5 hr of testing).

For each of the three 396-trial sessions, the listener sat in a different position relative to the circle, either in dead centre, or one foot ahead or behind this position (a movement along the line joining diagonal corners of the room). The listener always faced the same direction–a corner of the room— and used a cordless mouse, on a bench positioned near him or her, in order to affect the screen at the various distances away from it. Each of the 6 listeners received a different order of the positions, such that all possible orders were represented by the subjects (i.e., ahead, centre, behind; ahead, behind centre; centre ahead, behind, etc).

RESULTS

Direction as a function of CCW rotation. Considering the CW movement only, the trials represented 12 different sizes of spatial intervals, the smallest (1 unit) arising from presentation of one of the 12 tones, followed by the speaker to its adjacent right. The distance of 2 units was represented by pairs in which the 2nd speaker was 2 speakers to the right of the speaker that presented the 1st tone of the trial. The distance of 11 units was represented by pairs whose 2nd speaker was 11 tones CW from the first tone presented (i.e., just 1 unit away CCW). For each session of 396 trials, for each individual, the number of clockwise judgments for each of the 12 clockwise distances was calculated. The mean percentage of clockwise judgments is shown in Figure 1. It can be immediately seen that the number of clockwise judgments is a continuous function of distance and mirrors the pattern of directional judgments for circular pitch of Shepard (1964).

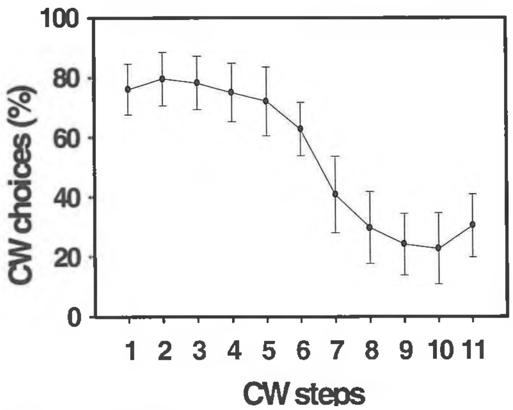

FIGURE 1. Mean percentage of CW judgments and SD as a function of CW step size collapsing over all sessions and subjects.

Front back confusions. An 11 x 12 matrix of CW or CCW judgements for each of the three blocks of data for each subject was compiled with a CW judgement given the value 1 and a CCW judgment given the value -1. These data were correlated with each of three templates of judgment based on the proximity rule (smallest distance governs the choice) and differing in the extent and type of front-back confusion. Template 1 (Circular) had no front-back confusion and assumed the location of all speakers was judged veridically. Template 2 (Front) represented the listener who heard tones emanating only from the speakers in the front hemisphere, with sounds from the back hemisphere heard as coming from the position mirrored in the front hemisphere. Template 3 (Back) represented the listener who heard tones only in the back hemisphere. A correlation of the actual data with the templates led to 3 correlation coefficients for each subject (however Templates 2 and 3 were different only in sign, and Template 3 will not be specifically referred to again). For each subject at least one of these correlations was statistically significant. Where correlations were high for one template, they were lower for the other.

For all listeners the Circular Template provided a better fit to the data when listeners were seated closer to the front speakers. For the majority of the listeners, changing proximity to the speakers by one foot changed the goodness-of-fit of the template. For only one listener, was the circular template the best-fit for all three locations. For three of the listeners the back position led to a best-fit with the Back Template, but for one listener in the back position, the best fit was the Front Template. For two listeners, the centre position was characterized by a Front Template for one listener, and a back template for the other.

The mean correlation obtained with the Circular Template for all six subjects for the ahead, centre, and behind positions was .73, .55 and .44 respectively. Thus, the appropriateness of the Circular Template is greatest for the in-front-of-centre position, and is least appropriate for the behind-centre position. To determine whether these differences were significant, for each subject, the correlation derived from the circular template was entered into a repeated measures ANOVA having one factor of seating position having three levels (ahead, centre, behind). The effect of body position was significant, F (2, 10) = 7.20, $p <$ .012, attributable to a linear trend, F (1, 10) = 22.9, $p < .005$. A similar analysis of correlations for the Front Template did not produce significant effects.

DISCUSSION

The present study illustrates that a relatively small change of a listener's position within a circular array can reverse the perceived direction of auditory motion. The result is explained by an increase or decrease in front-back confusion, with trials whose direction is switched being those with one or two speakers in the non-preferred hemisphere (i.e., if the listener hears all tones in the front, then a tone presented from a speaker in the back hemisphere will be heard as coming from its mirror image location).

The most important finding however is the fact that, at least in these conditions of testing, the most veridical hearing, that is, hearing without front-back confusion, and hearing in a full 360 degrees arises for five of the six listeners when they are not in the centre of the circle, but rather one foot forward. Moving ahead must be compensating for a tendency to hear the speakers in the back when one is truly centred. In spite of this general trend in the data, there were wide individual differences. These results have practical implications for those who would create impressions of spatial auditory vectors, in real-world surround-sound environments, such as home and public theatres.

REFERENCES

Cohen, A. J., Lamothe, M. J. R., MacIsaacs, R., Fleming, R., & Lamoureux, M. (2001). Does proximity govern judgments of auditory direction in the azimuthal plane? *Journal of the Acoustical Society of America, 109*, No. 5, Pt. 2, pMUa3 Abst.

Shepard, R. N. (1964). Circularity in judgements of relative pitch. *Journal of the Acoustical Society of America, 36*, 2346-2353.

Toole, F. (1970). In-head localization of acoustic images. *Journal of the Acoustical Society of America, 48*, 943-949.

Acknowledgements and author notes.
The research was supported by an NSERC Operating Grant to A. J. Cohen. The assistance of Robert MacIsaac who tested the subjects and of Robert Drew and Ian Toms who assisted in calibration is acknowledged. The multiplexing switch was developed by Michael Lamoureux and adapted by Richard Fleming.

Correspondence may be directed to either author at rlamothe@upei.ca or acohen@upei.ca respectively.

Rating Sound Level - An Overview Of Amendment 1 To Iso 1996-2

C. A. Krajewski
Ontario Ministry of the Environment, 2 St. Clair Avenue West, 12th Fl. Toronto, Ontario, M4V 1L5

1. INTRODUCTION

Environmental noise is a composition of sounds from many sources. The contributing sources may be separate or in various combinations as well as capable of changing their temporal and spectral characteristics. The method and procedures for the description and measurement of environmental noise must be applicable to sounds from all sources which, individually and in combination, contribute to the overall noise at the site, as well it must be related to human response to noise. However, the precise exposure/response relationship continue to be the subject of the scientific debate, and practicality of the applied method should be viewed in the context of the social, economic and political climate. For these reasons a number of different methods is currently in use for different type of noise in various jurisdictions. The evaluation of long-term noise annoyance was addressed, during the last two decades, using the equivalent continuous A-weighted sound level as a basic quantity supplemented by corrections or other descriptors applicable in various noise situations. However, this evaluation method had limitations, specifically in application to the assessment of impulsive and tonal sounds. The concept of the rating sound level, developed in the recent years, incorporates, in addition to the equivalent continuous A- weighted level, the impulse adjusted A-weighted level based on the sound exposure level measurements, and specific adjustments for different characteristics of impulsiveness as well as tonality.

2. RATING LEVEL

The rating sound level is determined over reference time intervals related to the characteristics of the sources(s) and receiver(s). For impulsive sounds there are two cases to consider:

In Case 1 the impulsive sounds can be identified and separately measured as single events from distinct source(s). For this case, the rating level for each reference interval is given by:

$$(L_{Ar,T})_i = 10\lg[10^{0.1[(L_{Aeq,T})i + (K_T)i]} + 10^{0.1[(L_{ArK1,T})_i]}]\mathrm{dB}$$

where:

$(L_{Aeq,T})_i$ - *equivalent continuous A-weighted SPL during the i th reference time interval*

$K_T)_i$ - *tone adjustment applicable to SPL during the i th reference time interval (5 to 6 dB if demonstrated* by 1/3 octave analysis, *2 to 3dB if demonstrated by narrow-band analysis)*

$(L_{A\,rK1,T})_i$ - *impulse adjusted A-weighted level ot the impulsive sound during the i th reference interval expressed by the following equation*:

$$(L_{ArK1,T})_i = 10\lg[(1/T\sum_{j=1}^{N} 10^{0.1(L_{AErj})_i}]\mathrm{dB}$$

In the above equation, $(L_{AE\,rj})_i$ represents the impulse adjusted sound exposure level as follows:

$$(L_{AE\,rj})_i = (L_{AE\,j})_i + (K_{1\,j})_i$$

where:

$(L_{AE\,j})_i$ - *sound exposure level of the j th impulse during the i th reference time interval*

$(K_{1\,j})_i$ - *impulse adjustment applicable to the j th impulse during the i th reference time interval (12 dB for each highly impulsive sound and 5 dB for each ordinary impulsive sound)*

The impulse adjustment applies when the equivalent sound level $(L_{Aeq,T})_i$ was measured inhibiting impulsive events. If the measured $(L_{Aeq,T})_i$ already includes the impulsive sound energy, the impulsive sound adjustment should be re-adjusted. The re-adjusted values K_{adj} can be calculated from the original values **K** by the equation:

$$K_{adj} = 10\lg(10^{0.1K} - 1)\ \mathrm{dB}$$

For $K = 12$ dB $K_{adj} = 11.7$ dB

For $K = 5$ dB $K_{adj} = 3$ dB

In **Case 2** the impulsive sounds cannot be separately measured as single events from distinct source(s). For this case, the rating sound level for each reference time interval is given by:

$$(L_{A\,r,T}) = (L_{A\,eq,T})_i + K_{T\,i} + K_{1\,i}$$

where:

$K_{T\,i}$ - *tone adjustment applicable to the ith reference time interval*

$K_{T\,i}$ - *impulse adjustment applicable to the ith refer-*

ence time interval. The value of this adjustment is 5 dB.

3. IMPULSE ADJUSTMENTS

According to findings documented in a large body of research the exposure to impulsive sounds is more annoying than exposure to noise from other sources when each produces the same equivalent sound level. Therefore, impulsive sound adjustments were introduced to provide numerical guidance to ensure proper rating of impulsive sounds. These adjustments were specified for the following categories of impulsive sound:

- **highly impulsive sound**, typically generated by small arms fire, hammering, stamping, forging, punching, cutting, forming, moulding, rail yard shunting operations.
- **high energy impulsive sound**, typically generated by quarry and mining explosions, sonic booms, demolition, industrial processes using high explosive, industrial circuit breakers and military ordnance.
- **ordinary impulsive sound**, including sounds that are sometimes described as impulsive, but are not normally judged to be as intrusive as highly impulsive sounds. Typically, sound sources of this category are car door slams, outdoor ball games, church bells, very fast passbys of vehicles, trains or low flying military aircraft

Research results show that the impulsive sound adjustments are not constant. With the exception of high-energy impulsive sounds, where the adjustment may be significantly greater, adjustments for impulsive sound typically range from 2dB to 15 dB. The value of the adjustment change with the type and character of the sound. The concept of "highly impulsive sounds" was developed by CEC research (references [2}, [3], [4] and [5]). Data obtained in various field surveys and laboratory studies indicate that for highly impulsive sounds, the adjustment ranges from 8 dB to 15dB. Research data also show that for ordinary impulsive sounds typical adjustments range from 2 dB to 7 dB.

In the revised ISO-2 standard 1996 (reference [1]), adjustments of 12 dB and 5 dB are applied to the sound exposure level of highly impulsive sounds and ordinary impulsive sounds respectively. The two values , 5 dB and 12 dB, provide adjustments that normally will be within 3 dB of research measured values.

For assessment of high-energy impulsive sounds, some countries use C-weighted sound exposure level, or peak level to determine a rating level. In other countries A-weighted sound exposure level is used. When the A-weighting is used, the value of the adjustment should be significantly greater than 12 dB. However, at the present time there is no agreement on the specific adjustment value.

4. TONAL ADJUSTMENTS

Tonal components in environmental sounds enhance noticeability or intrusion of those sounds within the general background of other non-tonal sounds. If tonal components are predominant characteristics of the sound within a specified time interval, an adjustment, $\mathbf{K_{Ti}}$, may be applied, for that time interval, to the measured equivalent continuous A-weighted sound pressure level. Procedures for assessing audibility of tones and specific correction factors to the measured data to account for the increased annoyance of the tonal components were developed by several researchers in the last four decades (references [6], [7], [8], [9] and [10]). In the revised ISO standard 1996 (reference [1]), it is suggested that, in practical case, a prominent tonal component may be detected in one- third octave spectra if the level of a one-third octave band exceeds the level of an average of the adjacent bands by 5 dB or more. However, a narrow-band frequency analysis may be required in order to detect precisely the occurrence of one or more tonal components in a noise signal.

If tonal components are clearly audible and their presence can be detected by a one-third octave analysis, the adjustments may be 5 dB to 6 dB.

If the components are only just detectable by the observer and demonstrated by narrow-band analysis, an adjustment of 2 dB to 3 dB may be appropriate. Tonal adjustment apply only to the part of reference interval during which tonal characteristics was present.

5. METHOD IMPLEMENTATION

A number of issues related to the method implementation is still subject to discussion by the ISO 1996 working group and further improvements to the standard are anticipated in future revised standard. The following are some issues subject to the working group discussions:

- In both Case 1 and 2, the reference time interval is specified as a time interval where specific impulse or tonal sound characteristics are clearly detectable. In practice, it may not be easy to separate time intervals with clearly determined sound characteristics.
- Relevance of the recommended impulse adjustments is based entirely on the source description, ignoring the range of the generated sound levels. Also, no consideration is given to the effect of impulse adjustments on assessment of impulse sources subjected to noise reduction; for a given category of impulse sound, the adjustment (penalty) will be the same with or without noise reduction measures.
- It is not clear that sounds from particular sources, at a distance from the sources, can be so definitely characterized as "impulsive", "highly impulsive" or "high-energy impulsive". The character of impulsive sound will change with distance from the source, as well when shielded, when under the influence of certain meteorological conditions and when propagated over different types of ter-

rain. It may be quite difficult to determine if the sound under investigation qualifies for assessment under Case 1 or Case 2, and what specific value of adjustment applies.. In practice, noise from some sources such as for example clay target shooting can exhibit characteristics typical for Case 1 and Case 2, even at the same receptor location and during a period of measurements as short as 30 minutes.

The perceived noise may be judged by a recipient in a different way. In implementing the method, discretion will have to be given to acoustic practitioners. However, it may be too complex for a layman to use.

- Categories of impulse sounds quoted in the standard are not inclusive enough. There is a lot of other sound sources having comparable characteristics and an equal degree of noisiness such as for example; metal processing plants (dropping of steel ingots), glass processing facilities, transportation sources ("jake" brakes), loading of transport containers, dock-yard rivetting and a variety of outdoor events (fireworks), etc.
- Reference is made in the revised ISO standard 1996 (reference [1]), to alternative methods of assessment for "high energy impulsive" sounds. However, specific recommendation on the selection of the sound descriptor for the assessment is not provided. Also, no specific adjustment value (higher than 12 dB) is recommended signifying that the status of the current research is insufficient to properly quantify the subjective effect of such sounds.

6. SUMMARY

An overview of the new method for description and measurement of environmental noise has been presented. Although some issues related to the method implementation remain, as yet, unresolved, the method represents a significant improvement over the currently used assessment procedures. A new approach to the assessment of impulsive noise is the main advantage of the method, as the existing impulse noise criteria tied to a number of impulses observed during the reference time period can be replaced by a single criterion based on the rating sound level.

The new method and all three Parts of the ISO 1996 standard were subject to review by the CSA 107.53 Working Group of the Industrial Noise Subcommittee over the past two years with the objective to endorse the ISO 1996 standard (references [11], [12] and [13]), and to assess its effectiveness for regulatory compliance. Alternative recommendations, supplementary notes/interpretations resulting from the CSA Working Group discussions were incorporated in a Prescriptive Annex to a proposed CSA standard.

In addition to the review work, the CSA Working Group developed tools for Round Robin Test of the rating sound level method, including selection of sample sound signals, instrumentation for the signals reproduction and development of computer spreadsheets for data analysis. An evaluation of results of the 1st phase of Round Robin Test is discussed in a companion paper.

7. REFERENCES

[1] ISO 1996-2, Acoustics-Description and measurement of environmental noise. Part 2, Acquisition of data pertinent to land use, Amendment 1 (1998)

[2] Berry, B. and Bisping, R. CEC Joint Project on Impulse Noise: Physical quantification methods. Proc. 5th Intl. Congress on Noise as a Public Health Problem, Stockholm, 1988, pp. 153-158.

[3] Berry, BF. Recent advances in the measurement and rating of impulsive noise. Proc. 13th ICA, Belgrade, 3, 1989, pp. 147-150.

[4] Rice, C.G. CEC Joint research on annoyance due to impulse noise. Proc. 4th Intl. Congress on Noise as a Public Health Problem, 2, 1984, pp. 1073-1084

[5] Rice, C.G. Human response to impulse noise: CEC studies: Review of 1987/1989 research programme. Proc. 13th ICA, Belgrade, 3, 1989, pp. 135-138.

[6] K.D. Kryter and K.S. Pearsons, "Judged noisiness of a band of random noise containing an audible pure tone.", J. Acoust. Soc. Am 38, 106-112 (1965)

[7] P.R. Williams & D.W. Robinson, "The detectability and tonal character of tones and other narrow-band stimuli in noise" ISVR TR 159, University of Southampton, (1988)

[8] D.W. Robinson, "The assessment of noise containing tonal components", ISVR TR 163, University of Southampton (1988)

[9] N.D. Porter, I.H. Flindell, and B.F. Berry, "An acoustic feature model for the assessment of environmental noise", Acoustics Bulletin, November/December 1993

[10] I.H. Flindell, " Sounds with tonal features-research methods and assessment", Inter-Noise 96, pp. 2473- 2478

[11] ISO 1996/1, Acoustics-Description and measurement of environmental noise-Part 1: Basic quantities and procedures.

[12] ISO 1996-2, Acoustics-Description and measurement of environmental noise-Part 2: Acquisition of data pertinent to land use.

[13] ISO 1996-3, Acoustics-Description and measurement of environmental noise-Part 3: Application to noise limits.

FSTC OF HIGH RISE CONCRETE WALL

James L. Feilders
Jade Acoustics Inc., 545 North Rivermede Road, Concord, Ontario, L4K 4H1

Introduction

Sound transmission loss tests following ASTM E336-84 procedures were conducted in a concrete framed high rise residential building. Tests were conducted on an 8 inch concrete shear wall with laminated drywall each side following initial noise complaints and remedial work. The field test results showed dramatic differences from FSTC 50 to 56 due to mounting of the drywall.

Initial Conditions

The wall construction separated two dwelling units with an open kitchen and living/dining area on one side (source) and a bedroom (receive) on the other. Voice communication could be carried out through the wall. A bare 8 inch thick concrete wall has a lab STC rating of 58. It is known that laminating gypsum board to the surface can degrade the acoustical performance.

The Field Sound Transmission Class (FSTC) was measured using a pink noise source and a Larson Davis 2800 Real Time Analyser. Reverberation time was calculated using the room surface characteristics. The STC value was automatically calculated by the analyser.

The FSTC was 50 as shown on Figure 1. A large dip occurred in the 400 Hz region where speech could pass.

Examination

The original solution proposed was to construct an additional insulated metal stud and drywall partition on the bedroom side. However, we recommended the drywall on the bedroom side be removed to check for any deficiencies as any damage to the wall surface would not matter because it would be covered by the new construction.

The bedroom wall was covered with three sheets of 4 foot by 8 foot drywall mounted vertically. One full sheet was first removed. It was discovered that the sheet was mounted with only 6 concrete nails around the perimeter and none in the field. In addition, the 2 inch diameter areas of drywall compound on six inch centres were adhered only to the gypsum board. This may have been due to dust on the concrete surface that was not removed.

The remainder of the drywall was removed and the wall retested. The FSTC was 56 and it was difficult to hear shouting through the wall.

The opposite side of the wall was inspected. Pushing on it caused it to move in and out indicating that it was constructed similarly to the other side. The contractor proposed to hammer in concrete nails over the entire surface but we were unable to do any follow-up testing to investigate the effect.

Conclusions

The poor performance of the initial wall condition appears to be due to the drywall sheets acting as sounding boards. No specific modelling of the phenomenon was performed but this may prove interesting.

Recommendations

The next revision of the National and Ontario Building Codes should include ratings for drywall laminated concrete walls and a cautionary note on the installation. The board should be firmly adhered to the concrete surface. The use of construction adhesive rather than drywall compound should be considered.

Figure 1

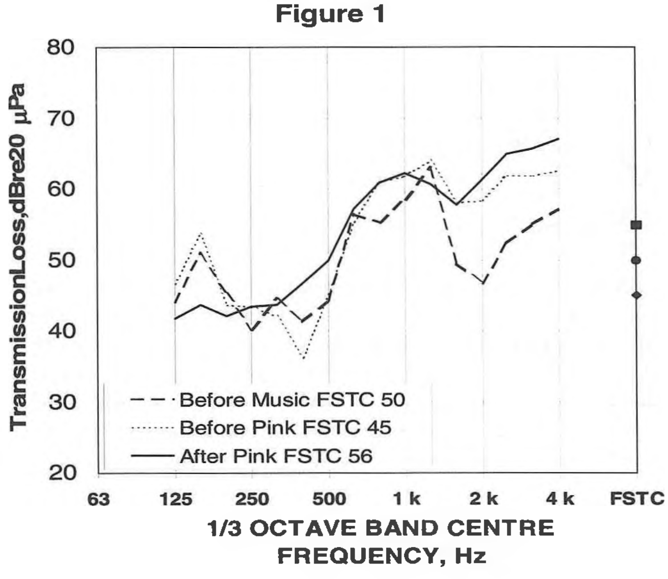

A Preview of The Draft CSA Guideline - Noise Emission Declarations For Machinery

Stephen Keith*, Stephen Bly* and Tim Kelsall**
*Health Canada, Radiation Protection Bureau, 775 Brookfield Rd. 6301B, Ottawa, ON, K1A 1C1
**Hatch Associates, 2800 Speakman Drive, Mississauga, ON, L5K 2R7

1.0 Introduction

Workplace noise is a major occupational health problem that results in thousands of disability claims per year. Community noise from workplaces can also be a significant source of annoyance. Industry works hard to avoid these concerns and to have a quiet workplace. The basic requirement for a quiet workplace is quiet machinery. Noise emission declarations assist the purchaser of quieter machinery by enabling manufacturers to formally provide sound level data in an agreed format.

To help reduce workplace and environmental noise, the Canadian Standards Association (CSA) is producing a guideline on noise emission declarations for machinery. The draft CSA guideline's recommendations are consistent with the requirements for the sale of machinery in the European Union (EU) as given in the EU Machinery Directive (EU directives are available from the Delegation of the European Commission in Canada, Ottawa, Ontario). The CSA document also provides guidance on the use of the series of measurement, declaration and verification standards of the International Organization for Standardization (ISO) (ISO standards are available from the Standards Council of Canada, Ottawa, Ontario). A worked example is provided to give step-by-step technical guidance on the use of the ISO measurement standards in a realistic scenario.

This paper provides excerpts from the draft CSA guideline to illustrate its use and to elicit further feedback from the acoustical community. For reference purposes the CSA guideline must be used; the excerpts in this paper are not an acceptable substitute.

2.0 Guidance For Purchasers

The starting points for use of the guideline are flow charts, one for purchasers and another for manufacturers. The steps for the purchaser are:

i) Determine Noise Design Goal
ii) Write Purchase Specifications
iii) Compare Machinery
Purchase?
Verify?
iv) Measure Sound Levels

i) Determine noise goal - The first step is to determine the noise design goal. For general plant areas the typical design criterion for employee exposure is 85 dBA. This value is generally used by industry even where the province does not yet require it, and organizations such as NIOSH and ACGIH recommend the use of 85 dBA. The CSA guideline also provides recommendations for unoccupied areas, lunch rooms, offices, outdoors, and nearby residences.

ii) Write purchase specification - The second step is the writing of purchase specifications. The draft CSA guideline provides a description of purchase specifications; an example is also given, referring to harmonized ISO standards. It is advantageous to use these standards as the basis for a purchase specification because they provide a convenient means for manufacturers to make measurements and prepare technical reports. Also, the EU Machinery Directive stipulates that conformity is presumed if these standards are used

The noise specification should contain the maximum acceptable declared sound pressure level. Generally this level should be at least 5 dB below the regulated noise limit to be met, i.e. 80 dBA at 1m is typically used if the employee exposure goal is 85 dBA. This difference is necessary because declared levels are obtained under controlled conditions for a single source, whereas the sound level encountered in the workplace includes contributions from multiple reflections and many sources. Where applicable, the corresponding sound power level should also be contained in the noise specification.

iii) Compare machinery - Next the purchaser must compare machinery. It is recommended that comparisons of noise emission data be based on the declared single-number values, which consist of a measured value plus the associated uncertainty. A small percentage of machines in a batch are expected to have noise emission values exceeding the declared value. Even for measurements made on a single machine, there is a small probability that the noise emission value will exceed the declared value.

The ISO harmonized standards allow machinery to be compared independent of the original measurement environments. However, it is important to make comparisons for operating conditions that are as close as possible. Use of the test code written for the class of machinery (e.g. electric motors), provides standard operating conditions and other machine specific recommendations for the tests. When a test code is not available, the CSA guideline provides recommendations on operating conditions.

Knowing which standard was used allows the measurement uncertainty to be estimated from tables in the CSA guideline. All other aspects being equal, noise emission values with a lower uncertainty are preferred.

iv) Measure sound levels - The decision to purchase and verify machinery may involve additional steps. If noise emission values are verified by measurement, the conditions and method of measurement of sound levels must be as close as possible to those required from the manufacturer. For verification of a single machine, the measured value should be less than the declared value. However, when using only one machine to verify an entire batch, the measured value should be 3 dB lower than the declared value. More details on verification are given in the guideline.

3.0 Guidance For Manufacturers

The flowchart for a manufacturer has the following steps:

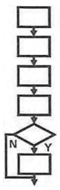

i) Determine Requirements
ii) Measure Sound Levels
iii) Estimate Uncertainty
iv) Document Results
> 1 batch?
v) Quality Control

i) Determine requirements - A noise emission declaration must appear in the operating instructions and documentation for the machinery. The declaration must contain the identification of the machinery, relevant operating conditions, the measurement method and reference to the standards used.

The information provided in a noise emission declaration includes the A-weighted sound pressure level, L_p, if the measured L_p plus uncertainty exceeds 70 dBA. The A-weighted sound power level is also required if the measured L_p plus uncertainty exceeds 85 dBA. In addition, for impulsive sounds, the C-weighted peak sound pressure level is also required if the measured value plus uncertainty exceeds 130 dBC peak. These requirements are consistent with those of the European Union Machinery Directive. Sound power level is required for the EU Outdoor Machinery Directive. The guideline contains excerpts from these Directives to indicate the many types of machines covered and some of the particular requirements for these machines. For example, some machines require the involvement of notified bodies to satisfy European marketing requirements. More details are provided in the CSA guideline.

ii) Measure sound levels - The next step is to measure the machinery noise levels. For a batch of machines, measurements may be made on a sample, instead of every machine. It is strongly recommended to use the CSA guideline and the referenced ISO standards for determination of the declared levels. This will also allow conformity with the existing European Union Machinery Directive and the EU Outdoor Machinery Directive. References to the pertinent standards and Directives, including points of contact for obtaining these documents, are given in the draft CSA guideline.

The operating, installation and mounting conditions of the machine would normally be specified in an ISO or European Committee for Standardization (CEN) noise test code. The conditions are typically reproducible and representative of the noisiest operation in typical usage. ISO and CEN are preparing test codes to ensure comparable and consistent operation of 800 different types of machines. The draft CSA guideline outlines recommended conditions to be used if a test code is not currently available. The guideline provides detailed technical guidance for selection of ISO measurement standards. A worked example is provided for additional guidance.

The standards most commonly used are ISO 11201 and ISO 3744 for sound pressure level and sound power level measurements, respectively. These standards provide for engineering grade measurements in an essentially free field above a reflecting plane. In the guideline, the suitability of these standards for given measurement conditions is summarized based on the floor characteristics, room size, room characteristics, background noise, and the distance to walls, pipes, and other small/large fixtures. Additional guidance is provided for 7 alternate standards.

Sound pressure measurements are made at the operator's position. For sound power measurements, nine or more measurements are made over an imaginary rectangular box that completely encloses the source. The box sides must be at least 25 cm away from the surface of the source. More detailed guidance on measurement positions is provided in the guideline.

iii) Estimate Uncertainty - Estimation of measurement uncertainty is the next step. The guideline illustrates how uncertainty is estimated from the accuracy of the measurement method and the repeatability of the machinery operation. Typically, for an engineering grade measurement, the uncertainty will work out to 5 dB, and for survey grade the uncertainty is 8 dB.

iv) Document results - For auditing purposes, the machinery manufacturer should maintain a technical file. This is a requirement for EU regulatory purposes. This file should include information on the operating conditions of the machinery during measurements and a statement of the noise test codes, standards and methods used to make the measurement. If harmonized ISO standards were not used, then the file should also contain the calculation notes, test results, etc., required to defend the noise emission declaration and the rationale for the use of a method other than specified in a harmonized ISO standard.

v) Quality control - When there is more than one batch of machines being produced, the manufacturer is advised to implement a quality control program. This is essentially a continuous verification process. Verification was briefly summarized above and more details are given in the draft CSA guideline.

4.0 Current Status

The guideline has been circulated in two drafts to a group of stakeholders and made available to subscribers of a popular Canadian e-mail list on Health and Safety (Health & Safety Canada [HS-Canada@list.ccohs.ca]). It is now in its 4th draft and has been approved by the CSA Industrial Noise Subcommittee who have passed it on to the Editorial Subcommittee for review, and to the Main Committee for balloting. The final guideline is expected to be published in 2002.

e-mail s_blv@hc-sc.gc.ca to request a draft for review purposes.

Song Memory: Are Text and Tune Asymmetrically Related in Recognition Memory?

Randall K. Jamieson and Lola L. Cuddy
Department of Psychology, Queen's University, Kingston, Ontario, Canada, K7L 3N6

1.0 Introduction

A song comprises two distinguishable and separate components - text and tune. Yet, hearing a song leaves the impression of a unified event. This incongruity has inspired the investigation into how song is represented in memory. *The integration hypothesis* proposes that text and tune are stored as a composite trace in which the meaning of the text-tune pairing eclipses the meaning of the parts (Crowder, 1993; Samson & Zatorre, 1991; Serafine, Crowder, & Repp, 1984; Serafine, Crowder, Davidson, & Repp, 1986). Associative theories propose that text and tune are represented as two separate memory traces bound by association (Peretz, 1993; Steinke, Cuddy, & Jakobson, in press).

Research has utilized a recognition task where listeners are asked to recognize the texts and tunes of song excerpts when presented with the same partner they were presented with at study (i.e., Match probes), or with a different, equally familiar, partner (i.e., Mismatch probes). The *integration effect* is the finding that a studied song component (i.e., a text or a tune) is recognized best when presented with the same partner it was presented with at study: $p(\text{Hit}|\text{Match}) > p(\text{Hit}|\text{Mismatch})$.

Research has provided evidence of the integration effect in tune recognition. That is, the tune of a song probe is better recognized as "old" in the context of a Match probe than in the context of a Mismatch probe (Crowder et al., 1990; Samson & Zatorre, 1991; Serafine et al., 1984, 1986). However, the integration effect has not reliably emerged in text recognition (Samson & Zatorre, 1991; Serafine et al., 1984). This disparity suggests an associative relationship between text and tune in memory in which a tune is more tightly associated with its text than the text of a song is associated with its tune. Thus far, an asymmetrical integration effect has been noted (Samson & Zatorre, 1991; Serafine et al., 1984), but it has not been investigated or discussed in much detail.

We investigated the relationship between the texts and tunes of songs in recognition memory. We expected that the integration effect would emerge in tune recognition but not in text recognition (i.e., *the asymmetrical integration effect*).

2.0 Method

2.1 Listeners. Thirty native English speakers from the Queen's psychology subject pool took part in the study (23 women and 7 men, *mean age* = 22.8 years, *SD* = 6.5). Music training was scored using a point system. One point was given for each year of private music lessons and one half point was given for each year of group music lessons. Half of the listeners had very little to no music training (M = .60, SD = .78, *range* = 0 – 2.5). The remaining listeners possessed considerably more music training (M = 10.50, SD = 3.88, *range* = 7 – 16.5).

2.2 Materials. Six pools of 20 songs were created and calibrated for the experiment. Tunes of songs were in 4/4 meter, were in the key of A^b-major, were two bars in length, and comprised 10 note events. Within pools, song texts possessed a similar stress pattern and were semantically congruous. All texts were eight syllables in length. All songs were sung by a professional male baritone.

2.3 Procedure. Testing sessions involved five sub-tests and took place a quiet room with groups of two to four listeners. In each sub-test, listeners were presented, twice, with a study-list of six songs. Listeners were then presented with two of each of five sorts of song probes: a) Songs that were in the study-list (i.e., Match probes); b) songs comprising a mismatched pairing of an old text and old tune from different songs in the study-list (i.e., O_{TX}:O_{TN} probes); c) songs that combined an old text from the study-list paired with a new tune (i.e., O_{TX}:N_{TN} probes); d) songs that paired a new text with an old tune from the study-list (i.e., N_{TX}:O_{TN} probes); and e) songs that paired a new text and a new tune, neither of which were in the study-list (i.e., N_{TX}:N_{TN} probes). Listeners provided old/new recognition judgments for each probe's tune, text, and text-tune pairing.

3. Results

'Old song', 'old tune', and 'old text' responses for each class of probe, across all five sub-tests of a testing session, were scored as proportions. The 'old song', 'old tune', and 'old text' data were analyzed separately using 5x2 mixed factors ANOVA designs with probe class as the repeated factor and training group as the between subjects factor.

3.1 Song Recognition. The 'old song' data are presented in Table 1. There was a main effect of probe class, $F(4, 112)$ = 74.38, p < .001. A contrast comparison revealed that listeners in both training groups discriminated old from new songs, $F(1,28)$ = 173.50, p < .001.

3.2 Tune Recognition. The 'old tune' data are presented in Table 2. There was a significant main effect of probe class, $F(4,112)$ = 40.66, p < .001, and a significant interaction between probe class and training, $F(4,112)$ = 3.84, p < .01. A first contrast revealed that trained listeners discriminated old from new tunes better than untrained listeners, $F(1,28) = 5.93$, $p < .05$. A second contrast confirmed the integration effect in tune recognition for both trained and untrained listeners, $F(1,28) = 24.53$, $p < .001$.

3.3 Text Recognition. The 'old text' data are presented in Table 3. There was a main effect of probe class, $F(4,112) = 160.87$, $p < .001$. A first contrast showed that listeners discriminated old from new texts, $F(1,28) = 332.83$, $p < .001$. A second contrast failed to confirm the integration effect in text recognition, $F(1,28) = 1.31$, $p > .25$.

4.0 Discussion

The results confirm the predicted *asymmetrical integration effect.* Recognition of a studied tune was best when presented with the same text it was paired with at study while recognition accuracy for a studied text was equivalent whether presented with the same tune it was paired with at study or with a different tune.

The asymmetrical integration effect contraindicates the integration hypothesis that demands a symmetrical integration effect. Associative theories, however, can accommodate the asymmetrical integration effect by proposing that text and tune are represented independently in memory with a stronger association from a song's tune to its text than the association from a song's text to its tune.

A third explanation for the asymmetrical integration effect is that the phonetic properties of a text impose subtle changes on the acoustical identity of a tune (e.g., note onsets, note offsets, timbral variations, and accent patterns). Since memory for a tune is acoustic in nature, the mental representation of a tune will incorporate elements of its accompanying text. In contrast, because memory for the text of a song is semantic in nature an accompanying tune would not alter a text's semantic representation in memory. Consequently, the recognition of a song's tune will display a context sensitivity for its originally paired text (i.e., the integration effect) while a song's text will not. This reasoning predicts the asymmetrical integration effect and , notably, describes the conditions under which the effect emerges.

Free of theoretical constraints, the current study shows a clear asymmetry in the relationship between text and tune in recognition memory. Unfortunately, the current study cannot address whether the asymmetrical integration effect emerges because of an asymmetrical association between text and tune in memory, or if it emerges as a consequence of the impositions of a paired text on the acoustical identity of a tune. Further investigation is needed to make this important distinction.

References

Crowder, R.G., Serafine, M.L., & Repp, B. (1990). Physical interaction and association by contiguity in memory for the words and melodies of songs. *Memory & Cognition, 18,* 469-476.

Crowder, R.G. (1993). Auditory memory. In McAdams, S. & Bigand, E. (Eds.), *Thinking in sound: The cognitive psychology of human audition* (pp. 113-145). Oxford: Clarendon Press.

Peretz, I. (1993). Auditory agnosia: A functional analysis. In McAdams, S. & Bigand, E. (Eds.), *Thinking in sound: The cognitive psychology of human audition* (pp. 199-230). Oxford: Clarendon Press.

Samson, S., & Zatorre R.J. (1991). Recognition memory for text and melody of songs after unilateral temporal lobe excision: Evidence for dual encoding. *Journal of Experimental Psychology: Learning, Memory, and Cognition, 17,* 793-804.

Serafine, M.L., Crowder, R.G., & Repp, B. (1984). Integration of melody and text in memory for songs. *Cognition, 16,* 285-303.

Serafine, M.L., Davidson, J., Crowder, R.G., & Repp, B. (1986). On the nature of melody – text integration in memory for songs. *Journal of Memory and Language, 25,* 123-135.

Steinke, W.R., Cuddy, L.L., & Jakobson, L.S. (in press). Dissociations among functional subsystems governing melody recognition after right hemisphere damage.

Table 1. *Mean proportion of 'old song' responses for each class of recognition probe for trained and untrained listeners. Bracketed values are standard deviations. Bolded values are hit rates.*

	Recognition Probe				
		New Songs			
Group	Match	O_{TX}:O_{TN}	O_{TX}:N_{TN}	N_{TX}:O_{TN}	N_{TX}:N_{TN}
Trained	**.64 (.15)**	.49 (.18)	.31 (.26)	.09 (.12)	.05 (.06)
Untrained	**.59 (.17)**	.45 (.17)	.43 (.23)	.10 (.16)	.07 (.17)

Table 2. *Mean proportion of 'old tune' responses for each class of recognition probe for trained and untrained listeners. Bracketed values are standard deviations. Bolded values are hit rates.*

	Recognition Probe				
		New Songs			
Group	Match	O_{TX}:O_{TN}	O_{TX}:N_{TN}	N_{TX}:O_{TN}	N_{TX}:N_{TN}
Trained	**.87 (.12)**	**.72 (.13)**	.49 (.21)	**.77 (.22)**	.40 (.16)
Untrained	**.83 (.12)**	**.74 (.18)**	.63 (.16)	**.63 (.13)**	.41 (.19)

Table 3. *Mean proportion of 'old text' responses for each class of recognition probe for trained and untrained listeners. Bracketed values are standard deviations. Bolded values are hit rates.*

	Recognition Probe				
		New Songs			
Group	Match	O_{TX}:O_{TN}	O_{TX}:N_{TN}	N_{TX}:O_{TN}	N_{TX}:N_{TN}
Trained	**.75 (.15)**	**.75 (.16)**	**.74 (.13)**	.14 (.12)	.14 (.15)
Untrained	**.80 (.15)**	**.72 (.21)**	**.76 (.18)**	.11 (.15)	.10 (.13)

This study was supported by a research grant to the second author from the Natural Sciences and Engineering Council of Canada.

STRUCTURE AND CORRELATION IN THE DETECTION OF MELODIC SEQUENCES

Jason Lee*, Frances Leung, Janakan Satkunasingham*, Winnie Wong** and Willy Wong*,****

*Edward S. Rogers Sr. Department of Electrical and Computer Engineering, University of Toronto **Institute of Biomaterials and Biomedical Engineering, University of Toronto

Introduction

It is known that higher animals perform well in the detection and recognition of familiar patterns under noisy conditions. Why is this so? We postulate that it is the inherent structure or redundancy in patterns that allows the sensory system to reconstruct familiar patterns from a noisy scene. In an earlier study by Wong and Barlow[1], it was found that for a well-known melody, the amount of signal and tolerable noise follows a power relationship, with the exponent approximately equaling two. I.e., doubling the amount of melody notes results in a four-fold increase of tolerable noise. This is to be contrasted with the results obtained from detecting signals without structure where tolerable noise level goes as a *linear* function of signal level (exponent equals one).

This experiment continues this study by measuring the detection performance of randomly generated signals of varying degrees of structural content. Fractal melodies were used and the degree of self-correlation (structural content) was changed in a continuous manner. If our postulate is correct, we would expect the exponent relating the tolerable noise and signal level to increase monotonically when the structural content of the signal increases.

This paper provides an overview of the experiment and discusses the hypothesis used in the experiment. Results of the experiment will be shown during the oral presentation.

Generating fractal melodies

It is known that signals with $1/f^{\beta}$ power spectrum, where β is constant and non-negative, have fractal properties [2]. Increasing β increases the self-correlation within the signal and vice versa. In particular, studies have shown that most music possess a 1/f power spectrum [3], [4]. Attempts have been made at generating music from $1/f^{\beta}$ spectrum. According to Voss [3], melodies generated from $1/f^2$ spectra lacks diversity (too correlated) and $1/f^0$ is too random (uncorrelated), while 1/f melody sounds more pleasant to most people. Signals with $1/f^0$, 1/f and $1/f^2$ spectrums are most commonly associated with white, pink and brown noise processes respectively.

In this experiment, we assume that the self-correlation of the signal represents its structural content, and by varying the parameter β, we can generate random melody with varying degree of structural content. In generating the melody, the discrete Fourier transform of the melody is first constructed with the following relationship to ensure $1/f^{\beta}$ power spectrum.

$$|X(k\,\Delta f)|^2 \propto 1/k^{\beta}, \quad k = 0, 1, 2, 3..... 511$$

The phase of the Fourier transform is randomly chosen between 0 to 2 PI for each value of k. The Fourier transform of negative frequency is set as the complex conjugate of that of positive frequency to ensure a real time series. FFT is then performed on the Fourier transform to generate the signal in time series with 1024 samples. The samples are then quantized into 21 levels, each corresponding to a musical note in the C major scale over a 3-octave range. Random rhythm is also added to the melody to make the melody sound more musical.

Experiment

In the experiment, the subject is presented with either a series of noise notes generated uniformly over the 3 octave range (a noise-only trial) or a fractal melody masked by noise notes (a signal-plus-noise trial). Both the noise-only and the signal-plus-noise trials have the same total number of notes. The melody is generated dynamically and differs from trial to trial. The subject chooses a response of either *noise-only* or *signal-plus-noise* after listening to an audio segment of approximately 10 secs in duration. Experiments are carried out over different values of β and over different lengths of the melodic sequence (both parameters are varied separately). The noise level or total number of noise notes changes dynamically, trial-by-trial, according to a Bayesian adaptive algorithm called QUEST [5]. The answer of the subject is recorded, and the percentage of correct answer is used to construct the psychometric function. We then noted the value of tolerable noise permitting 75% correct answers and tabulated such values for different values of beta and total signal or melodic length.

Discussion

The study by Wong and Barlow [1] showed that for a well-known melody, doubling the amount of melody notes results in a four-fold increase of tolerable noise. Hence, a log-log plot of tolerable noise level and signal length results in a line of slope two, meaning a power relationship with exponent equal to two. This is in contrast with the linear relationship between tolerable noise and signal for an unstructured signal, where a line of slope one was found on a log-log plot. Similar results have also been found in other recognition tasks in other modalities [6]. We postulate that it is the inherent structure of the signal that gives rise to the superior signal detection performance (a higher slope on a log-log plot). However, their experiment used the same tune throughout the experiment, and one may suggest that the *a priori* knowledge about the melody alone can contribute to the superior performance achieved by the subjects.

The major difference between this experiment and the above experiment is that the subject does not know ahead of time what the melody will be. Hence memory does not play a part in the detection of the melody, and the major cue is the structure, or the correlation in the melody. If the inherent structure of the melody can achieve superior performance in detection, the slope of the log-log plot of noise vs signal will increase when β, hence the correlation within the signal increases (see figure 1).

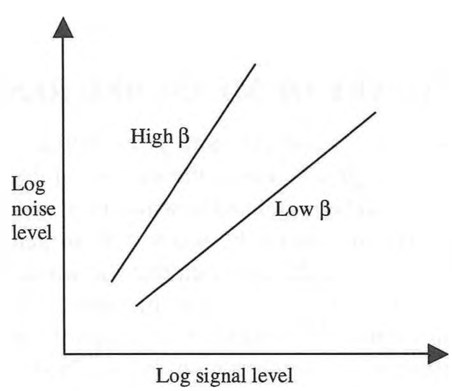

Figure 1: Expected Result from different β

References

[1] H. Barlow and W. Wong, "Tunes and templates," *Nature* vol. 404, pp. 952 – 953, Apr. 2000.

[2] P. Addison, "The colour and power of noise," in *Fractals and Chaos: An Illustrated Course*, London: Institute of Physics Publishing, 1997, pp. 80 – 81.

[3] R. F. Voss and J. Clarke, "'1/f noise' in music: Music from 1/f noise," *J. Acoust. Soc. Am.,* vol 63(1), pp. 258 – 263, Jan. 1978.

[4] R. F. Voss and J. Clarke, "'1/f noise' in music and speech," *Nature*, vol. 258, pp. 317 – 318, Nov. 1974.

[5] A. B. Watson and D .G. Pelli, "QUEST: A Bayesian adaptive psychometric method," *Perception and Psychophysics*, vol. 33(2), pp. 113 – 120, 1983.

[6] P. Neri, M. C. Morrone and D. C. Burr, "Seeing biological motion," *Nature*, vol. 395, pp. 894 – 896, Oct. 1998.

Investigation Of Wave Induced Motion Of A Breakwater Structure Using Automated Monitoring

Miroslav S. Ubovic, Robert D. Stevens
HGC Engineering, 2000 Argentia Road, Mississauga, Ontario, L5N 1P7

1.0 INTRODUCTION

Over recent years, a crack has been forming in a breakwater structure on the Lake Ontario shoreline. An investigative study was undertaken to determine if there is significant motion of the breakwater structure, and if so, whether this motion is wave-induced. Two automated seismographic monitors were fixed to the breakwater, one at each of the east and west ends of the structure, on either side of the crack (Figure 1), for a period of three months during the winter storm season. Motion was recorded in terms of peak particle velocity and was post-processed to compute peak displacement. Various important characteristics about the motion of the structure were evident.

2.0 MEASUREMENT INSTRUMENTATION AND METHOD

The two automatic seismograph monitors were used for this project equipped with external, triaxial geophones, to measure instantaneous velocity at a point (typically termed "peak particle velocity" or PPV, in units of mm/s), in the three principal directions: X, Y and Z. Because it was expected that the monitors would be inaccessible during the measurement period (due to ice build-up) each monitor was connected to a modem and phone line for remote data retrieval and reconfiguration.

Two different modes of data acquisition were employed during successive measurement periods, in order to gain different types of information. For the first two weeks, the monitors were configured in *interval* mode, during which the motion was monitored continuously and the maximum PPV occurring in each 15 minute interval was logged by the monitor, respectively in each of the three principal directions. This mode of operation allowed a manageable amount of information about the measured motion to be recorded continuously, with no gaps in the data. During the second measurement period, the monitors were configured in *threshold*

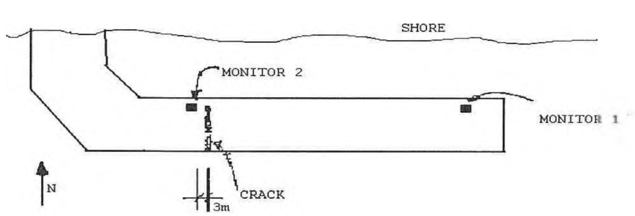

Figure 1: Shematic Plan of Monitor Locations

trigger mode. In this configuration, the monitors captured detailed information for a preset segment of time (e.g., 10 s) once the measured instantaneous motion exceeded a programmed threshold value. Although the monitoring is not continuous in trigger mode, this configuration allowed the unit to store a snapshot of the measured motion waveform, for post analysis. After two weeks of measuring in trigger mode, the monitors were configured back to interval mode to record data continuously for the remaining two months of the study period.

The data was post-processed in a variety of ways to highlight salient aspects of the measurement results. The post processing included integration of the measured velocity data [mm/s] into peak displacement [mm], correlation of motion of the breakwater to wind speed and direction, correlation of motion at Monitor 1 to motion at Monitor 2, and a general consideration of the motion measured in the three principal directions.

3.0 SUMMARY OF MEASURED RESULTS

A primary issue of concern during the initial monitoring period was the degree to which the motion on the breakwater structure could be correlated to wind speed and direction. Since the wave motion of the water will, in general, vary with wind speed, and the direction that the waves strike the breakwater will vary with wind direction, a correlation would indicate that the motion observed on the breakwater could be attributed to wave motion. Figure 2a shows hourly wind speed measured at Toronto Island Airport, obtained from Environment Canada. Figure 2b and Figure 2c show the motion measured at Monitor 1 and Monitor 2. Judging visually by the similarity in shape between the graphs of wind speed and measured breakwater motion, there is general correlation between high winds and pronounced motion. Figure 3 shows the result of an exponential regression calculation for each of the sets of monitored results against wind speed. From the trigger-recorded waveforms, it was evident that the true motion of the breakwater fell within the frequency range of about 2 to 8 Hz, while data falling outside this range was found to be noise (primarily spikes and hum on the A/C lines). The complete set of the data was separated into useful data and noise, during post-processing, based on the frequency range described above.

Figure 4 shows the correlation between the motion measured at Monitor 1 and Monitor 2. The slope of the best fit straight line shown in Figure 4 indicates that, on average, the motion

Figure 2a: Wind Data Jan 13-19, 2001

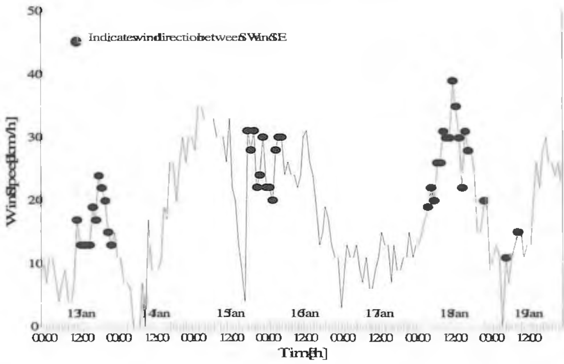

Figure 8a: PPV at Monitor 1 vs Monitor 2 - Lateral

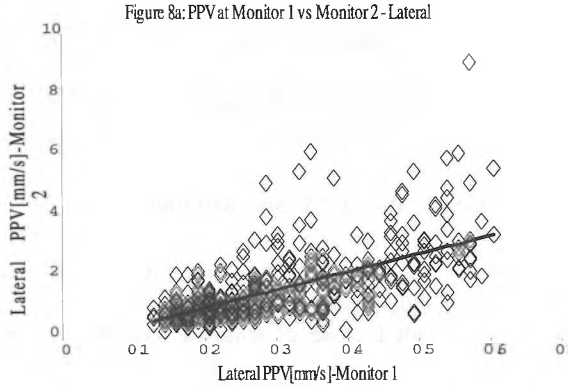

Figure 2b: Monitor 1 Jan 13-19, 2001

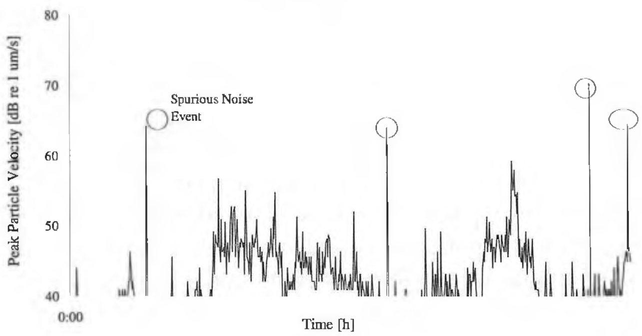

Figure 2c: Monitor 2 - Jan 13-19, 2001

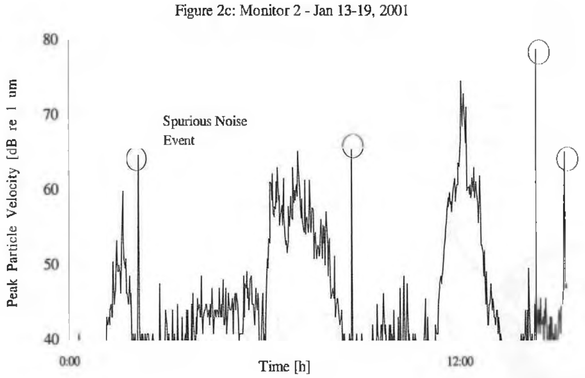

Figure 3: Wind Speed vs. Lateral PPV - Jan 13-19 2001

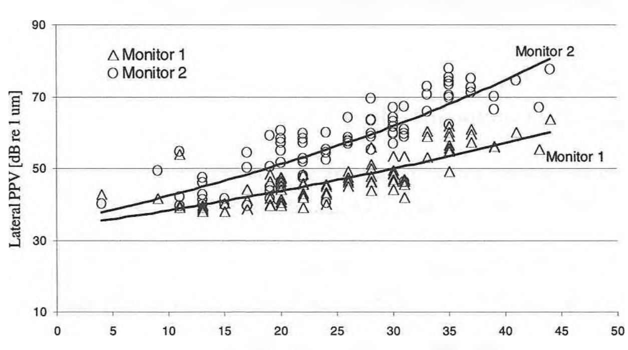

at Monitor 2 is a factor of 3 to 5 times greater than that at Monitor 1. Given that the driving force the two locations is effectively equal (wave impacts), this suggests that the mobility of the structure at Monitor 2 is significantly greater than that at Monitor 1. This observation and the relatively poor correlation (significant scatter in Figure 4) suggest that the two halves of the structure move essentially independently of one another. From a review of all the useful monitored data, the north-south motion at Monitor 2 was greater than that in the vertical or east-west direction, while at Monitor 1 the motion was no greater in north-south direction than in the other two principle directions. This suggests bulk motion is occurring at the west end of structure in the north-south direction. Also, since the wave impacts upon the breakwater occur primarily from the south (given its orientation), the motion in east-west and vertical directions is most likely a result of deformation (i.e. relative motion) rather then bulk motion of the structure as a whole.

4.0 CONCLUSION

The motion at the east and west ends of the breakwater was essentially non-correlated, suggesting that the two halves of the structure (on either side of the crack) move independently of each other. The west end of the structure was found to have displacement 3 to 5 times greater than that at the east end. The recorded data about the motion of the structure appears to indicate the possibility of both bulk motion and elastic deflection of the structure.

Recent Masters Theses At The University Of Western Ontario

Masking Overshoot In Young Versus Older Listeners

Erica F. Wong, M. Sc. (Audiology)

The threshold for the detection of a brief auditory signal in the presence of a longer-duration masker is elevated when the signal is presented close in time to the onset of the masker than when presented at longer delay times relative to the masker onset. This finding has been labeled "overshoot". This study examined the effect of aging on overshoot by comparing normal hearing young adults to normal hearing older adults. Also, the effect of hearing impairment was examined with an additional older adult subject group. Results of this study suggest that older adults exhibit a larger overshoot compared to young adults, and that hearing impairment does not appear to affect overshoot.

Leisure Noise Activites In A Sample Of Canadian High School Students

Lillian G. Ciona, M. Sc. (Audiology)

Recent interest in the prevalence of noise-induced hearing loss has shifted the focus from occupational noise levels to the noise levels of leisure activities. The recreational activities of youth, particularly those activities which utilize high fidelity, high intensity sound delivery systems (personal stereo systems, movie theatres), impulse noises (hunting, fireworks) and high powered motorized vehicles (motocross bikes, race cars) have been implicated as damaging to the human auditory system. An increased incidence of high-frequency hearing loss in young adults has been attributed to exposure of such leisure activities, however the level of participation of Canadian youth in such noisy activities has not been documented. This research was an initial attempt to quantify the participation by Canadian teens and young adults in noisy leisure activities in terms of participation rates, hours per activity, and frequency of participation. In the present study, a questionnaire was administered to a group of local high school students between the ages of 14 and 19. Participants indicated their participation in specific leisure activities during the previous one-week period, and the total duration of participation. The questionnaires were analyzed for number of activities, total participation time, and the noise immission level associated with each respondent's leisure noise exposure. The self-report questionnaires and previously published values of sound pressure levels of the reported activities were used to compute the NIL and risk of noise-induced hearing loss from leisure noise exposure. Approximately 66% of the students may be at risk, based on their responses. This determination of noise immission levels in teenagers can lead to noise control or legislation regarding permissible exposure levels in recreational activities and may motivate educational efforts (such as hearing conservation programs) to reduce hazardous noise exposure in the youth population, if the noise immission levels warrants such reductions.

Canadian Acoustical Association
Minutes of the Board of Directors Meeting -16 June 2001 - Toronto, Ontario

Present: J. Bradley, D. Giusti, T. Nightingale, K. Fraser, T. Kelsall, K. Fuller, R. Ramakrishnan, D. Stredulinsky

Regrets: N. Atalla, M. Cheesman, D. DeGagne, J. Hemingway, D. Jamieson, D. Whicker.

Meeting called to order at 10:06 a.m.

Minutes of the 28 September Board of Director's meeting were approved as written in the December 2000 issue of Canadian Acoustics. (Moved by R. Ramakrishnan, seconded by D. Giusti, carried).

President's Report

J. Bradley reported that, effective October 2000, Industry Canada approved the bylaw changes. The possibility of CAA involvement in the planning and organization of INTERNOISE 2002 to be held in Dearborn Michigan was discussed. No direct involvement by CAA was anticipated, although members may be asked to organize special sessions.

Secretary's Report

T. Nightingale was very pleased to report that in FY00/01 there was a 13% increase in membership (including non-voting journal subscriptions) which can be primarily attributed to the new members gained at the Sherbrooke Conference. As of June the total paid membership stands at 391with 80% being located in Canada, 10% in the USA, and 10% overseas.

The Secretary reported that the domain name "CAA-ACA.CA" was purchased and registered. Note: It must be renewed every twelve months. The new domain name has been linked (via a redirect) to the existing CAA web site hosted by UWO. (The cost for registration and the redirection was approximately $110.00) It was reported that the next steps in CAA having an independent web site is for the web mater(s) to design and create the web pages. Once complete, CAA can upgrade to a web-hosting package, which would have an annual cost of about $400 to $700 per year depending on the size of the site.

The Secretarial operating costs for the first ten months of FY00/01 were $995 which included the cost associated with domain name registration. There is $335 dollars in the Secretarial account. The Secretary moved that, "A cheque be issued for $300 to cover regular maintenance of the databases until the next Board meets next in October 2001." The motion was seconded by D. Giusti, carried.

The Secretary announced that he would not be seeking reelection at the October 2001 AGM.

(Acceptance of the Secretary's report was moved by D. Stredulinsky, seconded by T. Kelsall, carried).

Treasurer's Report

The Treasurer provided an itemized report of the Association's finances for the last three years. The report indicated a solid financial position. In all three fiscal years, revenues have exceeded operating costs. It was reported that the recent drop in interest rates has significantly reduced the rate of return for the investments, primarily bonds and GIC's. However, this was more than offset by the surplus from the 2000 Conference and the SPIF donation.

After discussion of the desired distribution of funds between the operating and capital accounts, D. Giusti moved that, "Twenty-five thousand dollars be transferred from the Operating Account to the Capital Account." The motion was seconded by Tim Kelsall. The Board also directed the Treasurer to continue to invest in fully guaranteed financial products that render a higher rate of return.

The Treasurer reported that a VISA merchant's account has been established and that the CAA should be able to accept payment by VISA for registration at the 2002 conference and for 2002 annual membership dues.

(Acceptance of the Treasurer's report was moved by R. Ramakrishnan, seconded by T. Kelsall, carried).

Editor's Report

R. Ramakrishnan reported on the possibility of publishing six issues of the Journal each year. Currently there is sufficient material (papers, articles, review, laboratory highlights, etc.) to warrant this. However, there was considerable discussion regarding the increased printing and mailing costs and if these costs could be covered by the existing budget and advertising. The editor was asked to prepare a detailed business plan indicating the anticipated cost, advertising revenues, and a target date. This would be presented at the next Board meeting and to the membership at the AGM in October for their consideration and discussion.

D. Giusti volunteered to investigate the possibility of a person to solicit advertising in Canadian Acoustics.

(Acceptance of the Editor's report was moved by T. Kelsall, seconded by D. Giusti, carried).

Past and Future Conferences

2000 Sherbrooke: The final report indicated there were 148 registrants (the most for any CAA conference to date) and a surplus of approximately $13k was realized. D. Guisti moved that, "The conference organizers, Noureddine Atalla and Alain Berry, be congratulated as the conference was both technically and financially very successful." Seconded by T. Kelsall, carried).

2001 Toronto: D. Giusti, reported that the conference will be held 01 –03 October at the Nottawasaga Inn, in Alliston North of Toronto. Conference chairs and session organizers have been very busy soliciting papers.

2002 Charlottetown: A. Cohen has agreed to organize the conference this year.

2003 Western Canada: Calgary or Edmonton were mentioned as possible locations.

Membership Chair's Report

D. Jamieson has announced his intent to resign as Membership Chairman. The Board accepted the resignation and thanked Don for his hard work over the years.

CAA Website

There was a review of recent progress, and the steps necessary, to create a site that is independently hosted. (See Secretary's report.) D. Stredulinsky volunteered to design the website drawing upon existing resources such as D. Whicker, J. Fielder, etc.

Award Coordinator's Report

K. Fuller reported that each prize has at least one applicant. There was general agreement that the awards brochure should be updated and the format changed to a one-page announcement since details and application forms are now available at the website. The Secretary was asked to provide an electronic copy of the membership database to Award Coordinator.

There was general discussion of the draft of the Underwater Acoustics Travel Subsidy. (This is a new award resulting from the $10,500 gift from NATO's Signal Processing Institute Fund received earlier this year.) A few issues needed to be clarified and/or resolved. These included a mechanism for adjudication, requirement to submit a conference report for publication the Journal, etc.

These discussions caused the Board to review the existing student travel subsidy whereby it was realized that existing wording prevents CAA student members studying outside of Canada from applying. This was felt to be too restrictive and K. Fuller moved, "The first eligibility requirement be changed to read, 'Full-time student, with priority being given to Canadian students.'" Seconded by K. Fraser, Carried.

K. Fuller reported that the Committee formed to draft the terms and conditions of the Raymond Hetu Undergraduate Book Prize has not reached consensus. After considerable discussion, K Fuller moved, "Subject to the approval of the Committee, one of the three student presentation awards would be given the name 'Ramynod Hetu Student Presentation Award for the best presentation at the annual CAA conference'. The sum would be $500." The motion was seconded by T. Kelsall, carried. K. Fuller agreed to inform the Committee of the Board's desire.

Partnering with Other Acoustics Related Organizations in Canada

The nature of potential partnerships included exchanging links on websites, publishing announcements in Canadian Acoustics, joint conferences, etc. The first task is to identify possible organizations, (AES, CSME, ASA, ASME, planners, etc.) This might be accomplished by requesting that conference registrants indicate other acoustical organizations in which they have a membership. R. Ramakrishnan volunteered to contact AES to get a half-page description of their organization and publish this in Canadian Acoustics.

Other Business

None was identified.

Adjournment

T. Kelsall moved to adjourn the meeting, seconded by K. Fuller, carried. Meeting adjourned at 3:10 p.m.

Special Action Items Arising from the Meeting

T. Nightingale

Forward electronic copy of the membership database to K. Fuller.

Purchase web-hosting package when draft of website has been created.

Update the wording of the Student Travel subsidy form and forward to A. Cohen organizer of 2002 conference.

D. Giusti

Transfer funds from the Operating to Capital fund as directed by the Board.

Contact suitable person to solicit Journal advertising.

R. Ramakrishnan

Prepare and present to the Board in October a business plan for increasing the frequency of Journal publication from four to six times a year.

D. Stredulinsky

With other CAA members, create a draft of the new CAA website and circulate html document to the Board for comment.

Revise the draft of the Signal Processing Student Travel Subsidy.

K. Fuller

Update the Prize Brochure and circulate to Board Members.

Discuss with the Raymond Hetu Prize Committee the possibility of changing it from a book prize to one of the student presentation awards.

West Caldwell Calibration Laboratories, Inc.
uncompromised calibration

Head Office: 1575 Pittsford-Victor Road, Victor
New York, NY 14564, U.S.A.
Phone: (716) 586-3900 Fax: (716) 586-4327

Branch Office: 5200 Dixie Road, Suite 118, Mississauga
Ontario, L4W 1E4, Canada
Phone: (905) 624-3919 Fax: (905) 624-3926

Web Site: www.wccl.com E-mail: info@wccl.com

A SINGLE SOURCE LABORATORY

for Calibration and Repair of
Sound, Vibration, and Electronic Test Instrumentation

SPECIALIZING IN:

- ACCELEROMETERS
- MICROPHONES
- SOUND LEVEL METERS
- VIBRATION METERS
- FIELD CALIBRATORS
- AUDIOMETRIC EQUIPMENT
- VIBRATION TEST EQUIPMENT
- FREQUENCY ANALYZERS

OUR AUTOMATED FACILITY ASSURES YOU OF:

CALIBRATIONS TRACEABLE TO N.I.S.T.
CERTIFICATION: ISO 9002
ACCREDITATION: ANSI/NCSL Z540-1-1994
ISO/IEC GUIDE 25 (1990)
COMPLIANCE MIL-STD-45662A
ISO 10012-0 1992 (E)
ISO 17025 (1999)

SUPERIOR WORKMENSHIP
COMPLETE TEST DOCUMENTATION
QUICK TURNAROUND TIME:
- TWO WEEK TURNAROUND
- 48 HOUR CALIBRATION SERVICE AVAILABLE FOR AN ADDITIONAL FEE.

OTHER SERVICES INCLUDE:

- CUSTOM SYSTEM INTEGRATION
- ON-SITE CALIBRATIONS

FREE INITIAL OR NEXT CALIBRATION, COMPLIMENTS FROM WCCL.
YOUR COST OF THE INSTRUMENT WILL BE MANUFACTURERS LIST PRICE.
We will be pleased to order for you, any instrument from the following manufacturers:

ACO PACIFIC	G.R.A.S.	PCB
BRUEL&KJAER	LARSON-DAVIS	RION
CEL	METROSONICS	SYMINEX
DYTRAN	NORSONIC	
ENDEVCO	NORWEGIAN ELECTRIC	

Authorized Calibration and Repair Center for:
- Rion
- Ono-Sokki
- Scantek Inc.

We service equipment Manufactured by:
- ACO Pacific
- Brüel & Kjær
- CEL
- Dytran
- Endevco
- Fluke
- G.R.A.S.
- Hewlett-Packard
- Larson Davis
- Metrosonics
- Norsonic
- Norwegian Electric
- PCB
- Rion
- Simpson
- Syminex
- Quest
- and others

(Contact for Details)

SAMPLE REPORT & CERTIFICATE:

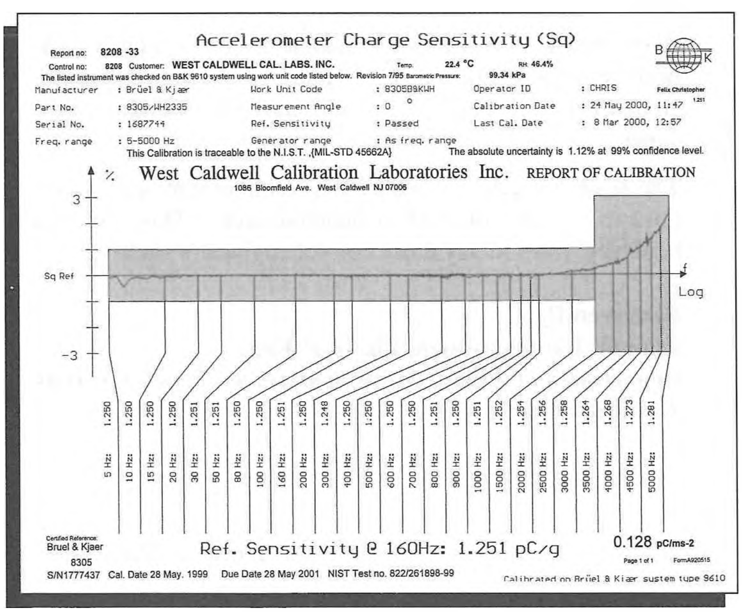

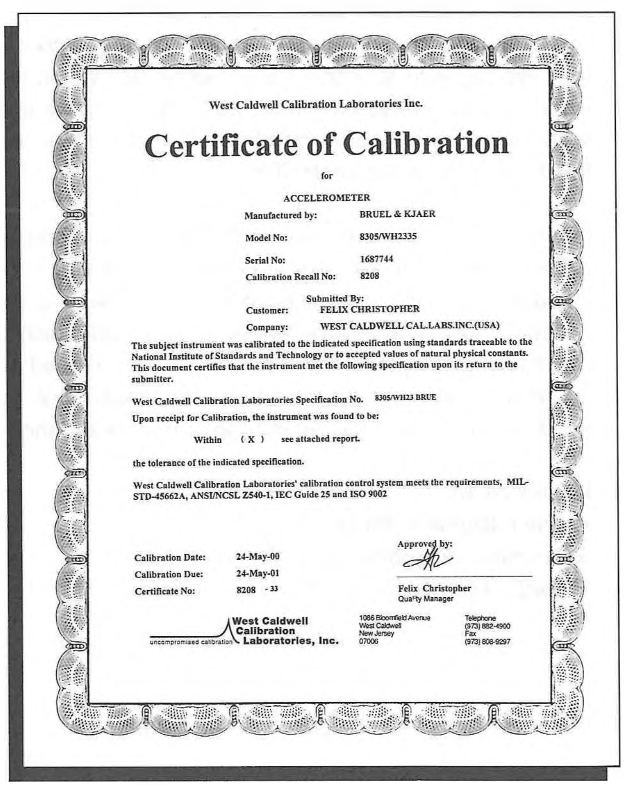

West Caldwell Calibration Laboratories Inc.

Certificate of Calibration

for

ACCELEROMETER

Manufactured by: BRUEL & KJAER
Model No: 8305/WH2335
Serial No: 1687744
Calibration Recall No: 8208

Submitted By:
Customer: FELIX CHRISTOPHER
Company: WEST CALDWELL CAL.LABS.INC.(USA)

The subject instrument was calibrated to the indicated specification using standards traceable to the National Institute of Standards and Technology or to accepted values of natural physical constants. This document certifies that the instrument met the following specification upon its return to the submitter.

West Caldwell Calibration Laboratories Specification No. 8305/WH23 BRUE

Upon receipt for Calibration, the instrument was found to be:

Within (X) see attached report.

the tolerance of the indicated specification.

West Caldwell Calibration Laboratories' calibration control system meets the requirements, MIL-STD-45662A, ANSI/NCSL Z540-1, IEC Guide 25 and ISO 9002

Calibration Date: 24-May-00
Calibration Due: 24-May-01
Certificate No: 8208 - 33

Approved by:
Felix Christopher
Quality Manager

West Caldwell Calibration Laboratories, Inc.
uncompromised calibration
1086 Bloomfield Avenue
West Caldwell
New Jersey
07006
Telephone
(973) 882-4900
Fax
(973) 808-9297

"Active Noise Control Primer," By Scott D. Snyder.

AIP Series in Modern Acoustics and Signal Processing - Springer-Verlag, New York Pages 159 2000. ISBN: 0-387-98951

The primer is aimed at the non-specialist who has little or no knowledge in acoustics, signal processing, or noise control. Ln order to provide at least a common basis, almost half of the 150 pages of text deals with general acoustics and passive noise control.

The topics covered include fundamentals of sound, mathematical methods used to describe sound, fundamentals of noise control and active noise control. The individual topics are presented in a qualitative manner. Simple easy to understand schematics and 'pictographs' are used throughout to enhance the descriptions. There is no mathematics.

The author frequently shares his experience in the field of noise control. This enhances the narrative, and non-specialists will probably take this as an easy guide to noise control. For those in the field, the side-lines are a collection of amusing anecdotes.

Once the reader has been sufficiently primed, it is time to look at active noise control in more detail. The remainder of the book deals with the controller algorithms. The exposition is quite clear and is indeed a useful primer for acousticians who want to know a little bit about active noise control.

There is no discussion on the transducers that are required to make the systems functional. This reflects the focus of many who are engaged in active noise control. However, to make these systems work, one must leave the software and deal with the many hardware problems that ultimately make or break an active noise controller.

Scott Snyder has written a useful primer to the concepts of noise control, both passive and active. As such it is recommended to project managers, who do not need a detailed understanding of acoustics, but do require some insight into the basic principles. The lack of equations and simple schematics make for easy reading. Those who look beyond the descriptive may only want to give it a brief glance.

Reviewed By:
Werner Richarz, Ph.D.
Aercoustics Engineering Ltd.,
Toronto, Ontario, Canada

"Understanding Active Noise Cancellation," By Colin H. Hansen

Spon Press, 162 Pages, 2001, £24.99
ISBN: 0-415-23377-1

Unlike the primer by Scott Snyder, Prof. Hansen's short text is aimed at practicing noise control specialists. In six short chapters, Colin Hansen was able to capture the interest of noise control engineer so that the engineer is able to start dwelling into the realm of active noise control.

Chapter 1 deals with a little history. The chapter not only provides the required background history regarding the early inventions and ideas of Coanda, Lueg and Olson, but also forecasts about future developments that can be expected.

Chapter 2, as expected, describes the foundations of active noise control. Hansen provides, within mere 18 pages, clear and concise descriptions of feedforward, feedback, adaptive, non-adaptive systems, their constituent parts as well as mechanisms that influence their performance such as control system power, placement and their optimization.

The next three chapters deal with the the basic details of components that make up the active noise cancellation systems. Hansen begins with the most complex component - could be called the heart of any active cancellation - the control system. Digital filters, the many available algorithms, and the issues that influence and determine a good control system, are described as required with clarity. The various active control sources and the issues that dominate the field of signal sensing and error sensing are also presented sucicntly, but with clarity.

The value of this book is its Chapter 6. Hansen has not only showed the different areas where active noise cancellation have been successful, he has also delineated the many areas where it is impractical to apply active noise cancellation. This chapter will be highly cherished by noise control engineers.

Even though this primer is valuable to noise control engineers, enough mathematical formulations have been provided to whet the appetite of any serious system design professional.

The book includes an exhaustive bibliography and useful links to websites of product manufacturers. This gem of a book is a must in any noise control engineer's shelf!

Reviewed By:
Ramani Ramakrishnan, Ph. D, P. Eng.
Department of Architectural Science, Ryerson University
Toronto, Ontario

NEWS / INFORMATIONS

CONFERENCES

The following list of conferences was mainly provided by the Acoustical Society of America. If you have any news to share with us, send them by mail or fax to the News Editor (see address on the inside cover), or via electronic mail to desharnais@drea.dnd.ca

2001

2-7 September: 17th International Congress on Acoustics (ICA), Rome, Italy. Fax: +39 6 4976 6932; Web: www.ica2001.it

10-14 September: International Symposium on Musical Acoustics (ISMA 2001), Perugia, Italy. Contact: Perugia Classico, Comune di Perugia, Via Eburnea 9, 06100 Perugia, Italy; Fax: +39 75 577 2255; Web: www.cini.ve.cnr.it/ISMA2001

1-3 October: Acoustics Week in Canada 2001, Nottawasaga Resort, Ontario. Contact: D. Giusti, Jade Acoustics Inc., 545 North Rivermede Road, Ste. 203, Concord, ON, L4K 4H1, Canada; Fax: 905-660-4110; Web: www.caa2001.com

7-10 October: 2001 IEEE International Ultrasonics Symposium Joint with World Congress on Ultrasonics, Atlanta, GA. Contact: W. O'Brien, Electrical and Computer Engineering, Univ. of Illinois, 405 N. Mathews, Urbana, IL 61801; Fax: 217-244-0105; WWW: www.ieee-uffc.org/2001

17-19 October: 32nd Meeting of the Spanish Acoustical Society, La Rioja, Spain. Contact: Serrano 144, Madrid 28006, Spain; Fax: +34 91 411 76 51; Web: www.ia.csic.es/sea/index.html

25-26 October: Fall meeting of the Swiss Acoustical Society, Wallis, Switzerland. Contact: Suva Akustik, P.O. Box 4358, 6002 Luzern, Switzerland; Web: www.sga-ssa.ch

29-31 October: NOISE-CON 2001 — 2001 National Conference on Noise Control Engineering, Portland, ME. Contact: INCE/USA, P.O. Box 3206 Arlington Branch, Poughkeepsie, NY 12603. Email: hq@ince.org

14-15 November: Institute of Acoustics Autumn Conference, Stratford-upon-Avon, UK. Contact: Institute of Acoustics, 77A St. Peter's Street, St. Albans, Herts, AL1 3BN, UK; Fax: +44 172 785 0553; Web: www.ioa.org.uk

16-18 November: Reproduced Sound 17, Stratford-upon-Avon, UK. Contact: Institute of Acoustics, 77A St. Peter's Street, St. Albans, Herts, AL1 3BN, UK; Fax: +44 172 785 0553; Web: www.ioa.org.uk

19-23 November: Russian Acoustical Society Meeting, Moscow, Russia. Contact: RAS, N.N. Andreyev Acoustics Institute, ul. Shvernika 4, Moscow 117036, Russia; Fax: +7 095 126 8411; Web: www.akin.ru/e_rao.htm

CONFÉRENCES

La liste de conférences ci-jointe a été offerte en majeure partie par l'Acoustical Society of America. Si vous avez des nouvelles à nous communiquer, envoyez-les par courrier ou fax (coordonnées incluses à l'envers de la page couverture), ou par courrier électronique à desharnais@drea.dnd.ca

2001

2-7 septembre: 17e Congrès international sur l'acoustique (ICA), Rome, Italie. Fax: +39 6 4976 6932; Web: www.ica2001.it

10-14 septembre: Symposium international sur l'acoustique musicale (ISMA 2001), Perugia, Italie. Info: Perugia Classico, Comune di Perugia, Via Eburnea 9, 06100 Perugia, Italy; Fax: +39 75 577 2255; Courriel: perugia@classico.it; Web: www.cini.ve.cnr.it/ISMA2001

1-3 octobre: Semaine canadienne d'acoustique 2001, Nottawasaga Resort, Ontario. Info: D. Giusti, Jade Acoustics Inc., 545 North Rivermede Road, Ste 203, Concord, ON, L4K 4H1, Canada; Fax: 905-660-4110; Web: www.caa2001.com

7-10 octobre: Symposium international IEEE 2001 sur les ultrasons, combiné avec le Congrès mondial sur les ultrasons, Atlanta, GA. Info: W. O'Brien, Electrical and Computer Engineering, Univ. of Illinois, 405 N. Mathews, Urbana, IL 61801; Fax: 217-244-0105; WWW: www.ieee-uffc.org/2001

17-19 octobre: 32e rencontre de la Société espagnole d'acoustique, La Rioja, Espagne. Info: Serrano 144, Madrid 28006, Spain; Fax: +34 91 411 76 51; Web: www.ia.csic.es/sea/index.html

25-26 octobre: Journées d'automne de la Société suisse d'acoustique, Valais, Suisse. Info: Suva Akustik, C.P. 4358, 6002 Luzerne, Suisse; Web: www.sga-ssa.ch

29-31 octobre: NOISE-CON 2001 — Conférence nationale 2001 sur le génie du contrôle du bruit, Portland, ME. Info: INCE/USA, P.O. Box 3206 Arlington Branch, Poughkeepsie, NY 12603. Courriel: hq@ince.org

14-15 novembre: Conférence d'automne de l'Institut d'acoustique, Stratford-upon-Avon, Royaume-Uni. Info: Institute of Acoustics, 77A St. Peter's Street, St. Albans, Herts, AL1 3BN, UK; Fax: +44 172 785 0553; Web: www.ioa.org.uk

16-18 novembre: Sons reproduits 17, Stratford-upon-Avon, Royaume-Uni. Info: Institute of Acoustics, 77A St. Peter's Street, St. Albans, Herts, AL1 3BN, UK; Fax: +44 172 785 0553; Web: www.ioa.org.uk

19-23 novembre: Rencontre de la Société russe d'acoustique, Moscou, Russie. Info: RAS, N.N. Andreyev Acoustics Institute, ul. Shvernika 4, Moscow 117036, Russia; Fax: +7 095 126 8411; Web: www.akin.ru/e_rao.htm

21-23 November: Australian Acoustical Society Annual Meeting, Canberra, Australia. Contact: Acoustics 2001, Australian Defense Force Academy, Canberra, ACT 2600, Australia; Email: nit@adfa.edu.au

3-7 December: 142nd Meeting of the Acoustical Society of America, Ft. Lauderdale, FL. Contact: Acoustical Society of America, Suite 1NO1, 2 Huntington Quadrangle, Melville, NY 11747-4502; Tel: 516-576-2360; Fax: 516-576-2377; Email: asa@aip.org; Web: asa.aip.org

2002

21-23 February: National Hearing Conservation Association Annual Conference, Dallas, TX. Contact: NHCA, 9101 E. Kenyon Ave., Ste. 3000, Denver, CO 80237; Tel.: 303-224-9022; Fax: 303-770-1812; Email: nhca@gwami.com; Web: www.hearingconservation.org/index.html

4-8 March: German Acoustical Society Meeting (DAGA 2002), Bochum, Germany. Contact: J. Blauert, Institute of Communication Acoustics, Ruhr-Universität Bochum, 44780 Bochum, Germany; Fax: +49 234 321 4165; Web: www.ika.ruhr-uni-bochum.de

27-30 May: Joint Meeting: Russian Acoustical Society and Conference on Ocean Acoustics, Moscow, Russia. Contact: Yu. A. Chepurin, P.P. Shirshov Institute of Oceanology, Russian Academy of Sciences, Nakhimovsky Prospekt 36, 117851 Moscow, Russia; Fax: +7 095 124 5983; Web: rav.sio.rssi.ru/Ixconf.html

3-7 June: 143rd Meeting of the Acoustical Society of America, Pittsburg, PA. Contact: Acoustical Society of America, Suite 1NO1, 2 Huntington Quadrangle, Melville, NY 11747-4502; Tel: 516-576-2360; Fax: 516-576-2377; Email: asa@aip.org; Web: asa.aip.org

4-6 June: 6th International Symposium on Transport Noise and Vibration, St. Petersburg, Russia. Contact: East-European Acoustical Association, Moskovskoe Shosse 44, St. Petersburg 196158, Russia; Fax: +7 812 127 9323; Email: noise@mail.rcom.ru

10-14 June: Acoustics in Fisheries and Aquatic Ecology, Montpellier, France. Contact: D.V. Holliday, BAE SYSTEMS, 4669 Murphy Canyon Road, Suite 102, San Diego, CA 92123-4333, USA; Web: www.ices.dk/symposia/

15-17 July: ACTIVE 2002 — 2002 International Symposium on Active Control of Sound and Vibration, Southampton, UK. Contact: Stephen J. Elliott, Institute of Sound and Vibration Research, Southampton University, University Road, Highfield, Southampton SO17 1BJ, United Kingdom; Tel.: +44 23 8059 2384; Fax: +44 23 8059 3190; Email: sje@isvr.soton.ac.uk; Web: www.isvr.soton.ac.uk /ACTIVE2002

19-21 August: Inter-Noise 2001 — 31st International Congress and Exposition on Noise Control Engineering, Dearborn, MI. Contact: Inter-Noise 2002 Congress Secretariat, Dept. Mechanical Engineering, Ohio State University, 206 West 18th Avenue, Columbus, OH 43210-1107, USA. Email: peersen.1@osu.edu; Web: www.internoise2002.org

21-23 novembre: Rencontre annuelle de la Société australienne d'acoustique, Canberra, Australie. Info: Acoustics 2001, Australian Defense Force Academy, Canberra, ACT 2600, Australia; Courriel: nit@adfa.edu.au

3-7 décembre: 142e recontre de l'Acoustical Society of America, Ft. Lauderdale, FL. Info: Acoustical Society of America, Suite 1NO1, 2 Huntington Quadrangle, Melville, NY 11747-4502; Tél: 516-576-2360; Fax: 516-576-2377; Courriel: asa@aip.org; Web: asa.aip.org

2002

21-23 février: Conférence annuelle de l'Association nationale de la conservation de l'audition, Dallas, TX. Info: NHCA, 9101 E. Kenyon Ave., Ste. 3000, Denver, CO 80237; Tél.: 303-224-9022; Fax: 303-770-1812; Courriel: nhca@gwami.com; Web: www.hearingconservation.org/index.html

4-8 mars: Rencontre de la Société allemande d'acoustique (DAGA 2002), Bochum, Allemagne. Info: J. Blauert, Institute of Communication Acoustics, Ruhr-Universität Bochum, 44780 Bochum, Germany; Fax: +49 234 321 4165; Web: www.ika.ruhr-uni-bochum.de

27-30 mai: Rencontre combinée: Société russe d'acoustique, et Conférence sur l'acoustique océanique, Moscou, Russie. Info: Yu. A. Chepurin, P.P. Shirshov Institute of Oceanology, Russian Academy of Sciences, Nakhimovsky Prospekt 36, 117851 Moscow, Russia; Fax: +7 095 124 5983; Web: rav.sio.rssi.ru/Ixconf.html

3-7 juin: 143e rencontre de l'Acoustical Society of America, Pittsburg, PA. Info: Acoustical Society of America, Suite 1NO1, 2 Huntington Quadrangle, Melville, NY 11747-4502; Tél: 516-576-2360; Fax: 516-576-2377; Courriel: asa@aip.org; Web: asa.aip.org

4-6 juin: 6e Symposium international sur le bruit et vibrations des transports, Saint-Pétersbourg, Russie. Info: East-European Acoustical Association, Moskovskoe Shosse 44, St. Petersburg 196158, Russia; Fax: +7 812 127 9323;

10-14 juin: Acoustique des pêches et écologie aquatique, Montpellier, France. Info: D.V. Holliday, BAE SYSTEMS, 4669 Murphy Canyon Road, Suite 102, San Diego, CA 92123-4333, USA; Web: www.ices.dk/symposia/

15-17 juillet: ACTIVE 2002 — Symposium international 2002 sur le contrôle actif du bruit et des vibrations, Southampton, Royaume-Uni. Info: Stephen J. Elliott, Institute of Sound and Vibration Research, Southampton University, University Road, Highfield, Southampton SO17 1BJ, United Kingdom; Tél.: +44 23 8059 2384; Fax: +44 23 8059 3190; Courriel: sje@isvr.soton.ac.uk; Web: www.isvr.soton.ac.uk /ACTIVE2002

19-21 août: Inter-Noise 2001 — 31e Congrès international et exposition sur le génie du contrôle du bruit, Dearborn, MI. Info: Inter-Noise 2002 Congress Secretariat, Dept. Mechanical Engineering, Ohio State University, 206 West 18th Avenue, Columbus, OH 43210-1107, USA. Courriel: peersen.1@osu.edu; Web: www.internoise2002.org

19-23 August: 16th International Symposium on Nonlinear Acoustics (ISNA16), Moscow, Russia. Contact: O. Rudenko, Physics Department, Moscow State University, 119899 Moscow, Russia; Email: isna@acs366b.phys.msu.su

16-21 September: Forum Acusticum 2002 (Joint EAA-SEA-ASJ Meeting), Sevilla. Fax: +34 91 411 7651; Web: www.cica.es/aliens/forum2002

2-6 December: Joint Meeting: 9th Mexican Congress on Acoustics, 144th Meeting of the Acoustical Society of America, and 3rd Iberoamerican Congress on Acoustics, Cancun, Mexico. Contact: Acoustical Society of America, Suite 1NO1, 2 Huntington Quadrangle, Melville, NY 11747-4502; Tel: 516-576-2360; Fax: 516-576-2377; Email: asa@aip.org; Web: asa.aip.org/cancun.html

2004

5-9 April: 18th International Congress on Acoustics (ICA2004), Kyoto, Japan. Web: ica2004.or.jp

19-23 août: 16e Symposium international sur l'acoustique non-linéaire (ISNA16), Moscou, Russie. Info: O. Rudenko, Physics Department, Moscow State University, 119899 Moscow, Russia; Courriel: isna@acs366b.phys.msu.su

16-21 septembre: Forum Acusticum 2002 (Rencontre conjointe EAA-SEA-ASJ), Séville. Fax: +34 91 411 7651; Web: www.cica.es/aliens/forum2002

2-6 décembre: Rencontres combinées: 9e Congrès mexicain d'acoustique, 144e rencontre de l'Acoustical Society of America, et 3e Congrès ibéro-américain d'acoustique, Cancun, Mexique. Info: Acoustical Society of America, Suite 1NO1, 2 Huntington Quadrangle, Melville, NY 11747-4502; Tél: 516-576-2360; Fax: 516-576-2377; Courriel: asa@aip.org

2004

5-9 avril: 18e Congrès international sur l'acoustique (ICA2004), Kyoto, Japon. Web: ica2004.or.jp

---

INCE/USA TO HOLD SEMINAR WITH NOISE-CON 2001

The Institute of Noise Control Engineering of the USA (INCE/USA) will sponsor a seminar titled "Noise Control and Low Noise Product Design" in conjunction with NOISE-CON 2001, the 2001 National Conference on Noise Control Engineering.

The seminar will be held on October 25-26 in Portland, Maine. It is designed to introduce basic concepts in acoustics and methods of low-noise design, noise control, and acoustical measurements. The seminar focuses on practical applications drawn from the presenters' extensive experience in the field. It is intended primarily for individuals working on controlling or measuring noise for products, buildings, factories, and outdoor environments. The key topics to be covered in the seminar are fundamentals of acoustics and noise control, noise criteria, principles of low-noise product design, noise measurements, and test facilities. Special "hot topics" sessions will cover noise control case histories, noise from computers and information technology equipment, noise from fans and other air-moving devices, and sound quality.

A copy of the seminar announcement and the NOISE-CON 2001 "Invitation to Participate" may be obtained from INCE/USA, P.O. Box 3206, Arlington Branch, Poughkeepsie, NY 12603. E-mail: hq@ince.org.

INSTRUCTIONS TO AUTHORS FOR THE PREPARATION OF MANUSCRIPTS

Submissions: The original manuscript and two copies should be sent to the Editor-in-Chief.

General Presentation: Papers should be submitted in camera-ready format. Paper size 8.5" x 11". If you have access to a word processor, copy as closely as possible the format of the articles in Canadian Acoustics 18(4) 1990. All text in Times-Roman 10 pt font, with single (12 pt) spacing. Main body of text in two columns separated by 0.25". One line space between paragraphs.

Margins: Top - title page: 1.25"; other pages, 0.75"; bottom, 1" minimum; sides, 0.75".

Title: Bold, 14 pt with 14 pt spacing, upper case, centered.

Authors/addresses: Names and full mailing addresses, 10 pt with single (12 pt) spacing, upper and lower case, centered. Names in bold text.

Abstracts: English and French versions. Headings, 12 pt bold, upper case, centered. Indent text 0.5" on both sides.

Headings: Headings to be in 12 pt bold, Times-Roman font. Number at the left margin and indent text 0.5". Main headings, numbered as 1, 2, 3, ... to be in upper case. Sub-headings numbered as 1.1, 1.2, 1.3, ... in upper and lower case. Sub-sub-headings not numbered, in upper and lower case, underlined.

Equations: Minimize. Place in text if short. Numbered.

Figures/Tables: Keep small. Insert in text at top or bottom of page. Name as "Figure 1, 2, ..." Caption in 9 pt with single (12 pt) spacing. Leave 0.5" between text.

Line Widths: Line widths in techincal drawings, figures and tables should be a minimum of 0.5 pt.

Photographs: Submit original glossy, black and white photograph.

Scans: Should be between 225 dpi and 300 dpi. Scan: Line art as bitmap tiffs; Black and white as grayscale tiffs and colour as CMYK tiffs;

References: Cite in text and list at end in any consistent format, 9 pt with single (12 pt) spacing.

Page numbers: In light pencil at the bottom of each page.

Reprints: Can be ordered at time of acceptance of paper.

DIRECTIVES A L'INTENTION DES AUTEURS PREPARATION DES MANUSCRITS

Soumissions: Le manuscrit original ainsi que deux copies doivent être soumis au rédacteur-en-chef.

Présentation générale: Le manuscript doit comprendre le collage. Dimensions des pages, 8.5" x 11". Si vous avez accès à un système de traitement de texte, dans la mesure du possible, suivre le format des articles dans l'Acoustique Canadienne 18(4) 1990. Tout le texte doit être en caractères Times-Roman, 10 pt et à simple (12 pt) interligne. Le texte principal doit être en deux colonnes séparées d'un espace de 0.25". Les paragraphes sont séparés d'un espace d'une ligne.

Marges: Dans le haut - page titre, 1.25"; autres pages, 0.75"; dans le bas, 1" minimum; latérales, 0.75".

Titre du manuscrit: 14 pt à 14 pt interligne, lettres majuscules, caractères gras. Centré.

Auteurs/adresses: Noms et adresses postales. Lettres majuscules et minuscules, 10 pt à simple (12 pt) interligne. Centré. Les noms doivent être en caractères gras.

Sommaire: En versions anglaise et française. Titre en 12 pt, lettres majuscules, caractères gras, centré. Paragraphe 0.5" en alinéa de la marge, des 2 cotés.

Titres des sections: Tous en caractères gras, 12 pt, Times-Roman. Premiers titres: numéroter 1, 2, 3, ..., en lettres majuscules; sous-titres: numéroter 1.1, 1.2, 1.3, ..., en lettres majuscules et minuscules; sous-sous-titres: ne pas numéroter, en lettres majuscules et minuscules et soulignés.

Equations: Les minimiser. Les insérer dans le texte si elles sont courtes. Les numéroter.

Figures/Tableaux: De petites tailles. Les insérer dans le texte dans le haut ou dans le bas de la page. Les nommer "Figure 1, 2, 3,..." Légende en 9 pt à simple (12 pt) interligne. Laisser un espace de 0.5" entre le texte.

Largeur Des Traits: La largeur des traits sur les schémas technique doivent être au minimum de 0.5 pt pour permettre une bonne reproduction.

Photographies: Soumettre la photographie originale sur papier glacé, noir et blanc.

Figures Scanées: Doivent être au minimum de 225 dpi et au maximum de 300 dpi. Les schémas doivent être scannés en bitmaps tif format. Les photos noir et blanc doivent être scannées en échelle de gris tifs et toutes les phoots couleurs doivent être scannées en CMYK tifs.

Références: Les citer dans le texte et en faire la liste à la fin du document, en format uniforme, 9 pt à simple (12 pt) interligne.

Pagination: Au crayon pâle, au bas de chaque page.

Tirés-à-part: Ils peuvent être commandés au moment de l'acceptation du manuscrit.

The Canadian Acoustical Association | l'Association Canadienne d'Acoustique

SUBSCRIPTION INVOICE

Subscription for the current calendar year is due January 31. New subscriptions received before July 1 will be applied to the current year and include that year's back issues of Canadian Acoustics, if available. Subscriptions received from July 1 will be applied to the next year.

FACTURE D'ABONNEMENT

L'abonnement pour la présente année est dû le 31 janvier. Les nouveaux abonnements reçus avant le 1 juillet s'appliquent à l'année courante et incluent les anciens numéros (non-épuisés) de l'Acoustique Canadienne de cette année. Les abonnements reçus après le 1 juillet s'appliquent à l'année suivante.

Check ONE Item Only: / Cocher la case appropriée:

CAA Membership	______	$50	______	Membre individuel
CAA Student membership	______	$10	______	Membre étudiant(e)
Institutional Subscription	______	$50	______	Membre institutionnel
Sustaining Subscription	______	$150	______	Abonnement de soutien
Total Remitted		$_______		Versement total

INFORMATION FOR MEMBERSHIP DIRECTORY / RENSEIGNEMENT POUR L'ANNUAIRE DES MEMBRES

Check areas of interest (max 3): / Cocher vos champs d'intérêt (max. 3):

Architectural Acoustics	1.	_____	1. Acoustique architecturale
Engineering Acoustics / Noise Control	2.	_____	2. Génie acoustique / Contrôle du bruit
Physical Acoustics / Ultrasound	3.	_____	3. Acoustique physique / Ultrasons
Musical Acoustics / Electroacoustics	4.	_____	4. Acoustique musicale / Electroacoustique
Psychological / Physiological Acoustics	5.	_____	5. Physio/psycho-acoustique
Shock and Vibration	6.	_____	6. Chocs et vibrations
Hearing Sciences	7.	_____	7. Audition
Speech Sciences	8.	_____	8. Parole
Underwater Acoustics	9.	_____	9. Acoustique sous-marine
Signal Processing / Numerical Methods	10.	_____	10. Traitement des signaux / Méthodes numériques
Other	11.	_____	11. Autre

Business telephone number (_____) _______________ Numéro de téléphone au bureau

Business facsimile number (_____) _______________ Numéro de télécopieur au bureau

Business E-Mail number __________________________________ Numéro de courier électronique au bureau

PLEASE TYPE NAME AND ADDRESS BELOW:

VEUILLEZ ECRIRE VOTRE NOM ET VOTRE ADRESSE CI-DESSOUS:

Faites parvenir ce formulaire à l'adresse suivante en prenant soin d'y joindre un chèque fait au nom de L'ASSOCIATION CANADIENNE D'ACOUSTIQUE:

Make cheques payable to THE CANADIAN ACOUSTICAL ASSOCIATION. Mail this form with payment to:

Trevor Nightingale
Secretary, Canadian Acoustical Association
P. O. Box 74068
Ottawa, Ontario K1M 2H9

The Canadian Acoustical Association
l'Association Canadienne d'Acoustique

SUSTAINING SUBSCRIBERS / ABONNES DE SOUTIEN

The Canadian Acoustical Association gratefully acknowledges the financial assistance of the Sustaining Subscribers listed below. Annual donations (of $150.00 or more) enable the journal to be distributed to all at a reasonable cost. Sustaining Subscribers receive the journal free of charge. Please address donation (made payable to the Canadian Acoustical Association) to the Secretary of the Association.

L'Association Canadienne d'Acoustique tient à témoigner sa reconnaissance à l'égard de ses Abonnés de Soutien en publiant ci-dessous leur nom et leur adresse. En amortissant les coûts de publication et de distribution, les dons annuels (de $150.00 et plus) rendent le journal accessible à tous nos membres. Les Abonnés de Soutien reçoivent le journal gratuitement. Pour devenir un Abonné de Soutien, faites parvenir vos dons (chèque ou mandat-poste fait au nom de l'Association Canadienne d'Acoustique) au secrétaire de l'Association.

ACO Pacific
Mr. Nolan Lewis - (650) 595-8588
www.acopacific.com - USA

Acoustec Inc.
Dr. J.G. Migneron - (418) 682-2331
courrier@acoustec.qc.ca - Canada

Aercoustics Engineering Limited
Mr. John O'Keefe - (416) 249-3361
aercoustics@aercoustics.com - Canada

Bruel & Kjaer Canada Ltd.
Mr. Bill Bailey, (514) 695-8225
- Canada

Dalimar Instruments Inc.
Mr. Daniel Larose - (450) 424-0033
daniel@delin.ca - Canaada

Dodge-Regupol Inc.
Mr. Paul Downey - 416-440-1094
pcd@regupol.com - Canada

Eckel Industries of Canada Ltd.
Mr. Blake Noon - (613) 543-2967
eckel@eckel.ca - Canada

H. L. Blachford Ltd.
Mr. D.E. Watson - (905) 823-3200
amsales@hlb.blachford.ca - Canada

Hatch Associates Ltd.
Mr. Tim Kelsall -(905) 855-7600
tkelsall@hatch.ca - Canada

HGC Engineering
Mr. Bill Gastmeier - (905) 826-4044
info@hgcengineering.com - Canada

Hydro-Quebec
Vice-presidence Environnement
- Canada

Industrial Metal Fabricators Ltd.
Mr. Frank Van Oirschot - (519) 354-4270
www.ciaccess.com/~indmetai - Canada

Integral DX Engineering Ltd.
Mr. Greg Clunis - (613) 761-1565
au741@ncf.ca - Canada

J. E. Coulter Associates Ltd.
Mr. John Coulter - (416) 502-8598
jcoulter@idirect.com - Canada

J. L. Richards & Assoc. Ltd.
Mr. Fernando Ribas - (613) 728-3571
mail@jlrichards.ca - Canada

Jade Acoustics Inc.
Ms. Dalila Giusti - (905) 660-2444
dalila@jadeacoustics.com - Canada

John Swallow Associates
Mr. John C. Swallow - (416) 798-0522
jcswall@attglobal.net - Canada

MJM Conseillers en Acoustique
M. Michel Morin - (514) 737-9811
mmroin@mjm.qc.ca - Canada

Nelson Industries Inc.
Mr. Ray Cheng - (608) 873-4370
- U. S. A.

Novel Dynamics Test Inc.
Mr. Andy Metelka - (519) 853-4495
metalka@aztec-net.com - Canada

OZA Inspections Ltd.
Mr. Gord Shaw - (416) 945-5471
oza@ozagroup.com - Canada

Peutz & Associés
Mr. Marc Asselineau - +33 1 45 23 05 00
asselino@worldnet.fr - France

Michel Picard
(514) 343-7617; FAX: (514) 343-2115
- Canada

Scantek Inc.
Mr. Peppin - (410) 290-7726
peppinr@asme.org - U. S. A.

Silex Inc.
(905) 612-4000
- Canada

SNC/Lavalin Environment Inc.
Mr. Allard - (514) 393-1000
allaj@snc-lavalin.com - Canada

Spaarg Engineering Limited
Dr. Robert Gaspar - (519) 972-0677
gasparr@kelcom.igs.net - Canada

State of the Art Acoustik Inc.
Dr. C. Fortier - 613-745-2003
sota@sota.ca - Canada

Tacet Engineering Ltd.
Dr. M.P. Sacks - (416) 782-0298
tacet@spectranet.ca - Canada

Valcoustics Canada Ltd.
Dr. Al Lightstone - (905) 764-5223
solutions@valcoustics.com - Canada

West Caldwell Calibration Labs
Mr. Stanley Christopher - (905) 624-3919
info@wccl.com - Canada

Wilrep Ltd.
Mr. Don Wilkinson - (905) 625-8944
www.wilrep.com - Canada